Design and Synthesis of Macrocyclic Ligands and Their Complexes of Lanthanides and Actinides

V. Alexander

Department of Chemistry, Loyola College, Madras-600 034, India

Received June 14, 1993 (Revised Manuscript Received July 16, 1994)

Contents

I. Introduction

Coordination chemistry of macrocyclic ligands has been a fascinating area of current research interest to the inorganic chemists all over the world. The continued interest and quest in designing new macrocyclic ligands stem mainly from their use as models for protein–metal binding sites in a substantial array of metalloproteins in biological systems, as synthetic ionophores, as models to study the magnetic exchange phenomena, as therapeutic reagents in chelate therapy for the treatment of metal intoxication, as cyclic antibiotics that owe their antibiotic actions to specific metal complexation, to study the guest–host interactions, and in catalysis. Recognition of the importance of complexes containing macrocyclic ligands has led to a considerable effort being invested in developing reliable inexpensive synthetic routes for these compounds.[1-4] Several classes of macrocyclic ligands, such as saturated polyazamacrocycles, imine Schiff base macrocycles, oxazolidine-containing macrocycles, polyoxamacrocycles, polyoxaazamacrocycles, polyoxa- and oxaazacoronands, crown ethers, lariat crown ethers, cryptands, cavitands, calixarenes, carcerands, cyclodextrins, cryptophanes, cyclophanes, hemispherands, catenanes, podands, compartmental macrocyclic ligands which form homo- and heterodinuclear complexes, structurally reinforced macrocycles, redox responsive macrocycles, photoresponsive macrocycles, pH-responsive macrocycles, chromogenic macrocycles, siderophores, sepulchrates, spherands, molecular clefts, bibracchial macrocycles, and macrocycles containing pendant arms have been synthesized. These macrocycles

0009-2665/95/0795-0273$15.50/0

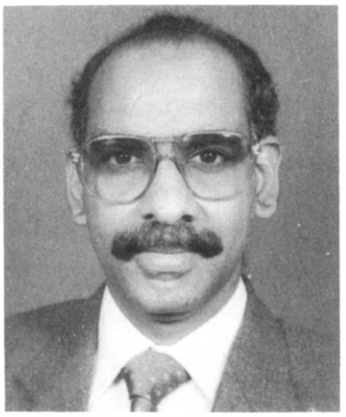

Vedhamonickom Alexander was born in 1956 in Kanyakumari District, the south end of India. He earned his B.Sc. from Madurai University through Christian College, Martandam, in 1976. He pursued his B.Ed. and M.Ed. degrees from the same university through St. Xavier's College of Education, Palayamkottai, in 1978 and 1979, respectively. After earning M.Sc. degree in chemistry from the University of Madras through St. Joseph's College, Tiruchirapalli, in 1981 he pursued research on model studies of coenzyme B_{12} from 1981 to 1984 under the supervision of Professor V. V. Ramanujam, the founding Professor of Inorganic Chemistry of the University of Madras and earned his Ph.D. in 1987. After serving in the American College, Madurai, as an Assistant Professor of Chemistry for a semester in 1985, he moved over to Loyola College, Madras, in July 1985 to take up the present position of Assistant Professor of Chemistry. He is teaching M.Sc. and M.Phil. courses and guiding research scholars for Ph.D. The broad area of his research interest are design and synthesis of macrocyclic ligands and their complexes of transition and inner-transition metal ions, binuclear macrocyclic complexes of transition and inner-transition metal ions, and spectroscopic and electrochemical investigations of the macrocyclic complexes of d- and f-block metal ions. He is a fellow of various scientific societies at home and a member of The Royal Society of Chemistry, American Chemical Society, and Sigma Xi. He is currently pursuing research on the macrocyclic complexes of lanthanides and actinides.

which contain varying combinations of aza (N), oxa (O), phospha (P), and sulfa (S) ligating atoms can be tailored to accommodate specific metal ions by the finetuning of the ligand design features, such as the macrocyclic hole size, nature of the ligand donors, donor set, donor array, ligand conjugation, ligand substitution, number and sizes of the chelate rings, ligand flexibility, and nature of the ligand backbone. The different types of macrocyclic ligands are particularly exciting because of the importance in generating new areas of fundamental chemistry and many opportunities of applied chemistry. The majority of macrocycles represent creative and focused efforts to design molecules which will have particular uses.

The ability of the lanthanide(III) metal ions to promote the Schiff base condensation of the appropriate diamine and dicarboxyl precursors, resulting in the formation of metal complexes of otherwise inaccessible macrocyclic ligands, is well established.[5,6] Macrocyclic ligands form stable complexes with lanthanides and actinides and hence they serve as a springboard to explore the coordination chemistry of these metal ions. Macrocyclic complexes of lanthanides are currently attracting much attention as radiopharmaceuticals,[7] in radioimmunotherapy,[7-12] in other medical applications, such as radioimmunoscintigraphy (γ-scintigraphy)[13,14] and positron emission tomography,[15,16] as contrast-enhancing agents in magnetic resonance imaging,[17-25] as NMR shift reagents,[26-33] as NMR shift and relaxation agents for proteins[34,35] and biological cations,[28,31,36] as fluorescent probes in fluoroimmunoassay[37-41] and in other clinical applications,[41] as luminescent labels in luminescence immunoassay,[42] as luminophores,[37,38] and as luminescent probes and luminescent concentrators.[38] Luminescent lanthanide complexes of chelating ligands have been suggested as markers in cytology and immunology and may serve as luminescent biomarkers.[43] Lanthanide luminscent probes[40,44-47] are presently extensively used for studying metal ion sites in macrocyclic complexes[48,49] and in biological systems,[40,48] There is an emerging interest in the application of macrocyclic ligands as effective metal ion chelators[50-57] and in the separation of lanthanides.[58-62] One of the most tantalizing applications of lanthanide(III) macrocyclic complexes is the efficient catalytic cleavage of RNA (transesterification of RNA).[63-65] Homodinuclear lanthanide complexes are used to study the nature and application of lanthanide metal−metal interactions in lasers[66,67] and phosphors,[68,69] to characterize complex biomolecules,[45,48] to determine the metal−metal distances[70] and the local coordination symmetry[48] in biomolecules and to determine the depth of the active sites from protein surfaces.[71-73] Dinuclear lanthanide(III) complexes are also important as novel tunable photonic devices[74] with potential application in biomedical diagnostics[75] and fluorescence imaging.[75,76] Possible applications of immobilized dinucleating chelates for the efficient separation and purification of the lanthanides are of great interest.[77,78] Dinuclear lanthanide complexes are also important in studying the molecular recognition processes which govern the lanthanide(III) cations' pairing events.[79]

Lanthanides and actinides form complexes of higher coordination numbers ranging from 7 to 12. This is attributed to the large size of these metal ions together with the ionic nature of the metal−ligand bonding. Studies on the involvement of f-electrons in metal−ligand bonding constitutes a challenging objective to be vigorously pursued. There is a need for synthesizing stable macrocyclic complexes of f-block metal ions to explore the bonding parameters and to tap their potential uses. The challenge is to design macrocycles with appropriate ligand design features required to form stable complexes. The rational design features for tailoring such macrocycles require a more detailed understanding of the subtle factors underlying the influence of structure and dynamics of the ligand on the stability of complexes.

A review of the various design and synthetic strategies developed by investigators in various laboratories to synthesize macrocyclic complexes of lanthanides and actinides is needed to develop new design and synthetic strategies for versatile ligand systems with requisite ligand design features. The design of ligands capable of forming stable lanthanide(III) complexes would not only allow further study of the coordination properties of the rare earth metal ions but would also enable chemists to exploit more fully certain important emerging properties of these complexes. No comprehensive review of the various design and synthetic strategies developed to

tailor macrocyclic complexes of lanthanides and actinides has been published. There are five reviews in this area which are listed together with the major area of emphasis in each case.

(1) P. Guerriero, P. A. Vigato, D. E. Fenton, and P. C. Hellier, "Synthesis and Application of Macrocyclic and Macroacyclic Schiff Bases", 1992.[80] The design and synthesis of macropolycyclic and macropolyacyclic Schiff bases which have the potential to act as metal-specific ligands and allow the simultaneous incorporation of two or more metal ions in well-defined homo- or heterodinuclear array is presented. The role of metal ions as templating devices and transmetalation reactions have been discussed briefly. Synthesis of functionalized macrocycles is also mentioned. Literature up to 1991 is covered.

(2) L. M. Vallarino, "Macrocyclic Complexes of the Lanthanide(III), Yttrium(III), and Dioxouranium(VI) Ions from Metal Templated Synthesis", 1991.[81] Template synthesis of the lanthanide(III) and yttrium-(III) complexes of "2 + 2" macrocyclic complexes derived from the pyridine or furan head units and aliphatic or aromatic lateral units have been discussed. Synthesis of dinuclear complexes of compartmental ligands and mono- and bicyclic polyamino ligands have been described. The UV–visible, IR, NMR, and FAB MS spectral properties have been well documented. X-ray crystal structures have been presented with crystallographic data. This is a comprehensive review article covering literature up to 1989.

(3) L. M. Vallarino, "Design, Synthesis, and Applications of Lanthanide Macrocyclic Complexes", 1989.[6] This is a brief review article with 23 references covering the synthesis and crystal structures of lanthanide(III) complexes of three 18-membered hexaazamacrocycles. A brief account of spectral properties and thermal stability are presented. Only selected literature up to 1987 is covered.

(4) D. E. Fenton and P. A. Vigato, "Macrocyclic Schiff Base Complexes of Lanthanides and Actinides", 1988.[5] Synthesis of macrocyclic complexes by coordination template effect using s-, p-, and d-block cations as templates and by transmetalation reaction has been introduced. Synthesis of lanthanide and actinide complexes of "1 + 1" and "2 + 2" symmetric macrocycles derived by the Schiff base condensation of pyridine, furan-2,5-dicarboxaldehyde, and phenol head units with aliphatic and aromatic dicarbonyl precursors as lateral units have been presented. The importance of cation–cavity "best fit" is illustrated. Structural aspects, kinetic phenomena, and some applications are very briefly mentioned. Literature up to 1987 is covered.

(5) G. Bombieri, "New Trends in the Structural Chemistry of Actinide and Lanthanide Coordination Compounds", 1987.[82] A critical survey of the various structures found for the lanthanide and actinide complexes of substituted amide ligands, substituted urea ligands, and 18-membered hexaazamacrocyclic ligands is presented. The relevant structural trends are related to steric and electronic effects.

Therefore, a review article which covers the various design and synthetic strategies developed to synthesize macrocyclic complexes of lanthanides and actinides, their structural features, quantitative studies on the stabilities of these complexes, their applications, and the structure–reactivity principle would be an asset for those who are actively engaged in this area of research. This review is also purported to give a comprehensive view of the current status of this area of research to the beginners and to highlight the application of this chemical research to emerging nonchemical applications to lure the potential workers. The coordination template effect provides a general strategy for the synthesis of a wide variety of discrete metal complexes. The principal conceptual and experimental development that have established and exploited this strategy are briefly outlined. A brief review of the coordination template effect and subsequent developments in the design of macrocyclic complexes of alkali, alkaline earth, and transition metal ions is presented as an essential basis for the rational design of new macrocyclic complexes of lanthanides and actinides. The exciting aspect of this chemistry is that in the majority of cases the molecules meet the design criteria very well. It is evident that in an increasing number of cases the driving force behind the synthetic effort is the desire to create a molecule which will enable the user to make specific applications.

II. Design of Macrocyclic Ligands by Coordination Template Effect

The macrocyclic complexes of metal ions are synthesized by the reaction of the required metal ion with the preformed macrocyclic ligands, but there are potential disadvantages in this method. The synthesis of a macrocycle in the free form often results in a low yield of the desired product with side reactions, such as, polymerization predominating. In order to circumvent this problem the ring-closure step in the synthesis may be carried out under conditions of high dilution[83] or a rigid group may be introduced to restrict rotation in the open-chain precursors[84–86] thereby facilitating cyclization. One effective method for the synthesis of macrocyclic complexes involves an *in situ* approach wherein the presence of a metal ion in the cyclization reaction markedly increases the yield of the cyclic product. The metal ion plays an important role in directing the steric course of the reaction and this effect is termed "metal template effect".[87] The metal ion may direct the condensation preferentially to cyclic rather than polymeric products (the kinetic template effect) or stabilize the macrocycle once formed (the thermodynamic template effect). Curtis has demonstrated the template potential of metal ions in the formation of the isomeric tetraazamacrocyclic complexes **1** and **2** by the reaction of $[Ni(en)_3](ClO_4)_2$ with acetone[88] as shown in Scheme 1. The first example of a deliberate synthesis of a macrocycle using this procedure was described by Thompson and Busch[89] to synthesize **3** as shown in Scheme 2. The diimine Schiff base macrocycles obtained by the condensation of one molecule each of the dicarbonyl and diamine precursors have been termed "1 + 1" macrocycles and the tetraimine macrocycles obtained by the condensation of two molecules of the dicarbonyl compounds with the two molecules of the diamine moiety have

Scheme 1. Illustration of the Formation of Macrocyclic Complexes by the Metal Template Method by Curtis (Synthesis of Curtis Ligands, Ref 88)

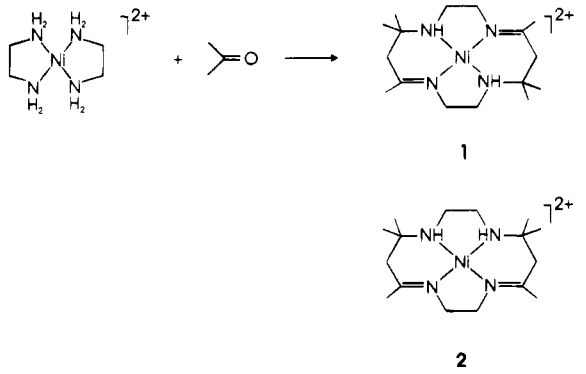

Scheme 2. The First Example of a Deliberate Synthesis of Macrocycle by the Metal Template Method by Thompson and Busch (Ref 89)

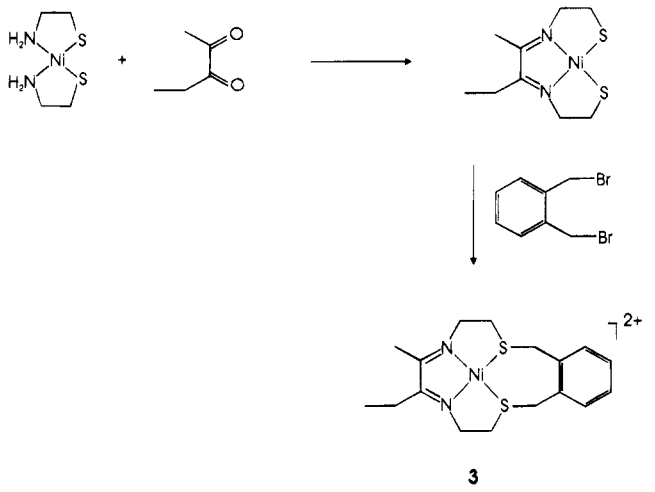

been termed "2 + 2" macrocycles as a consequence of the number of head and lateral units present.[90-92]

Coordination chemistry of polyazamacrocycles has undergone a spectacular growth since the early 1960s due to the pioneering independent contributions of Curtis[88,93,94] and Busch.[87,89] Since then a large number of synthetic polyaza macrocyclic ligands have been reported.[1-4] Synthesis of multidentate macrocyclic ligands by the metal template method has been recognized as offering high-yielding and selective routes to new ligands and their complexes.[1,3,5,87,95-99] Much of the early work featured the use of transition metal ions in the template synthesis of quadridentate macrocycles: the directional influence of the orthogonal d-orbitals was regarded as instrumental in guiding the synthetic pathway.[5] This technique has been extended in the last decade by using organotransition metal derivatives to generate tridentate cyclononane complexes.[100,101] The synthesis of macrocyclic complexes by the metal template method was extended by the use of s- and p-block cations as template devices to synthesize penta- and hexadentate Schiff base macrocycles[102-107] and a range of tetraimine Schiff base macrocycles[90,91] by the Sheffield[106-109] and Belfast[105,106,110] research groups.

The template potential of a metal ion in the formation of a macrocycle depends on the preference of the cations for stereochemistries (octahedral, tetragonal, square planar, or square pyramidal) in which the bonding d-orbitals are in orthogonal arrangements. This is exemplified by the observation that neither copper(II) nor nickel(II) acts as template[111] for the pentadentate "1 + 1" macrocycles **4**–**6**, derived by the Schiff base condensation of 2,6-diacetylpyridine with triethylenetetramine, *N*,*N*′-bis(3-aminopropyl)ethylenediamine, or *N*,*N*′-bis(2-aminoethyl)-1,3-propanediamine, respectively. However,

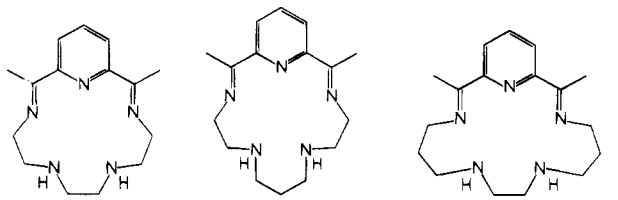

Mg^{2+}, Mn^{2+}, Fe^{2+}, Fe^{3+}, Co^{2+}, Zn^{2+}, Cd^{2+}, and Hg^{2+} serve as effective templates leading to the formation of 7-coordinate complexes of **4** and **5** with pentagonal bipyramidal geometries for Mg^{2+}, Mn^{2+}, Fe^{3+}, Fe^{2+}, Zn^{2+}, and Cd^{2+} and 6-coordinate pentagonal pyramidal geometries for Co^{2+}, Cd^{2+}, and Hg^{2+}.[112-121] The metal ion and the anion are important to the template process because the balance between the size of the cation and anion will determine the degree of dissociation of the metal salt in the reaction medium.[122]

During the synthesis of Schiff base macrocycles by the metal template method whether the reaction proceeds by an intramolecular mechanism to give the "1 + 1" macrocycle or via the bimolecular mechanism leading to the formation of the "2 + 2" macrocycle depends on one or more of the following factors: (i) if the diamine has insufficient chain length to span the two carbonyl groups then "1 + 1" macrocycle cannot be formed;[123] (ii) if the template ion is large with respect to the cavity size of the "1 + 1" ring, a "2 + 2" condensation may occur;[110,124] (iii) the electronic nature of the metal ion and the requirement of a preferred geometry of the complex; and (iv) the conformation of the "1 + 1" acyclic chelate.

A. Transamination in the Synthesis of Macrocyclic Ligands

During the course of the Schiff base condensation of the appropriate diamine and dicarbonyl precursors in the presence of an alkaline earth metal ion template macrocyclic complexes resulting from the condensation of one molecule of the dicarbonyl and two molecules of the diamine precursors are commonly isolated in good yield. An example is the complex **7**, obtained by the condensation of 2,6-diacetylpyridine with 3,6-dioxaoctane-1,8-diamine in the presence of Ba^{2+}. That this complex is a possible intermediate in the formation of the 30-membered "2 + 2" macrocycle **8** is indicated by its subsequent ring-closure reaction with 2,6-diacetylpyridine to obtain **8**.[90,92] Nevertheless, the reaction of **7** with 2,5-diformylfuran gives the Ba^{2+} complex of **9** containing both pyridyl and furan moieties.[90] This is a potential route to the synthesis of asymmetric macrocycles. An

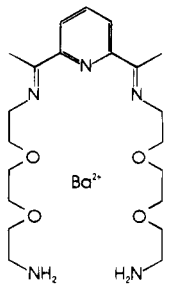

7

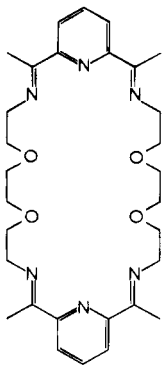

8

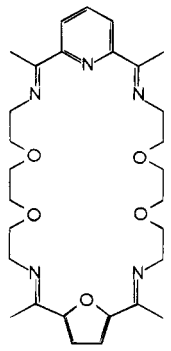

9

interesting observation is that **8** is also obtained in fairly good yield merely by warming **7** in dry solvent in the absence of the dialdehyde. A mechanism consisting of a sequence of nucleophilic additions (followed by deamination) of NH_2 groups at the coordinated >C=N centers was proposed. The results demonstrate the facility and reversibility of amine exchange (transamination) and its importance in the metal ion template synthesis of macrocyclic Schiff base ligands. The proposed mechanism involves two transaminations, one intermolecular and one intramolecular, and is consistent with the observation that macrocyclic formation is suppressed by the presence of an excess of free diamine or free metal ion. Also, in contrast to the behavior of [Ba(**7**)]$(ClO_4)_2$, the corresponding Sr^{2+} complex does not undergo ring closure either in the presence or absence of the dicarbonyl moiety to yield the complex of **8**. The study is extended to the alkaline earth metal ion controlled reactions between 2,6-diacetylpyridine and diethylenetriamine. The reaction in the presence of the perchlorate or nitrate of Mg^{2+}, Ca^{2+}, Sr^{2+}, or Ba^{2+} in a 1:1:1 mole ratio in methanol at ~20 °C yielded crystalline complexes of the open-chain Schiff base **10** containing two terminal primary amine groups.

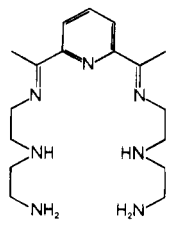

10

The same products were obtained by using different ratios of diketone to diamine although substantially increased yields were obtained by the use of excess of the amine.[125]

When the reaction is carried out in refluxing methanol complexes of the 18-membered macrocyclic ligand **11** is obtained (except for Mg^{2+}). It is interesting to note that the same set of 18-membered macrocyclic complexes are obtained in 50–70% yield when the complexes of the macroacyclic Schiff base **10** (except for Mg^{2+}) is refluxed in dry methanol for about 1 h or on standing at ~20 °C for 12–24 h as shown in eq 1.[125] The intermediacy of **10** in the

$$2[M(\mathbf{10})]X_2 \rightarrow [M(\mathbf{11})X_2] + 2X^- + 2\text{diene} \quad (1)$$

($M = Ca^{2+}$, Ba^{2+}, or Sr^{2+}; $X = ClO_4^-$ or NO_3^-)

formation of **11** can be shown by the ring closure reactions both in the presence and absence of added diketone. The crystal structure of the Ba^{2+} complex of **11** is solved, and the transamination mechanism is proposed to account for the ring closure in the absence of the added 2,6-diacetylpyridine. This consists of the addition of the secondary amine groups across the neighboring imine bonds with concomitant expulsion of two five-membered imidazolidine rings from the inner large ring of the macrocycle to give the 18-membered hexadentate macrocycle **11** instead of the expected 24-membered octadentate macrocycle **12**.[125] The X-ray crystal structure of [Ba(**11**)$ClO_4)_2$] is shown in Figure 1. The thermodynamic driving force for the ring contraction can be attributed to the mismatch of the macrocyclic cavity size in the corresponding ring-expanded macrocycle **12** and the radius of the alkaline earth metal ion. Treatment of **11** with $Cu(ClO_4)_2 \cdot 6H_2O$ gives the homodinuclear copper(II) complex of **12** with a concomitant ring expansion. The sequence of reactions involving ring closure by transamination with a concomitant ring contraction and reduction in ligand denticity and subsequent ring expansion in the presence of larger metal ions is illustrated in Scheme 3. The reaction of 1,3-diamino-2-hydroxypropane with 2,6-diacetylpyridine provides further evidence for the metal ion induced ring contraction. In the presence of Ba^{2+} the 20-membered macrocycle **13** is formed as its Ba^{2+} complex, whereas in the presence of the smaller Pb^{2+} cation ring contraction takes place to yield the 18-membered macrocycle **14** containing oxazolidine rings.[126,127] Parallel behavior is observed when 2,5-diformylfuran is condensed with 3,6-diox-

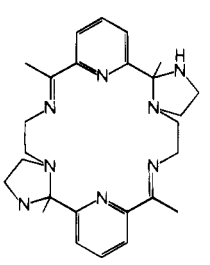

11

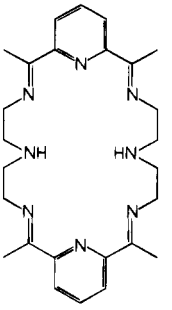

12

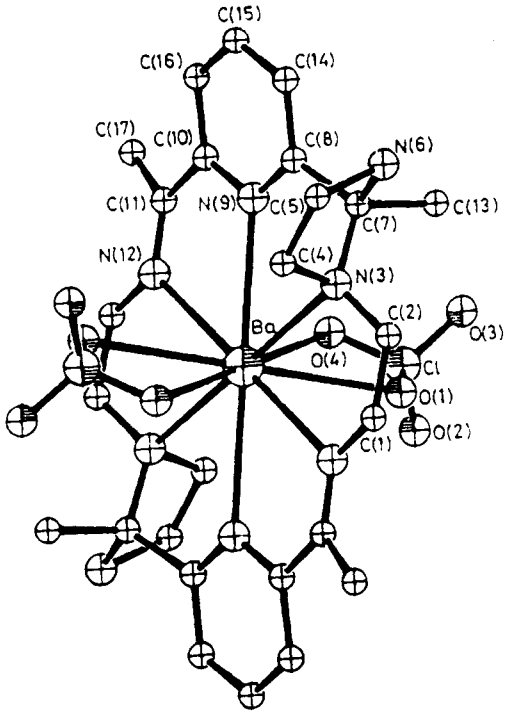

Figure 1. Structure of [Ba(**11**)$(ClO_4)_2$] together with the atomic numbering scheme. (Reprinted from ref 125. Copyright 1981 Royal Society of Chemistry.)

Scheme 3. Transamination and Ring Closure[a]

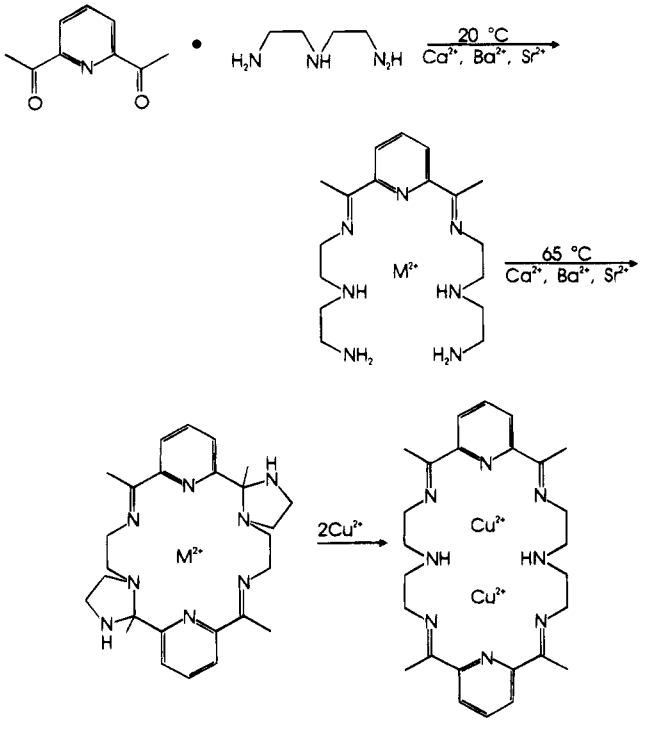

[a] When the metal ion is too small for the macorcyclic cavity, ring contraction takes place by transamination with a concomitant reduction in ligand denticity and ring size. The complex of the ring-contracted macrocycle undergoes ring expansion in the presence of larger metal ions.

aoctane-1,8-diamine in a 1:1 mole ratio in the presence of Ba^{2+} when the open-chain condensate **15** of two molecules of the diamine with one molecule of the dicarbonyl moiety is obtained. The yields are substantially increased when 2 mol of the diamine is condensed with 1 mol of the dialdehyde. No macrocyclic products were obtained under these conditions. Treatment of [Ba(**15**)]$(ClO_4)_2 \cdot 2H_2O$ with 2,5-diformylfuran afforded the complex of the 30-membered N_4O_6 macrocycle **16**. However, in contrast to [Ba(**7**)]$(ClO_4)_2$, the complex [Ba(**15**)]$(ClO_4)_2$ does not undergo ring closure in the absence of the dialdehyde.

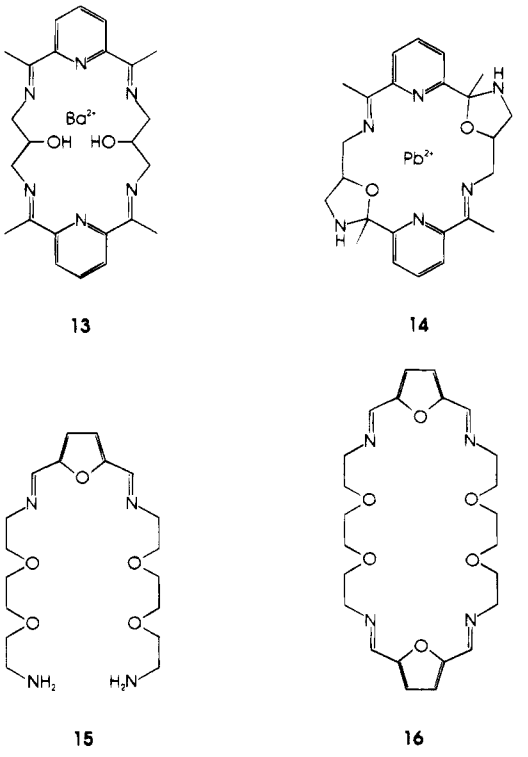

13 14

15 16

B. The Cation–Cavity "Best-Fit" in the Design of Macrocycles

The size of the cation used as the template has proved to be of importance in directing the synthetic pathway for the Schiff base systems. The compatibility between the radius of the templating cation and the "hole" of the macrocycle contributes to the

Scheme 4. Illustration of Cation–Cavity "Best Fit" In the Formation of "1 + 1" and "2 + 2" Schiff Base Macrocycles[a]

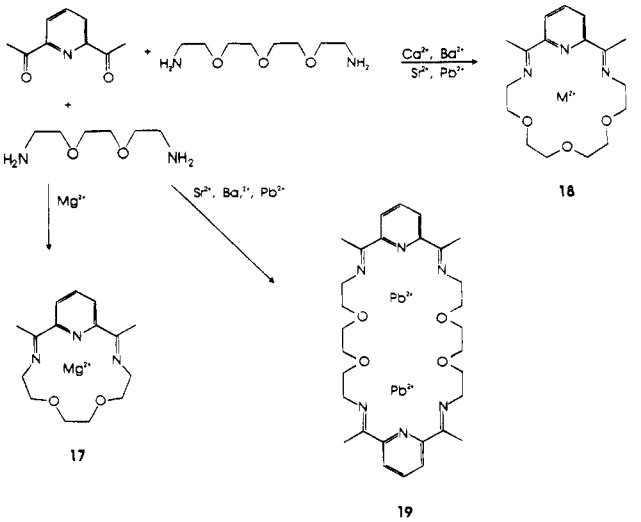

17 18 19

[a] The smaller metal ion favors the formation of "1 + 1" while the larger metal ion favors the formation of "2 + 2" macrocycle.

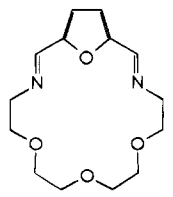

20

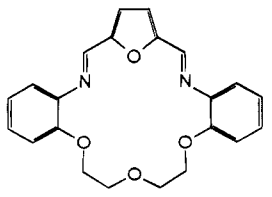

21

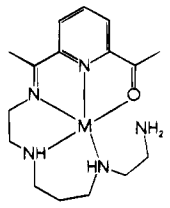

22

effectiveness of the synthetic pathway and to the geometry of the resulting complex. For example, cations of radii less than ~0.80 Å do not seem to generate complexes of **6**. The cation–cavity "best fit" in the formation of Schiff base macrocycles is diligently demonstrated by Fenton and his co-workers[103,104,106,107,124] by synthesizing oxaazamacrocycles using alkaline earth metal cations as templating devices. Of the alkaline earth cations, for example, only magnesium generates the pentadentate "1 + 1" macrocycle **17** but it is ineffective in generating the hexadentate "1 + 1" macrocycle **18** which is readily synthesized in the presence of larger cations such as Ca^{2+}, Sr^{2+}, Ba^{2+}, and Pb^{2+}. The preference for the formation of "1 + 1" or "2 + 2" Schiff base macrocycle in the metal template condensation depends on the cation radius. If it is too large for the "hole" then a "2 + 2" rather than a "1 + 1" condensation can occur. Thus the cations Sr^{2+}, Ba^{2+}, and Pb^{2+} generate the "2 + 2" macrocycle **19**[92,110] derived from the organic precursors giving the macrocycle **17** with Mg^{2+}. The cation–cavity "best fit" in the formation of the "1 + 1" and "2 + 2" macrocycles is illustrated in Scheme 4. Further illustration of the cation–cavity control factor is the synthesis of the "1 + 1" macrocycles **20** and **21** by the Schiff base condensation of furan-2,5-dicarboxaldehyde with 3,6,9-trioxaundecane-1,11-diamine and 1,5-bis(2-aminophenoxy)-3-oxapentane, respectively, using Ca^{2+}, Sr^{2+}, or Ba^{2+} as template. Mg^{2+} is ineffective in promoting the synthesis of these macrocycles.[104] The nature of the donor atom is also important in the formation of "1 + 1" or "2 + 2" macrocycle: while Pb^{2+} forms the 30-membered "2 + 2" macrocycle **19**, use of the corresponding nitrogen precursors yields the 15-membered "1 + 1" macrocycle **4**. This is due to the orientation of the terminal $-NH_2$ and >C=O groups of the probable intermediate **22**. If the interaction between the metal and the donor atoms of the diamine precursor is strong then the terminal $-NH_2$ and >C=O groups of **22** can be brought into the *cis* alignment as required for the ring closure to the "1 + 1" product. With weakly coordinating donors the probability of bringing the terminal functional groups in close proximity is less, and a "2 + 2" condensation results. This observation is clearly borne out from the X-ray crystal structures of $[Pb_2(\mathbf{19})(SCN)_4]$[110] and the related mononuclear complex $[Pb(\mathbf{18})(SCN)_2]$.[108] In both cases Pb^{2+} lies closer to the nitrogen donors than to the oxygen donors. Thus by extension of the functionally substituted α,ω-diamine chain length or donor capacity for a particular dicarbonyl precursor with an appropriate cation a desired macrocycle could be synthesized. Discrimination between alkali and alkaline earth metal cations can be made using macrocyclic and macrobicyclic polyether based ligands as a consequence of the "best fit" between the size of the cation and the cavity offered by the ligand.[128]

Scheme 5. Metal Ion Induced Ring Contraction[a]

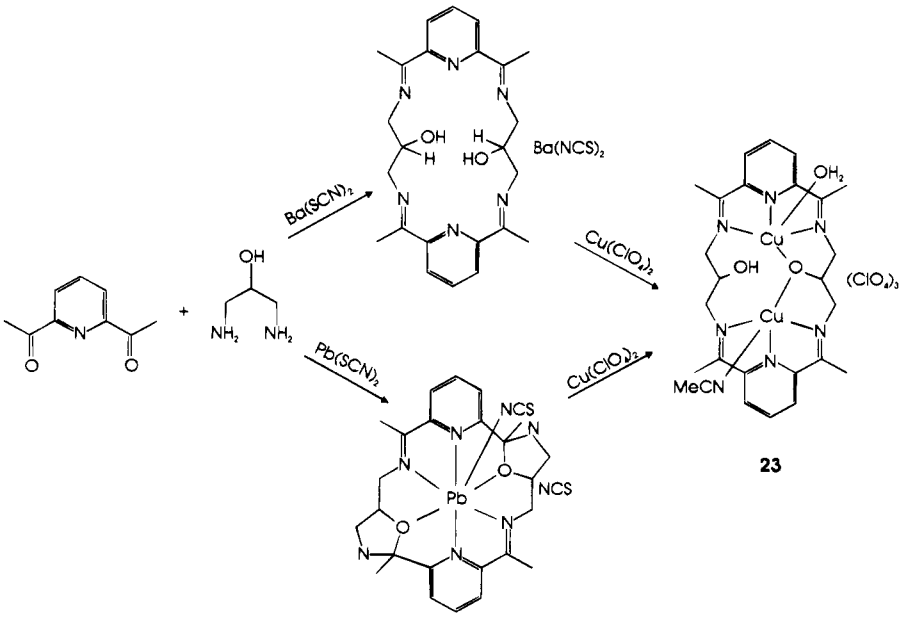

23

[a] The larger barium(II) ion gives **13** as the product from the reaction of 2,6-diacetylpyridine and 1,3-diamino-2-hydroxypropane, whereas the smaller lead(II) ion gives **14** with a reduction in ligand denticity and ring size. When the metal ion is too small for the macrocyclic cavity, ring contraction takes place by the addition of –OH function across the >C=N bond. Both **13** and **14** undergo transmetalation with Cu^{2+} to give the dinuclear copper(II) complex **23**.

A further size-related effect is the metal-induced ring contraction whereby if the metal ion is too small for the macrocyclic cavity and there is a functional group (=NH or −OH) available for addition to the imine bond then this can add to produce a smaller and more accommodating cavity for the available metal ion.[125,129] The formation of smaller macrocycles by the addition of the secondary amine group across the neighboring imine bond is discussed in section A on the metal ion controlled transamination. The reaction of 1,3-diamino-2-hydroxypropane with 2,6-diacetylpyridine provides further evidence for the metal ion control of ring contraction.[126,127] In the presence of Ba^{2+} the "2 + 2" macrocycle **13** is produced as its mononuclear Ba^{2+} complex, whereas when the smaller Pb^{2+} is used as the template a complete rearrangement of the ligand **13** occurs with a [20] → [18] ring contraction to give the macrocycle **14** containing oxazolidine rings. The sequence of reactions involving ring contraction and ring expansion according to the size of the templating cation is illustrated in Scheme 5. Both **13** and **14** on reaction with Cu^{2+} form the dinuclear copper(II) complex **23**. This is a typical example of the metal-controlled ring contraction resulting by the addition of the −OH function of the ligand framework across the >C=N bond.

III. The Anion Template Effect in the Synthesis of Macrocycles

As an alternate to the metal template synthesis of Schiff base macrocycles the metal-free ligand can be synthesized by an acid-catalyzed condensation. Sessler *et al.*[130] have synthesized pyrrole-containing macrocycles **24** and **25** by the acid-catalyzed Schiff base condensation of diformyltripyrrane with 1,2-diaminobenzene or 1,4-diaminobutane, respectively.

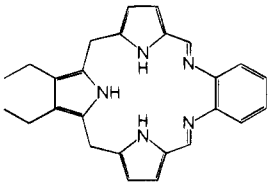

24

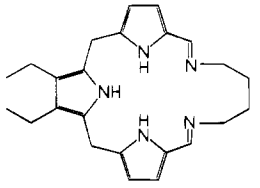

25

When the reaction was carried out in the presence of basic metal salts, such as $BaCO_3$, as a potential template no macrocycle could be isolated. Nor were any product isolated if the reaction was carried out in boiling benzene or methanol in the absence of a catalyst. However, **24** and **25** are obtained in high yields when the Schiff base condensation is effected in the presence of stoichiometric quantities of larger cations such as UO_2^{2+} and Pb^{2+}, provided that an acid catalyst is also employed.[130] In an attempt to synthesize the Schiff base macrocycle **26** in the free form the condensation of 3,4-diethylpyrrole-2,5-dicarboxaldehyde with 4,5-diamino-1,2-dimethoxybenzene was carried out by Sessler *et al.*[131] in the presence of HCl or HNO_3. Quantitative yields were obtained when HNO_3 rather than HCl was used as the acid catalyst. Under these conditions the free ligand was isolated as a protonated nitrate salt, **26**·2HNO_3. This nitrate

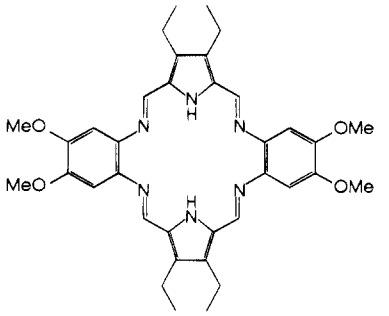

26

salt on washing with aqueous $NaHCO_3$ produced the free ligand **26**. This method of synthesizing this novel macrocycle by the acid-catalyzed Schiff base condensation led the authors to suggest a general "anion template effect". The anion template effect has been exploited in the synthesis of expanded porphyrins such as, rubyrin[132] and texaphyrins[133] by Sessler and his co-workers.

IV. Template Potential of Lanthanides

The similarity in ionic radii between the alkaline earth metal cations and the lanthanide(III) cations suggest that the latter could also be used as efficient templating devices. Furthermore, the steady decrease in ionic radius in the lanthanide series (the lanthanide contraction) could facilitate a fine control in the design of desired macrocycles. The lanthanide templates lack the metal-directing capabilities of the transition metals. The lanthanides are used to bring together two equivalents each of the diamine and dicarbonyl moieties to form macrocycles in good yield. Although the lanthanide template reactions leading to the formation of the carbon−nitrogen bonds of macrocycles parallel to those formed by the transition metal templates, the use of lanthanide ions as templates provide a more flexible coordination environment. Lanthanides resemble the alkali and alkaline earth metals in showing little directional character.[134]

A. "2 + 2" Macrocycles Derived from Pyridine Head Units and Aliphatic Lateral Units

The Schiff base condensation of 2 equiv of 2,6-diacetylpyridine with 1,2-diaminoethane in the presence of 1 equiv of hydrated lanthanum or cerium nitrate in refluxing methanol for 4−6 h gives complexes of the 18-membered hexaazamacrocycle **27**.

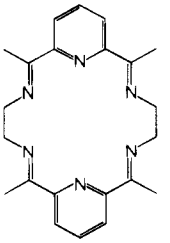

27

Analytically pure crystals of [Ln(**27**)$(NO_3)_3$] (Ln = La or Ce) were obtained in good yield. The discrete

nature of [La(**27**)]$(NO_3)_3$ is confirmed by X-ray crystallography.[135] The heavier lanthanide(III) cations were not found to be effective templating agents in the formation of analogous complexes under this reaction condition. The template potential of all the lanthanide(III) cations except the radioactive promethium has been demonstrated by De Cola *et al.*[136] in the synthesis of the macrocyclic ligand **27** by an appropriate combination of counterions and experimental conditions. The Schiff base condensation of 2,6-diacetylpyridine with 1,2-diaminoethane in the presence of lanthanide perchlorate (stored for several days in methanol over 4 Å molecular sieves) in refluxing methanol for 6 h containing ~0.1 M Cl^- yielded crystalline complexes of the composition Ln(**27**)$(ClO_4)_2(OH)\cdot nH_2O$ (Ln = La, Ce, Pr, Nd, Sm, Eu, Gd, Tb, Ho, Er, and Yb; n = 0 for La, Ce, Pr, Nd, Sm, and Er; n = 2 for Gd and Tb; n = 1 for Eu). Yields of the complexes range from 20 to 40% depending on the metal. No pure products were obtained for Tm and Dy. When the reaction is carried out under identical experimental conditions using lanthanide(III) acetate as the source of the metal template, complexes of the type Ln(**27**)$(CH_3COO)_2Cl\cdot nH_2O$ were obtained for all the lanthanides except Pm^{3+} and n varies from 3 to 6 depending on the metal. Yields of the complexes range from 70 to 80%. The values of the symmetric and antisymmetric stretching frequencies of the $-COO^-$ groups and their frequency separation, $\Delta\nu$, provide a reliable basis for structural assignments. A $\Delta\nu$ value smaller than that of the sodium salt is indicative of bidentate chelating coordination, whereas a greater $\Delta\nu$ value is diagnostic of a monodentate coordination; bidentate bridging carboxylates exhibit a $\Delta\nu$ value close to that of the free ion. The acetate–chloride complexes exhibit the ν_a(COO) absorption as a strong broad band centered at 1540 cm^{-1}, with shoulders at 1550 and 1530 cm^{-1}. The ν_s(COO) absorption appears as a pair of strong bands at 1445 and 1430 cm^{-1}, with shoulders (arising from the deformation modes of the CH_3 groups of the acetates) at 1443 and 1460 cm^{-1}. The δ(OCO) mode appears as a medium band at 670 cm^{-1}. Ionic acetate exhibits ν_a(COO) at 1550 cm^{-1} and ν_s(COO) at 1430 cm^{-1} with $\Delta\nu$ = 120 cm^{-1}, whereas the bidentate chelating acetate exhibits its ν_a(COO) at 1540 cm^{-1} and ν_s(COO) at 1455 cm^{-1} with $\Delta\nu$ = 85 cm^{-1}. The energies of the ν_a(COO) and ν_s(COO) absorptions and their energy separation in the acetate–chloride complexes are in conformity with the presence of both coordinated and ionic acetate ions which is in good agreement with the values reported in literature.[137,138] On the basis of the IR spectral evidences these complexes have been formulated as [Ln(**27**)$(CH_3COO)H_2O$][CH_3COO]$Cl\cdot nH_2O$, in which the central lanthanide(III) ion is 9-coordinate.

The heavier lanthanide cations (Tb^{3+}, Dy^{3+}, Ho^{3+}, Er^{3+}, Tm^{3+}, Yb^{3+}, and Lu^{3+}) are found to be effective in the synthesis of the smaller 14-membered hexaazamacrocycle **28** derived from the condensation of 2,6-diacetylpyridine with hydrazine: the complexes [Ln(**28**)$(H_2O)_2$]$(ClO_4)_3\cdot 4H_2O$ (Ln = Tb–Lu) are obtained. The lighter lanthanides (La^{3+} and Ce^{3+}) give complexes of the acyclic ligand **29**.[139] Thus the influence of the size of the templating cation on the formation of the macrocycle is well observed. Addition of water to the complexes of **28** also leads to ring opening to give the acyclic complexes [Ln(**29**)$(H_2O)_2$]$(ClO_4)_2\cdot 2H_2O$.

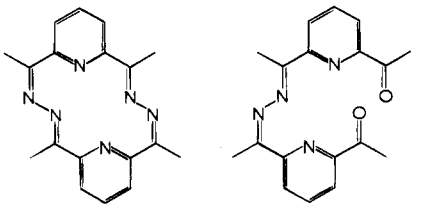

28 **29**

Condensation of 2,6-diformylpyridine with 1,2-diaminoethane in the presence of lanthanide(III) template yielded complexes of the macrocycle **30** for all the lanthanides except promethium.[140] These complexes have the formula [Ln(**30**)$(NO_3)_3]\cdot nH_2O$ (n = 0 for La–Pr; n = 1 for Nd–Gd and Dy; n = 2 for Tb and Ho–Yb; and n = 4 for Lu). The IR spectra of the complexes of the heavier lanthanides (Nd–Lu except Eu) are different from that of the lighter lanthanides (La–Pr and Eu) in that the former group of complexes exhibits a distinctive sharp band at ~3220 cm^{-1}, assignable to ν(NH) of the secondary amine group. Addition of a water molecule across an imine double bond leads to the formation of the carbinolamine species **31** as has previously been observed for some macrocyclic complexes of transition metals.[141,142] This is accompanied by an increase in

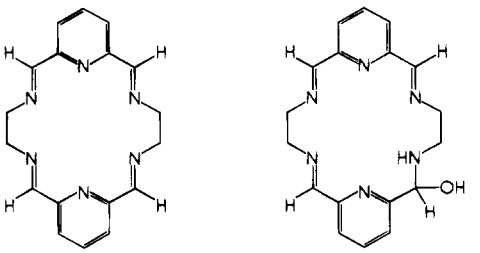

30 **31**

the flexibility of the macrocycle, making it capable of accommodating the smaller lanthanide cations. While the ^{13}C and ^1H NMR spectra of the lanthanum complex is simple as expected for the symmetric "2 + 2" macrocycle, the corresponding spectra of the Lu^{3+} complex is complicated indicating an equilibrium in solution between [Lu(**30**)$(NO_3)_3$] and [Lu(**31**)$(NO_3)_3$]. The samarium(III) complex of **31** on recrystallization yielded the complex of **30**, [Sm(**30**)$(OH)(NO_3)(H_2O)]NO_3$. The IR absorption band appearing in [Sm(**31**)$(NO_3)_3$] at 3210 cm^{-1}, assignable to ν(NH) of the secondary amine, disappears and a new band assignable to Sm–OH vibration appears in the new complex. The X-ray crystal structure, depicted in Figure 2, shows that it is a discrete complex cation [Sm(**30**)$(OH)(NO_3)(H_2O)]NO_3\cdot 2CH_3OH$.[143] The isolation of the carbinolamine complex suggests that it is probable that the formation of the tetraimine complexes could proceed via the formation of a carbinolamine intermediate prior to the elimination of water to yield the tetraimine. The isolation

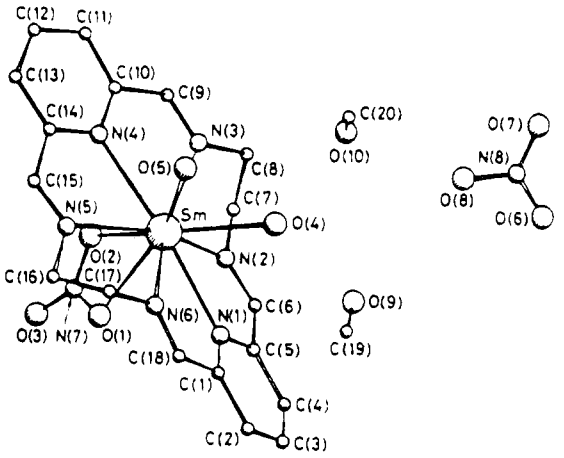

Figure 2. Crystal structure of $[Sm(\mathbf{30})(NO_3)(OH)(H_2O)]NO_3{\cdot}2CH_3OH$. (Reprinted from ref 143. Copyright 1984 Royal Society of Chemistry.)

of the complex of **31** suggests the stabilization of the carbinolamine intermediate via its facile coordination to the smaller lanthanide ions. On dissolution in water and recrystallization, a higher temperature is reached than in the original reaction in alcohol and this facilitates completion of the reaction. During the course of recrystallization there has been a reversion of the macrocycle from the carbinolamine derivative to the tetraimine form. It is probable that the optimal cation–cavity criteria has been met with and the samarium ion is accommodated by either form of the macrocycle. The initial bulk product isolated is a complex of the carbinolamine precursor to the tetraimine Schiff base, with the former being the kinetically favored product and the latter being the thermodynamically favored product. The samarium complex is also hydrolyzed during the recrystallization process. On prolonged exposure to water, dissociation of the complex occurs to give the free ligand and aquated Sm^{3+}. This seemingly facile hydrolysis of lanthanide complexes has been observed in related systems bearing compartmental ligands.[144]

The tetraimine Schiff bases **32** and **33**, derived from the condensation of 2,6-diformylpyridine with 1,2-diaminopropane or 1,3-diaminopropane, respectively, also form lanthanide complexes except for promethium. The ligand **32** forms complexes of the

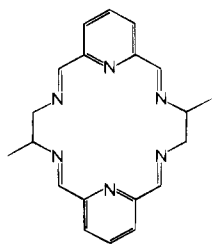

32

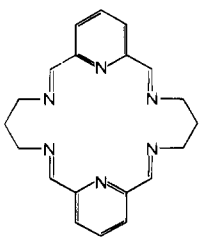

33

composition $[Ln(\mathbf{32})(NO_3)_3]{\cdot}nH_2O$ (n = 1 for Eu; n = 2 for La, Pr–Sm, Gd–Er, and Yb; and n = 3 for Ce, Tb, Tm, and Lu) and **33** forms complexes of the composition $[Ln(\mathbf{33})(NO_3)_3]{\cdot}nH_2O$ (n = 1 for La, Nd, Ho, Er, and Lu; n = 2 for Pr, Sm–Gd, and Dy; n = 3 for Ce, Tm, and Yb; and n = 4 for Tb). While the

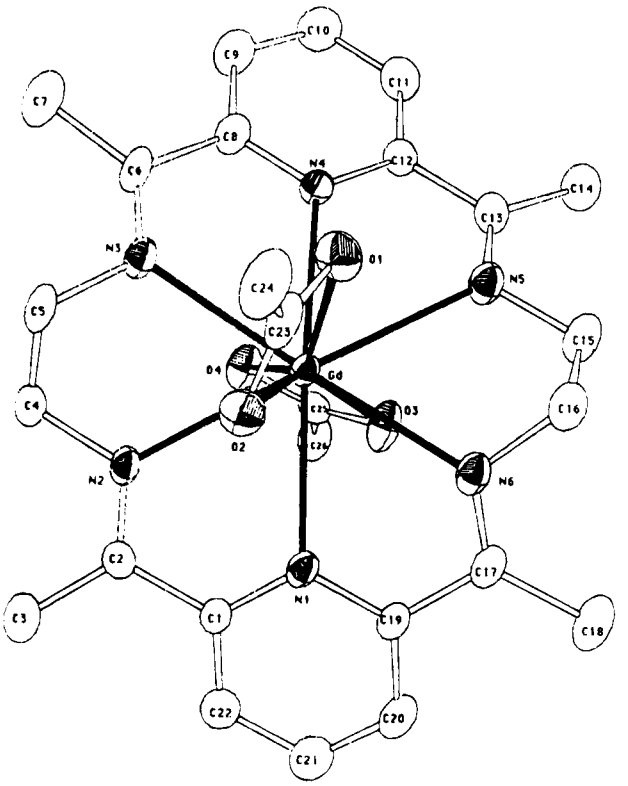

Figure 3. ORTEP labeling diagram for $[Gd(\mathbf{27})(CH_3COO)_2]Cl{\cdot}4H_2O$. (Reprinted from ref 148. Copyright 1989 American Chemical Society.)

tetraimine complexes are formed for all lanthanides with **33**, the heavier lanthanides (Nd–Lu) form complexes of the carbinolamine derivative of **32** as evidenced from the IR spectra.[140] The template potential of lanthanides has been exploited to generate a wide range of complexes of all metal ions from lanthanum to lutetium (except the radioactive promethium) with the "2 + 2" hexaazamacrocycles derived from the pyridine head units and aliphatic lateral units by an appropriate combination of counterions and experimental conditions.[135,136,140,143,145,146] The ease as well as the yield of the metal-templated macrocyclic synthesis appear to depend more on the counterion present than on the metal ion; good O-donor anions such as CH_3COO^- favor the reaction more than Cl^- or ClO_4^-. Once the complex cation is formed, addition of an appropriate combination of coordinating and noncoordinating anions favors the isolation of the complex in crystalline form. Treatment of the complexes with a variety of coordinating and noncoordinating counterions and with strong acids resulted in anion metathesis without any change in the macrocyclic cations. Anions of acetylacetone and dibenzoylmethane have also been successfully employed. X-ray crystal structures of $[La(\mathbf{27})(NO_3)_3]$,[135] $[Ce(\mathbf{27})(NO_3)_2(H_2O)]NO_3{\cdot}H_2O$,[146] $[\{Nd(\mathbf{27})(NO_3)(H_2O)_2\}_2]NO_3(ClO_4)_3{\cdot}4H_2O$,[146] $[Lu(\mathbf{27})(CH_3COO)H_2O](OH)(ClO_4){\cdot}CH_3OH$,[147] and $[Sm(\mathbf{30})(NO_3)(OH)(H_2O)]NO_3{\cdot}2CH_3OH$[143] indicate a decrease in coordination number for the lanthanide ions from La to Lu: La = 12, Ce = 11, Nd = 10, Sm = 10, and Lu = 9. This evidence suggests that the decrease in ionic radii along the $4f^n$ series may tend to lower their coordination numbers.

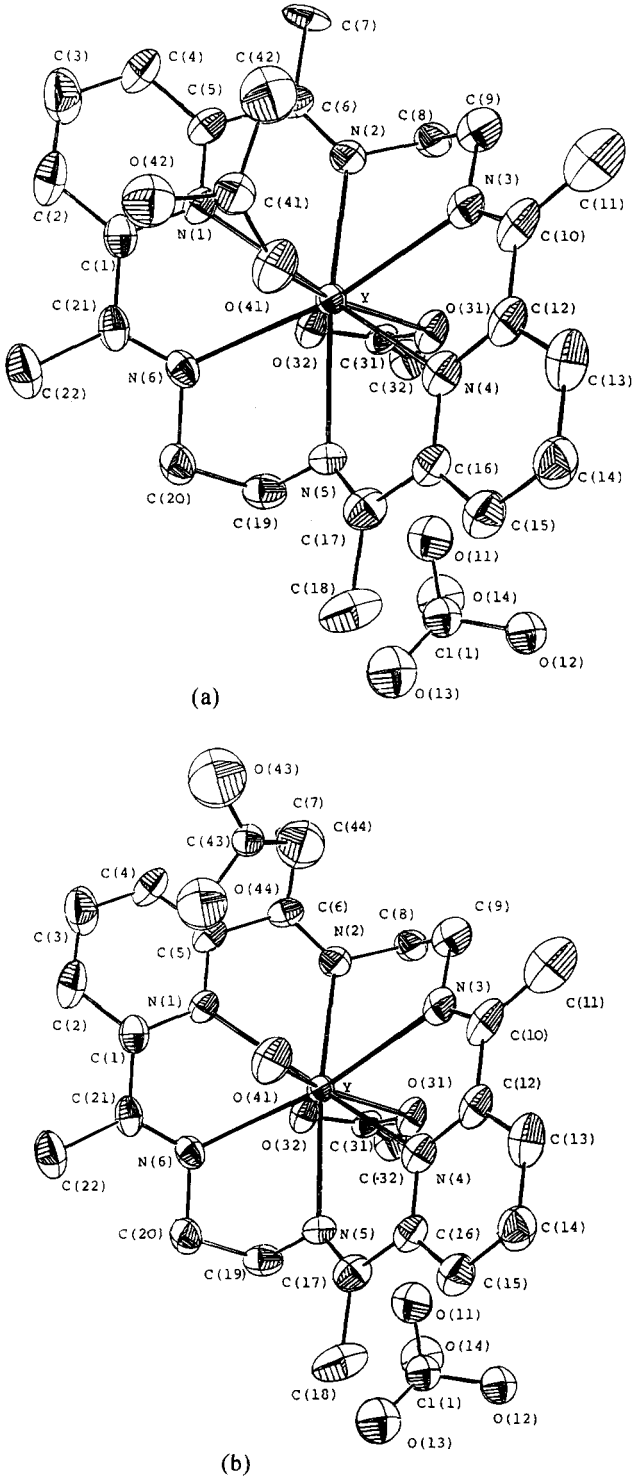

Figure 4. ORTEP perspective views of (a) [Y(**27**)($CH_3COO)_2$](ClO_4) and (b) [Y(**27**)(H_2O)(CH_3COO)](CH_3COO)-(ClO_4). The thermal ellipsoids are at 40% probability. (Reprinted from ref 149. Copyright 1989 Pergamon Press Ltd.)

The template synthesis of **27** with europium(III) or gadolinium(III) acetate as the template source in the presence of HCl yielded the complexes [Ln(**27**)-($CH_3COO)_2$]Cl·4H_2O (Ln = Eu or Gd). The X-ray crystal structure of the gadolinium complex,[148] depicted in Figure 3, shows that the metal ion is 10-coordinate with six nitrogen donors from the macrocycle and four oxygen donors from the two bidentate acetate anions. Electrochemical study demonstrates the stabilization of Eu^{3+} relative to Eu^{2+} in the

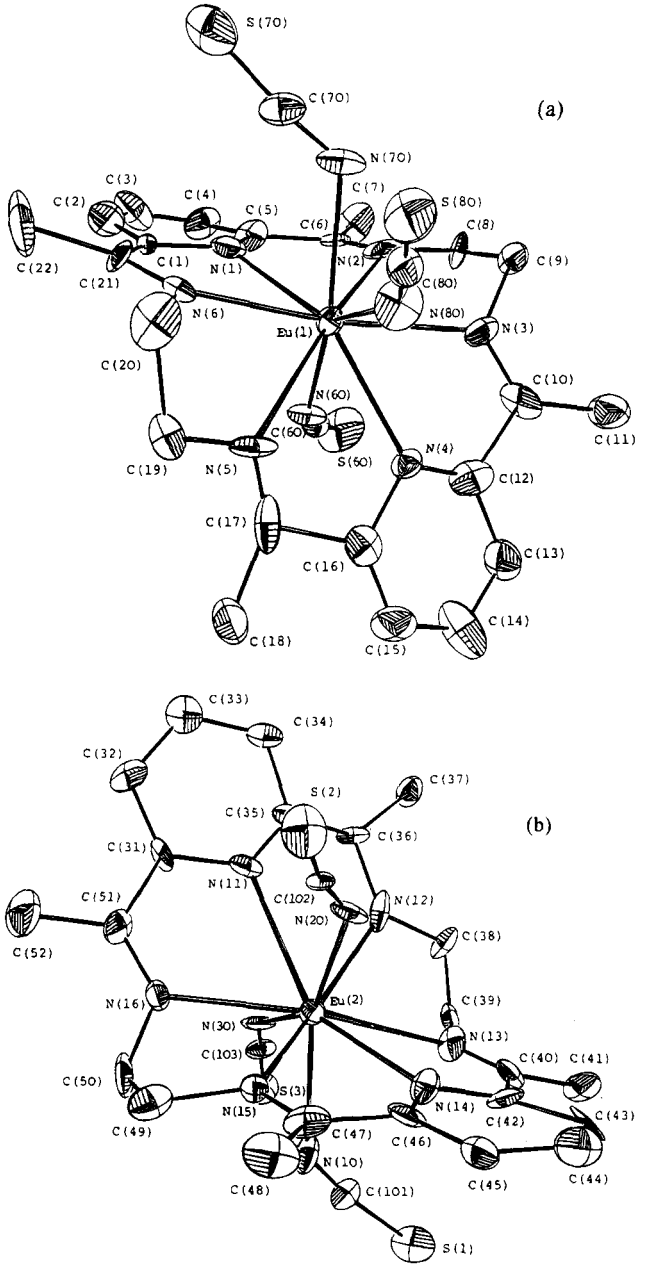

Figure 5. ORTEP view of the two independent molecules present in the crystal of [Eu(**27**)($NCS)_3$] (ellipsoids are at 40% probability; hydrogen atoms are omitted for clarity). (Reprinted from ref 150. Copyright 1989 Pergamon Press Ltd.)

macrocyclic cavity by a factor of $10^{4.6}$ as a consequence of "best fit" between the size of the Eu^{3+} and the cavity of **27**. In an attempt to develop a parallel series of macrocyclic complexes of yttrium(III) with the lanthanide(III) ions, Bombieri *et al.*[149] have synthesized yttrium(III) complexes of the macrocycles **27** and **30** by the template method. The metal-templated synthesis and general properties of the Y^{3+} complexes of **27** and **30** closely resemble the corresponding complexes of the lanthanide(III) ions.[135,136,146] Treatment of [Y(**27**)($CH_3COO)_2$Cl]·4H_2O with a variety of coordinating and noncoordinating counterions as well as with strong acids resulted in anion metathesis without disruption of the macrocyclic entity. Thus, reaction with stoichiometric quantity of aromatic monocarboxylic acids resulted in exchange of the acetates by other monocarboxyl-

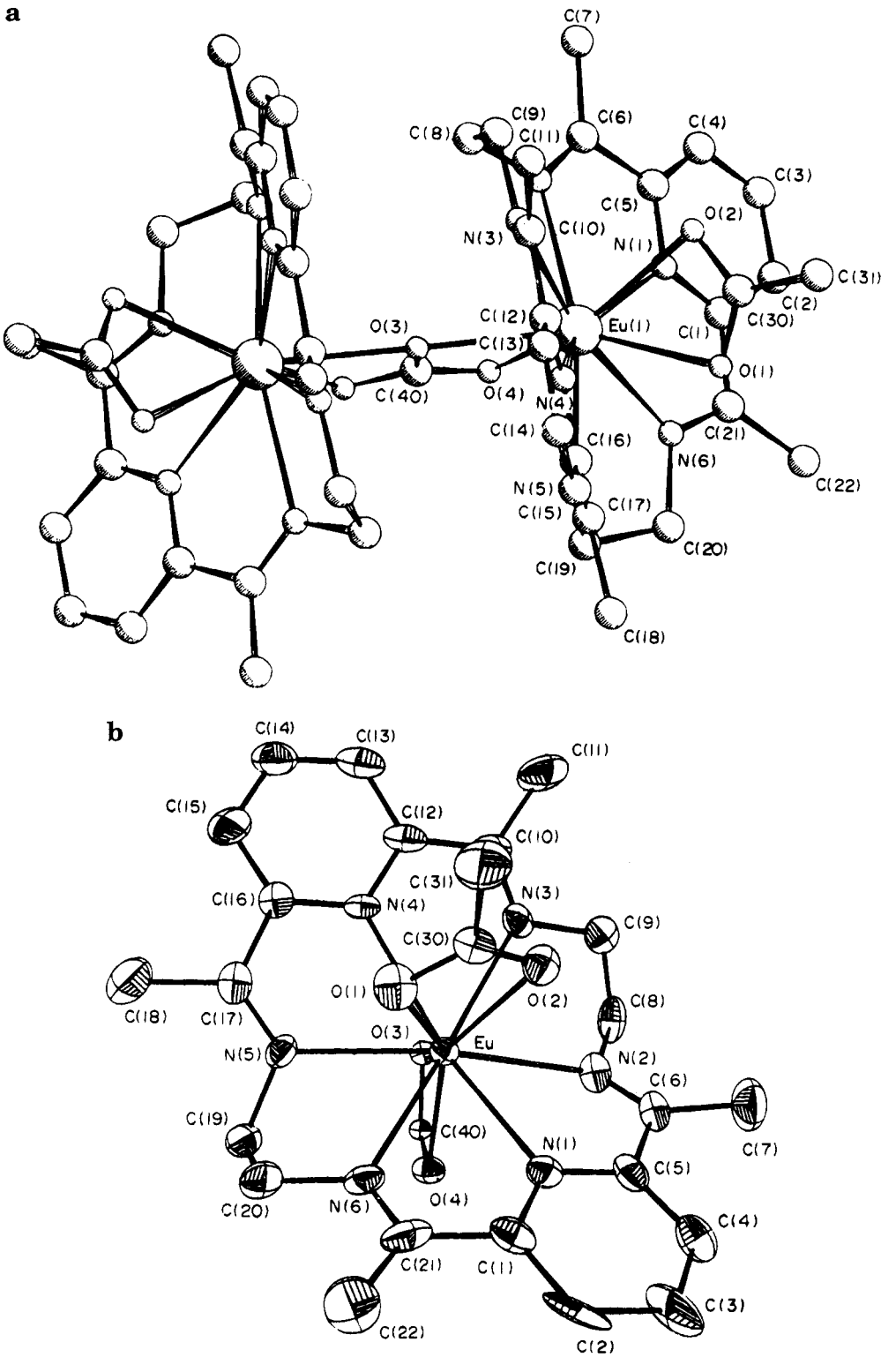

Figure 6. (a) Structure of the dimeric complex cation $[\{Eu(\mathbf{27})(CH_3COO)\}_2(\mu\text{-}CO_3)]^{2-}$ (PLUTO view) and (b) ORTEP view of the asymmetric half-dimer of $[\{Eu(\mathbf{27})(CH_3COO)\}_2(\mu\text{-}CO_3)]^{2+}$. (Reprinted from ref 151. Copyright 1991 Pergamon Press Ltd.)

ates and formation of complexes with the general formula $Y(\mathbf{27})X_2Cl{\cdot}nH_2O$ (X = benzoate, 2-furancarboxylate, 2-hydroxobenzoate, or 2-aminobenzoate). Treatment of the complex with an excess of $LiClO_4$ resulted in exchange of chloride by perchlorate, yielding a complex of the stoichiometry $Y(\mathbf{27})(CH_3COO)_2ClO_4{\cdot}0.5H_2O$. Substitution of both acetates and chloride was achieved by treatment with a 2-fold excess of concentrated hydrobromic acid or a 5-fold excess of $LiBF_4$, resulting in complexes of the formula $Y(\mathbf{27})X_3{\cdot}nH_2O$ ($X = Br^-$, $n = 5$; $X = BF_4^-$, $n = 2$). Partial exchange of the acetates by chloride was accomplished by treating the diacetate–chloride complex with hydrochloric acid in methanol and complex of the composition $Y(\mathbf{27})(CH_3COO)_{0.5}Cl_{2.5}{\cdot}5H_2O$ was obtained as colorless microcrystals.[149] The NMR spectra are consistent with a highly symmetric structure. The crystal structure of the Y^{3+} complex

of **27** reveals the presence of two different complex cations, $[Y(\mathbf{27})(CH_3COO)_2]^+$ and $[Y(\mathbf{27})(CH_3COO)(H_2O)]^{2+}$, present in a 1:1 ratio in the crystal lattice. In each case yttrium(III) is 9-coordinate. The X-ray crystal structures of the two cations are presented in Figure 4. The anion metathesis is exploited to generate the tris(isothiocyanato) complexes of yttrium(III) and europium(III) with the macrocycles **27** and **30**.[150] The X-ray crystal structures of the complexes of these metal ions with **27** show the coexistence in the same crystal of two kinds of 9-coordinate molecules with different macrocyclic conformations. The X-ray crystal structures of the two independent molecules present in the crystal of $[Eu(\mathbf{27})(NCS)_3]$ is depicted in Figure 5. The two complexes are isostructural.[150] The complex cations of Y^{3+} and Eu^{3+} display an unusual preference for the N-donor atom of NCS^-. Unlike the other complexes of these macrocycles they show no tendency to include solvent molecules in either the metal coordination sphere or the crystal lattice. The electronic and steric requirements of the central metal ions appear to be fully satisfied by coordination to the six nitrogen donors of the macrocycle and three nitrogen donors of NCS^-. The remarkable stability of this nine nitrogen coordination sphere is attributed to the nearly identical folding of the macrocycle in the complexes despite the difference in the ionic radii of these metal ions. The yields of the macrocyclic complexes do not vary appreciably with the ionic size of the metal within the first part of the lanthanide series. As the metal ionic radius decreases beyond dysprosium, however, the yields of the macrocyclic complexes gradually decrease and are usually the smallest for lutetium. There are no major differences in the general synthetic methods and structural features of the macrocyclic complexes obtained from 2,6-diacetylpyridine and 2,6-diformylpyridine except that the latter gives the complex of a partly hydrolyzed carbinolamine macrocycle as the main product. No such species has so far been observed with the complexes derived from pyridine diketone.

The interaction of the paramagnetic complex $[Eu(\mathbf{27})(CH_3COO)_2]Cl{\cdot}4H_2O$ with a series of oxygen-containing organic substrates such as alcohols, phenols, ketones, and carboxylic acids and their anions have been studied by Fonda *et al.*[29] to evaluate its performance as an NMR shift reagent and to identify exocyclic ligands that might enhance its luminescence intensity to practically useful levels. Complexes of the formula $[Eu(\mathbf{27})(RCOO)_2]Cl{\cdot}nH_2O$ (R = C_6H_5, C_4H_3O, C_4H_3S, C_4H_3NH, or C_5H_4N, n = 2–4) were prepared by metathesis between $[Eu(\mathbf{27})(CH_3COO)_2]Cl{\cdot}4H_2O$ and the respective aromatic or heteroaromatic monocarboxylic acid. These complexes are colorless crystalline solids, soluble in water and polar organic solvents. IR spectral data show that in the complexes containing benzoate, 2-furancarboxylate, 2-pyrrolecarboxylate, or 2-thiophenecarboxylate the $-COO^-$ groups act as bidentate chelating ligands. The ring heteroatom of the carboxylates cannot be coordinated to the Eu^{3+} center since the "bite" of the ligand is not sufficient to permit tridentate chelation. The ^1H NMR resonance of anionic or acidic substrates were greatly shifted in the presence of the europium complex, whereas those of uncharged substrates remain essentially unchanged. Neutral N-donor ligands, such as, 1-aminobutane, 2-aminobutane, 2-amino-2-methylbutane, 1,2-diaminoethane, aniline, pyridine, 1,10-phenanthroline, and 2,2′-bipyridyl do not interact with the metal center of the complex as evidenced from the NMR and luminescence titration experiments.[151] Attempts to isolate the 1,10-phenanthroline complex of the europium macrocycle produced the novel yellow crystalline complex $[\{Eu(\mathbf{27})(CH_3COO)\}_2(\mu\text{-}CO_3)](OH)_2{\cdot}7H_2O$, which incorporated atmospheric carbon dioxide. The X-ray crystal structure shows that the compound is ionic with dimeric complex cations consisting of two Eu(**27**) moieties linked through a bridging as well as chelating carbonate. Each europium ion is further bonded to a bidentate chelating acetate. The structure of the dimeric complex cation $[\{Eu(\mathbf{27})(CH_3COO)\}_2(\mu\text{-}CO_3)](OH)_2{\cdot}H_2O$, and the ORTEP view of the asymmetric half dimer are depicted in Figure 6, parts a and b, respectively.[151]

In order to establish the maximum number of exocyclic carboxylates which can coordinate to the metal center of the Eu(**27**) macrocyclic moiety, the triacetato complex $[Eu(\mathbf{27})(CH_3COO)_2]CH_3COO{\cdot}9H_2O$ was synthesized and its structure determined by X-ray crystallography.[29] The complex cation consists of a 10-coordinate europium bonded to six nitrogen donors of the macrocycle and to two bidentate chelating acetates situated on opposite sides of the macrocycle. An uncoordinated acetate balances the ionic charge of the complex cation. An ORTEP view of the cation and anion units in $[Eu(\mathbf{27})(CH_3COO)_2]CH_3COO{\cdot}9H_2O$ is shown in Figure 7.

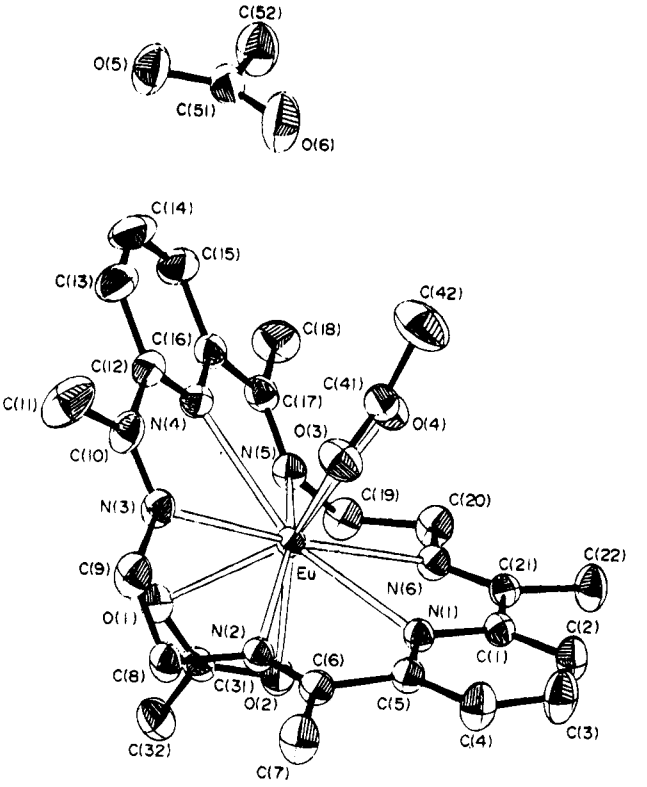

Figure 7. ORTEP view of the cation and anion units in the $[Eu(\mathbf{27})(CH_3COO)_2]CH_3COO{\cdot}9H_2O$ complex. The water molecules are omitted for clarity. (Reprinted from ref 29. Copyright 1993 Pergamon Press Ltd.)

B. "2 + 2" Macrocycles Derived from Pyridine Head Units and Aromatic Lateral Units

The Schiff base condensation of 2,6-diacetylpyridine with 1,2-diaminobenzene was first studied by Stotz and Stoufer,[152] who reported the formation of an yellow crystalline product ($C_{30}H_{26}N_6$) formulated as the 18-membered macrocyclic ligand **34**. Reinvestigation by Cabral *et al.*[153] showed the yellow compound to have the tricyclic structure **36**, consisting of a central 12-membered ring flanked by two identical 7-membered rings. The condensation of

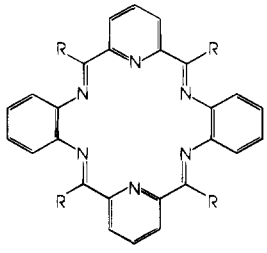

34, R = CH_3

35, R = H

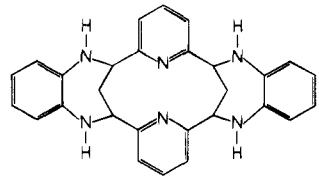

36

these precursors in the presence of the nitrates of the larger lanthanides (La, Ce, Pr, and Nd) has been reported to give $[Ln(\mathbf{34})(NO_3)_2]\cdot 2H_2O$.[154,155] The presence of a peak corresponding to the free macrocycle in the mass spectrum and IR spectral data led to the proposal that the complexes contained 12-coordinate lanthanide cations; the three nitrate anions were predicted to be bidentate. When the reaction was carried out in the presence of the metal template the chief product was the tricyclic compound **36**.[154,155] However, very low yields of the desirable complexes having the general formula $[Ln(\mathbf{34})(NO_3)_3]\cdot nH_2O$ (Ln = La^{3+}, Pr^{3+}, and Nd^{3+}; $n = 0.5-3.0$) were reported by Benetollo *et al.*[155] The authors have also isolated the "1 + 1" macrocycle **37** and the tricyclic compound **36** by the nontemplated condensation. Metathesis by other counteranions yielded the new crystalline complexes $[Pr(\mathbf{34})(NO_3)_2(CH_3OH)]ClO_4\cdot 0.5H_2O\cdot 0.5CH_3OH$ and $Nd(\mathbf{34})(OH)(NO_3)_{0.5}(ClO_4)_{1.5}\cdot 2H_2O$. The X-ray crystal structure of the praseodymium complex, depicted in Figure 8, reveals that the metal ion is 11-coordinate, being linked to the six nitrogen donors of the macrocycle, to a bidentate chelating nitrate ion, and to a methanol molecule on one side of the macrocycle and to the another bidentate chelating nitrate on the other side. The facile recovery of the compound **36** during the metal-templated synthesis led to the conclusion that steric crowding inhibited the formation of **34**. This could arise via interaction of the methyl groups with proximal aromatic hydrogen atoms. In contrast, the related condensation of 1,2-diaminobenzene with 2,6-diformylpyridine in the presence of the Ca^{2+}, Sr^{2+}, Ba^{2+}, or Pb^{2+} templates readily gives complexes of the hexaazamacrocycle **35**.[156]

The nitrates of all lanthanide(III) ions promoted the formation of the complexes of **35**.[157] Yields are quite high for the larger lanthanides (80–60% for La–Nd) and gradually decreases with decreasing size of the metal ions (less than 5% for Lu). The size of

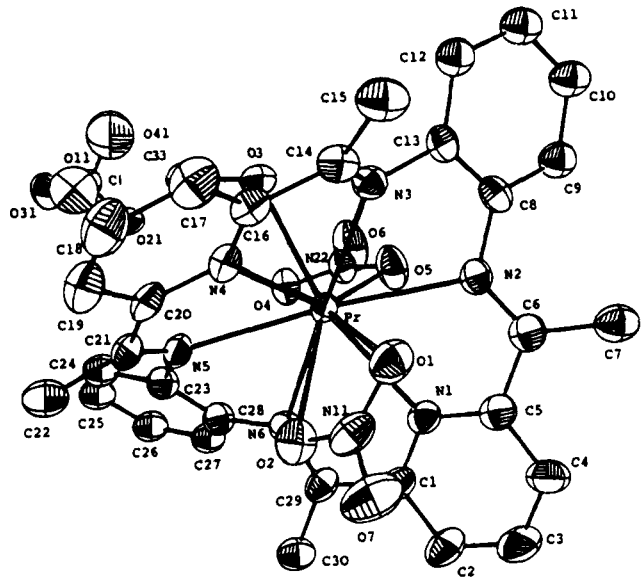

Figure 8. Perspective view of $[Pr(\mathbf{34})(NO_3)_2(CH_3OH)]ClO_4$. The thermal ellipsoids are at 50% probability. (Reprinted from ref 155. Copyright 1989 American Chemical Society.)

the metal ion also affects the stoichiometry of the complexes: the larger lanthanides (La–Gd) form the trinitrates, $[Ln(\mathbf{35})(NO_3)_3]\cdot nH_2O$ ($n = 0-4.5$), whereas the smaller ions (Tb–Lu) yielded the nitrate–hydroxide complexes, $[Ln(\mathbf{35})(NO_3)_{3-x}(OH)_x]\cdot nH_2O$ ($n = 0.5-1.5$). This change in stoichiometry most likely results from the steric requirements of the nitrate ligands, which becomes increasingly forbidding upon traversing the series, and also from the increased tendency of the smaller metal ions to hydrolyze. The triflates and acetates of the larger lanthanides also act as templates, but yields are lower than for the corresponding nitrates. In general, the synthesis is favored by coordinating anions that form sparingly soluble final products.[157] This behavior contrasts with that of the corresponding macrocyclic complexes of **34**, which are best synthesized as the highly soluble diacetate chlorides.[136] As the yields of the macrocyclic complexes from the template synthesis gradually decrease along the lanthanide series, proportionately increasing amounts of nonmacrocyclic organic byproducts were formed. In every case the major product is 2,6-bis(2-benzimidazolyl)pyridine (**38**), both as free base and as the protonated salts or nonstoichiometric metal adducts.[157] The formation

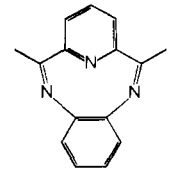

37

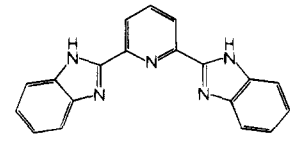

38

of N-protonated organic byproducts has been observed in the metal-templated synthesis of **34**.[155] When the condensation of 2,6-diformylpyridine with 1,2-diaminobenzene is carried out in the presence of cerium(III) acetate or europium(III) nitrate in a 4:4:1 precursor-to-metal mole ratio minor quantities of a different organic byproduct **39** is obtained. The complexes of **35** are microcrystalline solids and their

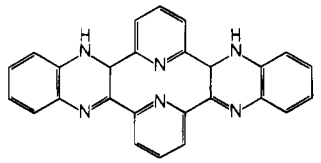

39

solubility in organic solvents depends on the metal–counterion combination and are generally lower for the complexes of the larger lanthanides. The insoluble complexes dissolve in warm methanol or ethanol containing strong base such as NaOH, but the resulting solutions are stable only for a limited time. All the lanthanide complexes of **35** undergo partial or complete anion metathesis when placed in contact with appropriate competing counterions. Reactions are practically instantaneous for the soluble complexes, showing the metal–anion association to be very labile. A similar behavior is reported for the complexes of **27** and **34**.[136,147,155]

The Schiff base condensation of 2,6-pyridinedicarboxaldehyde with chiral 1,2-diaminocyclohexane in the presence of lanthanide(III) nitrate hexahydrate in boiling methanol yielded complexes of the chiral 18-membered macrocycle **40**. Complexes of the type

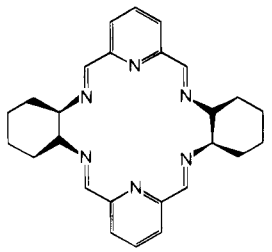

40

[Ln(**40**)](NO$_3$)$_3$·$^3/_2$H$_2$O (Ln = La^{3+}, Eu^{3+}, or Tb^{3+}) were isolated as colorless crystals. The yield ranges from 33% for La^{3+}, 34% for Eu^{3+}, to 47% for Tb^{3+}. The *RR*- and *SS*-enantiomers have been prepared under similar reaction conditions using 1(*R*),2(*R*)- and 1(*S*)-2(*S*)-diaminocyclohexane, respectively. The structures of these complexes were characterized by NMR and luminescence spectroscopy to have D_2 molecular symmetry and the absolute chiral structures were determined from CD data.[158] These chiral macrocyclic complexes are very good materials suited for studying the chiroptical properties of lanthanide complexes in solution.

C. "2 + 2" Macrocycles Derived from Furan-2,5-dicarboxaldehyde

The metal template procedure has been used to prepare complexes of the "2 + 2" symmetric macrocycles **41**–**43** by the Schiff base condensation of furan-2,5-dicarboxaldehyde with aliphatic diamines as the lateral units. The larger lanthanides readily form trinitrato complexes with these macrocycles. The following complexes are reported by Abid and Fenton:[159] [Ln(**41**)(NO$_3$)$_3$]·*n*H$_2$O (Ln = La^{3+}–Eu^{3+} except Pm^{3+}, *n* = 0–2); [Ln(**42**)(NO$_3$)$_3$]·*n*H$_2$O (Ln = La^{3+}, Ce^{3+}, and Pr^{3+}, *n* = 0–2); and [Ln(**43**)(NO$_3$)$_3$]·*n*H$_2$O (Ln = La^{3+}, Ce^{3+}, and Pr^{3+}, *n* = 0, 1).

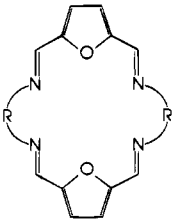

41, R = CH_2CH_2
42, R = $CH_2CH(CH_3)$
43, R = $CH_2CH_2CH_2$

When the condensation is carried out in the presence of heavier lanthanides (Gd–Lu) with 1,2-diaminoethane as the lateral units, complexes of the composition [Ln$_3$(**41**)$_2$(NO$_3$)$_9$]·4H$_2$O were obtained.[159,160] Formation of these complexes with this unexpected stoichiometry is attributed to the decreased size of the metal ions as the hole of the 18-membered macrocycle may be too large for these cations and a sandwich structure in which groups of donors are shared is proposed.[159] In the corresponding reactions with 1,3-diaminopropane or 1,2-diaminopropane as the lateral units intractable compounds were recovered.[159] In contrast to the pyridine-based macrocycles, the complexes of **41**–**43** decompose in water. This may be attributed to the lability of metal ions as a consequence of the divergence from the "best fit" situation as the "bite" in the terminal furandiimine moiety would be larger than that in the corresponding pyridinediimine moiety thereby giving a cavity of slightly larger diameter and a diminished metal–ligand interaction. In addition, the weakly donating furan head unit would help in labilizing the system. The liberation of the free macrocycle in solution was observed from the ^{1}H NMR spectrum in DMSO-d_6.

D. "2 + 2" Symmetric Macrocycles Derived from 2,6-Diformylphenols

Since the first report by Pilkington and Robson[161] of a dinucleating Schiff base macrocycle derived from 2,6-diformyl-4-methylphenol many examples of similar dinuclear systems have been reported, both macrocyclic[162–165] and macroacyclic.[166–171] The coordination chemistry of transition metal complexes of these ligands has been well explored and reviewed.[172] The template synthesis often does not afford the desirable "2 + 2" symmetric macrocyclic complexes and hence the use of the preformed macrocyclic ligands is preferred. However, reaction of the metal ion with the preformed ligand causes problems owing to their low solubility in alcohols. The best route is not to isolate these ligands but to prepare the desired one *in situ* by a step by step reaction of the appropriate organic precursors and to treat with the appropriate lanthanide salts. This allows a better control of the reaction to get the desired product. The Schiff bases behave as neutral or dianionic ligands according to the synthetic procedures employed. The generation of macroacyclic ligands **44** and **45** and their complexes **50** and **51**, macrocyclic symmetric "2 + 2" macrocycles **46** and **47** and their complexes **52**–**55**, and the unsymmetric macrocycles **48** and **49** from the reaction of 2,6-diformyl-4-chlorophenol with polyamines under various reaction conditions are

Scheme 6. Synthesis of Macrocyclic and Macroacyclic Ligands and Their Complexes of Lanthanides by the Reaction of 2,6-Diformylphenol with Polyamines under Various Reaction Conditions[a]

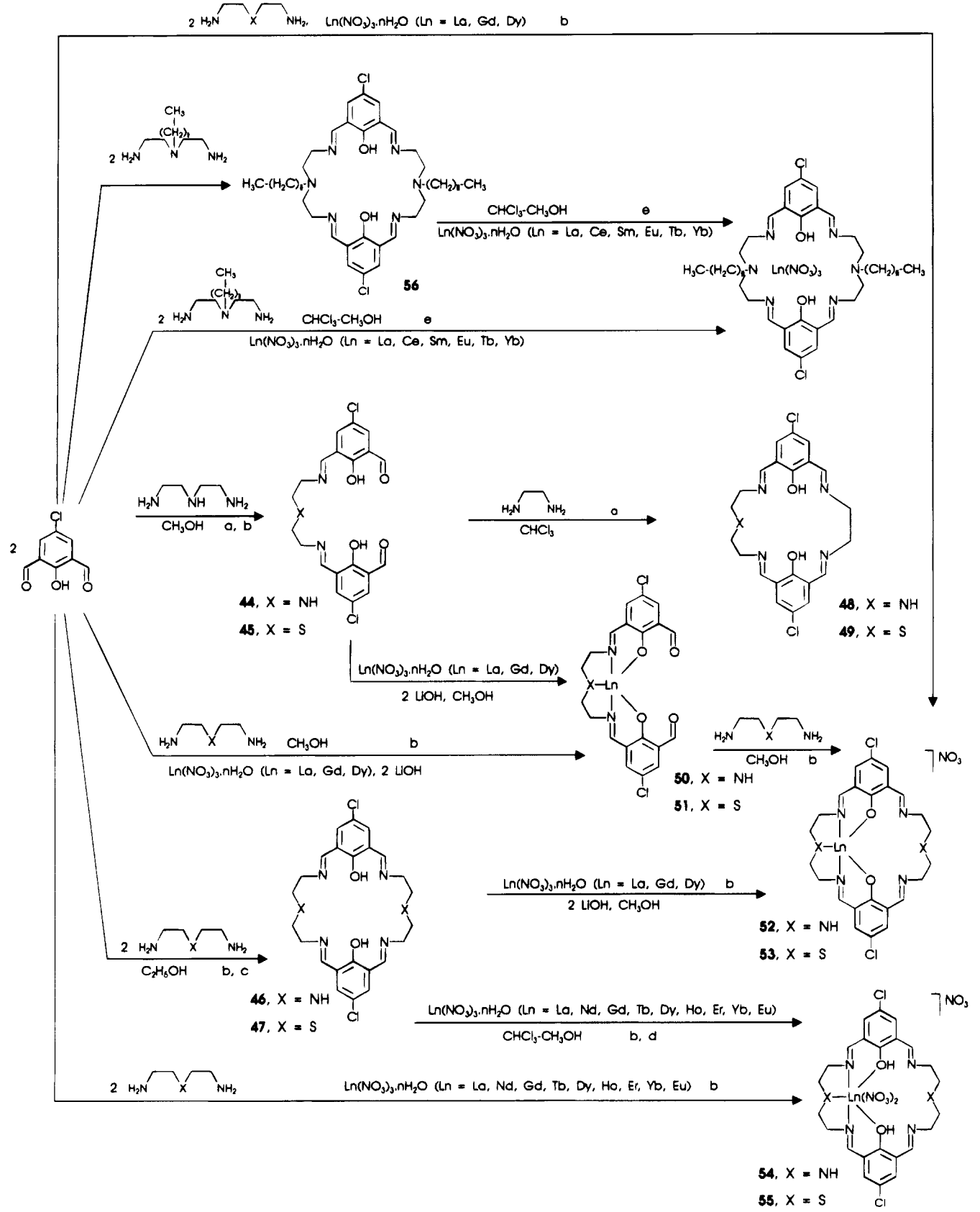

[a] Reference 174. [b] Reference 173. [c] Reference 176. [d] Reference 175. [e] Reference 177.

presented in Scheme 6.[173-177] The presence of a base (LiOH or NaOH) deprotonates the macrocycles **46** and **47** and promotes the formation of the complexes **52** and **53** containing one nitrate group, whereas in the absence of the base the ligands act as neutral ones and complexes containing two chelating nitrate ions have been obtained. In an attempt to obtain lanthanide complexes which are soluble in organic solvents for use in separation techniques Bullita *et al.*[177] synthesized the macrocycle **56** having a long

Scheme 7. Metal-Induced Ring Contraction[a]

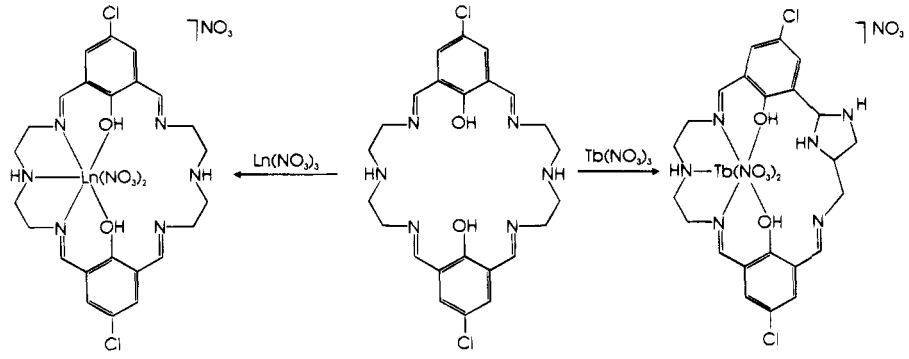

57

[a] On reaction of **46** with the smaller terbium ion ring contraction takes place through the formation of an imidazoline ring in the aliphatic chain of the free compartment. With the larger lanthanide ions the macrocycle coordinates intact.

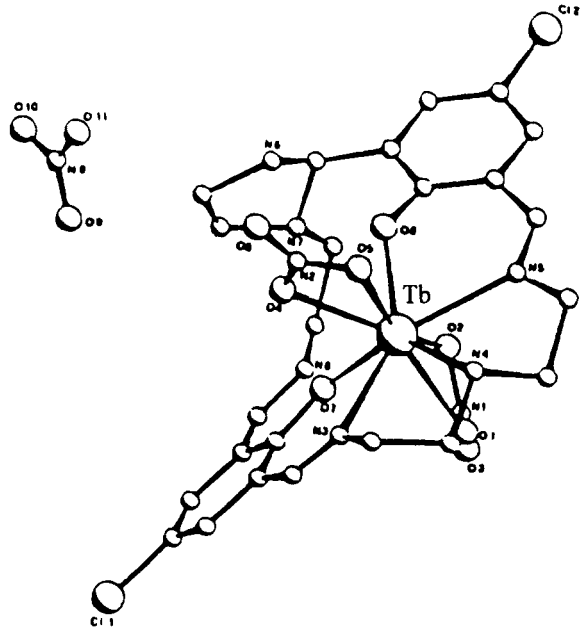

Figure 9. The crystal structure of $[Tb(\mathbf{46})(NO_3)_2]NO_3$. (Reprinted from ref 173. Copyright 1987 Elsevier Sequoia.)

aliphatic chain in the lateral unit by the condensation of 2,6-diformyl-4-chlorophenol with *N*-dodecyldiethylenetriamine. Reaction of **56** with lanthanide nitrates yielded the complexes $[Ln(\mathbf{56})(NO_3)_3]$ (Ln = La, Ce, Sm, Eu, Tb, and Yb). The metal-templated condensation also yielded the respective complexes.[177] This ligand has been used for the extraction of lanthanide ions from aqueous to organic solvents. The *in situ* generated macrocycle **46** on treatment with smaller lanthanide ions undergoes ring contraction: this allows a diminution of the macrocyclic cavity and reduction in ligand denticity. This makes the ligand more suitable for the smaller metal ions employed. The related macrocycle **47** does not undergo ring contraction and it coordinates intact as a pentadentate ligand with the lanthanide ions. The metal ion induced ring contraction is illustrated in Scheme 7. The X-ray crystal structure of the terbium complex **57**[173] of the contracted form of **46**, depicted in Figure 9, shows that the terbium ion is 9-coordinate, being bound to five donor atoms of the macrocycle and to four oxygen atoms of two bidentate

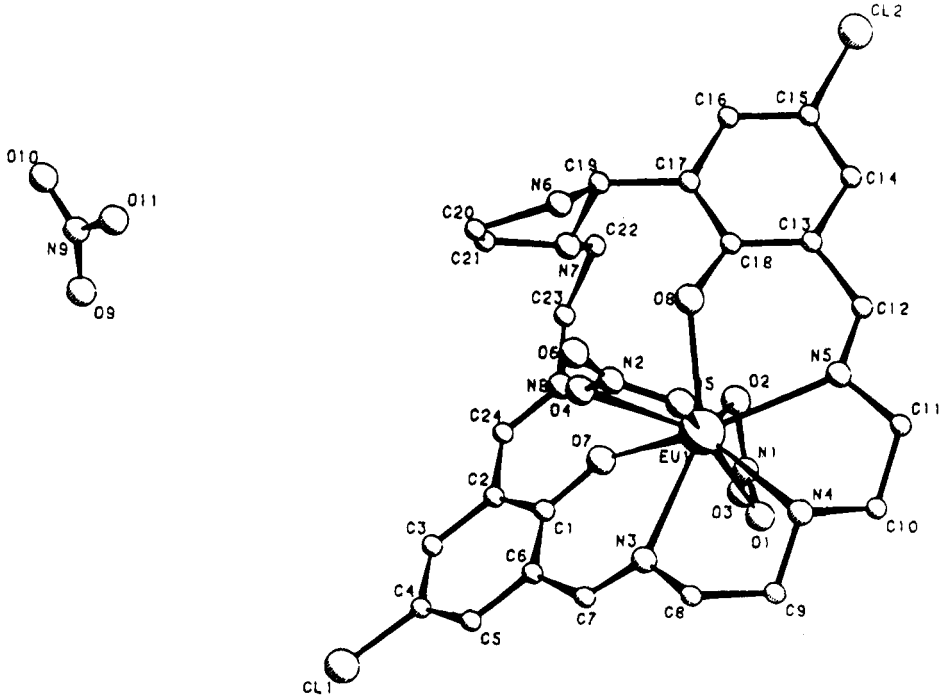

Figure 10. The molecular structure of $[Eu(\mathbf{46})(NO_3)_2]NO_3$. (Reprinted from ref 175. Copyright 1988 Elsevier Sequoia.)

nitrate ions. The metal ion sits in the lateral compartment of the macrocycle derived from the open chain amine and the imidazoline ring containing compartment is empty. In the corresponding europium(III) trinitrato complex no ring contraction is observed. It crystallizes in two isostructural forms, yellow and red.[175] The europium ion is 9-coordinate and is isomorphous with the terbium analog. The coordination polyhedron around both these metal ions can be best described as a distorted tricapped trigonal prism.[173,175] The X-ray crystal structure of [Eu(**46**)$(NO_3)_2$]NO_3 is presented in Figure 10.

E. "1 + 1" Macrocyclic Complexes of Lanthanides

Transition metal complexes of "1 + 1" Schiff base macrocycles containing pyridinyl head units have been well studied to explore their capability for generating high coordination geometries at the metal centers.[90,91] The condensation of 2,6-diacetylpyridine or 2,6-diformylpyridine with short-chain primary diamines such as 1,2-diaminoethane and 1,2-diaminobenzene in the presence of lanthanide templates has yielded mononuclear complexes of the "2 + 2" symmetric macrocycles (vide sections IV.A and IV.B). But condensation of 2,6-diacetylpyridine with the long chain diamine $H_2NCH_2CH_2(-OCH_2CH_2-)_3NH_2$ in the presence of early lanthanide nitrates resulted in the formation of mononuclear complexes of the "1 + 1" macrocycle **58** rather than complexes of the "2 + 2" ligand **59**.[178] The template procedure has

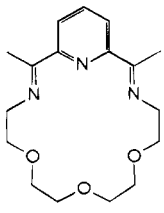

58

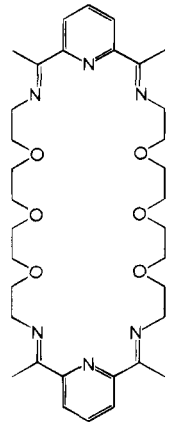

59

yielded several other lanthanide complexes of the "1 + 1" macrocycles **60**–**62** containing pyridinyl head unit and other long-chain diamines.[178] The following complexes have been reported for these ligands: [La(**58**)$(NO_3)_3$]·$n$$H_2O$, [La(**60**)$(NO_3)_3$]·$n$$H_2O$, [La(**61**)$(NO_3)_2$(OH)]·$n$$H_2O$, and [La(**62**)$(NO_3)_2$(OH)]·$n$$H_2O$. When $La(NCS)_3$ is used as template, mixed (NCS)(OH) complexes are obtained throughout: [La(**58**)$(NCS)_2$(OH)], [La(**60**)(NCS)$(OH)_2$], [La(**60**)$(NCS)_2$(OH)], and [La(**62**)(NCS)$(OH)_2$]. The presence of the macrocycle is confirmed by spectral studies. The X-ray crystal structure of [La(**58**)$(NO_3)_3$],[178] presented in Figure 11, shows that the lanthanum ion is 12-coordinate by three oxygen and three nitrogen donors of the macrocycle and three bidentate nitrate anions. The

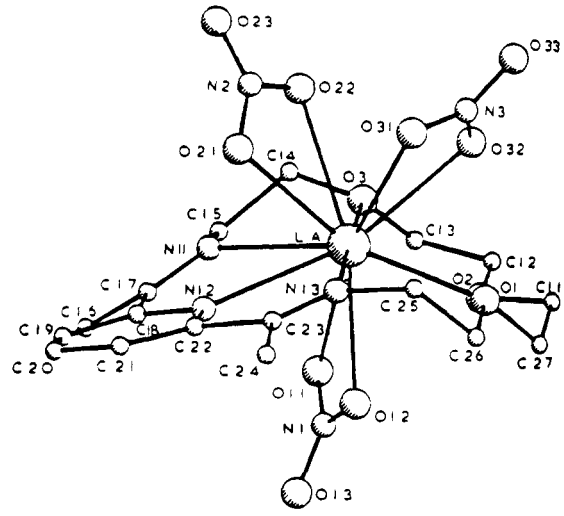

Figure 11. Crystal structure of [La(**58**)$(NO_3)_3$]. (Reprinted from ref 178. Copyright 1985 Elsevier Sequoia.)

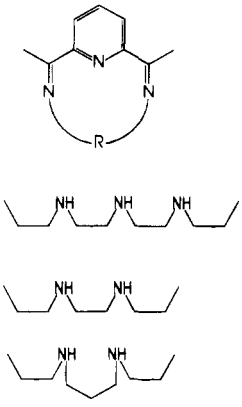

lanthanum ion is equally disposed toward the oxygen and nitrogen donors of **58** as has been observed in the alkaline earth metal complexes [Ca(**58**)]$(NCS)_2$ and [Sr(**58**)]$(NCS)_2$·H_2O.[107] This is in contrast to the preferential disposition of Pb^{2+} toward the nitrogen donors in [Pb(**58**)](NCS)(SCN).[108] In this case the affinity of the metal for the softer ligand environment is evidenced. There appears to be a consistency in the 12-coordination of lanthanum in its complexes of 18-membered hexadentate macrocycles.

F. Lanthanide Complexes of Amine Cage Macrocycles

In an attempt to prepare kinetically inert complexes of lanthanides in which the metal ion is completely encapsulated in a macrocyclic structure, Raymond and his co-workers[179,180] have prepared macrocyclic amine complexes of La, Yb,[179] Ce, Pr, Eu, and Y[180] in which the metal ion is surrounded by a covalently linked cage of amine-ligating groups. Amines have three covalent bonds in addition to their lone pair metal binding sites and hence their topology is ideal for the synthesis of complex polycyclic ligands. The synthesis of the cobalt cage complex, the "sepulchrate", by Creaser *et al.*[181] from $[Co(en)_3]Cl_3$, formaldehyde, and ammonia is a spectacular example of this principle and suggests the use of formaldehyde as a general amine coupling agent. A combination

of the approaches used to prepare the cobalt sepulchrate and the lanthanide Schiff base macrocycles has been used in the lanthanide template synthesis of amine cage complexes from tris(2-aminoethyl)-amine [$N(CH_2CH_2NH_2)_3$] and bis(dimethylamino)-methane [$CH_2(N(CH_3)_2)_2$], a formaldehyde derivative. Due to the hydrolytic instability of lanthanide amine complexes the use of formaldehyde was precluded, because the reaction produces water; but the formaldehyde equivalent, bis(dimethylamino)methane, reacts to give methylene bridges[182] without producing water. The advantages of using this particular formaldehyde derivative as a coupling reagent are 4-fold: (1) The reaction of this compound with an amine produces dimethylamine, which is volatile and eventually leaves the reaction mixture as a gas, thereby driving the reaction toward the desired product. (2) The reaction does not produce water, which reacts with lanthanide amine complex to form insoluble lanthanide hydroxides. (3) Schiff base reactions are in general reversible, which may allow this reaction to proceed to the thermodynamically stable product, thereby decreasing the side products. (4) The small bite angle of the NCH_2N moiety favors high coordination numbers around the metal.

The macrocyclic amine ligand 1,9-bis(2-aminoethyl)-1,4,6,9,12,14-hexaazacyclohexadecane (**63**) has been prepared by the metal template reaction of 2 equiv of tris(2-aminoethyl)amine with an excess of bis(dimethylamino)methane in the presence of 1 equiv of the lanthanide triflate in acetonitrile. The

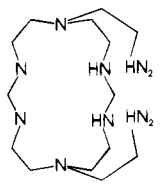

63

lanthanum complex is 10-coordinate with eight nitrogens from the macrocycle and two oxygens from the two triflate anions. The coordination geometry around lanthanum is not highly regular but can be viewed as a distorted bicapped square antiprism in which one triflate oxygen and four nitrogens from the macrocycle make up each of the two eclipsed square pyramids. The tertiary nitrogens form the caps of the square antiprism. If one ignores the orientation of the triflate anion, the complex has a noncrystallographic C_2 axis passing through the lanthanum ion and bisecting the O1–La–O4 angle. The X-ray crystal structure of [La(**63**)$(CF_3SO_3)_2$]CF_3SO_3·CH_3CN[179] is shown in Figure 12. The analogous ytterbium complex is 9-coordinate with one triflate anion and eight nitrogens from the macrocycle. The coordination geometry around ytterbium can be described as a monocapped square antiprism. The X-ray crystal structure of [Yb(**63**)(CF_3SO_3)]$(CF_3SO_3)_2$·CH_3CN[179] is shown in Figure 13. The ^{13}C and ^1H NMR spectra of [La(**63**)$(CF_3SO_3)_2$]CF_3SO_3·CH_3CN suggests that the complex has a C_2 axis in solution (on the NMR time scale) and is consistent with the approximate C_2 axis observed in the solid state.[179] Analysis of the NMR spectra of the complexes of

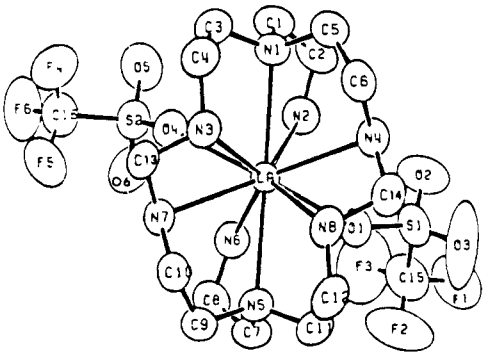

Figure 12. ORTEP drawing of [La(**63**)$(CF_3SO_3)_2$]CF_3SO_3·CH_3CN drawn with 50% probability ellipsoids and the crystallographic numbering scheme. (Reprinted from ref 179. Copyright 1985 American Chemical Society.)

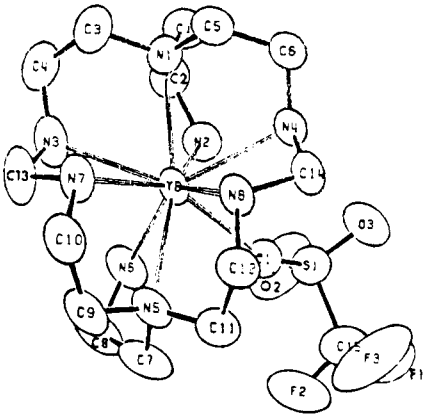

Figure 13. ORTEP drawing of [Yb(**63**)(CF_3SO_3)]$(CF_3SO_3)_2$·CH_3CN drawn with 50% probability ellipsoids and the crystallographic numbering scheme. (Reprinted from ref 179. Copyright 1985 American Chemical Society.)

other lanthanide cations indicates that a change in coordination number from 10-coordinate to 9-coordinate occurs between praseodymium and europium. The reduction potentials of the europium and ytterbium complexes of **63** are −0.68 and −1.37 V (vs SCE in propylene carbonate), respectively, suggesting that the dibridged macrocycle imparts a large stabilization of the 3+ oxidation state relative to the 2+ state.

In the lanthanum complex the macrocycle is somewhat "closed" in comparison to the "open" conformation of the macrocycle in the ytterbium complex. This difference is illustrated by the difference in the N1–Ln–N5 angles of 162.4 and 148.8° for the lanthanum and ytterbium complex, respectively. In the ytterbium species it appears that if the conformation of the macrocycle were to adapt the conformation seen in the lanthanum species, the formation of a third methylene bridge would be facilitated. Thus, the formation of a completely encapsulated lanthanide environment, analogous to the sepulchrate transition metal complexes, is envisaged.[182] Indeed, the fully encapsulated ytterbium(III) complex of the tribridged ligand 1,4,6,9,12,14,19,21-octaazabicyclo[7.7.7]tricosane (**64**) is synthesized by the template reaction of 2 equiv of $N(CH_2CH_2NH_2)_3$ with 10 equiv of bis(dimethylamino)methane in the presence of 1 equiv of ytterbium triflate. The most exciting feature of the fully encapsulated ytterbium complex, Yb(**64**)$(CF_3SO_3)_3$·CH_3CN, is its apparent stability toward hydrolysis. Acetonitrile solutions of [La(**63**)]$(CF_3$-

$SO_3)_2]CF_3SO_3 \cdot CH_3CN$ and $[Yb(\mathbf{63})(CF_3SO_3)](CF_3SO_3)_2 \cdot CH_3CN$ form precipitates of $Ln(OH)_3$ immediately upon addition of water, whereas Yb(**64**)$(CF_3SO_3)_3 \cdot CH_3CN$ is soluble in water without precipitation of $Yb(OH)_3$.

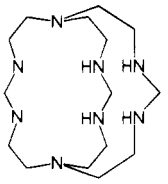

64

G. Lanthanide Complexes of Texaphyrins

The new class of pyrrole-based aromatic "expanded porphyrins", the so called "texaphyrins", developed by Sessler and his co-workers[130,183-186] are capable of binding a variety of metal cations and stabilizing a range of unusual coordination geometries. The texaphyrin **65** forms hydrolytically stable Gd^{3+} complex.[187] The complex is insoluble in water and its half-life for decomplexation and/or decomposition is found to be 37 days in 1:1 water–methanol. In an attempt to prepare a new type of analogous Gd^{3+} texaphyrin complex that would be soluble in water Sessler *et al.*[133] have prepared a full range of lanthanide(III) complexes of the texaphyrins **66**, **67**, and the lutetium(III) complex of **68**. The texaphyrins **67** and **68** have been designed by appending several hydroxy substituents around the periphery of the texaphyrin **24**. The texaphyrin **66** was synthesized

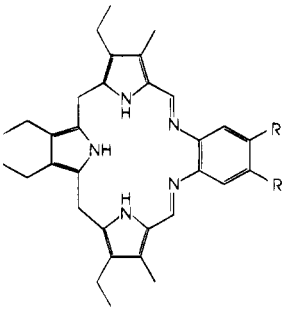

65, R = CH_3
66, R = OCH_3
68, R = $O(CH_2)_3OH$

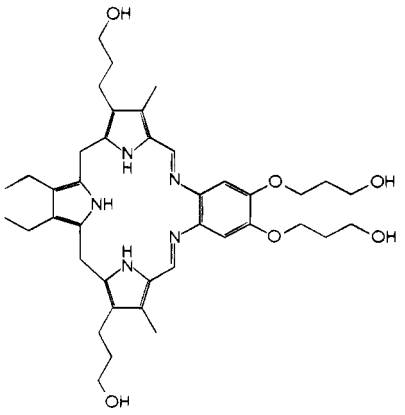

67

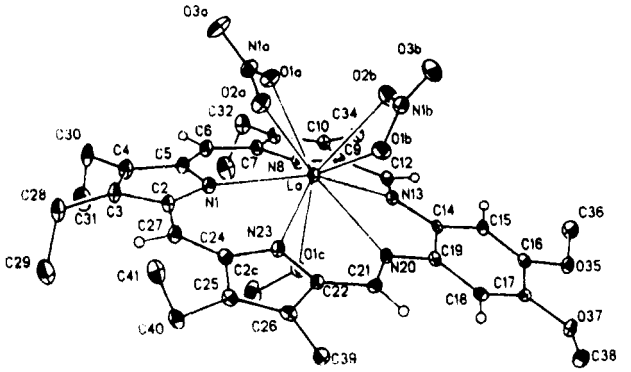

Figure 14. View of lanthanum(III) texaphyrin La(**66**) showing the representative labeling scheme for the macrocycle. Thermal ellipsoids are scaled to the 30% probability level. Most hydrogen atoms are omitted for clarity. (Reprinted from ref 133. Copyright 1993 American Chemical Society.)

by the acid-catalyzed condensation of 2,5-bis[(3-ethyl-5-formyl-4-methylpyrrol-2-yl)methyl]-3,4-diethylpyrrole with 1,2-diamino-4,5-dimethoxybenzene.[186] The reaction of the preformed texaphyrin **66** with $Ln(NO_3)_3 n H_2O$ and triethylamine in oxygenated methanol yielded complexes of the type Ln(**66**)$(NO_3)_2$ for Ln = La^{3+}, Eu^{3+}, Tm^{3+}, Yb^{3+}, and Lu^{3+}; Ln(**66**)$(NO_3)_2 \cdot H_2O$ for Ln = Ce^{3+}, Sm^{3+}, Ho^{3+}, Tb^{3+}, and Er^{3+}; Ln(**66**)$(NO_3)_2(CH_3OH)_{0.5}$ for Ln = Pr^{3+} and Nd^{3+}; and Gd(**66**)$(NO_3)_2(CH_3OH)_{1.5}(H_2O)_{0.5}$. Yields of the purified complexes vary from ~55 to 70% for the heavier lanthanides (Nd–Lu, except Pm) to ~30% for the lighter lanthanides (La–Pr). All these complexes are 1:1 metal–ligand complexes as characterized by mass spectrometry and microanalytical data. All the complexes exhibit the characteristic electronic absorptions, with the Soret-like and Q-type bands in the 473 and 728–743 nm regions, respectively.[133] The spectra of all these complexes are very similar to the spectrum of the Gd^{3+} complex of the texaphyrin **65**.[187] The ^1H NMR spectrum of the diamagnetic lanthanum(III) complex of **66** shows the general features[183,184,188] which are typical of other analogous aromatic expanded porphyrins[185] such as sapphyrin,[189-192] pentaphyrin,[193,194] rubyrin,[132] and hexaphyrin.[195]

The La^{3+} complex of **66** is 10-coordinate, being bound to all the five nitrogen donors of the texaphyrin, two bidentate nitrate ions, and to one molecule of methanol. The X-ray crystal structure of [La(**66**)$(NO_3)_2(CH_3OH)$] is shown in Figure 14. The Gd^{3+} complex of **66** has both 9- and 10-coordinate species present in the solid state. The 9-coordinate Gd^{3+} is ligated by the texaphyrin, one bidentate nitrate ion, and two methanol molecules. In the second structure the metal ion is 10-coordinate, being surrounded by two bidentate nitrate ions and one molecule of methanol. The crystal structure of Gd(**66**) is shown in Figure 15.

The texaphyrin **68** was synthesized by the acid-catalyzed condensation between 2,5-bis[(3-ethyl-5-formyl-4-methylpyrrol-2-yl)methyl]-3,4-diethylpyrrole and 1,2-diamino-4,5-bis[(3′-hydroxypropyl)oxy]-benzene in anhydrous toluene–methanol (5:1 v/v). The hydrochloride salt of the sp^3 texaphyrin **68** was obtained in 93% yield.[133] Oxidative metalation of the

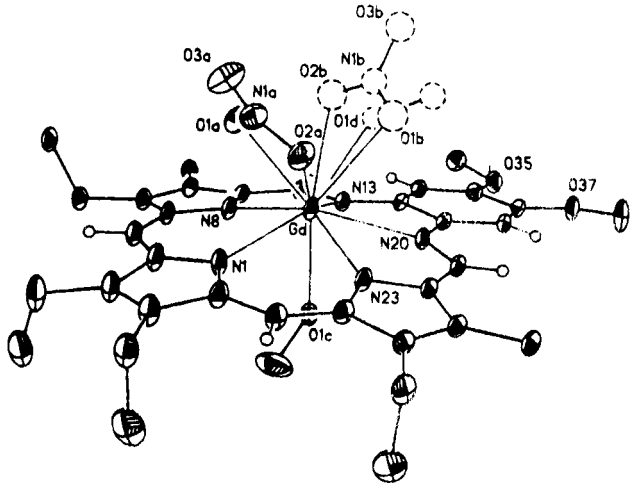

Figure 15. View of gadolinium(III) texaphyrin Gd(**66**) showing the 9- and 10-coordinate Gd(III) species present in the solid state. The disordered atoms are represented as dashed circles. Thermal ellipsoids are scaled to the 30% probability level and all heteroatoms are labeled. Most hydrogen atoms are omitted for clarity. (Reprinted from ref 133. Copyright 1993 American Chemical Society.)

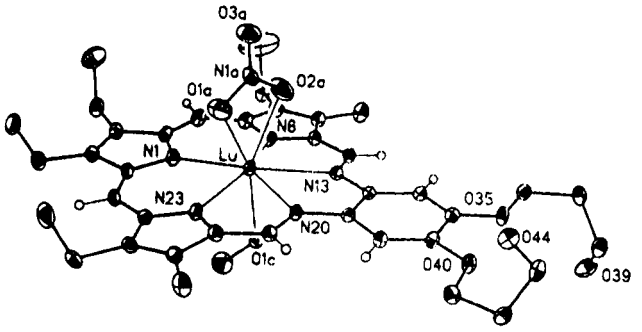

Figure 16. View of the lutetium(III) texaphyrin Lu(**68**) with the heteroatoms labeled. Thermal ellipsoids are scaled to the 30% probability level, and most hydrogen atoms are omitted for clarity. The methanol coordination is shown. (Reprinted from ref 133. Copyright 1993 American Chemical Society.)

hydrochloride salt of **68** carried out in the presence of $Lu(NO_3)_3 \cdot H_2O$ in refluxing methanol containing triethylamine yielded the complex $[Lu(\mathbf{68})(NO_3)(CH_3OH)]^+$ in ~37% yield. The X-ray crystal structure of $[Lu(\mathbf{68})(NO_3)(CH_3OH)]^+$, depicted in Figure 16, shows that the Lu^{3+} cation is 8-coordinate, being bound to the five nitrogen donors of the macrocycle, one bidentate nitrate ion, and one molecule of methanol. The lutetium complex of **68** is insoluble in water but soluble in organic solvents. In an attempt to prepare water-soluble lanthanide complexes, the tetrahydroxylated texaphyrin **67** was synthesized as its hydrochloride salt in quantitative yield by the Schiff base condensation of 2,5-bis[(5-formyl-3-(3-hydroxypropyl)-4-methylpyrrol-2-yl)methyl]-3,4-diethylpyrrole with 1,2-diamino-4,5-bis[(3′-hydroxypropyl)oxy]-benzene in refluxing toluene–methanol (5:1 v/v) mixture in the presence of HCl as the catalyst in an inert atmosphere. Oxidation and metalation of **67** in the presence of 1.5 equiv of $Ln(NO_3)_3 \cdot nH_2O$, 2–3 equiv of tetrabutylammonium nitrate, and triethylamine in refluxing methanol yielded complexes of the composition $[Ln(\mathbf{67})(NO_3)_2(H_2O)_2]$ (Ln = La and Tm); $[Ce(\mathbf{67})(NO_3)_2(H_2O)_3]$; $[Ln(\mathbf{67})(NO_3)_2(CH_3OH)(H_2O)]$ (Ln = Pr, Gd, Tb, and Ho); $[Ln(\mathbf{67})(NO_3)_2(CH_3OH)]$;

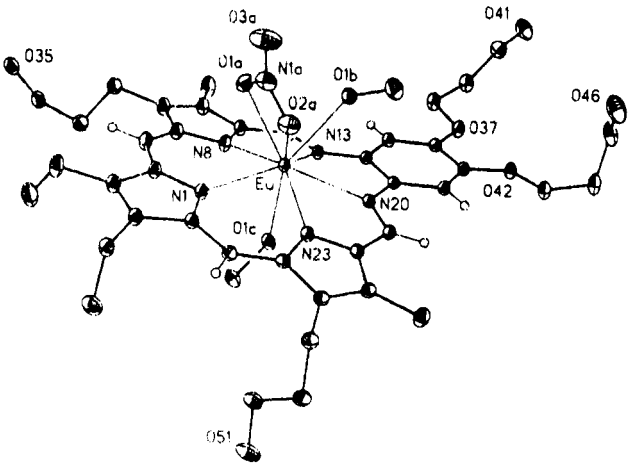

Figure 17. View of europium(III) texaphyrin Eu(**67**) with the heteroatoms labeled. The analogous Gd(III) complex Gd(**67**) is isomorphous and is not shown. Thermal ellipsoids are scaled to the 30% probability level. Most hydrogen atoms are omitted for clarity. (Reprinted from ref 133. Copyright 1993 American Chemical Society.)

(Ln = Nd, Sm, and Er); $[Ln(\mathbf{67})(NO_3)_2(H_2O)]$ (Ln = Eu and Dy); and $[Ln(\mathbf{67})]^{2+}$ (Ln = Yb and Lu). The yields of the complexes vary from 34 to 75%. All these complexes are water soluble to a greater or lesser degree. Thus the choice of appending four peripheral hydroxyl groups on the macrocycle solved the critical problem of solubility. However, the solubility in water was found to be remarkably reduced in the case of the heavier congeners. The single-crystal X-ray crystal structures of the Eu^{3+} and Gd^{3+} complexes of **67** show that they are isomorphous. In both cases the metal ions are 9-coordinate, being bound to the five nitrogen donors of the macrocycle, one bidentate nitrate ion, and two molecules of methanol. The crystal structure of Eu(**67**) is shown in Figure 17.

The X-ray crystal structure of the La^{3+}, Eu^{3+}, Gd^{3+}, and Lu^{3+} complexes of the texaphyrins reveal that the Ln^{3+} cations are coordinated to all five nitrogen donors of the macrocycle and that these complexes are bonafide 1:1 complexes in the solid state. The so-called sp^3 nonaromatic texaphyrins are quite stable. Oxidation and metalation of the texaphyrins in the presence of lanthanide(III) cations and triethylamine in oxygenated solvent yield lanthanide(III) complexes of aromatic texaphyrins **69** in which the texaphyrins lose one proton and act as monoanions. Thus the texaphyrins provide a unique opportunity to explore the lanthanide coordination

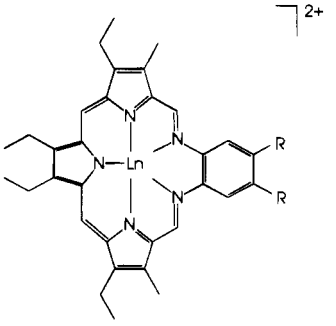

69

chemistry. The crystal structures of these complexes reflect both the decrease in coordination number and the intrinsic contraction in cation size observed as the lanthanide series is traversed.

V. Template Potential of Actinides

The template potential of actinides in generating Schiff base macrocycles was demonstrated by the formation of the so-called superphthalocyanine (**70**) by the reaction of 1,2-dicyanobenzene with dioxouranium(VI) dichloride in DMF.[196-200] The interme-

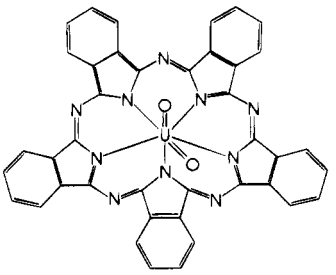

70

diate size of the cation (1.00 Å) and the preference for equatorially directed bonding suggest that dioxouranium(VI) ion could promote the formation of flat macrocyclic systems. In recent years considerable effort has been developed to preparing well-characterized complexes of UO_2^{2+} and a variety of ligands have been synthesized.[155,177,201-208] A few of these macrocycles are pyrrole-based ones: superphthalocyanine (**70**),[196-200] pentaphyrin (**71**),[193] and sapphyrin (**72**).[209] In these ligands the uranyl ion is chelated

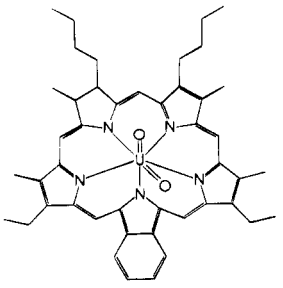

71

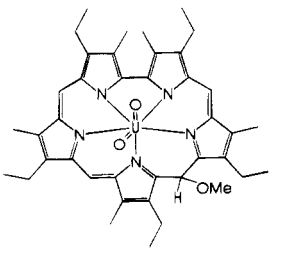

72

in a saddle-shaped pentagonal planar arrangement and in the case of sapphyrin, uranyl chelation induces a chemical modification of the ligand framework. In an attempt to synthesize pyrrole-based porphyrin-like systems incorporating hexagonal planar ligand fields Sessler *et al.*[131] have reported the hexaazamacrocycle **26**. The metal template condensation of 3,4-diethylpyrrole-2,5-dicarboxaldehyde with 4,5-diamino-1,2-dimethoxybenzene in the presence of uranyl nitrate yielded the complex **73** in 75% yield. Alternatively, the metal-free ligand, prepared by an acid-catalyzed condensation, readily reacts with UO_2^{2+} to give the same complex. In the latter reaction use of *N,N,N',N'*-tetramethyl-1,8-naphthalenediamine (proton sponge) prevents the formation of the protonated nitrate salt of **26**. Single-crystal X-ray crystal structure of **73**, depicted in Figure 18, shows that the uranyl cation is coordinated to all six nitrogen donors

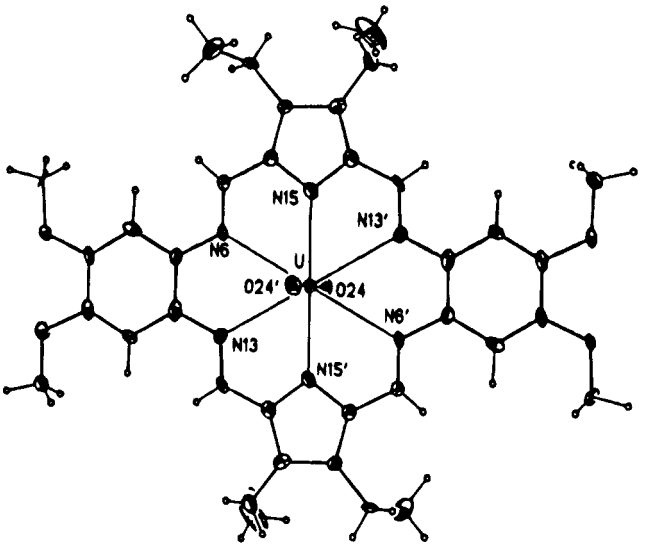

Figure 18. View of $[UO_2(\mathbf{26})]$ showing the hexagonal bipyramidal coordination around uranium. (Reprinted from ref 131. Copyright 1992 American Chemical Society.)

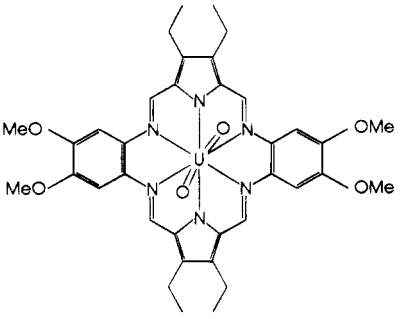

73

in a planar fashion. Although not formally aromatic the complex is remarkably planar. The structure of **73** is thus very different from the saddle-shaped conformations seen in the uranyl chelates of the formally aromatic "expanded porphyrin" ligands **70** and **71**. The condensation of pyridinyl head units with 1,2-diaminoethane proceeds smoothly with UO_2^{2+} to yield the complexes $[UO_2(\mathbf{27})]X_2$ and $[UO_2(\mathbf{30})]X_2$[207] (X = ClO_4^-, NO_3^-, or I^-). Spectral evidence suggests that all the six nitrogen donors are coordinated to uranium and that the metal ion has a D_{6h} site symmetry.

The reaction of 2,6-diformyl-4-chlorophenol with diethylenetriamine in the presence of uranyl nitrate hexahydrate in a 2:1:1 mole ratio in absolute ethanol yielded the mononuclear macroacyclic complex **74** which could be cyclized on further reaction with the appropriate diamine to give the mononuclear macrocyclic complexes **75**–**78**.[210] These cyclic complexes act as ligands toward transition metal ions and give heterodinuclear complexes of the type **79** in which the uranyl ion and a transition metal ion are held in close proximity within the dinucleating macrocyclic periphery.[211] Extension of this synthetic strategy has afforded the symmetric and asymmetric macrocycles and their mononuclear UO_2^{2+} complexes **80**–**82**.[174,211,212] The complex **81** has also been prepared by the reaction of the preformed macrocycle **47** with uranyl acetate dihydrate in the presence of LiOH. The X-ray crystal structure of $[UO_2(\mathbf{47})]$ (**81**),[212] shown in Figure 19, confirms that the UO_2^{2+} is

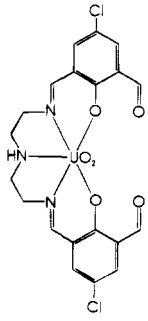

74

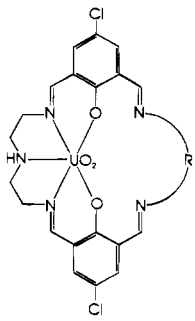

R

75, CH_2CH_2

76, $CH_2CH_2CH_2$

77, $CH_2CH(CH_3)$

78, C_6H_4

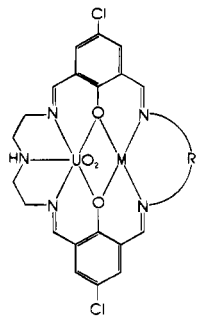

R

79, CH_2CH_2
$CH_2CH_2CH_2$
$CH_2CH(CH_3)$

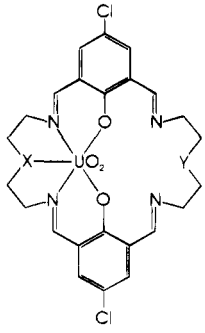

80, X = Y = NH

81, X = Y = S

82, X = NH, Y = S

equatorially bonded to the N_2O_2S donors of one of the two identical compartments. The ligand has a second compartment which, at least in principle, could act as a second coordination center. Nevertheless, the peculiar conformation of the ligand indicates that it will be difficult for a second metal ion to be coordinated. The physicochemical properties of the UO_2^{2+} ion do not favor the formation of homodinuclear cyclic complexes. Attempts to prepare the homodinuclear uranyl(VI) complexes were not successful. The second UO_2^{2+} ion seems to be too large to enter into the second chamber when the first one is occupied by UO_2^{2+} ion. On the contrary, this compartment can serve as a coordinating site for a second smaller metal ion such as Ni^{2+} and Cu^{+}, and the heterodinuclear complexes $[UO_2(\mathbf{46})Cu](ClO_4)\cdot 2C_2H_5OH$,[213] and $[UO_2(\mathbf{46})Ni](ClO_4)_2$[154] have been obtained. The presence of $Cu^{I}U^{VI}$ species is observed by cyclic voltammetry.

By the reaction of 2,6-diformyl-4-chlorophenol and polyamines of the type $NH_2(CH_2)_2X(CH_2)_2NH_2$ (X = NH or S) in the presence of uranyl(VI) acetate the complexes reported in Scheme 8 have been obtained.[174,177,210-213] In the symmetric macrocyclic mononuclear complexes the metal ion occupies one of the two identical compartments: obviously the change from one coordination site to the other does not involve any variation in the physicochemical properties of the complex. The difference in the coordination ability of the two compartments in the asymmetric macrocyclic ligands is not always too high as to make one chamber selective for a particular metal ion. Consequently, in the related mononuclear complexes it becomes easy for the central metal ion to change the coordination compartment depending on the physicochemical properties of the donor site and of the metal ion. The two cyclic uranyl complexes obtained by the reaction of **83** with diethylenetriamine and by the reaction of **74** with 1,5-diamino-3-thiapentane were found to be the same

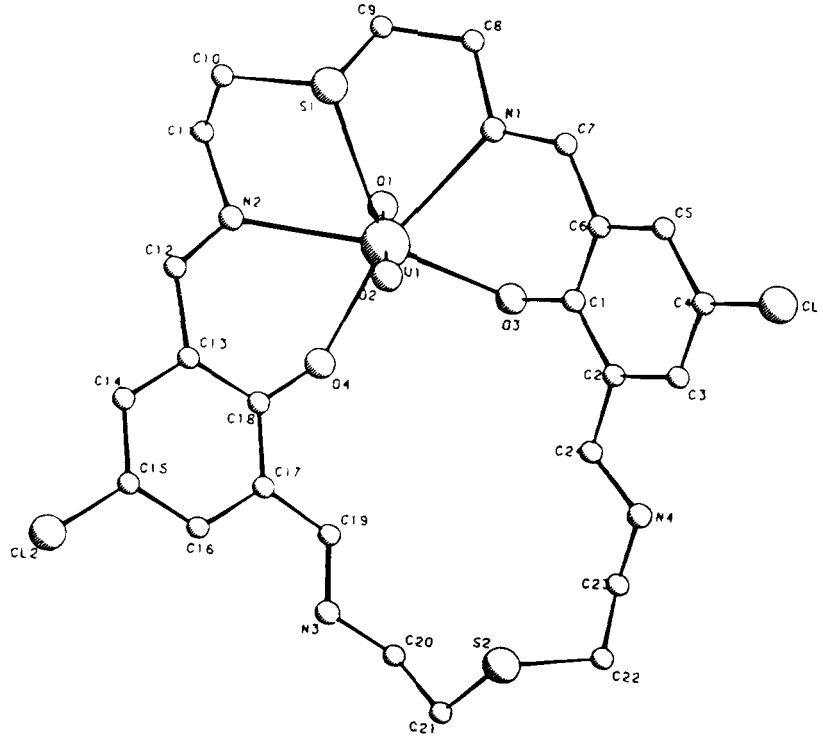

Figure 19. Crystal structure of $[UO_2(\mathbf{47})]$ (**81**) with atom numbering. H atoms are omitted for the sake of clarity. (Reprinted from ref 212. Copyright 1986 Elsevier Sequoia.)

Scheme 8. Synthesis of Uranyl Complexes of Macroacyclic Ligands and Symmetric and Asymmetric Macrocycles Derived from 2,6-Diformyl-4-chlorophenol with Various Polyamines

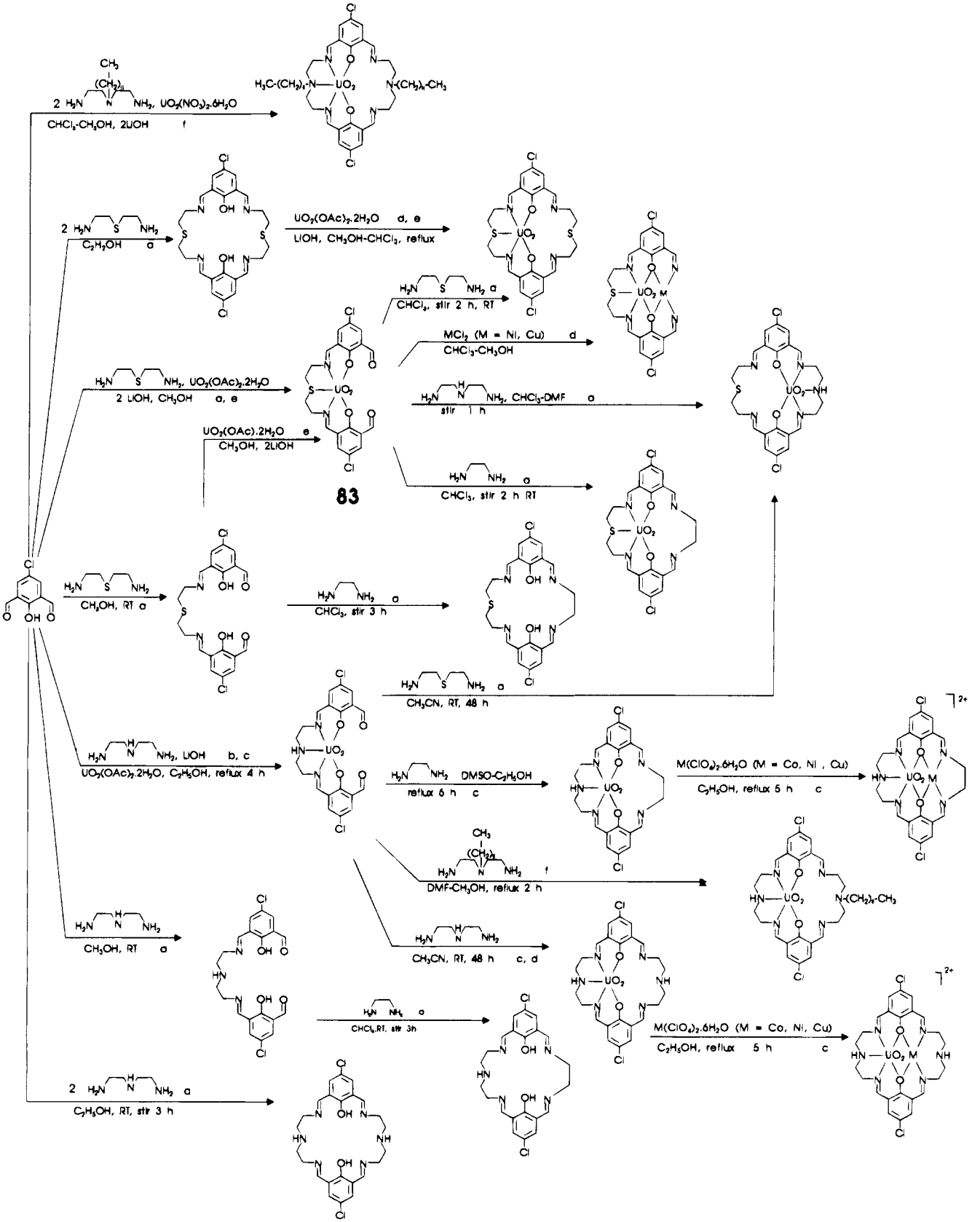

[a] Reference 174. [b] Reference 210. [c] Reference 211. [d] Reference 213. [e] Reference 212. [f] Reference 177.

and the UO_2^{2+} ion occupies the harder N_3O_2 site instead of the softer N_2O_2S compartment in both the cases. Thus uranyl ion has undergone a coordination site change from the N_2O_2S compartment of **83** to the N_3O_2 compartment during the cyclization process.[213]

The cocomplexation of a neutral guest molecule by a host molecule both by hydrogen bonding and coordination with a metal ion is frequently observed

in metalloenzymes such as urease where urea is believed to bind at the active site of the enzyme both through a coordination bond to a nickel ion and by means of hydrogen bonds with the carboxylate groups of the polypeptide chain.[214] Mimicry of such an enzyme binding site has been accomplished by synthesizing uranyl complexes of the larger polyazaoxa macrocycles **84**–**88**.[206,215] The macrocycles **84** and **85**

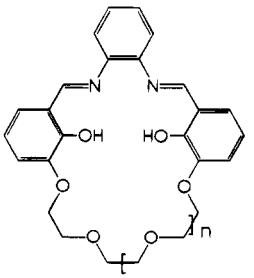

84, n = 1

85, n = 2

86, n = 3

87, n = 4

88, n = 5

were prepared by the reaction of the phenolate anion, obtained by the reaction of 2,3-dihydroxybenzaldehyde with NaH in DMSO, with tri- or tetraethylene glycol, respectively, followed by the condensation of the resulting dialdehyde with 1,2-diaminobenzene in the presence of $Ba(ClO_4)_2$ or $Ba(CF_3SO_3)_2$. The larger analogs **86**–**88** were synthesized by the reaction of 2-(allyloxy)-3-hydroxybenzaldehyde, obtained by the selective protection of 2,3-dihydroxybenzaldehyde by reacting it with 1 equiv of NaH followed by the reaction of the resulting phenolate anion with 3-bromo-1-propene, with penta-, hexa-, or heptaethylene glycol ditosylate, respectively, followed by removal of the protecting allyl groups by reaction with 5% Pd/C and a trace of acid in CH_3OH/H_2O under reflux, and condensation with 1,2-diaminobenzene in the presence of $Ba(ClO_4)_2$ or $Ba(CF_3SO_3)_2$ template.[215] The barium ion which is coordinated in the polyether cavity is removed by reaction of the complexes with guanidium sulfate in a two-phase system of water and chloroform. The free ligands on treatment with $Ni(CH_3COO)_2$, $Cu(CH_3COO)_2$, or $Zn(CH_3COO)_2$ in alcohol yield the corresponding metal complexes in which the metal ion is coordinated within the Schiff base moiety. Reaction of the barium complexes of **84**–**88** with uranyl acetate in refluxing methanol yielded the corresponding UO_2^{2+} complexes. The uranyl ion occupies the Schiff base compartment. The uranyl complex of **88** on treatment with 1 equiv of urea in CH_3OH yielded the 1:1 complex **89**. X-ray crystal structure of **89** shows that the uranyl ion is held in the Schiff base compartment, and the urea molecule in the polyether compartment. The urea is coordinated with the cation via the carbonyl oxygen and is hydrogen bonded to five oxygen donors of the polyether chain and one phenolic oxygen. The uranyl complexes of similar macrocycles act as macrocyclic carriers for the transport of neutral molecules through supported liquid membranes.[202] The macrocyclic uranyl complexes **90**–**93**, obtained by replacing the

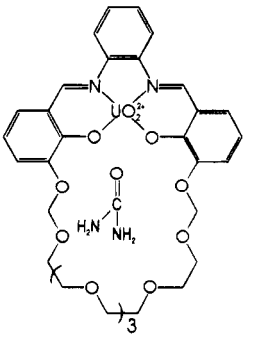

89

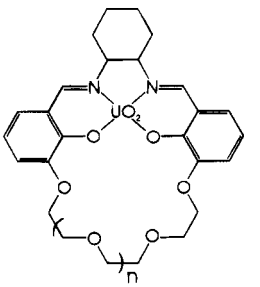

90, n = 2

91, n = 3

92, n = 4

93, n = 5

benzene ring of the salophene part of the UO_2^{2+} complexes of **85**–**88** by the 1,2-cyclohexyl moiety, are more soluble than the corresponding salophene metallomacrocycles. These compounds have been used as carriers in a supported liquid membrane composed of a porous polymeric support (Accurel) impregnated with *o*-nitrophenyl *n*-octyl ether to investigate the relation between the ring size of the metallomacrocycle and the rate of the urea transport. To improve the lipophilicity and thereby to improve the partition coefficient of these receptors the crown ether salophene derivative has been modified by the binaphthyl function to obtain **94**.[202]

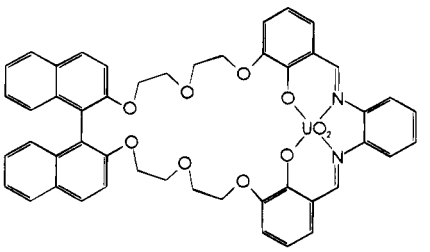

94

VI. Dinuclear Macrocyclic Complexes of Lanthanides and Actinides

The synthesis of homodinuclear complexes of Schiff base macrocycles was first accomplished by the condensation of 2,6-diacetylpyridine with 3,6-dioxaoctane-1,8-diamine in the presence of Pb^{2+} template.[110,124] The resulting macrocycle **8** binds with two Pb^{2+} ions to give the dinuclear complex $[Pb_2(\mathbf{8})](NCS)_4$. The first example of the homodinuclear macrocyclic complexes of lanthanides have been

synthesized by the condensation of 2,6-diformyl-4-methylphenol with triethylenetetramine in the presence of lanthanide nitrates or perchlorates (Ln = La–Gd): complexes of the general formula $[Ln_2(\mathbf{95})(NO_3)_4]\cdot nH_2O$ (n = 0 or 2) and $[Ln_2(\mathbf{95})(NO_3)_x(OH)_{4-x}]$ (x = 2 or 3) have been obtained.[216] In the

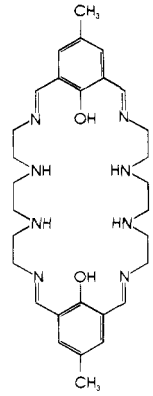

95

latter complexes the number of hydroxyl ions bonded to the metal ions depends on the reaction conditions. The hydroxo complexes were converted into the corresponding nitrato complexes when the complex was allowed to stand in methanol containing triethylenetetramine. The conversion was found to be quantitative when the complex is refluxed in methanol containing the free amine and a 3-fold excess of $Ln(NO_3)_3$. When perchlorates are used as the templates, complexes of the type $[Ln_2(\mathbf{95})(ClO_4)_x(OH)_{4-x}]$ were obtained. The coordination of the perchlorate ions is inferred from the splitting of the υ_3 and υ_4 band of ClO_4^- at ~1100 and 630 cm^{-1}, respectively. The dinuclear nature of these complexes was established by positive ion mode fast atom bombardment mass spectra. The prominent feature of the spectra is the occurrence of oxo clusters such as LnO^+, $Ln_2O_2^+$, $Ln_2O_3^+$, $Ln_3O_4^+$, $Ln_4O_6^+$, and $Ln_5O_7^+$. In the case of Ln = La and Y, which are monoisotropic, higher oxocluster peak intensities were found at m/z corresponding to $Ln_6O_8^+$, $Ln_7O_{10}^+$, and $Ln_9O_{13}^+$. In those cases where the lanthanide cations are polyisotropic the calculated and observed isotopic patterns were identical.[216]

The organizational role of the lanthanide cations in the assembly of the binucleating macrocycle was evidenced by the recovery of intractable materials when the condensation of 2,6-diformyl-4-methylphenol and triethylenetetramine is carried out in the presence of Ca^{2+}, Sr^{2+}, Ba^{2+}, and Pb^{2+} as putative templates. Direct condensation in the absence of the lanthanide cations led to the formation of intractable oils. It is also interesting to note that even under a 2-fold excess of dialdehyde or 10-fold excess of triethylenetetramine the exclusive products are the complexes of the "2 + 2" symmetric macrocycle **95**.

Condensation of 2,6-diformyl-4-methylphenol with 3,6-dioxaoctane-1,8-diamine in the presence of lanthanide(III) nitrate yielded homodinuclear complexes $[Ln_2(\mathbf{96})(NO_3)_4]\cdot H_2O$ (Ln = La^{3+}–Tb^{3+}) in 70–100% yield.[216] The yields of the complexes decrease with decreasing size of the cations. The X-ray crystal

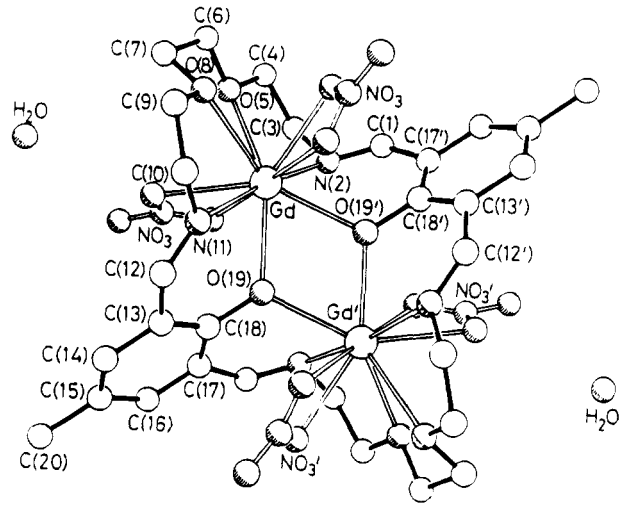

Figure 20. The molecular structure of $[Gd_2(\mathbf{96})(NO_3)_4]\cdot H_2O$. (Reprinted from ref 217. Copyright 1989 Royal Society of Chemistry.)

structure of the dinuclear gadolinium(III) complex $[Gd_2(\mathbf{96})(NO_3)_4]\cdot H_2O$[217] indicates that both gadolinium ions are coordinated to the macrocycle and are bridged by the two phenolate oxygen atoms. Each gadolinium ion is 10-coordinate, being bound to two oxygen and two nitrogen donors of the macrocycle, two phenolate oxygens, and four nitrate oxygens. The coordination geometry around the metal ion is a distorted bicapped dodecahedron. The X-ray crystal structure of $[Gd_2(\mathbf{96})(NO_3)_4]\cdot H_2O$ is shown in Figure 20. Molecular recognition events in the formation of heterolanthanide(III) cation pairs have been studied by synthesizing heterodinuclear complexes $[(Ln_{1-x}Eu_x)_2(\mathbf{96})(NO_3)_4]\cdot H_2O$ (Ln = La, Ce, Pr, Nd, Sm, Gd, Tb, or Dy) and $[(Ln_{1-x}Tb_x)_2(\mathbf{96})(NO_3)_4]\cdot H_2O$ (Ln = Ce, Pr, Nd, Sm, Eu, Gd, or Dy). Molecular recognition processes which govern the template condensation of 2,6-diformyl-4-methylphenol with 3,6-dioxaoctane-1,8-diamine to yield **96** and its dilanthanide complexes are more selective toward the larger Ln^{3+} cations. Reaction mixtures containing equimolar amounts of Eu^{3+} and Ln^{3+} (Ln = La–Dy, except Pm) deposited crystalline $[(Ln_{1-x}Eu_x)_2(\mathbf{96})(NO_3)_4]\cdot H_2O$ complexes which exhibit variable compositions depending on the nature of Ln^{3+}. The measured europium levels are generally lower when the competing heterocation is the larger lanthanide (Ln = La–Gd), but with smaller lanthanide (Ln = Tb^{3+} and Dy^{3+}) preferential enrichment of Eu^{3+} is observed. In the $[(Ln_{1-x}Tb_x)_2(\mathbf{96})(NO_3)_4]\cdot H_2O$ complexes, preferential incorporation of the larger lanthanide cations is encountered. There is a systematic increase in the concentration of Tb^{3+} on going from Ce^{3+} to Gd^{3+}, but with smaller lanthanides (Ln = Gd–Dy) the heterodilanthanide crystalline products become increasingly richer in Tb^{3+}. The luminescence decay dynamics of $[(Sm_{1-x}Eu_x)_2(\mathbf{96})(NO_3)_4]\cdot H_2O$ and $[(Pr_{1-x}Tb_x)_2(\mathbf{96})(NO_3)_4]\cdot H_2O$ indicates that the formation of the dinuclear lanthanide complexes of **96** is governed by molecular recognition process in which the homo- or heterolanthanide cations are recognized and paired on the basis of their cooperative effects.[79]

Condensation of 2,6-diformyl-4-chlorophenol with 3,6-dioxaoctane-1,8-diamine in a 1:1 mole ratio af-

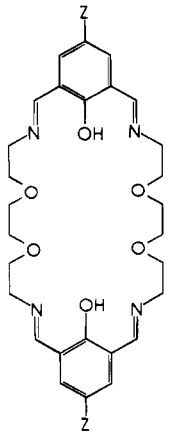

96, Z = CH_3

97, Z = Cl

forded the macrocycle **97**.[218] The homo- and heterodinuclear lanthanide(III) complexes have been prepared in 80% yield from an *in situ* procedure by treating the macrocycle formed in solution with LiOH followed by the addition of the appropriate $Ln(NO_3)_3 \cdot nH_2O$. When the condensation of the organic precursors is carried out in the presence of the lanthanide template the yield is very low (15–20%). Homodinuclear lanthanide(III) complexes of the composition $[Ln_2(\mathbf{97})(NO_3)_4] \cdot nH_2O$ (Ln = La, Pr, Sm, Eu, Gd, Tb, or Dy; n = 1 for La, Sm, Eu, and Dy; and n = 2 for Pr, Gd, and Tb) and heterodinuclear complexes of the general formula $[Ln_xLn'_{2-x}(\mathbf{97})(NO_3)_4] \cdot nH_2O$ (Ln, Ln' = La, Sm; La, Gd; La, Dy; La, Eu; Dy, Gd; Dy, Eu; Gd, Eu; Gd, Tb; Eu, Tb; or La, Tb; and n = 1 for La, Dy; Dy, Eu; and Gd, Tb; and n = 2 for La, Sm; La, Gd; La, Eu; Dy, Gd; Gd, Eu; Eu, Tb; and La, Tb; x = 1 or 2) were synthesized. Electron microscopy and X-ray fluorescence analysis show that the distribution of the two metal ions in the various crystals is homogeneous. The homogeneity of the complexes results from the equal occupancy of the two compartments of the ligand. The two compartments of the ligand are not selective enough totally to prevent metal exchange between the two coordination sites; positional heterodinuclear complexes and scrambling can occur. For instance, crystals of $[LaSm(\mathbf{97})(NO_3)_4] \cdot 2H_2O$, grown from the mother liquor, have the correct Ln:Cl ratio but the samarium content is about four times that of lanthanum, suggesting a stoichiometry of the type $[La_{0.4}Sm_{1.6}(\mathbf{97})(NO_3)_4]$. A similar behavior was found for the crystals containing lanthanum and dysprosium, the dysprosium content being about a tenth of the lanthanum content. This indicates the selectivity of the ligand compartments with respect to the ionic radius of the metal. Integration of back-scattered X-rays gave the Ln:Cl ratios: in homodinuclear complexes the ratio is found to be 1:1 while in the heterodinuclear complexes the Ln:Ln':Cl ratio is found to be 1:1:2. Attempts to prepare mononuclear complexes of **97** failed. Laser-excited luminescence spectra confirm the presence of heterodinuclear complexes. Dinuclear complexes of **97** are versatile to study the absorption of energy by the ligand and the energy transfer from the ligand to the lanthanide(III) ions inside the macrocycle and the energy transfer from one lanthanide ion to the other within the macrocyclic framework. Such an energy transfer has been well defined for the complex $[EuTb(\mathbf{97})(NO_3)_4] \cdot 2H_2O$.[218] The intermetallic distance was evaluated by quantifying the yield of the $Tb^{3+} \rightarrow Eu^{3+}$ energy transfer and the metal–metal distance computed is consistent with the interionic distance measured from the space-filling molecular models.

Ziessel *et al.*[219] have synthesized dinuclear complexes of the branched hexaazacyclooctadecane ligand **98** containing six 2,2′-bipyridine pendant units. Homodinuclear complexes of the type $[Ln_2(\mathbf{98})]Cl_6 \cdot nH_2O$ (Ln = Gd, Tb, and Eu; n = 6 for Gd and n = 8 for Tb and Eu) have been obtained by the reaction of the preformed macrocycle with the respective $LnCl_3 \cdot 6H_2O$ in a 1:1 mole ratio in 20–28% yield. Each molecule of **98** coordinates with two metal ions. The space-filling model shows that the two metal ions are lodged on opposite sides of the plane defined by the macrocyclic ring, each one being surrounded by three bipyridine units.

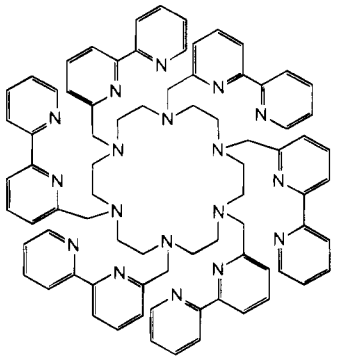

98

The importance of favorable ligand conformation required for the metal ion to fit into the macrocyclic cavity is evidenced from the X-ray crystal structure of the dinuclear gadolinium complex $[Gd_2(\mathbf{99})_2(H_2O)_2] \cdot 14H_2O$ in which the metal ions are located between the two ligand molecules[220] as shown in Figure 21. The related macrocycle **100** containing an additional $-CH_2-$ group onto the macrocyclic ring increases the flexibility of the ligand and results in the formation of the mononuclear Gd^{3+} complex $[Gd(\mathbf{100})(H_2O)] \cdot 3H_2O$. The ligands **99** and **100** are synthesized by the condensation of diethylenetriaminepentaacetic dianhydride with 1,2-diaminoeth-

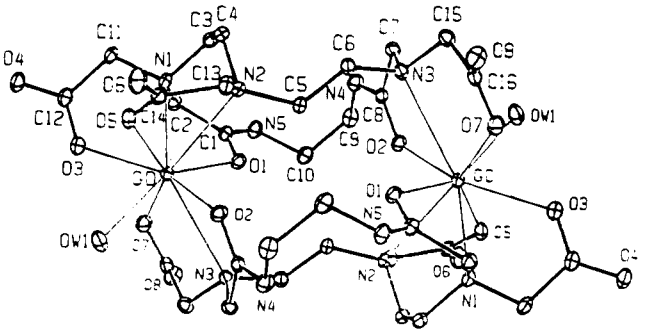

Figure 21. Molecular structure of $[Gd_2(\mathbf{99})_2(H_2O)_2] \cdot 14H_2O$. Atoms are shown at the 20% probability level. (Reprinted from ref 220. Copyright 1993 Elsevier Sequoia.)

ane or 1,3-diaminopropane, respectively.[220,221] The formation of the dinuclear Gd^{3+} complex with **99** and mononuclear Gd^{3+} complex with **100** demonstrates the dependence of the structural properties of macrocyclic complexes on the geometrical properties of the ligand.

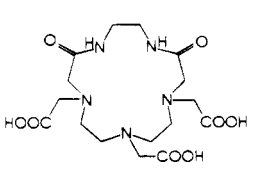

99

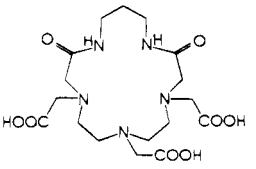

100

VII. Trinuclear Macrocyclic Complexes of Lanthanides

The Schiff base condensation of 2,6-diacetylpyridine with 1,3-diamino-2-hydroxypropane in the presence of a metal template forms macrocyclic complex. The nature and the ring size of the resultant macrocycle appears to be determined by the metal ion used as the template as illustrated in Scheme 5. When $Ba(SCN)_2$ is used as the template the "2 + 2" macrocycle incorporating one barium predominates; the OH groups on the macrocycle remain intact and the two thiocyanato ligands balance the charge of the metal ion. When $Pb(ClO_4)_2$ is used as the metal template, a complete rearrangement of the ligand occurs to form the ring-contracted macrocycle **14** containing oxazolidine rings. Transmetalation of the barium complex with $Cu(ClO_4)_2$ produces the dinuclear copper complex in which a proton is lost from one of the OH groups of the ligand and the alkoxide bridges both copper ions. When $Mn(ClO_4)_2$ is used in the transmetalation reaction with the barium complex the "4 + 4" macrocycle with four Mn^{2+} ions is formed in low yield.[222]

The versatility of the ligands obtained by the condensation of 2,6-diacetylpyridine with 1,3-diamino-2-hydroxypropane is further demonstrated by Fenton *et al.*[223] by carrying out the Schiff base condensation in the presence of a lanthanide template to obtain the first known trinuclear lanthanide complex of the "3 + 3" macrocycle **101**. The trinuclear complex $La_3(\mathbf{101})(NO_3)_6 \cdot 3CH_3OH$ is obtained as yellow crystals from methanol at 50 °C. ^1H NMR decoupling

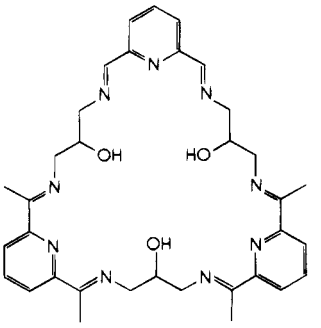

101

and NOE difference spectra confirm the presence of

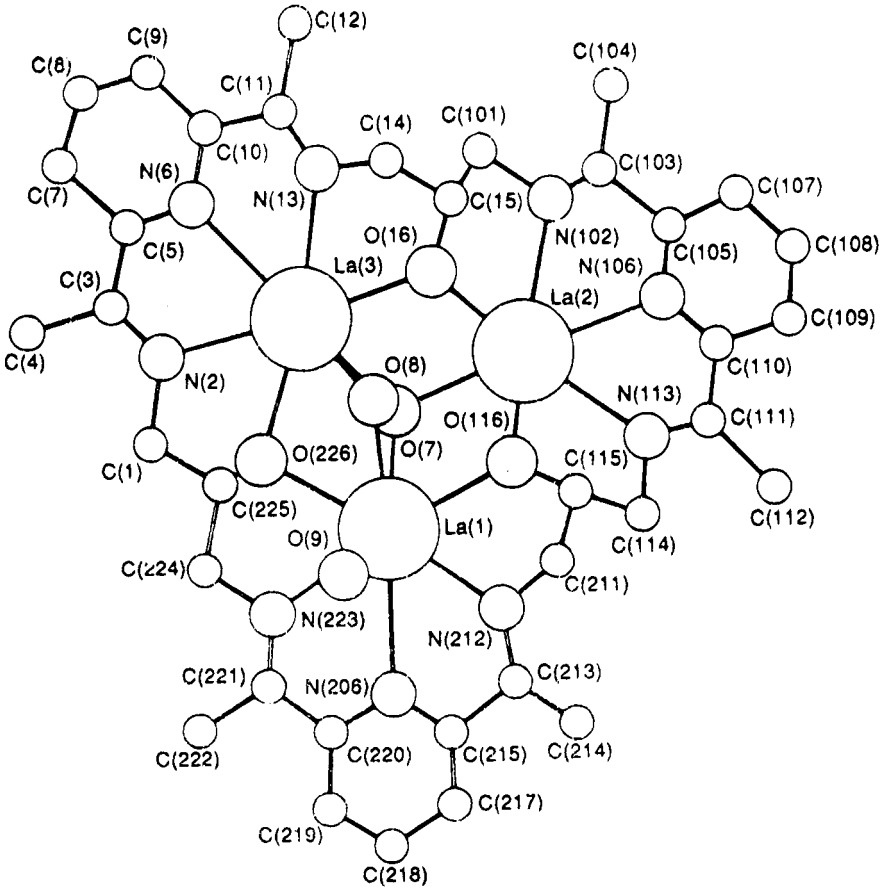

Figure 22. The structure of the $[La(\mathbf{101})(\mu_3\text{-}OH)(OH)(NO_3)_4] \cdot 7H_2O$. The nitrate ions and the water molecules are omitted for clarity (Reprinted from ref 224. Copyright 1993 Royal Society of Chemistry.)

a 2-fold axis of symmetry where two sides of the macrocycle are identical and different from the third. The template potential of the lanthanides in the assembly of the trinucleating "3 + 3" macrocycle **101** is extended with other lanthanides by Aspinall *et al.*[224] very recently. When the template condensation is carried out in the presence of lanthanide nitrates homotrinuclear lanthanide complexes $[Ln_3(\mathbf{101})(OH)_2(NO_3)_4]\cdot 4H_2O$ (Ln = La, Pr, Eu, or Gd) were isolated. Analogous reactions with $Ln(NCS)_3 \cdot nH_2O$ as template give $[Ln_3(\mathbf{101})(OH)(NCS)_5]\cdot 7H_2O$ (Ln = La, Pr, Eu, or Gd). The yields of the complexes decrease with decrease in ionic radii for both the nitrato and thiocyanato complexes. No complex was formed when perchlorates or acetates were used as the templates. The single-crystal X-ray crystal structure of the trinuclear lanthanum complex indicates that the complex obtained is $[La_3(\mathbf{101})(\mu_3\text{-}OH)(OH)(NO_3)_4]\cdot 7H_2O$. This is the first structurally characterized example of a trinuclear lanthanide Schiff base complex.[224] The structure is illustrated in Figure 22. The three lanthanide ions form an equilateral triangle of edge 4 Å. Each metal ion is 9-coordinate, being bonded to three nitrogen and two oxygen donors of the macrocycle and to four oxygen donors of OH^-, NO_3^-, and H_2O. The trinuclear lanthanum nitrate complex decomposes slowly in aqueous solution, precipitating $La(OH)_3$.

VIII. Synthesis of Macrocyclic Complexes by Transmetalation Reactions

Replacement of the coordinated metal ion by other metal ions which are not effective as templates is usually readily achieved by the transmetalation (metal exchange) reaction. In this way a wide range of mono- and dinuclear complexes have been prepared. A metal which cannot serve as a template for a particular macrocycle can effectively coordinate to form stable complexes if reacted with the free macrocycles. For the larger Schiff base macrocycles the transition metal ions are ineffective as templates. Consequently, the kinetic lability of the metal ions present in the macrocyclic complexes of the s- and p-block cations enable the generation of the corresponding transition and inner-transition metal complexes by transmetalation reactions. On treating the kinetically labile complexes with a second metal ion the liberated macrocycle is captured and stabilized by coordination to the new metal ion before decomposition. In this way a range of Ni^{2+} and Cu^{2+} complexes of **5** and other macrocycles have been obtained which are not accessible by the direct template method.[90,91,102-107,124,142,225] The transmetalation is the resultant of the stability differentials of the parent complex and the complex of the transmetalating ion. Thus, for the transmetalation to be feasible the stability of the complex of the transmetalating ion should be greater than that of the parent complex. Transmetalation has been exploited to synthesize a range of dinuclear complexes of "2 + 2" macrocycles from the corresponding mononuclear complexes. For example, reactions of the Ba^{2+} complex of the "2 + 2" macrocycle **13** and the Pb^{2+} complex of the ring-contracted macrocycle **14** with Cu^{2+} give the dinuclear copper(II) complex **23**. Similarly, Ca^{2+}, Ba^{2+}, and Sr^{2+} complexes of **11** also give the dinuclear copper(II) complex of **12**. In some cases transmetalation is accompanied by a change in geometry of the resulting complex: for example, when Ag^+ in $[Ag(\mathbf{5})]_2(ClO_4)_2$ is exchanged by Ni^{2+} in dry ethanol or methanol the octahedral complex of the more flexible macrocycle **102** is obtained by the addition of ROH across one of the azomethine bonds of **5**. When the reaction is carried out in the same

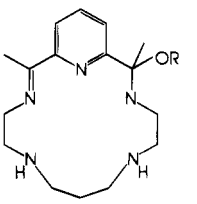

102

solvent containing water, hydrolysis occurs to give the octahedral complex of the ring opened ligand **22**. Molecular models and various structural analysis show that **5** cannot fold so as to occupy five octahedral positions. A strong preference of Ni^{2+} for the orthogonal disposition of metal–ligand bonds is the driving force for **5** to add ROH across one of the >C=N bonds or replacement of Ag^+ by Ni^{2+} thereby acquiring the necessary flexibility to attain the octahedral geometry.[111] Both the dinuclear Pb^{2+} and the mononuclear Ba^{2+} complexes of **8** undergo a facile transmetalation reaction to generate the homodinuclear copper(II) complex.

Furthermore, when some metal ions are used in the transmetalation reaction new types of macrocyclic ligands arising from ring expansion or contraction are obtained. This depends on the demands and the size of the transmetalating ion.[90,226,227] For example, while none of the transition metal complexes of **10** undergo ring closure to give the macrocyclic complex of **12**, transmetalation of the alkaline earth metal complexes of **11** by transition metal ions affords both mono- and dinuclear complexes of **12**. In this case a macrocyclic ring expansion from [18] to [24] occurs. There is considerable literature[92,228,229] on the synthesis of copper macrocyclic complexes by transmetalation reaction, and most of these reactions were carried out using alkaline earth complexes and in particular barium complexes as the starting material.

The kinetic lability of the lanthanide complexes has also been exploited to generate the corresponding complexes of the transition metals. For example, the reaction of the lanthanum(III) complex of **33** with Cu^{2+} yields dinuclear copper(II) complexes depending on the reaction conditions as shown in eqs 2 and 3.[140]

$$1[La(\mathbf{33})(NO_3)_3] + 2Cu(ClO_4)_2\cdot 6H_2O \xrightarrow{EtOH} [Cu_2(\mathbf{33})(OH)_2](ClO_4)_2\cdot 3H_2O + La(NO_3)_3 \quad (2)$$

$$1[La(\mathbf{33})(NO_3)_3] + 6Cu(ClO_4)_2\cdot 6H_2O \xrightarrow{EtOH} [Cu_2(\mathbf{33})(\mu\text{-}OH)](ClO_4)_3 + La(NO_3)_3 \quad (3)$$

The lanthanum(III) complex of **30** also undergoes transmetalation reaction to give the dinuclear copper-

(II) complex.[140] The lanthanide complexes of **43** are labile and transmetalation reaction of [La(**43**)]$(NO_3)_3$ with $Cu(ClO_4)_2 \cdot 6H_2O$ affords the dinuclear copper(II) complex, $[Cu_2(\mathbf{43})(\mu\text{-}OH)_2](ClO_4)_2 \cdot 3H_2O$.[159] This differs only in the number of water molecules present in the corresponding complex prepared via transmetalation of [Ba(**43**)]$(ClO_4)_2 \cdot C_2H_5OH$.[230,231] The dicopper(I) complexes are also obtained by the reaction of the barium complex with $[Cu(CH_3CN)_4]ClO_4$.[231] The reactions are represented in eqs 4–6.

$$[\text{La}(\mathbf{43})](NO_3)_3 + Cu(ClO_4)_2 \cdot 6H_2O \xrightarrow[\text{reflux}]{\text{EtOH}} [Cu_2(\mathbf{43})(\mu\text{-}OH)_2](ClO_4)_2 \cdot 3H_2O \quad (4)$$
(green)

$$[\text{Ba}(\mathbf{43})](ClO_4)_2 \cdot \text{EtOH} + Cu(ClO_4)_2 \cdot 6H_2O \xrightarrow[50-60\ ^\circ C]{\text{EtOH}} [Cu_2(\mathbf{43})(\mu\text{-}OH)_2](ClO_4)_2 \cdot H_2O \quad (5)$$
(green)

$$[\text{Ba}(\mathbf{43})](ClO_4)_2 \cdot \text{EtOH} + [Cu(CH_3CN)_4]ClO_4 \xrightarrow[\text{Ar}]{CH_3CN-\text{EtOH}} [Cu_2(\mathbf{43})(CH_3CN)_2](ClO_4)_2 \quad (6)$$
(yellow)

Trinitrato complexes of the larger lanthanides (La–Nd) with **35** were obtained by Gray and Hart[232] and by Benetollo *et al.*[157] by transmetalation from the corresponding bimacrocyclic Ba^{2+} complex, $[Ba(\mathbf{35})_2](ClO_4)_2$. When the nitrates of the smaller lanthanides (Dy–Yb) are used in the transmetalation reactions, a yellow solution resulted from which no pure complex could be isolated on concentration. Addition of an excess of NaSCN or $LiNO_3$ to the solution caused the precipitation of the lanthanide complexes in 30–50% yields as mixed thiocyanate–perchlorates or nitrate–perchlorates, respectively.[157] All solutions obtained from the transmetalation reactions contain small quantities of 2,6-bis(2-benzimidazolyl)pyridine (**38**).

Complexes of some of the heavier lanthanides have also been prepared by transmetalation reaction in which the barium complex [Ba(**27**)]$(ClO_4)_2$ echanges metal with the lanthanide ion to give two types of complexes: $[Ln(\mathbf{27})(NO_3)_2(H_2O)]NO_3 \cdot H_2O$ (Ln = La, Ce, or Pr) and $[\{Ln(\mathbf{27})(NO_3)_2(H_2O)\}_2]NO_3(ClO_4)_3 \cdot 4H_2O$ (Ln = Nd, Sm, Eu, Gd, Tb, Dy, Ho, or Er).[146] The smaller lanthanides appear to have too small an ionic radius to coordinate effectively with the macrocycle in competition with barium. The cerium and samarium complexes of **58** are prepared by the use of transmetalation from the barium complex.[178] The transmetalation reaction has also been exploited to effect slight modification in the inner-coordination sphere. For example, condensation of equimolar amounts of 2,6-diacetylpyridine with 1,2-diaminoethane in the presence of hydrated lanthanum(III) or cerium(III) nitrate yields pure crystalline trinitrato complexes, $[Ln(\mathbf{27})(NO_3)_3]$, while transmetalation of $[Ba(\mathbf{27})(ClO_4)_2]$ with $Ln(NO_3)_3$ (Ln = La, Ce, or Pr) yields the corresponding dinitrato(aqua) complex by the replacement of one of the bidentate nitrate ions by a water molecule.[146] Transmetalation reaction has also been used to synthesize macrocyclic complexes of lanthanides in pure form when the synthesis of the corresponding complexes by the metal template method yields impure complexes. For example, when the Schiff base condensation of equimolar amounts of 2,6-diacetylpyridine and 1,2-diaminoethane is carried out in the presence of hydrated nitrates of heavier lanthanides no pure complex could be isolated. But analytically pure crystalline complexes $[\{Ln(\mathbf{27})(NO_3)(H_2O)_2\}_2]NO_3(ClO_4)_3 \cdot 4H_2O$ (Ln = Nd, Sm, Eu, Gd, Tb, Dy, Ho, or Er) were obtained in 50–75% yield by the transmetalation reactions of [Ba(**27**)]$(ClO_4)_2$ with the lanthanide(III) nitrates in water.[146] Transmetalation of Ba^{2+} complexes of **86**–**88** with uranyl acetate in refluxing methanol yielded the hydrated uranyl complexes as deep red crystals as illustrated in Scheme 9. In these cases transmetalation is accompanied by a change in coordination site from the ether compartment for Ba^{2+} to the Schiff base compartment for UO_2^{2+}.[215]

Scheme 9. Transmetalation Reaction[a]

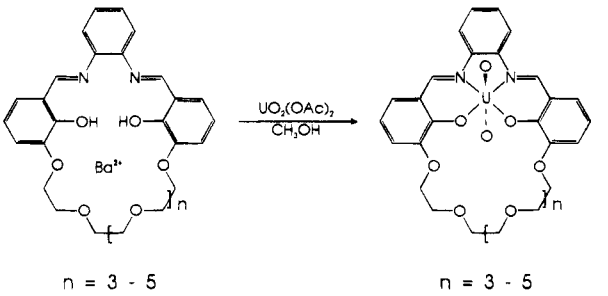

[a] Reaction of the Ba^{2+} complexes of **86**–**88** with $UO_2(OAc)_2$ gives the corresponding uranyl complexes. During the course of transmetalation there is a change in the coordination site from the ether compartment for Ba^{2+} to the Schiff base compartment for UO_2^{2+} (ref 215).

IX. Thermal Stability of Macrocyclic Complexes of Lanthanides and Actinides and Kinetic Inertness toward Cation Release

The lanthanide and actinide complexes of macrocycles exhibit high thermal stability and remarkable kinetic inertness. Thermogravimetric analysis shows that the lanthanide complexes of **27** have very high thermal stability and have been found to undergo reversible thermal dehydration in the crystalline state and irreversible anion loss. The hydrated complexes readily lose water at low temperature (below 60 °C) and the resulting anhydrous products are immediately rehydrated upon exposure to the atmosphere, returning exactly to their original masses. This lower temperature (<60 °C) dehydration–rehydration sequence could be repeated several times with reproducible results. The diacetate chloride compounds lose one of the acetates between 180 and 220 °C irreversibly, but the macrocyclic cations themselves remain unchanged up to 240–260 °C.[136] The complexes of **35** are crystalline solids with high thermal stability. Any solvent present in the crystal lattice is released between 80 and 150 °C, but the complex cation remains unchanged up to 250 °C. The uranyl complex **73** is quite stable, undergoing no apparent decomposition or demetalation when stirred

for several hours in a 5:1 (v/v) solution of chloroform and trifluoroacetic acid. The complex is quite stable up to 300 °C.[131]

In solution the macrocyclic cations are unaffected by strong acids: treatment of the lanthanide complexes of **27** having coordinated acetates with a 10-fold excess of HCl in methanol yielded the corresponding trichlorides. The cations are also unaffected by strong bases. The lanthanide complexes are remarkable for their exceptional inertness toward metal release in solution—a feature that contrasted with the common behavior of these very labile ions and made possible a detailed study of the luminescence of the europium(III) complex in dilute aqueous solution.[233] In solution the macrocyclic moiety remains unaltered even in the presence of good oxygen donor solvents such as water and DMSO. This inertness is confirmed by the observation that typical precipitating agents of the lanthanide ions such as F^-, OH^-, and $C_2O_4^{2-}$, fail to remove the metal ion from the macrocyclic system. For example, $[Pr(\mathbf{27})(NO_3)_2(H_2O)]NO_3 \cdot H_2O$ is stable for some time in KOH solution before $Pr(OH)_3$ is precipitated, and with KF no ready precipitation occurs. The complexes are also stable to decomposition in the presence of DTPA in aqueous solution. The ^1H and ^{13}C NMR spectra in neutral and acidic aqueous solutions show the hydrolytic stability of the europium complex.[148] This is in contrast with the behavior of $[Pr(18\text{-crown-6})(NO_3)_3]$ which gave instant precipitation with both the reagents.[146] Because of this unique inertness and their solubility in both water and organic solvents, the complexes of the paramagnetic lanthanides, and in particular those of Pr, Eu, and Yb, should prove to be useful and versatile NMR shift reagents. The conductivity study shows that the complexes of **27** exist as $[Ln(\mathbf{27})(H_2O)_n]^{3+}$ in aqueous solution. The uranyl complexes of **27** and **30** exhibit exceptional inertness in solution toward the release of UO_2^{2+}, even toward strong acids or strong ligands, which suggest that systems of this type may be of value when efficient sequestering of actinide ions is necessitated. The insoluble complexes of **35** dissolve in warm methanol or ethanol containing strong base such as NaOH, but the resulting solutions are stable only for a limited time. In contrast, these complexes are extremely stable to acids and are recovered unchanged after prolonged contact with an excess of HCl in either water or methanol. ^1H NMR studies show that the complexes are remarkably stable to dissociation in H_2O and DMSO and the macrocycle is resistant to hydrolysis. In both DMSO-d_6 and $CDCl_3$ the ^1H NMR spectra of both the La^{3+} and Lu^{3+} acetate chloride complexes of **27** remained unchanged over a period of weeks. The ^1H NMR spectra of the nitrato complexes of **27** reveal fairly considerable contact shifts. However, it is likely that for the smaller lanthanides (Tb–Er) structural changes occur in solution. It could not be ascertained whether this is by means of an NMR rapid equilibrium between two or more discrete structures which changes as the series is traversed or whether one structure is present for each metal ion but progressively alters with ionic radius. The lanthanide complexes are kinetically stable against metal ion exchange. Thus the NMR spectrum of $[La(\mathbf{27})(NO_3)_3]$ in D_2O is unaltered for 24 h after the addition of Ce^{3+}. Similarly the NMR spectrum of $[Ce(\mathbf{27})(NO_3)_2(H_2O)]^+$ is unaltered by the addition of La^{3+}. Xylenol orange, which forms a characteristic deep pink complex with lanthanide ions in aqueous solution, fails to give that color when treated with the lanthanide complexes of **27**, showing that they are inert to ligand replacement by this dye.[146]

X. Ligand Design Features and Metal Ion Discrimination

The main target in macrocyclic design is to synthesize macrocycles which are able to discriminate among the different metal cations. Many factors influencing the selectivities of macrocycles for cations have been determined. These include macrocyclic cavity dimensions, shape and topology, substituent effect, conformational flexibility/rigidity, and donor atom type, number, and arrangement.[2,3,234–239] For the first row transition metal ions the consecutive increments in radii are not large so it becomes difficult to effect discrimination solely on the cation–cavity "best fit". The other features involved are (i) the natural order of stability constants, (ii) the metal ion–ligand donor compatibility derived from hard and soft acid and base character, and (iii) the preferential site symmetry required by the metal ion.[240] The match between the cation and the macrocyclic cavity diameter is especially visible in small cryptands and other preorganized macrocycles, such as calixarenes and spherands. In these cases, size selectivity goes together with lack of flexibility of the ring which is too rigid to undergo conformational changes upon complexation. The influence of the cavity shape is envisaged in some calixarenes which exhibit very high "coordination-geometry selectivity" toward UO_2^{2+}.[241] Molecules of rigid types such as small cryptands and other preorganized macrocycles discriminate between cations that are either smaller or larger than the one with the optimum size—"peak selectivity". Macrocycles of flexible type, such as larger crown ethers and cryptands, discriminate principally among smaller cations—"plateau selectivity".[235]

Incorporating benzene, cyclohexane, pyridine rings, and other constituents into flexible macrocyclic skeletons lead to their stiffening and may alter both ligand binding strength and selectivity. Selectivities may also be modified by variation of side arms: 1,-10-diaza-18-crown-6 containing two carboxylate groups as side arms shows unique selectivity toward lanthanide cations as a group.[242] The number, kind, and arrangement of donor atoms also play important roles in macrocyclic selectivities: oxygen donors in classical crown ethers have the largest affinities for alkali, alkaline earth, and lanthanide cations, nitrogen donor atoms favor transition metal cations, sulfur donor atoms favor Ag^+, Pb^{2+}, and Hg^{2+}.[235] For example, the extremely large stability differential (up to 10^{10} for Cu^{2+}) among macrocycles may be achieved solely through variation of the number, nature, and array of donor atoms within the specific ligand framework employed.[243] It is often difficult to predict with confidence the relative binding preferences of

many polydentate ligands, particularly multidonor ligand systems, toward particular metal ions because of the number of variables, such as the nature of the donor atoms, the number and size of the chelate rings formed, the flexibility of the system, the relative position of the donor atom, and the nature of the ligand backbone. For macrocyclic systems, the macrocyclic ring size may be another important parameter. Thus the cyclic ligands have additional stereochemical constraints which may influence metal ion binding and hence thermodynamic discrimination.

Fenton and his co-workers[240,244,245] have investigated the design and synthesis of oxaazamacrocyclic ligands with varying ring sizes and flexibilities including both weak and strong donor atoms in varied donor sets and sequences in order to define the principles underlying transition metal selectivity by macrocyclic ligands. Such discrimination is found to be structurally or stereochemically based. This behavioral trend is well documented through the work of Tasker and his co-workers.[246,247] Lindoy and his co-workers[248] have developed design strategies for new macrocyclic ligand systems which are able to recognize particular transition and post-transition metal ions. Differences in log K values were used both as a monitor and control of the ligand synthesis. That is, starting from a particular macrocyclic ligand which gives rise to discrimination, related derivatives are synthesized in a systematic tuning up process by employing a typical three-dimensional structural matrix procedure by varying the macrocyclic hole size along one direction, increasing macrocyclic ring substitution along another direction, and varying the donor atom type along the third. This matrix procedure enables the effects of incremental structural variations on log K differences to be followed. Their studies demonstrate the extremely large stability differentials that may be achieved solely through donor atom variation within a given ligand framework.[243] When used in conjunction with the ring size variation, the combined procedure provides a potentially very powerful means for achieving metal ion discrimination.

Lindoy and his co-workers[243,246,249–252] have studied the discrimination of metal ions by ligands by following the occurrence of "structural dislocation" along a series of closely related mixed donor ligand systems. Structural dislocation is associated with a sudden change in the K value for cation–macrocycle interaction for a particular metal ion with a series of closely related macrocyclic ligands.[250,251] Such dislocation occurs when the gradual change of properties along the ligand series induces a sudden change in coordination geometry for the complexes of adjacent ligands. The influence of solvent[253–260] and counteranion[261–264] on macrocyclic selectivities are also well known and have been extensively studied. The subtle factors underlying such discrimination have been elucidated using a combination of solution equilibrium, kinetic, NMR, molecular mechanics, and X-ray diffraction techniques.

XI. Macrocyclic Substitution and Complex Stability

It has been found that macrocycles with substituents will greatly restrict the possible conformations on coordination to a metal ion. The stabilities of complexes of sterically hindered ligands are generally much lower than those for the unsubstituted parent rings.[252] For example, the X-ray crystal structure and molecular model studies of the complexes of the dioxatriazamacrocycle **103** containing N-benzyl sub-

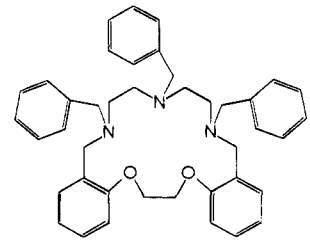

103

stituents indicate that the tribenzyl substituent will greatly restrict the conformation able to be adopted by **103** on coordination to a metal ion. A comparison of the log K values of the Co^{2+}, Ni^{2+}, Zn^{2+}, Cd^{2+}, Pb^{2+}, and Ag^{+} complexes of **103** with those of the parent ring indicates that the stabilities of the complexes of the sterically hindered ligand are generally much lower than that of the unsubstituted parent ring.

Macrocyclic ligands with pendant donor groups represent a class of ligands deliberately synthesized to achieve metal ion discrimination. Macrocycles with pendant groups bearing neutral oxygen donors have been synthesized in abundance mainly due to the synthetic simplicity.[265–271] The hydroxyethyl pendant groups produce a marked decrease in complex stability for small metal ions and a moderate increase in complex stability for the larger Pb^{2+} ion. This is in accordance with the rule regarding the effect of neutral oxygen donors on complex stability in relation to metal ion size. This leads to a simple generalization that in order to increase the selectivity of macrocycles for larger metal ions, all that is necessary is to add groups bearing neutral oxygen donors.[272] This is illustrated for the ligand **104**, which has a modest selectivity for the larger Pb^{2+} ion over the smaller ions. Greater selectivity is easily achieved by adding more oxygen donors to **104** to yield **105**.[271] Macrocyclic ligands with ethylamine

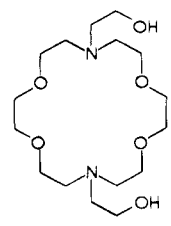

104

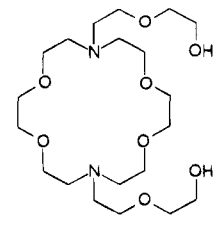

105

pendant groups represent another class of ligands synthesized to achieve metal ion coordination. A useful synthon for the introduction of an ethylamine group onto a molecule is the 3-membered heterocycle

N-(*p*-tolylsulfonyl)aziridine (*N*-tosylaziridine).[273-275] Murase and his co-workers[276,277] have reported that addition of *N*-tosylaziridine to cyclam followed by detosylation with HBr−CH_3COOH yielded the tetrakis(2-aminoethyl) pendant armed cyclam. Variations on this procedure have allowed the addition of pendant arms onto other macrocycles.[278-281]

N-Acetate-substituted macrocycles, particularly the tetraazamacrocycles with four added *N*-acetates, are another class of ligands with pendant side arms.[282,283-290] These ligands allow strong complexation of large metal ions that can achieve the coordination number of 8 required for full coordination of the donor atoms of the ligand. Thus, the Ca^{2+} complex of **106** is the most stable known complex of Ca^{2+} with a log *K* value of 16.5.[283,284] The *N*-acetate-substituted tetraazamacrocycles form stable complexes with lanthanides as these metal ions can expand the coordination number to meet the potential octadentate coordination provided by these ligands.[282] The ligand **106** is well known to form thermodynamically stable complexes with a wide range of divalent and trivalent metal ions.[291,292] In particular, it is a sterically efficient ligand for the coordination of lanthanides[293] and forms very stable complexes.[282,286,294-296] The formation constant for [Gd(**106**)]$^-$ is high with the reported values[282,297-299] ranging from 10^{22} to 10^{25}, and the complex is kinetically inert to the metal ion release. The low-temperature limiting ^1H and ^{13}C NMR spectral study of [Ln(**106**)]$^-$ (Ln = La^{3+}, Pr^{3+}, Nd^{3+}, Sm^{3+}, Eu^{3+}, Tb^{3+}, Dy^{3+}, Ho^{3+}, Er^{3+}, Tm^{3+}, Yb^{3+}, and Lu^{3+}) by Aime *et al.*[300] suggests the remarkable nonlability of the Ln−O bonds for the [Ln(**106**)]$^-$ chelates as also found by Wang *et al.*[297] in a kinetic study. The X-ray crystal structure of the Eu^{3+} complex of **106** shows a rigid 9-coordinate structure with an additional coordination of water.[301]

The analogous 14-membered *N*-acetate-substituted macrocycle **107** also forms more stable complexes with lanthanides.[296] However, one of the drawbacks with these macrocyclic ligands is their slow rate of complexation.[296,302,303] In an attempt to design new ligand systems which could give a faster rate of complexation, Kodama *et al.*[304] have synthesized the macrocyclic pentaamino pentacarboxylate ligand **108** and the hexaamino hexacarboxylate ligand **109** and studied their complexation with lanthanides (La^{3+}−Lu^{3+}, except Pm^{3+}). The stability trends of these complexes are almost parallel to those of DTPA and **106**. In contrast to **106** and **107**, **108** and **109** interact with lanthanides much faster. A comparison of the stability constants of the lanthanide complexes of the *N*-acetate-substituted macrocycles **106**−**109** indicates that as the nitrogen atoms in the macrocycle increases the 1:1 complex becomes more stable; thus the complexes of **109** are more stable than the corresponding complexes of **106**−**108**. The stability constants of the lanthanide complexes of these macrocycles are presented in Table 1. Measurements of the thermodynamic parameters ΔH and ΔS show that ΔS is the major contributor to the complex stability. The pseudo-first-order rate constants for the formation of lanthanide(III) complexes of polyaza polycarboxylates (k_{obs}) increase with an increase in ring size. Thus **109** forms Lu^{3+} and Y^{3+} complexes about 100 times faster than **106** and it reacts about 10 times more slowly than DTPA. The order of the relative rates indicates that the rate-determining step in the complexation is mainly controlled by the ligand flexibility and not by the coordination number. The pseudo-first-order rate constants for the Ln^{3+}−polyaza polycarboxylate complex formation are given in Table 2.

Table 1. Stability Constants (log K_{ML}) of Macrocyclic Complexes of Lanthanides at 25 °C and μ = 0.2 M $NaNO_3$[a]

	macrocycle					
metal ion	**107**	**108**	**109**	DTPA[b]	**106**	**130**
La^{3+}	12.74	13.57	19.11	19.5		
Ce^{3+}	13.12	14.16	19.59	20.3	23.0[c]	19.7[d]
Nd^{3+}	13.76	14.85	20.36	21.6		
	14.51[e]					
Sm^{3+}	14.47	15.35	21.24	22.3		
	14.97[e]					
Eu^{3+}	14.66	15.59	22.68	22.4	28.2[f]	
	15.46[e]					
Gd^{3+}	14.73	15.88	22.95	22.5	24.6[c]	21.1[g]
	15.75[e]					
Tb^{3+}	14.81	15.91	23.15	22.7	28.6[f]	
Ho^{3+}	14.95	16.48	23.88	22.8		
Tm^{3+}	15.15	16.61	24.09	22.7		
Lu^{3+}	15.31	16.71	24.26	22.4	29.2[f]	23.0[d]
					25.5[c]	
Y^{3+}	14.77	16.07	24.04	22.1	24.9[h]	21.1[g]
Dy^{3+}	16.04[e]					
Er^{3+}	16.49[e]					
Yb^{3+}	16.55[e]					

[a] K_{ML} = [ML]/[M][L] (M^{-1}). Three titrations were conducted for each system. The standard deviations at the 95% confidence level for the complexation constants are 0.05 unless otherwise noted (ref 304). [b] Reference 393. [c] Reference 282. [d] Reference 326. [e] At 80 °C and μ = 1.0 M NaCl (ref 296). [f] Determined by gravimetric method (ref 296). [g] Reference 329. [h] References 291 and 292.

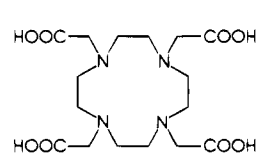

106

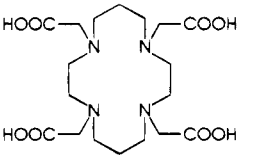

107

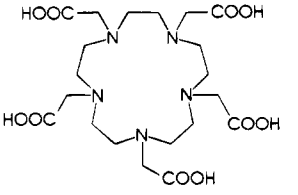

108

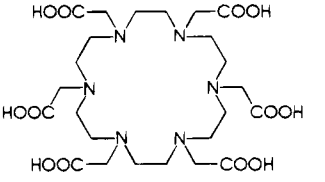

109

In order to investigate the effect of the ring size and rigidity of macrocycles as well as ring substituent effects on the kinetic properties of lanthanide complexes, Brucher and Sherry[305] studied the kinetics of formation and dissociation of Ce^{3+}, Gd^{3+}, and Er^{3+} complexes of the triaza triacetate macrocycle **110**. The stability constants of the [Ln(**110**)] complexes increase with increasing atomic number of the lanthanides, whereas the rates of both the spontaneous and proton-catalyzed dissociations decrease significantly as the ionic radius decreases. The complexes

Table 2. Pseudo-First-Order Rate Constants for M^{3+}–Polyaza Polycarboxylate Complex Formation at pH 7.8, 25 °C, and μ = 0.1 M ($NaClO_4$ + 25 mM HEPES Buffer)[a]

	k_{obs}, min^{-1}			
	106	**108**	**109**	DTPA
Lu^{3+}	6.3×10^{-3}	9.6×10^{-2}	5.8×10^{-1}	4.6
Y^{3+}	4.6×10^{-3}	2.0×10^{-1}	6.3×10^{-1}	7.3

[a] The standard deviations at the 95% confidence level for k_{obs} values are within 20%. Five measurements were conducted for each system (ref 304).

undergo spontaneous dissociation at physiological pH[305] in contrast to the behavior of [Ce(**106**)]$^-$.[302] This reflects the differing sizes and rigidities of the tetraazamacrocycle **106** versus the triazamacrocycle **110**. This is likely to be a consequence of the small size of the cyclononane ring of this chelate.[306] The thermodynamic and kinetic stabilities of [Gd(**110**)] are lower than that of [Gd(**106**)]$^-$ and [Gd(DTPA)]$^{2-}$.[282,305] The dissociation of [Gd(**106**)]$^-$, investigated by scavenging the liberated Gd^{3+} with an ion exchanger, is exceedingly slow.[297] It exhibits remarkable kinetic inertness. The role of the stereochemical requirements of **106** in determining the kinetic inertness of its lanthanide complexes is particularly notable when compared with the dissociation of lanthanide complexes of **110**[305] or **111**.[307]

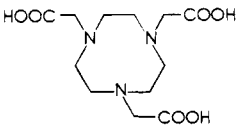

110

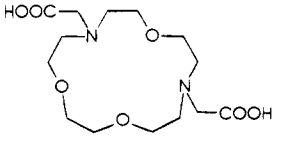

111

The former macrocycle is smaller than **106**, and the latter is larger. Both are less rigid and they feature less coordinating groups. When compared to [Gd(DTPA)]$^{2-}$, [Gd(**106**)]$^-$ presents the major advantage of dissociating much more slowly even in acidic media. With a half-life of 85 days at pH 2 and of more than 200 days at pH 5, [Gd(**106**)]$^-$ is indeed kinetically remarkably inert. In an attempt to determine the effect of the macrocyclic hole size and rigidity on the complexation properties, Sherry and his co-workers have designed the 12-membered triaza triacetate macrocycle **112**[308] and the 10-membered triaza triacetate ligands **113**–**115**.[309] An increase in

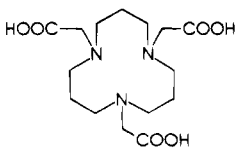

112

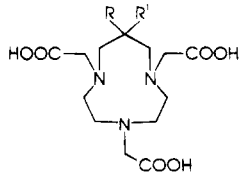

113, R = R' = H

114, R = CH_3, R' = H

115, R = R' = CH_3

the ring size from 9 to 12 of the triaza triacetate macrocycles **110** and **112** affects both the protonation and complexation properties of these macrocycles. The protonation constants increase significantly with an increase in size of the macrocycles, apparently due to a decrease in electrostatic repulsion between the protonated nitrogen atoms. The stability differentials of the complexes are the result of a combination of factors including metal ion size, macrocyclic hole size, and the degree of metal ion–donor atom covalency.[308] The formation rates (k_{OH}) of [Gd(**113**)] and [Gd(**114**)] are identical but are about 2 orders of magnitude lower than the k_{OH} value found for [Gd(**110**)]. This indicates that an increase in the ring size from 9 to 10 has a substantial effect upon the reactivity of these macrocycles. Both the spontaneous and the proton-assisted dissociation rates decrease in the order [Gd(**115**)] ≫ [Gd(**110**)] > [Gd(**113**)] > [Gd(**114**)]. Both the rate constants are significantly affected by ring size and ring substitution. An increase in ring size from 9 (**110**) to 10 (**113**) leads to

Table 3. Stability Constants, Formation Rate Constants, and Spontaneous and Proton-Assisted Dissociation Rate Constants of Macrocyclic Complexes of Lanthanides as a Function of Ring Size and Ring Substitution of Macrocycles and Ionic Radii of Metal Ions[a]

	stability constants[b]		formation rate constants:[c]	dissociation rate constants		
complex	log K'	log K_{LnL}	K_{OH}, M^{-1} s^{-1}	K_d^0, s^{-1}	K_d^1, M^{-1} s^{-1}	ref
[Gd(**106**)]		24.6[d]	$(5.9 \pm 0.2) \times 10^6$ [e]	null[f]	$(8.4 \pm 0.4) \times 10^{-6}$ [g]	297
[Ce(**106**)]		23.0[d]		*h*	$(8 \pm 2) \times 10^{-4}$	302
[Gd(**110**)]	2.30 ± 0.17	13.7 ± 0.2	$(7.1 \pm 1) \times 10^7$	$(8.3 \pm 1) \times 10^{-6}$	$(2.3 \pm 0.3) \times 10^{-2}$	305
[Ce(**110**)]			$(6.3 \pm 1) \times 10^7$	$(2.5 \pm 0.3) \times 10^{-5}$	$(4.3 \pm 0.5) \times 10^{-2}$	305
[Er(**110**)]			$(5.5 \pm 0.7) \times 10^7$	$(2.7 \pm 0.5) \times 10^{-6}$	$(1.6 \bullet 0.3) \times 10^{-3}$	305
[Gd(**113**)]	0.30 ± 0.17	15.1 ± 0.3	$(8.2 \pm 2) \times 10^5$	$(5.7 \pm 1) \times 10^{-6}$	$(4.5 \pm 0.6) \times 10^{-3}$	309
[Gd(**114**)]	-0.64 ± 0.27	14.7 ± 0.3	$(7.3 \pm 1.6) \times 10^5$	$(3.3 \pm 0.6) \times 10^{-6}$	$(1.6 \pm 0.2) \times 10^{-3}$	309
[Gd(**115**)]	-3.47 ± 0.10	10.4 ± 0.2	$(3.8 \pm 1) \times 10^4$	$(8.3 \pm 1) \times 10^{-4}$	0.5 ± 0.1	309
[Ce(**130**)]		19.7 ± 0.4		$(1.8 \pm 0.8) \times 10^{-3}$	$(1.12 \pm 0.04) \times 10^{-1}$	326
[Gd(**130**)]		21.0 ± 0.2	$(2.1 \pm 0.1) \times 10^7$ [i]	$(4.4 \pm 0.1) \times 10^{-4}$	*h*	326
[Lu(**130**)]		23.0 ± 0.2		*h*	*h*	326
[Ce(**131**)]				$(1.4 \pm 0.2) \times 10^{-4}$	$(2.00 \pm 0.04) \times 10^{-3}$	326
[Gd(**131**)]			$(1.23 \pm 0.04) \times 10^7$ [i]	*h*	*h*	326
[Gd(**133**)]		25.3	$(7.2 \pm 0.3) \times 10^4$ [i]	3.7×10^{-5}	$(5.2 \pm 0.5) \times 10^{-4}$	329

[a] At 25.0 ± 0.1 °C, μ = 1 M NaCl; k_d^0 and k_d^1 are the direct and proton-assisted dissociation rate constants, respectively, of the monoprotonated chelate, [MLH]. [b] Stability constant, K', corrected for proton competition by the second and third protonations only. [c] The specific base-assisted second-order rate constants for the dissociation of the intermediate M(*LH) (*HL is the monoprotonated intermediate, L is the macrocycle.) [d] Reference 282. [e] The kinetic data of Wang *et al.* (ref 297) was reanalyzed by Kumar and Tweedle (ref 327) and computed the value of K_{OH}. [f] Error on $K_d^0 = 5 \times 10^{-8}$ s^{-1}. [g] The proton assisted dissociation rate constants is also represented as k_d, H. [h] Not observed. [i] Reference 327.

an increase in kinetic stability because the Gd^{3+} ion fits into a 10-membered macrocycle better than a 9-membered macrocycle. Substitution of a methyl group onto a ring carbon of the ligand increases the rigidity of the macrocycle, yielding a complex with even greater kinetic stability, [Gd(**114**)] versus [Gd(**113**)]. The substitution of two methyl groups onto a ring carbon, however, results in a significant decrease in both the thermodynamic and kinetic stabilities of the resulting Gd^{3+} complex.[309] The ionic size of the lanthanides seems to have a drastic effect on the kinetic phenomena. Brucher *et al.*[302] reported the proton-assisted dissociation rate constant for $[Ce(\mathbf{106})]^-$ which is 2 orders of magnitude higher than the value obtained by Wang *et al.*[297] for $[Gd(\mathbf{106})]^-$. The stability constants, formation rate constants, and the spontaneous and proton-assisted dissociation rate constants (k_d^0 and k_d^1, respectively) for the lanthanide complexes of **106**, **110**, and **113**–**115** are presented in Table 3.

The edta bis(amide) chelate **116** exerts high selectivity for Gd^{3+} over Zn^{2+}. The logarithmic selectivity

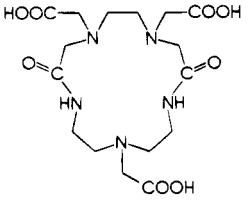

116

constant of **116** for Gd^{3+} over Zn^{2+} is 6.12.[310] Aime *et al.*[311] have synthesized Gd^{3+} complexes of **117**–**120** which are the functionalized derivatives of **106**.

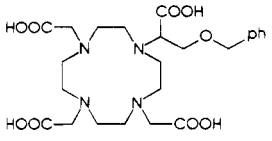

117

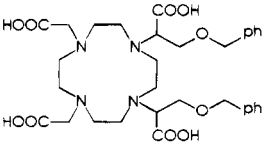

118

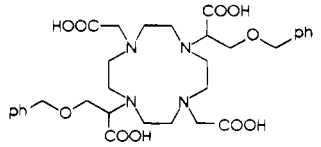

119

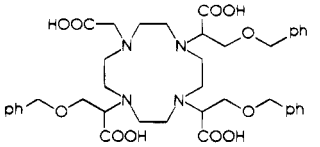

120

These ligands are synthesized by the stepwise alkylation of 1,4,7,10-tetraazacyclododecane first with 2-chloro-3-(benzyloxy)propionic acid and then with bromoacetic acid. The stability constants for [Gd(**117**)] and [Gd(**118**)] are only 1 order of magnitude lower than that of $[Gd(\mathbf{106})]^-$ and significantly higher than that reported for the Gd^{3+} complexes of DTPA and the amide and ester conjugates of **106**.[303,312] Gd^{3+} complexes of **121** and **122** containing a polyhydroxy (benzyloxy)propionamide substituent and the corresponding derivatives **123** and **124** with a primary alcoholic function, synthesized by modifying **106** by Aime *et al.*,[313] do not alter the coordination capabilities of these macrocyclic ligands as evidenced by their high formation constants. The high formation constants of [Gd(**121**)] and [Gd(**122**)] (log $K_{[GdL]}$ = 25.9

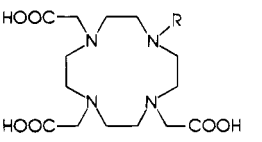

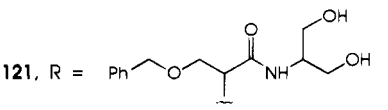

121, R =

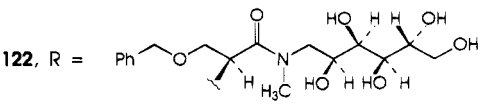

122, R =

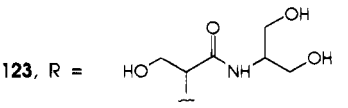

123, R =

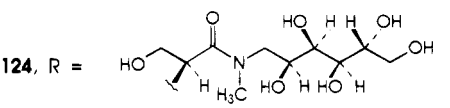

124, R =

and 26.4, respectively) support the direct involvement of the amide functionality in the coordination cage. This was revealed by the crystal structure of [Gd(**121**)].[313]

The ligand **125** having four methylenephosphonic acid pendant groups forms stable complexes with lanthanide(III) cations. The first preparation of **125** was reported[314] in 1984, and since then several synthetic procedures have appeared[28,35,315,316] each leading to different yields or products with subtly differing chemical characteristics. The ligand **125** was prepared by the reaction of 1,4,7,10-tetraazacyclododecane tetrahydrochloride with paraformaldehyde and phosphorous acid. It reacts more rapidly

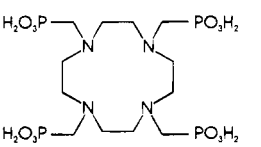

125

with lanthanide(III) ions than does **106** under similar solution conditions[315,316] and unlike the $[Ln(\mathbf{106})]^-$ complexes, the $[Ln(\mathbf{125})]^{5-}$ complexes tend to aggregate to a small extent in aqueous solution.[317] These observations may be related to the conformational preferences of the side chain phosphonates in **125** versus the carboxylates in **106**.[316] Lazar *et al.*[316] have optimized the synthetic procedure so as to get **125** in 78–82% yield in pure form. The tetraazacyclododecane derivative **126** with four alkylphosphinic acid pendant groups forms monoanionic complexes under strongly acidic conditions.[318] In addition, a phosphinic acid oxygen is a better σ-donor than a carboxylate oxygen for cations of high charge density. Reaction of cyclen with paraformaldehyde and $CH_3P(OC_2H_5)_2$ in tetrahydrofuran yielded the tetraester **126** as a mixture of four possible diastereoisomers. Acid hydrolysis (6 M HCl, 18 h, 125 °C) of **126** yielded the tetraacid **127** as the hydrochloride salt.[319] Stability constant for the complexation of **127** with Y^{3+} (log

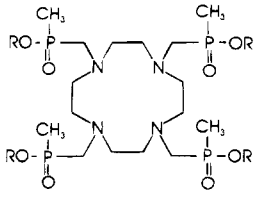

126, R = C_2H_5

127, R = H

$K_{[Y(\mathbf{127})]^-}$ = 25.1) is higher than that reported for **106** (log $K_{[Y(\mathbf{106})]^-}$ = 24.9).[291,292] The yttrium complex of **127** was formed as a single diastereoisomer (δ_p (D_2O, pD 6) = 44.4) in which the configuration at each of the four stereogenic centers at phosphorous is most likely to be the same, i.e., *RRRR* or *SSSS*. In this configuration the methyl groups are oriented away from the plane of the [12]N_4 ring. Resolution of this chiral complex is feasible with a suitable enantiomerically pure base.[319] Thus the cyclen macrocycle is a good ligand framework to build ligands for lanthanide(III) cations.

Morrow and Chin[320] synthesized the ligand 1,4,7,-10-tetrakis(2-hydroxyethyl)-1,4,7,10-tetraazacyclododecane (**128**) by incorporating four 2-hydroxyethyl pendant groups onto the cyclen framework. The La^{3+}

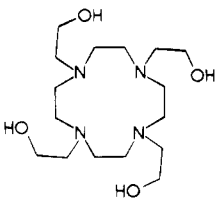

128

and Eu^{3+} complexes of **128** are prepared under anhydrous conditions by the treatment of Ln(CF_3SO_3)$_3$ with **128**. The use of dry acetonitrile and the addition of the drying agent trimethyl orthoformate is necessary to prevent the formation of lanthanide hydroxides. Both the La^{3+} and Eu^{3+} complexes are stable in water at neutral pH. Dissociation of Eu(**128**)(CF_3SO_3)$_3$ proceeds much more slowly than the lanthanum complex. The europium complex has a half-life of 270 h compared to the half-life of 21 h for the lanthanum complex at pH 6.0. A better fit of the smaller Eu^{3+} ion into the macrocyclic cavity of **128** may be responsible for the greater kinetic inertness of the europium complex to the metal ion release.[320] In addition, the difference in ionic radius between La^{3+} and Eu^{3+} may result in different coordination numbers for the complexes in water.[321] Variable-temperature ^1H and ^{13}C NMR studies indicate that the ethylenic groups of **128** are rigid on the NMR time scale at low temperature (−40 °C), and all adopt the same conformation. Macrocyclic rigidity is lost at elevated temperatures and a dynamic process involving conformational changes of the ethylenic groups is consistent with the NMR data. A similar dynamic process is observed for the Ln^{3+} complexes of **106**.[293,300] Comparison of the energy barrier of 52 ± 0.7 kJ mol^{-1} for the dynamic process of La(**128**)(CF_3SO_3)$_3$, calculated from the line-shape analysis of ^{13}C NMR spectra at different temperatures, with an activation energy of 60.7 ± 1.2 kJ mol^{-1} for [La(**106**)][322] indicates that **128** when bound to La^{3+} is less rigid than **106** bound to La^{3+}. This suggests that pendant groups contribute to the overall rigidity of the macrocyclic ring.

The 18-membered macrocyclic triaza trioxa triacetic acid **129** forms stable complex with Gd^{3+}. This is

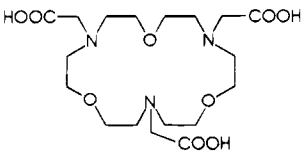

129

the first example of a 9-coordinate Gd^{3+} complex of a macrocyclic ligand in which all the nine donor atoms are derived from the same ligand framework.[323] The stability constant of [Gd(**129**)] is found to be 18.02.[324] A comparison of the stabilities of the complexes of di- and trivalent transition metal ions and Gd^{3+} with macrocyclic triaza triacetic acids of varying cavity sizes suggest that the 18-membered macrocycle **129** which is more flexible adapts better to the size of the metal ions and brings the donor atoms near to the metal ions.[324] The crystal structure of [Gd(**129**)][323] confirms this hypothesis; in the solid state the gadolinium atom lies within the macrocycle and is 9-coordinate, being bound to all donor atoms of the macrocycle.

The stability constants of lanthanide complexes of the 12-membered tetraaza triacetic acid **130**[325] increase with the decreasing ionic radii or increasing charge density of Ln^{3+}.[326] Derivatization of **130** on the unique nitrogen of the macrocyclic ring with 2-hydroxypropyl pendant group yields the octadentate macrocycle **131** which forms more stable lanthanide(III) complexes than **130**. The stability differences between the complexes of the heptadentate **130** and the octadentate **131** and **106** are due to the differences in the number and type of donor atoms and the number of chelate rings formed. Replacement of the neutral hydroxypropyl coordinating group in **131** by the ionizable carboxylate group in **106** increases the stability by 2 orders of magnitude.[326] The additional negative charge on **106** provides additional stability of lanthanide complexes, which supports the preference of ionic bonding of lanthanides. The relative kinetic inertness of the Gd^{3+} complexes in 0.1 M HCl follows the order **106** > **131** > **130** > **110**. The cavity size of **110** is too small for the lanthanides and consequently its complexes are relatively labile. The stability constants and kinetic inertia of lanthanide complexes increase with increasing charge density of the metal ion, but for the relatively more rigid octadentate ligands **106**

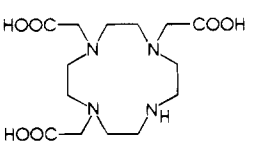

130

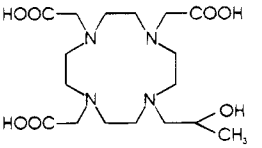

131

and **131**, the stability constants of Gd^{3+} and Lu^{3+} are controlled by the cavity size match and/or structural changes.[326] The recent kinetic study by Kumar and Tweedle[327] indicates that the rate of formation of gadolinium complexes of macrocyclic polyamino carboxylates is much slower than the rate of formation of linear polyamino carboxylate complexes of Gd^{3+} due to the greater rigidity and basicity of these macrocycles.

The influence of the alkyl groups attached onto the acetate pendant groups also alters the rigidity of the macrocyclic ring. For example, the luminescence and NMR study by Brittain and Desreux[328] indicates that the Eu^{3+} and Tb^{3+} chelates of **132** are more rigid than those of **106**, with the conformation of the ethylenic groups of the macrocyclic ring undergoing very slow inversion between 0 and 100 °C, demonstrating that the introduction of the α-methyl groups increases the rigidity of the amino carboxylate macrocyclic framework. The effect of additional rigidity caused by the α-methyl groups onto the carboxylate pendant arms was also reported by Kang *et al.*[329] by studying the stability, lability, and relaxivity of the Gd^{3+} and Y^{3+} complexes of (1*R*,4*R*,7*R*)-α,α′,α″-trimethyl-1,4,7,10-tetraazacyclododecane-1,4,7-triacetic acid (**133**), synthesized by the simultaneous hydrogenolysis and deformylation of 10-formyl-1,4,7-tris[[(benzyloxy)carbonyl]methyl]-1,4,7,10-tetraazacyclododecane. Treatment of either the triethylammonium salt of **133** with gadolinium acetate or the free acid **133** with gadolinium oxide in water resulted in the formation of the diastereomerically pure Gd(**133**). X-ray crystal structure analysis of Gd(**133**) reveals that all the three asymmetric carbons bearing α-methyl groups have the (*R*) configuration and that the complex crystallizes as a dimer, $[Gd(\mathbf{133})(H_2O)]_2 \cdot 4H_2O$, in which both the gadolinium atoms are 9-coordinate. The stability constant of Gd(**133**) ($\log K_{[Gd(133)]} = 25.3$)[329] is nearly as high as that of Gd(**106**) ($\log K_{[Gd(106)]} = 25.8$)[329] contrary to expectation based on the difference in coordination number between these two complexes (CN = 7 for [Gd(**133**)] and 8 for $[Gd(\mathbf{106})]^-$). This is explained on the basis of the relative basicities of the two ligands; the sums of the pK_a values for the neutral ligands **106** and **133** are 29.8 and 27.8, respectively. This enhanced stability of the complexes of **133** due to the α-methyl groups is consistent with the findings of Matthews *et al.*[330] on the stabilities of indium and gallium complexes of **110** and **134**. No release of free Gd^{3+} ion was observed by HPLC (<0.002 mol %) upon storing Gd(**133**) as a 0.5 M solution at physiological pH for three months. The complex is 10-fold more inert than Gd(**130**) in 0.1 M HCl. This large difference in kinetic inertness is attributed to additional rigidity of Gd(**133**) imposed by the α-methyl groups. The stability constants and the formation and dissociation rate constants of the lanthanide(III) complexes of the macrocyclic polyamino carboxylates, **106**, **130**, **131**, and **133** are given in Table 3.

The water-soluble Gd^{3+} complex of the texaphyrin **67** is stable in aqueous media in the presence of challengers, such as, EDTA, oxalate, and phosphate over a period of 45 days. The observable species in solution over the entire 45 days period is Gd(**67**). This

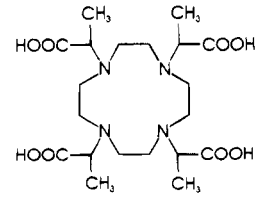

132

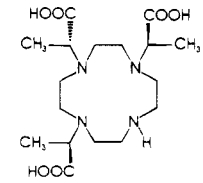

133

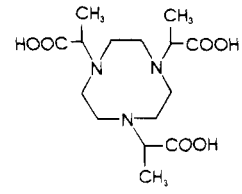

134

conclusion is supported by the lack of any observable shifts in the position of the Soret and Q-type bands over the 45 day period; if appreciable amounts of free macrocycle is being formed, a shift in the position of these bands would be expected. These results indicate that the Gd^{3+} complex of **67** is stable *in vitro* in the presence of strong chelating agents, such as, EDTA and precipitating agents, such as, oxalate and phosphate at pH 7.[133] The stability of Gd(**67**) is in marked contrast to the Gd^{3+} porphyrins, which are known to demetalate rapidly in the presence of EDTA.[331-333] The kinetic study of the stabilities of other lanthanide texaphyrin complexes shows a high degree of nonlability in aqueous solution under ambient laboratory conditions.[133]

Properties, such as coordination number, ionic radius, and Lewis acidity of the metal ion, macrocyclic substitution, rigidity of the macrocycle, basicity of the macrocycle, macrocyclic hole size, and the degree of metal ion–ligand donor covalency may all influence the inertness of the macrocyclic complex to the metal ion release. An important consideration in the synthesis of lanthanide(III) tetraaza macrocyclic complexes that are kinetically inert to the metal ion release is the size of the macrocyclic ring.

XII. Covalency in Metal–Ligand Bonding in the Complexes of Lanthanides and Actinides

A brief account is now given of the quantitative studies on the covalent character and the involvement of metal f-electrons in metal–ligand bonding in the organometallic compounds of lanthanides and actinides as an essential basis to emphasize the covalent character and the involvement of metal f-electrons in metal–ligand bonding in (nonalkyl)-lanthanide and -actinide complexes. The higher coordination numbers of lanthanides and actinides in their complexes is attributed to their large size together with the ionic nature of metal–ligand bonding. Study on the participation of f-electrons and covalent character in metal–ligand bonding constitutes a challenging objective to be vigorously pursued. Investigations on the degree of covalent bonding in cyclooctatetraenyl and cyclopentadienyl complexes of f-elements has been the subject of interest ever since the isolation of uranocene.[334] Spectroscopic

and physical evidence suggest that substantial metal–ligand covalent character exists in many organolanthanide and actinide complexes.[335–341] Evidence for covalent bonding in cyclopentadienyl complexes of the f-block elements was sought from the linear relationship between metal radii and metal–cp distances in over 200 structurally characterized compounds.[342] A comparison of bonding in several organometallic compounds of uranium, neptunium, plutonium, and transplutonium metals with that of lanthanides and a transition metal analog by the Xα-SW molecular orbital calculation with quasi relativistic correction by Bursten and his co-workers[343–345] reveals that the metal 6d-orbitals are more important in bonding with the cp ligands than the 5f-orbitals.[345] The principal function of the 5f-orbitals is to act as a reservoir for metal-based electrons.[344] Discovery of facile migratory insertion of CO into uranium bonds with various ligands sparked new interest in this area.[336,346–350] Brennan *et al.*[351] have synthesized the first molecular actinide carbonyl complex stable in solid state and solution. IR spectroscopy provides evidence for back-bonding. This is the first report of the back-bonding interaction in a discrete actinide complex.[351] Quasi relativistic Xα-SW molecular orbital calculation by Bursten and Strittmatter[352] on the model compound cp_3UCO reveals extensive U 5f → CO 2π-back-bonding.

Evidence for the covalent character in the lanthanide–ligand bonding is sought from the energies of f–f transitions. For example, the unusually high energies of the f–f transitions, such as, $^7F_0 \rightarrow {}^5D_0$ for Eu^{3+}, $^7F_6 \rightarrow {}^5D_4$ for Tb^{3+}, and $^2F_{5/2} \rightarrow {}^2F_{7/2}$ for Yb^{3+}, in the dinuclear lanthanide(III) complexes of *p-tert*-butylcalix[8]arene, reported by Bunzli *et al.*,[353] are indicative of metal–ligand covalent character. In highly luminescent lanthanide compounds there is an efficient ligand to metal energy transfer which implies overlap of the metal and ligand orbitals so that the complexes present a very high Ln^{3+} emission through ligand excitation. It has been demonstrated that the energy transfer from the ligand to the metal takes place through an exchange interaction originating from the overlap of the electronic cloud of the atoms participating in the metal–ligand bond.[354]

XIII. Structural Features of Lanthanide and Actinide Complexes of Higher Coordination Numbers

The structural chemistry of lanthanide and actinide elements has recently undergone considerable development and a wide variety of coordination numbers and geometries have been observed. This structural versatility arises from the lack of strong crystal field effects for the 4f- and 5f-electronic configurations and from the large ionic radii of these metal ions. The major differences in electronic structure which establish the chemical differences between actinides and lanthanides are (i) for the lighter actinides the 5f-orbitals are not completely shielded from the influence of the 6s- and 6f-electrons, allowing radial expansion of 5f-orbitals sufficient for overlapping with the ligand orbitals and, as a consequence, they are rather versatile in their oxidation numbers; (ii) on going along the actinide series the increase in nuclear charge causes a contraction of the 5f-orbitals with decreasing metal–ligand overlap and the trivalent oxidation state dominates with an even more highly ionic character in bonding; and (iii) in the lanthanides the 4f-orbitals are more shielded by the 5s- and 5p-electrons and they are greatly contracted along the series, and their ionic radii decrease monotonically with increasing atomic number. The large ionic radii of the lanthanide and actinide ions together with the increased ionic character of the metal–ligand bonding in their complexes led to the generation of complexes with higher coordination numbers.[355] The ratio of the ionic radius of the metal ion to the cavity diameter, the flexibility of the macrocycle, and the nature of the counteranion are the most important factors which determine the type of the complex obtainable. Preformed macrocyclic ligands having four or five donor atoms whose cavity size is too small to accommodate the metal ion coordinate on one side while the remaining exocyclic ligands in the complex coordinate on the opposite side.[82]

A. Structural Features of Mononuclear Macrocyclic Complexes of Lanthanides and UO_2^{2+}

The X-ray crystal structures of the hexaazamacrocycles **27**, **30**, and **34** derived from pyridine head units have been reported. A common feature observed in all the complexes of **27** and **30** is the hinging of the macrocycle at the two flexible $-CH_2-CH_2-$ lateral units, resulting in a folded butterfly configuration. This folding relieves steric strain within the macrocycle and also minimizes repulsion among the coordinated exocyclic ligands, thus allowing the central metal ion to attain its highest possible coordination number. The macrocyclic plane may be viewed as generating two hemispheres, one above and one below the plane of the donor atoms, and the exocyclic ligands will occupy sites within these hemispheres. The lanthanum ion is 12-coordinate in [La(**27**)$(NO_3)_3$],[135,146] being bonded to the six nitrogen donors of the macrocycle and to two bidentate nitrate on one side of the macrocycle and to the other bidentate nitrate ion on the other side as has been found in the complex [Ln(18-crown-6)$(NO_3)_3$].[356] The molecular structure of [La(**27**)$(NO_3)_3$] and the folding of the macrocycle along the $-CH_2CH_2-$ unit are depicted in Figure 23, parts a and b, respectively.

The cerium ion in [Ce(**27**)$(NO_3)_2(H_2O)$]$NO_3 \cdot H_2O$ is 11-coordinate. The metal ion is coordinated to the six nitrogen donors of the macrocycle, to one of the bidentate nitrate ions on one side of the macrocycle, and to the second nitrate ion and to a water molecule on the other side.[146] The two coplanar conjugated sections of the ligand show a larger interplanar angle of 59.0° than in [La(**27**)$(NO_3)_3$]. The ligand is folded away from the hemisphere containing the water molecule. There is a striking difference between the two halves of the macrocycle: one half has Ce–N at 2.722 Å (average), while the other is appreciably more closely bonded with Ce–N at 2.625 Å (average). The molecular structure of [Ce(**27**)$(NO_3)_2(H_2O)$]$NO_3 \cdot H_2O$ is shown in Figure 24. In the complex of the slightly smaller neodymium ion, [{Nd(**27**)$(NO_3)(H_2O)_2$}$_2$]$(NO_3)(ClO_4)_3 \cdot 4H_2O$,[146] the metal ion is 10-coordinate, being

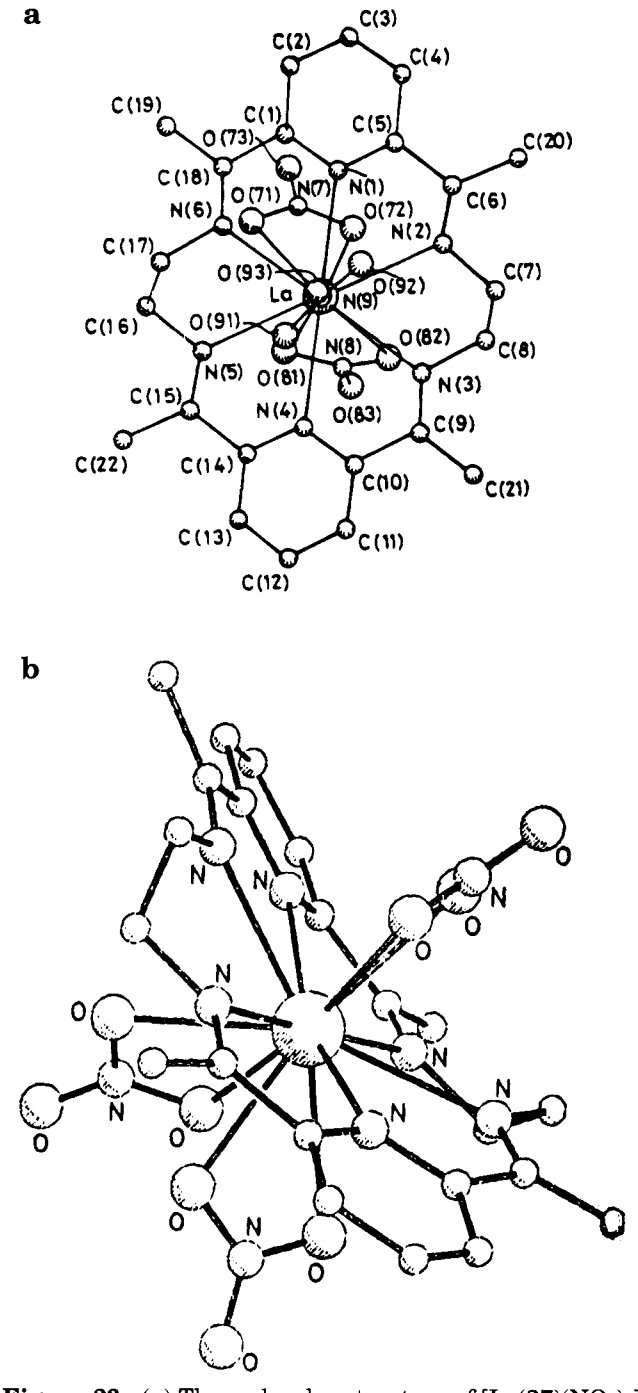

Figure 23. (a) The molecular structure of $[La(\mathbf{27})(NO_3)_3]$ and atom numbering scheme and (b) the molecular structure of $[La(\mathbf{27})(NO_3)_3]$ showing the folding of the macrocycle along the $-CH_2CH_2-$ lateral unit. (a: Reprinted from ref 146. Copyright 1987 Royal Society of Chemistry. b: Reprinted from ref 135. Copyright 1979 Royal Society of Chemistry.)

bonded to the six ring nitrogen donors of **27**, to the chelating nitrate ion on one side of the macrocycle, and to the two water molecules on the other side. The ligand is folded away from the hemisphere containing the two water molecules. This is a direct demonstration of the smaller steric requirement of bidentate nitrate as compared with the water molecules. The X-ray crystal structure of $[Nd(\mathbf{27})(NO_3)(H_2O)_2]^{2+}$ ion is depicted in Figure 25. The crystal lattice of the lutetium(III) complex $[Lu(\mathbf{27})(CH_3COO)(H_2O)_{0.5}(CH_3OH)_{0.5}](ClO_4)(OH)(CH_3OH)_{0.5}$[147] consists of two species having the structural formula $[Lu(\mathbf{27})(CH_3COO)(H_2O)](ClO_4)(OH)(CH_3OH)$ and $[Lu(\mathbf{27})(CH_3COO)(CH_3OH)](ClO_4)(OH)$. In the former complex species, the macrocycle surrounds the metal ion with all nitrogen donors bound to it, the acetate ion is chelated to the metal ion as a bidentate ligand on one side of the macrocycle, and the water molecule on the opposite side completes the coordination sphere. The latter complex species differs from the first species only by having a methanol molecule coordinated to the metal instead of a water molecule. In both cases the perchlorate counterion is distorted. The coordination number of lutetium is 9 in both cases. The conformation of the macrocycle is characterized by two approximately planar sections with deviations from planarity ranging from −0.17 to +0.23 Å. The two sections are hinged along an axis passing midway between the two $-CH_2CH_2-$ lateral units and are folded toward the singly coordinated ligand (water/methanol); the dihedral angle between the two planes is 114.4(1)°. The X-ray crystal struc-

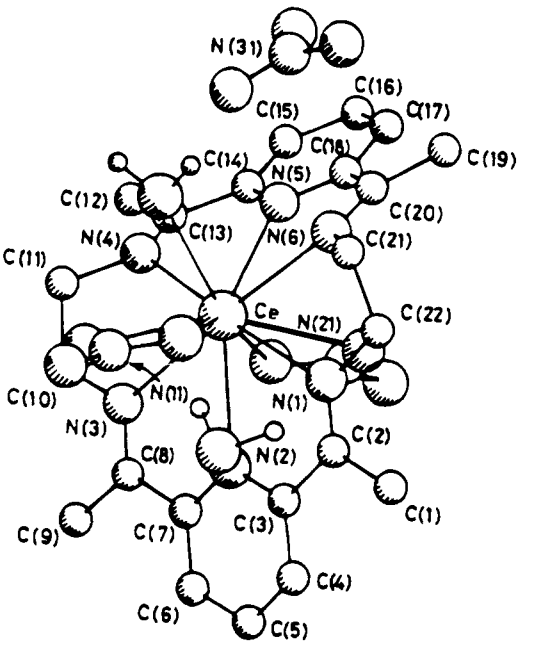

Figure 24. The molecular structure of $[Ce(\mathbf{27})(NO_3)_2(H_2O)]NO_3 \cdot H_2O$ and atom numbering scheme. (Reprinted from ref 146. Copyright 1987 Royal Society of Chemistry.)

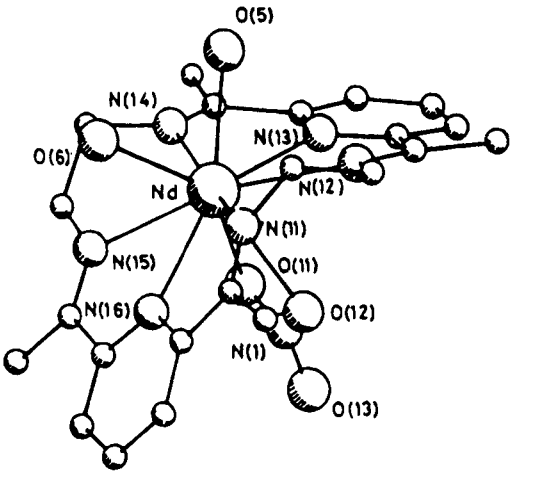

Figure 25. The molecular structure of $[Nd(\mathbf{27})(NO_3)(H_2O)_2]^{2+}$ ion and atom numbering scheme. (Reprinted from ref 146. Copyright 1987 Royal Society of Chemistry.)

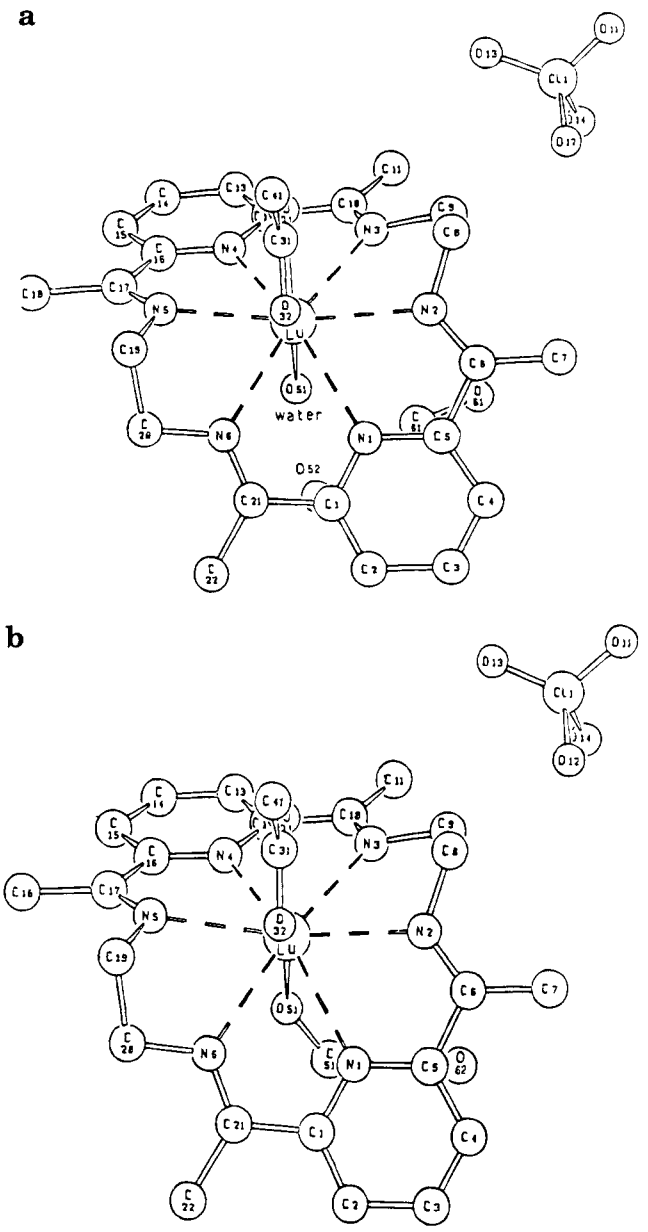

Figure 26. Perspective view of $[Lu(\mathbf{27})(CH_3COO)(H_2O)](CH_3OH)(OH)(ClO_4)$ (a) and $[Lu(\mathbf{27})(CH_3COO)(CH_3OH)](OH)(ClO_4)$ (b). (Reprinted from ref 147. Copyright 1986 American Chemical Society.)

tures of the two crystalline forms of the lutetium complex are shown in Figure 26, parts a and b, respectively.[147]

The yttrium(III) complex of **27** contains two different complex cations, $[Y(\mathbf{27})(CH_3COO)_2]ClO_4$ and $[Y(\mathbf{27})(CH_3COO)(H_2O)](CH_3COO)(ClO_4)$, present in a 1:1 mole ratio in the crystal lattice.[149] In each case the metal is 9-coordinate and is bonded to the six nitrogen donors of the macrocycle, which is slightly folded in a butterfly configuration. In addition, the metal ion is bonded to the two oxygen atoms of the bidentate acetate on the convex side of the macrocycle and to either a monodentate acetate or a water molecule on the opposite side. The coordination geometry is the same for both complex cations and is best described as a monocapped square antiprism and the capping position is occupied by the pyridine nitrogen. The macrocycle is folded in the direction of the singly coordinated ligand (water or acetate) with a dihedral angle of 115.7° and consists of two nearly planar sections with deviations from their best mean planes ranging from −0.17 to 0.20 Å. The metal coordination sphere is characterized by three slightly different pairs of yttrium−nitrogen bond lengths, the bonds of each pair being trans to each other. The X-ray crystal structures of the two crystalline forms of the yttrium complex are given in Figure 4. The structure of $[Lu(\mathbf{27})(CH_3COO)(H_2O)_{0.5}(CH_3OH)_{0.5}](OH)(ClO_4)(CH_3OH)_{0.5}$ is similar to that of the yttrium(III) complex, but differs only in the identity of the monodentate exocyclic ligands (50% monodentate acetate and 50% water for Y^{3+}, 50% CH_3OH and 50% water for Lu^{3+}) that occupy the axial coordination site on the concave side of the macrocycle. This facile interchange of neutral and anionic axial ligands within the crystal structure is consistent with the high lability of the exocyclic ligands observed in solution.

The crystal of the europium complex $[Eu(\mathbf{27})(NCS)_3]$[150] was also found to contain two distinct molecules having the same formula as well as the same metal coordination environment, but differing in the conformation of the macrocycle. The structures of the two molecules are illustrated in Figure 5. In both cases the macrocycle is hinged at the lateral units giving a folded butterfly configuration. The Eu^{3+} ion is bonded to the nitrogen donors of the three thiocyanate ions, two on the convex side of the macrocycle and the third on the opposite side. The coordination number of the metal ion in both cases is 9. The coexistence of two species with different stoichiometries and/or slightly different conformations appear to be a common feature in macrocyclic complexes of the lanthanides.[146,147,149,150,357,358] The structure of the yttrium(III) complex $[Y(\mathbf{27})(NCS)_3]$ is found to be isostructural with the europium analog and, similar to it, was characterized by the presence in the crystal lattice of two molecules of identical formula but different ligand conformations. The two planar halves of the macrocycle form an angle of 111.1° and 103.2° in the two molecules. The isothiocyanato ligands are coordinated in an angular fashion as has been observed in the europium analog. The coordination polyhedron in both the europium and yttrium complexes is based on an approximately planar pentagon defined by the two nitrogens of the pyridine rings and the three nitrogens of the NCS^- moieties. Two nitrogens of one diimine moiety are below this five-nitrogen plane and the nitrogens of the other diimine are above it.[150]

The crystal structures of $[Nd(\mathbf{27})(CH_3COO)_2]Cl{\cdot}4H_2O$ and $[Eu(\mathbf{27})(CH_3COO)_2]Cl{\cdot}4H_2O$ reveal a 10-coordination polyhedron for the metal ions, being bonded to the six nitrogen donors of **27** and to two bidentate chelating acetates situated on opposite sides of the macrocycle.[359] The two acetates are staggered and the angle between their planes is 94.8° in both complexes. The macrocycle has the folded butterfly configuration usually found in the lanthanide complexes of **27**.[135,146−150] The structures consist of two approximately planar sections containing the pyridine rings by hinging at the $-CH_2CH_2-$ side chains with dihedral angles of 132.82° for Nd^{3+} and 132.37° for Eu^{3+}. The orientation of the coordinated acetates

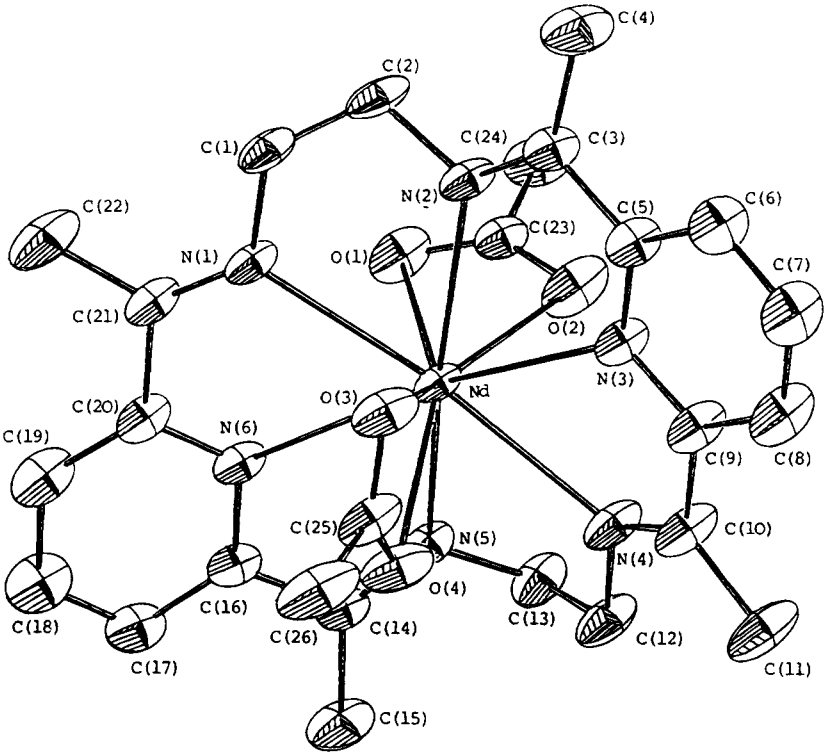

Figure 27. ORTEP view of $[Nd(\mathbf{27})(CH_3COO)_2]Cl{\cdot}4H_2O$. (Reprinted from ref 359. Copyright 1990 Pergamon Press Ltd.)

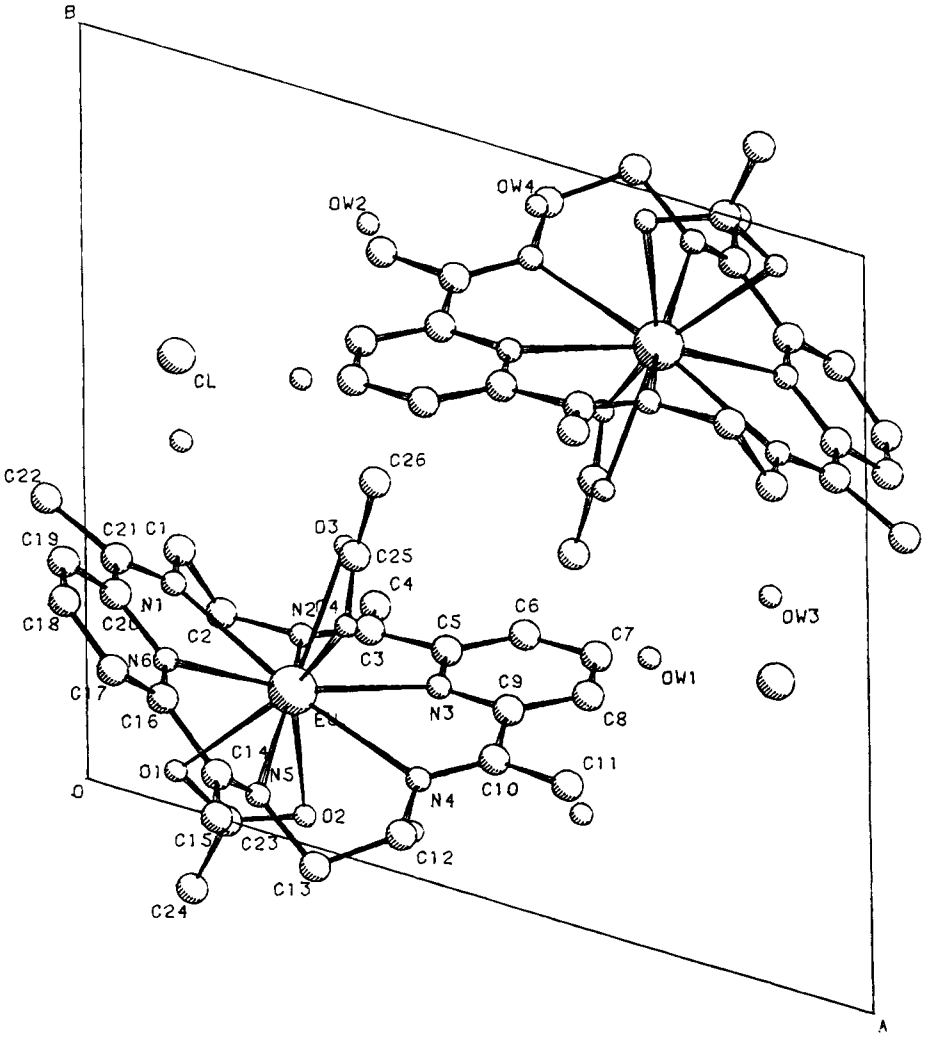

Figure 28. PLUTO view down C of the cell constant for $[Eu(\mathbf{27})(CH_3COO)_2]Cl{\cdot}4H_2O$. (Reprinted from ref 359. Copyright 1990 Pergamon Press Ltd.)

appears to be dictated primarily by steric requirements. Comparison of bond lengths shows that the metal–acetate distances are longer for neodymium (average $N-O_{acetate}$ = 2.514 Å) than for europium (average $Eu-O_{acetate}$ = 2.481 Å), in agreement with the decrease in metal ionic radius from Nd^{3+} to Eu^{3+}. In contrast, all metal–nitrogen distances are shorter for Nd^{3+} than for Eu^{3+}. The crystal structures of the neodymium and europium complexes are shown in Figures 27 and 28, respectively. A comparison between the X-ray crystal structures of the complex cations present in the triacetate complex [Eu(**27**)-$(CH_3COO)_2$]$(CH_3COO)\cdot 9H_2O$[29] and the diacetate–chloride complex [Eu(**27**)$(CH_3COO)_2$]$Cl\cdot 4H_2O$[359] reveals qualitative similarities and quantitative differences. In both compounds the macrocycle has the folded butterfly conformation common to other complexes of **27** and consists of two approximately planar sections that include the pyridine rings and are hinged at the $-CH_2CH_2-$ side chains. The folding of the macrocycle, however, is considerably more pronounced in the triacetate complex; the angle between the two planar sections being 122.50° vs 132.37° in the diacetate–chloride species. The torsion angles of the two $-CH_2CH_2-$ side chains of the triacetate complex differ significantly from the corresponding angles of the diacetate–chloride species. In both cases the two acetates are staggered and the acetate on the concave side of the macrocycle is oriented approximately along the fold line of the macrocycle and leans toward one of the two planar sections. The two $Eu-O_{acetate}$ bond lengths on the concave side of the macrocycle are more symmetrical and slightly longer than those on the convex side. In the triacetate complex the Eu–N bond lengths are shorter than that in the diacetate–chloride species. Clathrated water molecules (nine per complex unit) form an extensive network of hydrogen bonds that runs in channels through the crystal and includes the oxygen atoms of the coordinated and ionic acetates. An ORTEP view of the cation and anion units in [Eu(**27**)$(CH_3COO)_2$]$(CH_3COO)\cdot 9H_2O$[29] is shown in Figure 7. The crystal structure of [Gd(**27**)$(CH_3COO)_2$]-$Cl\cdot 4H_2O$[148] reveals that the metal ion is 10-coordinate. The metal ion lies 0.05 Å from the least-squares plane defined by the six nitrogens, and the mean deviation of the nitrogens from that plane is 0.36 Å. The acetate ions are coordinated on opposite sides of the metal ion, and the dihedral angle between the planes of the two $Gd(CH_3COO)_2$ fragments is 95.1°. As has been observed with the other lanthanide complexes of **27** the two diiminopyridine fragments are not coplanar. The conformation of the macrocycle across the lanthanide series ranges from being almost purely twisted for the lanthanum complex to primarily bent for the lutetium complex. The gadolinium complex appears to be some combination of these two extremes. These distortions would be expected to decrease the cavity size of the macrocycle relative to a planar form. The X-ray crystal structure of [Gd-(**27**)$(CH_3COO)_2$]$Cl\cdot 4H_2O$ is presented in Figure 3.

The samarium(III) complex [Sm(**30**)$(NO_3)(OH)$-(H_2O)]$NO_3\cdot 2CH_3OH$[143] is the solitary example of the complex of **30** for which X-ray crystal structure is available. The metal ion is 10-coordinate, being

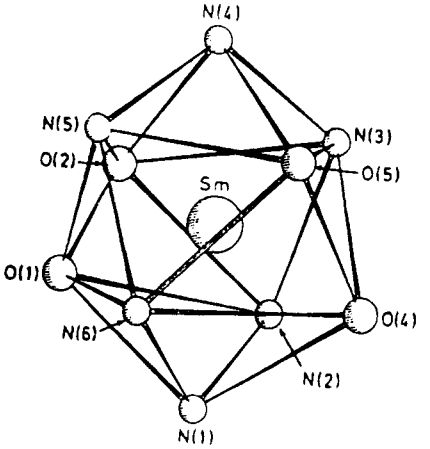

Figure 29. Coordination polyhedron around Sm^{3+} in [Sm-(**30**)$(NO_3)(OH)(H_2O)$]$NO_3\cdot 2CH_3OH$. (Reprinted from ref 143. Copyright 1984 Royal Society of Chemistry.)

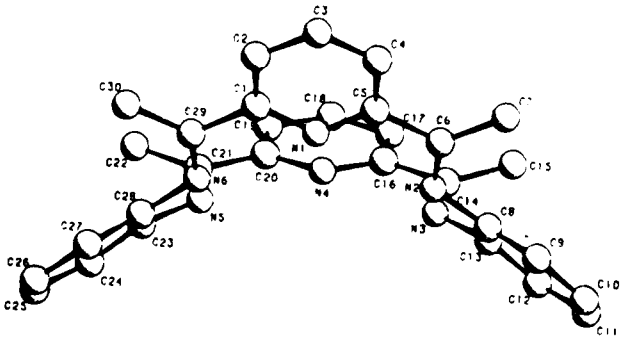

Figure 30. Conformation of the macrocyclic ligand **34** in [Pr(**34**)$(NO_3)_2(CH_3OH)$]ClO_4. (Reprinted from ref 155. Copyright 1989 American Chemical Society.)

bonded to the six nitrogen donors of the macrocycle, to the bidentate nitrate ion on one side of the macrocycle, and to the hydroxyl ion and to the water molecule on the other side. The coordination polyhedron can be described as an irregular antiprism capped on its square faces by the pyridine nitrogen donors. The $Sm-N_{pyridine}$ bond lengths are significantly longer than the $Sm-N_{imine}$ bond lengths, and all the Sm–N distances are shorter than those found in [La(**27**)$(NO_3)_3$]. The differences may be due to the different coordination number in the complexes as well as to the diminished radius of the central metal ion. The X-ray crystal structure of the samarium complex and the coordination polyhedron around the samarium ion are shown in Figures 2 and 29, respectively.

The only known complex of **34** for which X-ray crystal structure is available is the praseodymium-(III) complex [Pr(**34**)$(NO_3)_2(CH_3OH)$]ClO_4.[155] The metal ion is 11-coordinate. The macrocycle is folded with the two pyridine rings directed away from the hemisphere containing the NO_3^- and CH_3OH ligands. The molecular structure is shown in Figure 8. The conformation of the macrocycle, shown in Figure 30, is fairly symmetrical and is characterized by a dihedral angle of 110.3° between the planes of the two pyridine rings and by a dihedral angle of 112.0° between the planes of the two *o*-phenylene rings. This extensive bending prevents conjugation among the four aromatic sections of the macrocycle. The torsion angles indicate that the *o*-phenylene groups consider-

ably reduce the flexibility of the macrocycle compared to that of the ligand **27**, in which the $=NCH_2CH_2N=$ side chains function as adjustable hinges. A comparison of the crystallographic data of the lanthanide complexes of **27** indicates that the M−N bond lengths decrease fairly regularly as the metal ionic radii decrease along the lanthanide series. In the Pr^{3+} complex of **34**, however, all the M−N bonds become equal within the limits of their standard deviations. Thus, the greater rigidity of **34** results in an increased regularity in the metal−nitrogen bond lengths. The dihedral angle between the halves of the macrocycle containing the pyridine rings also decrease with decreasing metal ion radius, but the variation is far from regular. For the ligand **27**, the change in angle is 32° from La^{3+} to Ce^{3+} (Δionic radius 0.03 Å), 5° from Ce^{3+} to Nd^{3+} (Δionic radius 0.04 Å), and 2° from Nd^{3+} to Lu^{3+} (Δionic radius 0.15 Å). In the Pr^{3+} complex of **34** the py−py dihedral angle is 11° smaller than that of the Ce^{3+} complex of **27**, even though the difference in the metal ion radius is less than 0.02 Å. The folding of the macrocycle is the result of various cooperative factors, of which the rigidity of the ligand, the size of the metal ion, and the number and bulk of the exocyclic ligands appear to be the most important.

It is instructive to compare the bending of the macrocycle **27** in the various lanthanide complexes. The values of the macrocyclic folding (dihedral angles) together with the coordination numbers, ionic radii of the central metal ions, the average Ln−N and Ln−O bond lengths are given in Table 4. The conformational differences observed among the various complexes of the macrocycle **27** has been attributed to changes in the metal center, number and steric requirements of the exocyclic ligands, and also by interaction with species present in the outer-coordination sphere. For the nitrato complexes, the progressive departure from planarity from lanthanum(III) to neodymium(III) is due to the requirement to maintain 6-coordination as the radius of the central metal ion decreases.[146] A similar trend is observed for the yttrium(III)[149] and lutetium(III)[147] with acetates as anionic ligands. In contrast, for the isothiocyanato complexes, the folding of the macrocycle does not match with the values of the ionic radii.[150] Furthermore, the presence of two complex entities within the same crystal having the same formula but different macrocycle conformations suggest that the NCS^-, being less bulky than either nitrate or acetate, allows a greater flexibility of the macrocycle. The near-identical folding of the macrocycle in the yttrium(III) and europium(III) complexes, which is not observed in the other yttrium and lanthanide complexes containing O-donor exocyclic ligands, is due to the remarkable stability of the nine nitrogen coordination sphere. The coexistence of different macrocycle conformations within the same crystal suggests the operation of several cooperative factors that include not only the ionic radius of the metal ion but also the crystal packing forces and steric requirements of the exocyclic ligands.

A comparison of the crystal structures of the lanthanide complexes of related macrocycles points to some interesting generalizations. In the crystalline complexes the coordinated exocyclic anionic ligands are bound to the central metal ion more strongly than the nitrogen donors of the macrocycle, and this is true for both oxygen and nitrogen donor ligands. This observation confirms the kinetic origin of the extreme resistance to decomposition of the $[ML_6]$ (L_6 = macrocycle) entity, compared to the ease of exchange of the exocyclic anions.[359] Second, the folding of the macrocycle appears to be a consequence of the ligand buckling to accommodate the metal ion and to maintain the hexadentate coordination rather than being the result of different steric requirement of the exocyclic ligands on either side of the macrocycle: the folding of the macrocycle allows close approach of the exocyclic ligands and is always in the direction of the hemisphere containing the single exocyclic ligand. The noncoplanarity of the macrocycle increases in the same sequence as does the coordination number. Third, the presence of at least one anionic exocyclic ligand in the primary coordination sphere suggests that its coordination greatly contributes to the stability of the complexes and will occur whenever a suitable anion is present. Coordination of additional anionic ligands appears to be controlled by a fine balance of steric requirements and/or crystal lattice effects.

The europium complex $[Eu(\mathbf{46})(NO_3)_2]NO_3$[173] consists of two isostructural crystalline forms (yellow and red) which is isomorphous with the terbium analog, $[Tb(\mathbf{46})(NO_3)_2]NO_3$,[173] and the differences are ascribed to the larger ionic radius of Eu^{3+} with respect to Tb^{3+}. The crystal structures of the terbium and europium complexes are presented in Figures 9 and 10, respectively. In both these complexes the metal ion is 9-coordinate. The $Eu-O_{nitrate}$ mean bond length (2.50 Å), $Eu-O_{macrocycle}$ mean bond length (2.28 Å), and $Eu-N_{macrocycle}$ mean bond length (2.57 Å) are longer than those found in the terbium complex. (Mean bond lengths are 2.46, 2.25, and 2.54 Å, respectively.) The coordination polyhedron around the metal ions may be described as a distorted tricapped trigonal prism. Distortions from the idealized geometry mainly arise from the asymmetry of the pentadentate ligand and from the geometrical constraints due to the rigid structure of the nitrate groups. It is noteworthy that the Ln−O distances with the macrocycle are significantly shorter than the corresponding distances with the chelating nitrate groups. This indicates that the $Ln-O_{nitrate}$ distances are largely determined by the geometry of the ligands. The pentagon formed by the three nitrogen and two oxygen donors of the macrocycle presents the same distortion around the europium and terbium ions. The distortion of the macrocycle and the coordination polyhedron around terbium ion are depicted in Figure 31, parts a and b, respectively.

The octadentate ($S_2N_4O_2$) macrocycle **47** coordinates with UO_2^{2+} as a pentadentate ligand with severe deviations of atoms from the equatorial plane due to structural constraints. The crystal structure of $[UO_2(\mathbf{47})]$[212] is shown in Figure 19. The five donor atoms of the ligand form a strongly puckered pentagon. Although the molecule has no imposed symmetry, the two wings of the ligand are symmetrical, forming dihedral angles of 40° and 47° with the

Table 4. X-ray Crystallographic Data (Coordination Number, Ln–N and Ln–O Bond Lengths, Dihedral Angle of the Folding of the Macrocycle) of Lanthanide Complexes of "2 + 2" Macrocycles Derived from Pyridine Head Units and Aliphatic and Aromatic Lateral Units

complex	CN	ionic radii,[a] Å	Ln–N(py), Å		Ln–N(imine), Å		Ln–O(exocyclic ligands), Å		dihedral angle[c]	ref
			bond lengths[b]	average	range[b]	average	range[b]	average		
[La(**27**)$(NO_3)_3$]	12	1.061	2.764, 2.746	2.755	2.672–2.729	2.706	2.689–2.767	2.726	153.3	146
[Ce(**27**)$(NO_3)_2(H_2O)$]$(NO_3)\cdot H_2O$	11	1.034	2.726, 2.637	2.682	2.617–2.720	2.670	2.648–2.745 (NO_3), 2.569 (H_2O)	2.692	121	146
[{Nd(**27**)$(NO_3)(H_2O)_2\}_2$]$NO_3(ClO_4)_3\cdot 4H_2O$	10	0.995	2.614, 2.628	2.621	2.573–2.671	2.610	2.598, 2.617 (NO_3) 2.493, 2.516 (H_2O)	2.608 2.505	116.1	146
[Lu(**27**)$(CH_3COO)(H_2O)_{0.5}(CH_3OH)_{0.5}$]$(ClO_4)(OH)(CH_3OH)_{0.5}$[d]	9	0.848	2.555, 2.552	2.554	2.471–2.608	2.540	2.325, 2.368 (OAc), 2232 (H_2O)	2.347	114.4	147
[Y(**27**)$(CH_3COO)_{1.5}(H_2O)_{0.5}$]$(CH_3COO)_{0.5}ClO_4$[e]	9	1.075[f]	2.579, 2.584	2.582	2.498–2.623	2.567	2.355, 2.415 (OAc[g]), 2.274 (OAc[h] or H_2O)	2.385	115.7	149
[Eu(**27**)$(NCS)_3$][i]	9	0.950	2.656, 2.542	2.599	2.489–2.668	2.572	2.475–2.527 (NCS)	2.505	111.3	150
[Eu(**27**)$(NCS)_3$][i]	9	0.950	2.719, 2.569	2.649	2.560–2.639	2.601	2.411–2.439 (NCS)	2.426	102.1	150
[Gd(**27**)$(CH_3COO)_2$]$Cl\cdot 4H_2O$	10	0.938	2.627, 2.642	2.635	2.565–2.654	2.616	2.442–2.494 (OAc)	2.467		148
[Nd(**27**)$(CH_3COO)_2$]$Cl\cdot 4H_2O$	10	0.995	2.587, 2.591	2.589	2.609–2.640	2.624	2.498–2.545 (OAc)	2.514	132.86	359
[Eu(**27**)$(CH_3COO)_2$]$Cl\cdot 4H_2O$	10	0.950	2.638, 2.639	2.639	2.590–2.665	2.632	2.458–2.505 (OAc)	2.481	132.37	359
[Y(**27**)$(NCS)_3$][j]	9	1.075[f]	2.58, 2.57	2.575	2.50–2.63	2.565	2.39–2.49 (NCS)	2.427	111.1	150
[Y(**27**)$(NCS)_3$][j]	9	1.075[f]	2.65, 2.55	2.60	2.46–2.72	2.558	2.35–2.53 (NCS)	2.427	103.2	150
[Sm(**30**)$(OH)(H_2O)(NO_3)$]$NO_3\cdot 2CH_3OH$	10	0.964	2.66, 2.65	2.655	2.60–2.64	2.62	2.51, 2.52 (NO_3), 2.46 (H_2O), 2.52 (OH^-)	2.515		143
[Pr(**34**)$(NO_3)_2(CH_3OH)$]ClO_4	11	1.013	2.651, 2.661	2.656	2.657–2.681	2.669	2.557–2.705 (NO_3) 2.592 (CH_3OH)	2.657	113.0[k] 112.1[l]	155
[Eu(**27**)$(CH_3COO)_2$]$(CH_3COO)\cdot 9H_2O$	10	0.950	2.613, 2.599	2.604	2.568–2.649	2.606	2.454–2.519 (OAc)	2.49	122.50	29
[{Eu(**27**)$(CH_3COO)\}_2(\mu\text{-}CO_3)$]$(OH)_2\cdot 7H_2O$[m]	10	0.950	2.64, 2.63	2.635	2.56–2.66	2.608	2.52, 2.55 (OAc) 2.493, 2.394 (CO_3)	2.535 2.444	131.8	151

[a] Taken from Shannon, R. D.; Prewitt, C. T. *Acta Crystallogr., Sect. B* **1969**, *25*, 925. [b] Esd's which are available for a few cases are not indicated for the sake of uniformity. [c] Dihedral angle is otherwise referred as wing's angle. [d] The crystal lattice consists of two species having the structural formula [Lu(**27**)$(CH_3COO)(CH_3OH)$]$(ClO_4)(OH)$ and [Lu(**27**)$(CH_3COO)(H_2O)$]-$(ClO_4)(OH)(CH_3OH)$. [e] The complex exists as two different complex cations, [Y(**27**)$(CH_3COO)_2$]ClO_4 and [Y(**27**)$(CH_3COO)(H_2O)$]$(CH_3OH)ClO_4$. [f] According to Shannon for IX coordination: Shannon, R. D. *Acta Crystallogr., Sect. A: Cryst. Phys., Diffraction Theor. Gen. Cryst.* **1976**, *A32*, 751. [g] Bidentate acetate. [h] Monodentate acetate. [i] The crystal lattice contains two distinct molecules having the same formula as well as the same 9-coordinate metal coordination environment, but differing in the conformation of the macrocycle. [j] X-ray analysis of the complex shows the coexistence in the same crystal of two kinds of 9-coordinate molecules with different macrocyclic conformations. [k] Dihedral angle between the two halves of the pyridine rings. [l] Dihedral angle between the two halves of the benzene rings. [m] The dimeric complex cation consists of two Eu(**27**) moieties linked through a bridging as well as chelating carbonate.

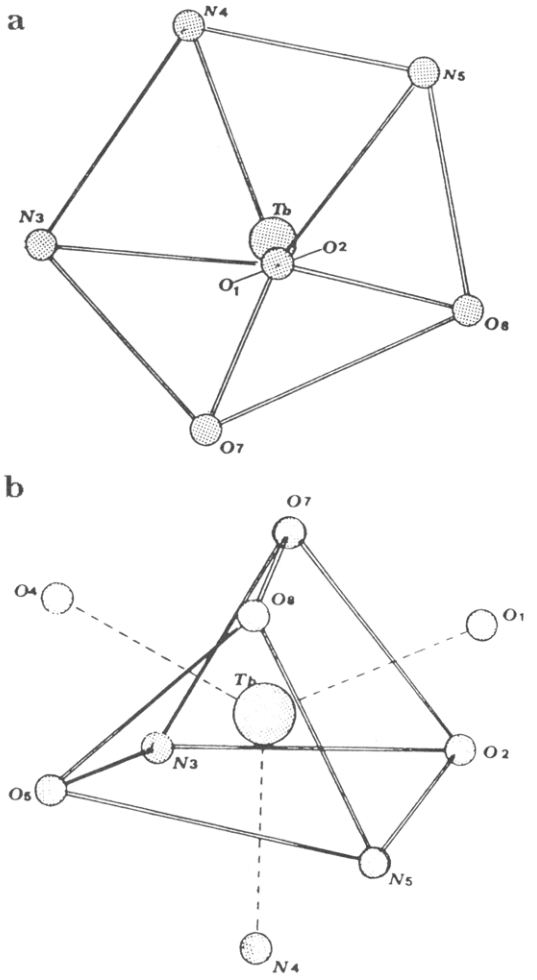

Figure 31. The crystal structure of [Tb(**46**)$(NO_3)_2$]NO_3. The five donor atoms of the macrocycle form a distorted pentagon around Tb. (a) The coordination polyhedron around Tb in [Tb(**46**)$(NO_3)_2$]NO_3 (b) can be described as a distorted tricapped trigonal prism. (Reprinted from ref 173. Copyright 1987 Elsevier Sequoia.)

coordinated plane. The wings are strongly inclined to each other so that the ligand has the shape of an umbrella as shown in Figure 32. The peculiar conformation of the ligand and the reciprocal position of the available donor atoms indicate that it would be difficult for a second metal ion to be coordinated. Indeed, attempts to synthesize the homodinuclear uranyl complex was not successful. The uranyl complex of the hexadentate pyrrole derived macrocycle **26**[131] is the only known example of an actinide complex in which the metal ion is coordinated in a planar fashion. The complex is remarkably planar and the coordination geometry around the uranyl atom is hexagonal bipyramid. The presence of a regular polyhedron structure around the actinide ion overthrows the speculation that it would be futile to try to define lanthanide and actinide complexes in terms of a particular polyhedron.

B. Structural Features of Lanthanide Complexes of Macrocyclic Polyamino Carboxylates

The structure of Na[Eu(**106**)(H_2O)][301] is shown in Figure 33a. The macrocycle forms a shell around the europium ion, which is linked to the four nitrogen atoms and to the four carboxyl oxygen atoms of the

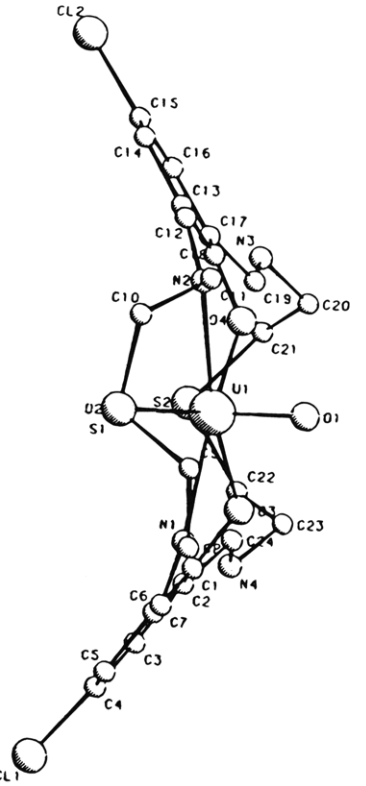

Figure 32. Crystal structure of [UO_2(**47**)]: the two wings of the ligand are inclined with respect to the coordination plane. (Reprinted from ref 212. Copyright 1986 Elsevier Sequoia.)

ligand. It is also bonded to one water molecule attaining the coordination number of 9. The variation among the Eu–N and Eu–O distances are statistically significant and ranges from 2.519 to 2.900 Å and from 2.247 to 2.511 Å, respectively. As expected, the Eu–N distances are much longer than the Eu–O distances. The coordination polyhedron about europium is best described in terms of a distorted capped square antiprism: the donor atoms of **106** are at the vertices of the two square bases and the water oxygen is in the axial position as shown in Figure 33b. The two planes are parallel within 0.25°, and the europium ion is displaced by 0.7 Å from the second plane toward the inside of the shell of **106**. The complex adopts a very crowded conformation and appears to be highly strained as evidenced by marked deviation from the expected values of several valency angles and of the bond lengths. No such effects have been observed in the case of the terbium complex of **107**, a ligand which is similar to **106** but exhibits a larger internal cavity. The terbium ion in Na[Tb(**107**)]·$6H_2O$·0.5NaCl[286] is completely encapsulated by the macrocycle and is linked to the four nitrogen donors and to the four carboxylic groups of the ligand. The coordination polyhedron is a severely distorted dodecahedron. The terbium ion is found 1.249 Å above the mean plane of the nitrogen atoms and 1.212 Å below the mean plane of the oxygen atoms. The maximum deviations from the mean Tb–N (2.599 Å) and Tb–O (2.315 Å) distances are 0.024 and 0.015 Å, respectively, i.e., much smaller than reported for Na[Eu(**106**)(H_2O)]. Thus, the larger size of the internal cavity of the macrocycle **107** brings about no significant changes in the metal–donor atom distances. However, **107** is more flexible and

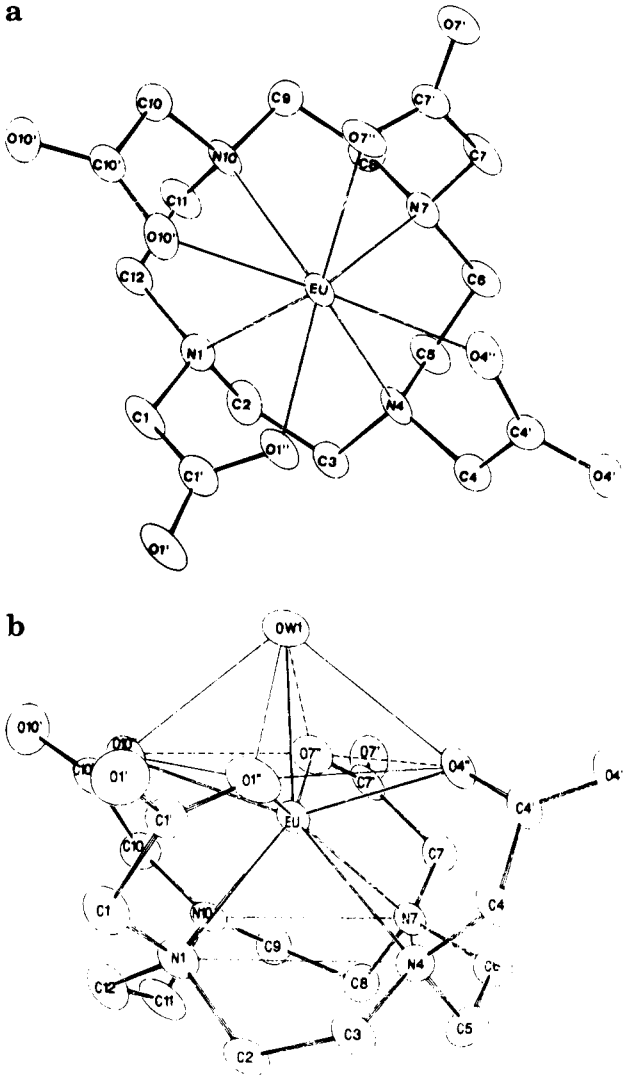

Figure 33. Perspective view of the Na[Eu(**106**)(H_2O)] (a) and the coordination polyhedron in Na[Eu(**106**)(H_2O)] (b). (Reprinted from ref 301. Copyright 1984 American Chemical Society.)

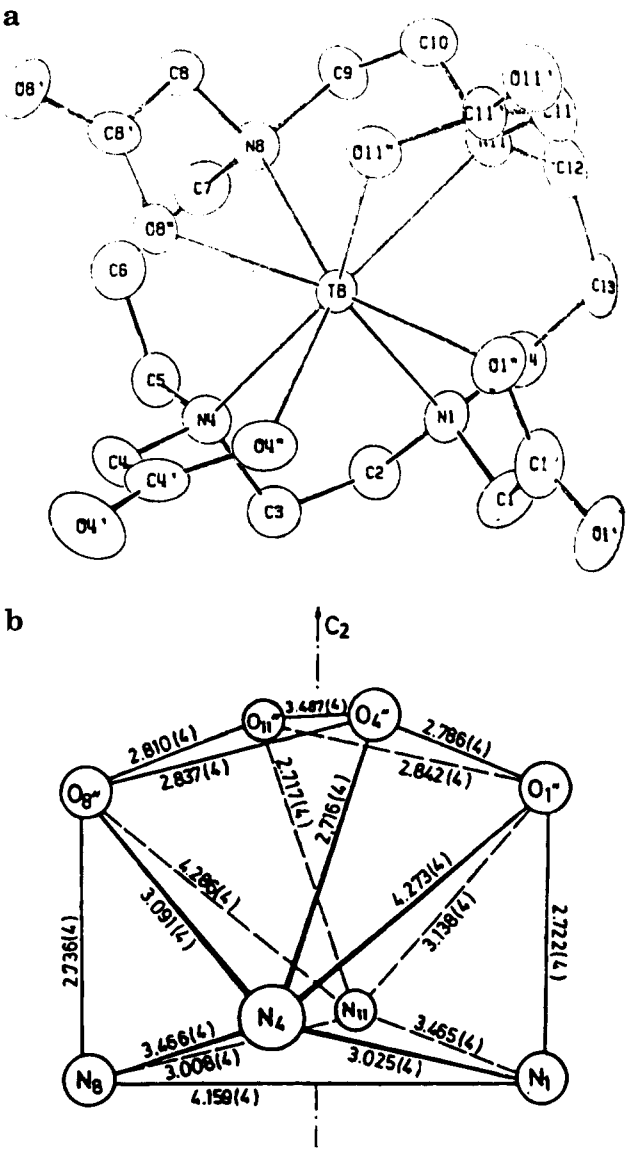

Figure 34. Perspective view of the Na[Tb(**107**)]·$6H_2O$·0.5NaCl (a) and coordination polyhedron about the terbium ion in Na[Tb(**107**)]·$6H_2O$·0.5NaCl (b). (Reprinted from ref 286. Copyright 1984 American Chemical Society.)

can wrap itself around the terbium ion in a more effective way. Accordingly, the hydration numbers of [Eu(**106**)]$^-$ and [Tb(**107**)]$^-$ are different. The complex of **106** is found to be monohydrated both in the crystal[301] and in solution; their square antiprismatic structures leave enough room for coordination by a water molecule. On the contrary, in the dodecahedral conformation of [Tb(**107**)]$^-$ the oxygen atoms are in close contact; they are not separated by more than two van der Waals radii and there is no space left for a water molecule. The X-ray crystal structure of the terbium complex and the coordination polyhedron about the terbium ion are depicted in Figure 34, parts a and b, respectively.

The complexes Na[Ln(**106**)(H_2O)]·$4H_2O$ (Ln = Y,[360] Eu,[301] and Gd[361]) are crystallographically isostructural and have similar geometries. The 9-coordinate metal in the C_4 symmetric anion is coordinated to the four nitrogens and an oxygen atom from each of the four carboxylate arms of the macrocyclic ligand. The ninth coordination site is occupied by a water molecule which caps the square antiprismatic arrangement of the other ligating atoms. The X-ray crystal structure of Na[Y(**106**)(H_2O)]·$4H_2O$ is depicted in Figure 35. The 16-membered macrocycle **100** forms the mononuclear gadolinium complex [Gd(**100**)(H_2O)]·$3H_2O$ in which the metal ion is 9-coordinate, being bonded to two amide oxygen atoms, three carboxylate oxygen atoms, and three amine nitrogen atoms of the macrocycle and a water oxygen. The coordination polyhedron around the metal ion is described as a distorted tricapped trigonal prism.[220] The crystal structure of [Gd(**100**)(H_2O)]·$3H_2O$ is shown in Figure 36.

The structure of [Gd(**121**)(H_2O)][313] shows a 9-coordinate stereochemistry for Gd^{3+}. The coordinating sites are occupied by the four amine nitrogens, three carboxylate oxygens, one carboxamide oxygen, and the water oxygen. The coordination polyhedron can be described as a distorted square antiprism capped with the coordinated water oxygen in the axial position. The X-ray crystal structure of the complex and the coordination polyhedron about the Gd^{3+} ion are shown in Figure 37, parts a and b, respectively.

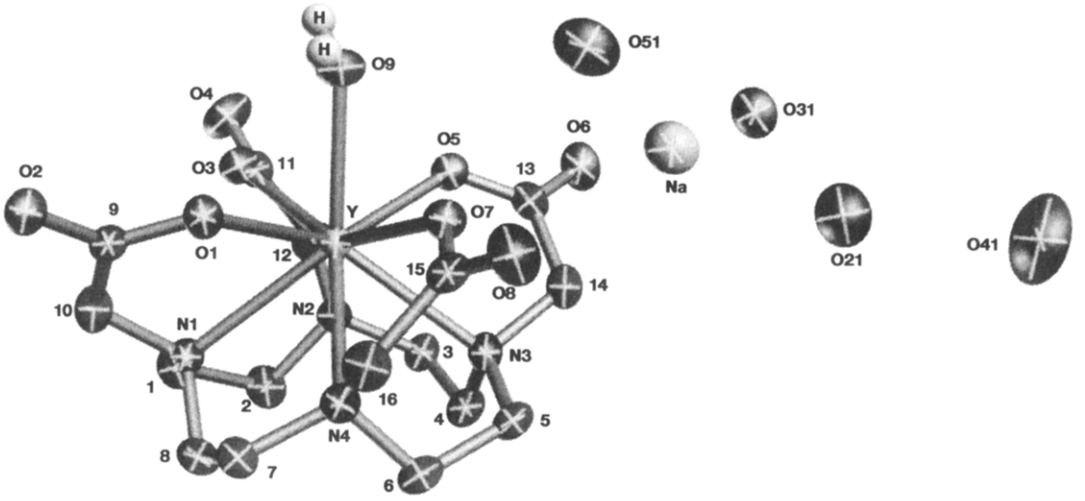

Figure 35. Solid state conformation of the Na[Y(**106**)(H_2O)]·4H_2O complex. All nonhydrogen atoms are represented by (50% probability) ellipsoids consistent with refined anisotropic thermal parameters. (Reprinted from ref 360. Copyright 1993 American Chemical Society.)

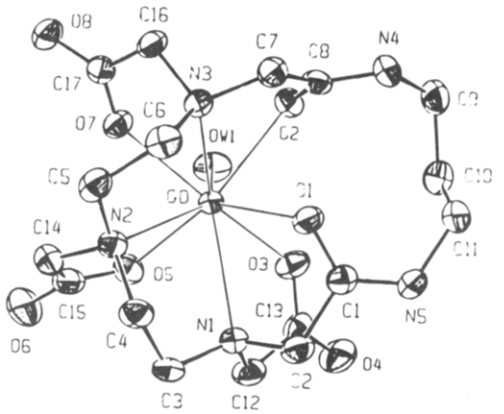

Figure 36. Structure of [Gd(**100**)(H_2O)]·3H_2O. Atoms are shown at the 50% probability level. (Reprinted from ref 220. Copyright 1993 Elsevier Sequoia.)

The Gd−O distances (Gd−O_{av} = 2.37 Å) are significantly shorter than those observed for the Gd−N bonds (Gd−N_{av} = 2.67 Å). The coordinated water oxygen is at 2.43 Å from the gadolinium atom, and this value is comparable with the Ln−OH_2 distances observed in other complexes. The four nitrogen and the oxygen donors of the macrocycle coordinated to gadolinium lie in two mean planes. The two planes are parallel within 0.5°.

The crystal structure of the gadolinium(III) complex of the triaza trioxa triacetic acid **129**[323] has a propeller conformation with no crystallographically imposed symmetry. The gadolinium atom lies within the macrocycle and is 9-coordinate, being bonded to the three nitrogen, three oxygen, and the three acetate oxygen donors of the macrocycle. The shortest contacts are the Gd−$O_{acetate}$ bonds, in the range of 2.31−2.34 Å. The Gd−O_{ether} bond lengths are comparable to those found in the 9-coordinate dichloro(ethanol)(18-crown-6)gadolinium(III) chloride.[362] The molecular structure of [Gd(**129**)] is presented in Figure 38.

In the crystal structure of [Gd(**130**)]$_3$·Na_2CO_3·17H_2O,[360] the three crystallographically independent Gd(**130**) units have essentially the same structure, conformation, and chirality. The four nitrogens and

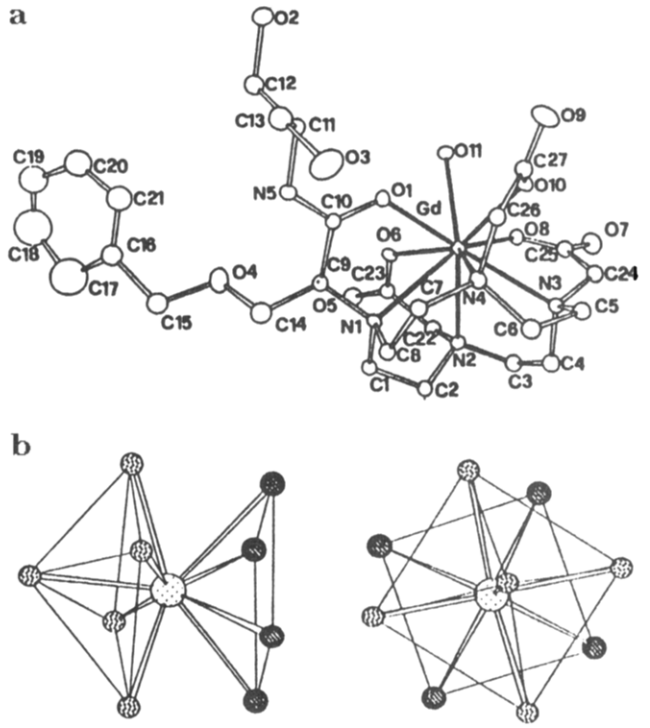

Figure 37. ORTEP drawing of [Gd(**121**)(H_2O)] (a) and coordination polyhedron formed by the ligand atoms about the Gd^{3+} ion in [Gd(**121**)(H_2O)] (b). (Reprinted from ref 313. Copyright 1992 American Chemical Society.)

an oxygen from each of the three carboxylate arms bind the ligand to the metal. The eighth and ninth coordination sites for all three Gd(**130**) units are occupied by a single carbonate ion. No water molecule is coordinated to the gadolinium atoms in the crystal structure. The X-ray crystal structure of [Gd(**130**)]$_3$·Na_2CO_3·17H_2O is shown in Figure 39. The trimeric arrangement appears to gain some additional stability from the interaction of each secondary N−H group with a carboxylate oxygen from another Gd(**130**) unit in the trimer. The two sodium ions cap the trimer at the opposite ends through coordination to carboxylate oxygens.

The X-ray crystal structure of Gd(**133**)[329] shows that in the solid state two crystallographically inde-

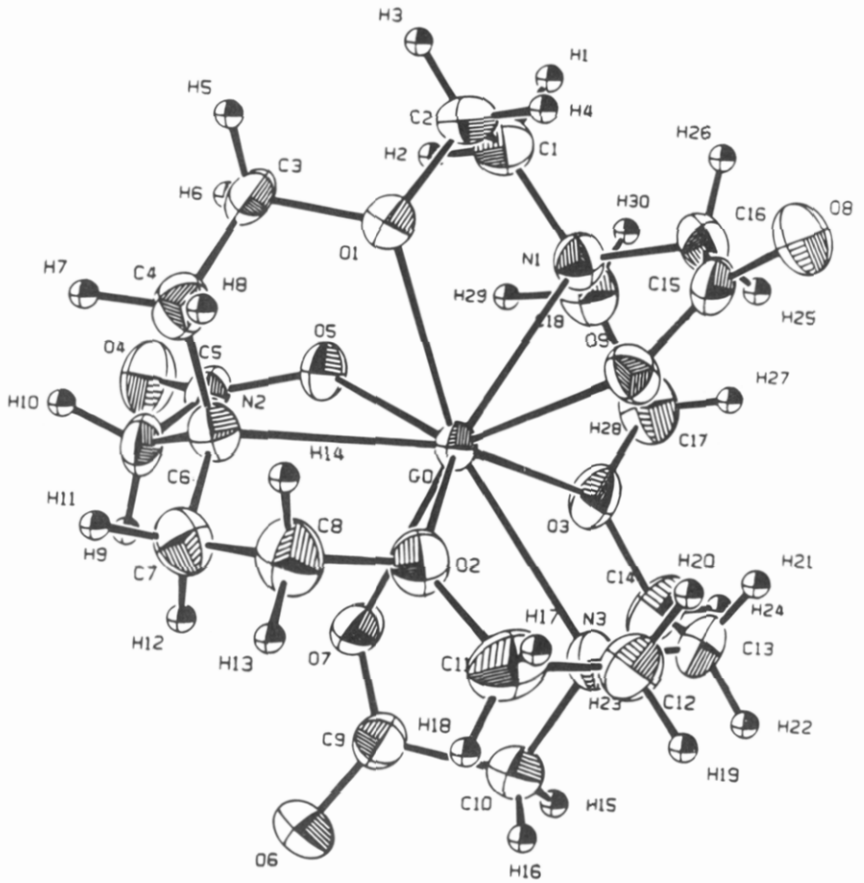

Figure 38. ORTEP diagram of the X-ray crystal structure of [Gd(**129**)]. Thermal ellipsoids are shown at the 50% probability level. (Reprinted from ref 323. Copyright 1990 American Chemical Society.)

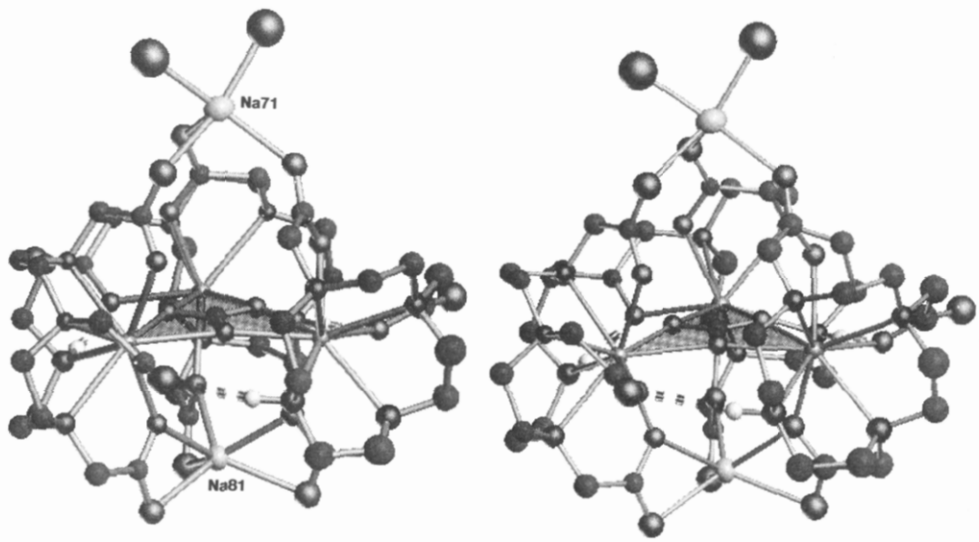

Figure 39. Stereoscopic drawing of the $[Gd(\mathbf{130})]_3 \cdot Na_2CO_3 \cdot 17H_2O$ complex. Only the two water molecules associated with the external sodium atom (top) are shown. Atoms are represented by (50% probability) surfaces consistent with refined thermal parameters. (Reprinted from ref 360. Copyright 1993 American Chemical Society.)

pendent Gd(**133**) complexes and two water molecules are joined to form a dimeric unit. For each independent Gd(**133**) unit the macrocycle adopts a distorted quadrangular [3333] conformation. An oxygen atom from each of the three carboxyl arms and the four essentially coplanar nitrogens of the macrocycle are coordinated to the embedded gadolinium atom. The three $Gd-N_{tert}$ distances (2.66 Å) are longer than the $Gd-N_{sec}$ distance (2.58 Å). In addition to the seven ligating atoms of the ligand, two other external oxygens are also coordinated to the metal, thus the metal ion is 9-coordinate. One of the external oxygen atoms lies approximately in the equatorial plane of the three coordinating carboxyl oxygens while the other external oxygen atom occupies the apical position. All bond lengths are averaged over the two complex units and presented in Table 5. The gadolinium atom lies 1.62 Å above the least-squares plane of the nitrogens, and 0.83 Å below the least-squares plane of the four equatorial oxygen atoms. The apical

Table 5. X-ray Crystallographic Data of Macrocyclic Complexes of Lanthanides and UO_2^{2+}

complex	CN	ionic radii,[a] Å	M−N(macrocycle), Å		M−O(macrocycle), Å		M−O(exocyclic), Å		ref
			range[b]	average	range[b]	average	bond lengths[b]	average	
[UO_2(**26**)]	8[c]		2.418−2.748	2.633[d]			1.770 (UO_2)[e]		131
[Eu(**46**)(NO_3)$_2$]NO_3	9	0.950	2.54−2.58	2.56	2.28, 2.28	2.28	2.48−2.53 (NO_3)	2.49	175
[Tb(**46**)(NO_3)$_2$]NO_3	9	0.923	2.52−2.55	2.54	2.26, 2.24	2.25	2.42−2.51 (NO_3)	2.458	173
[UO_2(**47**)]	7		2.60, 2.54	2.57	2.22, 2.25	2.235			212
[La(**63**)(CF_3SO_3)$_2$](CF_3SO_3)·CH_3CN	10	1.061	2.669−2.816	2.734			2.585, 2.632 (CF_3SO_3)	2.609	179
[Yb(**63**)(CF_3SO_3)](CF_3SO_3)$_2$·CH_3CN	9	0.859	2.442−2.611	2.523			2.390 (CF_3SO_3)		179
[La(**66**)(NO_3)$_2$(CH_3OH)]	10	1.061	2.484−2.685	2.584			2.640−2.749 (NO_3) 2.722 (CH_3OH)	2.677	133
[Gd(**66**)(NO_3)$_2$(CH_3OH)][f]	10	0.938	2.404−2.579	2.494			2.508−2.649 (NO_3) 2.512 (CH_3OH)	2.601	133
[Eu(**67**)(NO_3)(CH_3OH)$_2$]$^+$	9	0.950	2.388−2.538	2.468			2.495, 2.499 (NO_3) 2.491 (CH_3OH)	2.497	133
[Gd(**67**)(NO_3)(CH_3OH)$_2$]$^+$	9	0.938	2.383−2.536	2.464			2.489, 2.484 (NO_3) 2.491 (CH_3OH)	2.487	133
[Lu(**68**)(NO_3)(CH_3OH)]$^+$	8	0.848	2.312−2.455	2.388			2.378, 2.373 (NO_3) 2.269 (CH_3OH)	2.376	133
[Gd$_2$(**96**)(NO_3)$_4$]·7H_2O	10	0.938	2.46, 2.70	2.58	2.34−2.68	2.495	2.47−2.67 (NO_3)	2.543	217
[Gd$_2$(**99**)$_2$(H_2O)$_2$]·14H_2O[g]	9	0.938	2.611−2.915[h]	2.762	2.449, 2.406 2.380−2.381	2.428[i] 2.381[j]	2.412 (H_2O)		220
[Gd(**100**)(H_2O)]·3H_2O	9	0.938	2.618−2.748[h]	2.677	2.451, 2.439 2.332−2.391	2.445[i] 2.365[j]	2.474 (H_2O)		220
[La$_3$(**101**)(μ_3-OH)(OH)(NO_3)$_4$]·7H_2O[k]	9	1.061	2.697−2.880	2.755	2.383−2.571	2.473	2.371−2.745[l]	2.584	224
Na[Eu(**106**)(H_2O)]·4H_2O	9	0.950	2.519−2.900	2.680	2.247−2.511	2.393[j]	2.480 (H_2O)		301
Na[Y(**106**)(H_2O)]·4H_2O	9		2.633−2.666	2.646	2.316−2.327	2.323	2.435 (H_2O)		360
Na[Tb(**107**)]·6H_2O·0.5NaCl	8	0.923	2.575−2.620	2.599	2.302−2.330	2.315[j]			286
[Gd(**121**)(H_2O)]	9	0.938	2.627−2.719	2.675	2.337−2.392	2.367[j]	2.429 (H_2O)		313
[Gd(**129**)]	9	0.938	2.641−2.686	2.656	2.467−2.609 2.310−2.341	2.528 2.326[j]			323
[Gd(**130**)]$_3$·Na_2CO_3[m]	9[n]	0.938	2.56−2.63	2.595	2.34−2.35	2.35[j]			360
[Gd(**131**)(H_2O)]$_2$[o,p]	9	0.938		2.66[q] 2.58[r]		2.35[j]	2.451 (H_2O)$_{equatorial}$ 2.56 (H_2O)$_{axial}$		329

[a] Taken from Shannon, R. D.; Prewitt, C. T. *Acta Crystallogr., Sect. B* **1969**, *25*, 925. [b] Esd's which are available for a few cases are not indicated for the sake of uniformity. [c] Six nitrogen donors of the macrocycle and two oxygens of the uranyl ion. [d] The U−N bond lengths presented are only for three adjacent U−N bonds. [e] Oxygen atoms of the uranyl ion. [f] The complex has two distinct crystal structures in the unit cell. The 10-coordinate species is coordinated to the five nitrogen donors of the texaphyrin, two bidentate nitrate ions, and a molecule of methanol. The 9-coordinate species is bound to the five nitrogen donors of the texaphyrin, one bidentate nitrate ion, and to two molecules of methanol. [g] The data presented are for each [Gd(**99**)(H_2O)]·7H_2O unit. [h] Amine nitrogen donor of the macrocycle. [i] Amide oxygen donor of the macrocycle. [j] The acetate pendant arm of the macrocycle. [k] Each lanthanum is coordinated to three nitrogens and two oxygen donors of the macrocycle and to the oxygen donors of OH^-, NO_3^-, or H_2O. The average of the three La−X values are given. [l] Oxygen donors of OH^-, NO_3^-, or H_2O. [m] The data given are for each of the three crystallographically independent |Gd(**130**)| units. [n] The eighth and ninth coordination sites for all the three Gd(**130**) units are filled by a single carbonate ion. [o] In the solid state, two crystallographically independent Gd(**131**) complexes and two water molecules are joined to form a dimeric unit. The two external oxygen ligands (one equatorial and one axial) are water molecules in one complex, while in the other complex the two external oxygens are donated by a bridging carboxyl group of the other complex. [p] Only the average Gd−X distances are given. [q] Tertiary Nitrogen donor of the macrocycle. [r] Secondary Nitrogen donor of the macrocycle.

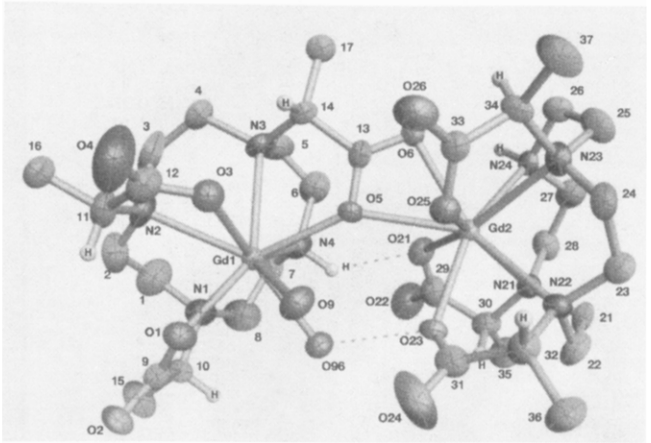

Figure 40. Dimeric structure of Gd(**133**). Only two of the six water molecules in the asymmetric unit are shown. Anisotropic thermal parameters are represented by 50% probability ellipsoids. (Reprinted from ref 329. Copyright 1993 American Chemical Society.)

oxygen lies 1.69 Å above the equatorial oxygen plane. The plane of the nitrogens and the plane of the equatorial oxygens are nearly parallel (dihedral angle = 4°). In the two independent Gd(**133**) complex units the tetraazacyclododecane macrocycle are enantiomeric and therefore the two complexes have diastereomeric conformations. The two external oxygen ligands are water molecules in one complex, while in the other complex the two external oxygens are donated by a bridging carboxyl group of the other complex. This bridging carboxyl group is therefore a tridentate ligand in which one of its oxygens is apical with respect to one complex and equatorial with respect to the other. The X-ray crystal structure of the dimeric complex of Gd(**133**) is shown in Figure 40. X-ray crystallographic data (coordination numbers of the central metal ions, M−O and M−N bond lengths) of the complexes of **46**, **47**, **96**, **99**, **100**, **101**, **106**, **107**, **121**, **129**, **130**, and **133** are presented in Table 5.

C. Structural Features of Dinuclear Macrocyclic Complexes of Lanthanides

The X-ray crystal structure of the carbonato-bridged complex $[\{Eu(\mathbf{27})(CH_3COO)\}_2(\mu\text{-}CO_3)](OH)_2 \cdot 7H_2O$[151] consists of two Eu(**27**) moieties linked through a bridging as well as chelating carbonate. The two moities are related by a crystallographic 2-fold axis passing through the carbon atom and one of the oxygen atoms of the carbonato bridge. Each europium ion is further linked to a bidentate chelating acetate on the external side of the $[EuCO_3Eu]$ core. The two macrocyclic moieties of the dimer are folded toward the external acetates and have the butterfly configuration found in other lanthanide complexes of **27**. Each macrocycle consists of two quasi-planar sections containing the pyridine rings and hinged at the $-CH_2CH_2-$ side chains, with an angle of 131.8°. This value is very close to that found in the monomeric complex $[Eu(\mathbf{27})(CH_3COO)_2]Cl \cdot 4H_2O$.[359] A ring puckering analysis of the six N-donor atoms shows a minor deviation from planarity in a twisted boat conformation. The two acetate ligands of the dimeric complex are staggered with respect to the bridging carbonate and are oriented along the fold line of the respective macrocycle. The $Eu-O_{acetate}$ distances are, on the average, appreciably longer for the dimeric complex (Eu−O = 2.53 Å) than the average $Eu-O_{acetate}$ distances of $[Eu(\mathbf{27})(CH_3COO)_2]Cl \cdot 4H_2O$ (Eu−O = 2.48 Å) and $[Eu(\mathbf{27})(CH_3COO)_2](CH_3COO) \cdot 9H_2O$ (Eu−O = 2.49 Å). This difference among the europium complexes having the same macrocycle and the same coordination number shows that substitution of an acetate by a bridging carbonate influences, either sterically or electronically, the strength of the bonding between the metal and the acetate on the opposite side of the macrocycle. The bridging carbonate ion acts as a chelating ligand to both the europium ions and is symmetrically positioned between the two halves of the dimer due to the presence of the crystallographic 2-fold axis.

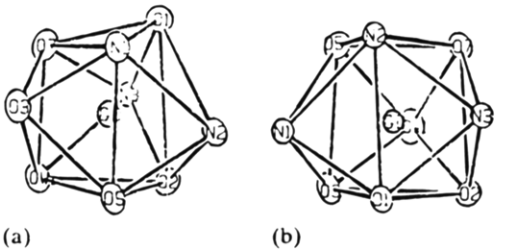

Figure 41. Tetrahedron around gadolinium ion in $[Gd_2(\mathbf{99})_2(H_2O)_2] \cdot 14H_2O$ (a) and in $[Gd(\mathbf{100})(H_2O)] \cdot 3H_2O$ (b). (Reprinted from ref 220. Copyright 1993 Elsevier Sequoia.)

The X-ray crystal structure of $[Gd_2(\mathbf{96})(NO_3)_4]H_2O$ shows that the complex has a propeller conformation with approximate noncrystallographic D_2 symmetry. The crystallographic 2-fold axis passes through the center and is normal to the mean plane of the macrocycle. Both gadolinium atoms lie within the macrocycle and are bridged by the two phenolate oxygen atoms. Each gadolinium atom is 10-coordinate, being bound to two nitrogen and two oxygen atoms of the macrocycle, four nitrate oxygens, and two phenolate oxygen atoms. The coordination geometry is a distorted bicapped dodecahedron. The metal−ligand bond lengths are in the range 2.34−2.69 Å, the shortest bond length being $Gd-O_{phenolate}$.[217]

The X-ray crystal structure of $[Gd_2(\mathbf{99})_2(H_2O)_2] \cdot 14H_2O$, depicted in Figure 21, shows that the two gadolinium ions are located between the two ligand molecules and the averaged molecular planes of the two macrocyclic rings are parallel to each other. Each metal ion is 9-coordinate, being bound to an amide oxygen atom, two carboxylate oxygen atoms, and two amine nitrogen atoms from one ligand molecule and to an amide oxygen atom, a carboxylate oxygen atom, and an amine nitrogen atom from the second ligand molecule and a water oxygen atom. The coordination geometry around the metal ion is described as a distorted tricapped trigonal prism (tetradecahedron). The crystal structures of $[Gd_2(\mathbf{99})_2(H_2O)_2] \cdot 14H_2O$ and $[Gd(\mathbf{100})(H_2O)] \cdot 3H_2O$ are quite different from each other; the sequences of the coordinated atoms in the tetradecahedron are different from each other as shown in Figure 41. In addition, the tetradecahedron in $[Gd_2(\mathbf{99})_2(H_2O)_2] \cdot 14H_2O$ is highly distorted from the ideal D_{3h} geometry when compared to that in $[Gd(\mathbf{100})(H_2O)] \cdot 3H_2O$. These structural differences are explained by the geometrical properties of the two macrocyclic ligands.

In both the ligands each amide group is located on a single plane. This planarity of the amide groups generates inflexibility in the ligand. The extreme distortion of the tetradecahedron around a Gd^{3+} ion in $[Gd_2(\mathbf{99})_2(H_2O)_2]\cdot 14H_2O$ is also attributable to the rigidity of the ligand. The introduction of an additional $-CH_2-$ group onto the macrocyclic ring increases the flexibility of the ligand and results in the mononuclear structure in $[Gd(\mathbf{100})(H_2O)]\cdot 3H_2O$ and the tetradecahedral coordination geometry is close to the ideal D_{3h} geometry.[220]

D. Structural Features of Trinuclear Macrocyclic Complexes of Lanthanides

The X-ray crystal structure of the trinuclear lanthanum complex $[La_3(\mathbf{101})(\mu_3\text{-}OH)(OH)(NO_3)_4]\cdot 7H_2O$ is illustrated in Figure 22. The $La_3(\mathbf{101})$ unit has an approximate mirror plane symmetry. The three lanthanum ions form an equilateral triangle of edge 4 Å. The 30-atom macrocyclic ring is made up of three planar seven-atom sections containing the pyridine rings and the imine linkages. The conformation around one of the $-CH_2CH(O^-)CH_2-$ chains is different from the other two. Each lanthanum is 9-coordinate, making five bonds to the macrocycle and four to the oxygen atoms of OH^-, NO_3^-, or H_2O. The average La–N and La–O bond lengths are presented in Table 5. Pairs of $La_3(\mathbf{101})$ units are joined by two La–OH–La bridges to make a unit containing six lanthanum atoms lying across a crystallographic inversion center, with La(1)–La(3) distance of 4.62 Å. There is an extended intricate network of hydrogen bonding involving OH^-, NO_3^-, and lattice water.[224]

E. Structural Features of Lanthanide Complexes of Texaphyrins

The lanthanide(III) texaphyrin complexes, La-$[(\mathbf{66})]^{2+}$, $[Gd(\mathbf{66})]^{2+}$, $[Eu(\mathbf{67})]^{2+}$, $[Gd(\mathbf{67})]^{2+}$ which is isomorphous with $[Eu(\mathbf{67})]^{2+}$, and $[Lu(\mathbf{68})]^{2+}$ exhibit several distinctive structural features.[133] They differ from one another slightly in relation to coordination number and distortion of the macrocyclic ligand framework. Nonetheless, these structures resemble each other quite closely and serve to define several interesting trends relating both to lanthanide coordination chemistry and texaphyrin metal chelation. In all the complexes the metal ion is coordinated to all the five nitrogen donors of the texaphyrin, to one or two nitrate ions, and to a methanol molecule on the opposite sides of the macrocycle. The coordination number varies from 10 for La^{3+} in $[La(\mathbf{66})]^{2+}$ to 8 for Lu^{3+} in $[Lu(\mathbf{68})]^{2+}$. These structures reflect a decrease in coordination number with the intrinsic contraction in cation size as the lanthanide series is traversed. For instance, an average decrease in nitrogen to metal bond length of 0.12 Å is found when comparing the 10-coordinate $[La(\mathbf{66})]^{2+}$ to the 9-coordinate $[Gd(\mathbf{67})]^{2+}$ and a decrease of 0.075 Å is observed when comparing $[Gd(\mathbf{67})]^{2+}$ to the 8-coordinate $[Lu(\mathbf{68})]^{2+}$. The 10-coordinate La^{3+} center in $[La(\mathbf{66})]^{2+}$ is found to be 0.91 Å from the mean plane through the five nitrogen donors of the macrocycle while the 8-coordinate Lu^{3+} center in $[Lu(\mathbf{68})]^{2+}$ is only 0.27 Å from the plane. The root mean square deviation from planarity for the nitrogen donors of the macrocycle is 0.15 Å in $[La(\mathbf{66})]^{2+}$ and only 0.072 Å in $[Lu(\mathbf{68})]^{2+}$, as compared to 0.097, 0.122, and 0.120 Å in $[Gd(\mathbf{66})]^{2+}$, $[Eu(\mathbf{67})]^{2+}$, and $[Gd(\mathbf{67})]^{2+}$, respectively. The Lu^{3+} cation in $[Lu(\mathbf{68})]^{2+}$ lies slightly above the plane of the macrocycle, being displaced by approximately 0.27 Å from the mean plane of the five nitrogens. This texaphyrin structure thus stands in marked contrast to that of the 5-coordinate, η^4 lutetium(III) octaethylporphyrin complex in which the metal was found to be approximately 0.92 Å above the macrocyclic plane.[363] This difference in "nearly in plane" versus "essentially out of plane" binding is considered to be a direct reflection of the expanded nature of the texaphyrin binding core which has been estimated to be ~20% larger than that of the corresponding tetradentate porphyrins.[183,184,188] This conclusion of better size matching for the texaphyrins is also apparent by inspection of the other Ln^{3+} texaphyrin structures.[133] In these cases the Ln^{3+} to N5 plane distance ranges between 0.60 and 0.91 Å. This is significantly shorter than the metal to porphyrin mean N4 plane distances found in the corresponding lanthanide porphyrin structures.[363,364–369] The increased binding core of the pentadentate texaphyrins accommodate the Ln^{3+} cation in a 1:1 fashion. This is in marked contrast to Eu^{3+} and Ce^{3+} octaethylporphyrin complexes which have been structurally characterized as 2:1 sandwich or 3:2 triple decker sandwich. In all the crystal structures of La^{3+} texaphyrins a certain degree of buckling in the macrocyclic framework was observed depending on the size of the lanthanide cation. In general, the greater the Ln^{3+} cation, greater is the degree of buckling. For instance, the maximum deviation from planarity is 0.15 Å for $[La(\mathbf{66})]^{2+}$ but only 0.072 for the smaller Lu^{3+} analog $[Lu(\mathbf{68})]^{2+}$. The X-ray crystallographic data of the lanthanide complexes of texaphyrins are presented in Table 5.

XIV. Macrocyclic Complexes as Contrast-Enhancing Agents in Nuclear Magnetic Resonance Imaging

Imaging used in diagnostic medicine is similar to spectroscopy in chemistry. Incident radiation from some source is changed as a result of interaction with a sample, and the changes are monitored with a detector. In medical imaging the sample is the human body. Diagnostic imaging procedures have been benefited by the availability of relatively safe pharmaceuticals called contrast agents which, when introduced into body cavities, are easily detected in an image. The presence or absence and the kinetic behavior of the agents in the tissues is used by physicians to determine the status of normal and diseased tissues. There are currently three types of medical imaging where lanthanides might be used as contrast agents: nuclear imaging,[7] X-ray imaging,[370] and nuclear magnetic resonance imaging.[17–25] The development of new lanthanide complexes as suitable contrast-enhancing agents is the primary focus of this chapter. The use of lanthanides in the

other two techniques have been discussed in detail elsewhere.[19] In recent years, magnetic resonance imaging (MRI) has been recognized as a powerful diagnostic tool in clinical practice.[371] NMR imaging is a tomographic technique yielding what are essentially three-dimensional images in the form of slices of tissue. Practical medical imaging is restricted to protons because they are the most sensitive nuclei, and mostly water protons because they are by far the most abundant *in vivo*. Movement of protons from one position to another during the relaxation experiment affects the signal intensity and for this reason moving blood usually has no detectable signal. The development of magnetic resonance imaging as a clinical diagnostic modality has created the need for a new class of pharmaceuticals called MRI contrast agents. These pharmaceuticals are paramagnetic substances which function to provide contrast between diseased and normal tissue and/or show the status of organ function and blood flow. Paramagnetic compounds are presently undergoing extensive evaluation as contrast agents in MRI. These agents increase contrast in MRI by differentially localizing in tissues where they increase the relaxation rates of nearby water protons. The images, which are mainly due to the NMR signal of water protons, are the result of the complex interplay between a number of parameters, such as proton density, flow, and longitudinal and transverse relaxation times T_1 and T_2. An improvement in the contrast may be achieved by administering exogenous chemicals that significantly alter the NMR properties of water resonance.[20,372]

Strongly chelated complexes of Gd^{3+}, Fe^{3+}, Mn^{2+}, and Cr^{3+} are most commonly suggested for use as contrast agents. Gd^{3+} has the largest magnetic moment ($\mu_{eff}^2 = g^2S(S + 1) = 63$) and long electron spin relaxation times[20] and so with other variables approximately equal, one would expect the Gd^{3+} complexes to have the largest longitudinal relaxivity, R_1, values ($f = 20$ MHz). Gadolinium(III) complexes containing coordinated water in the inner-coordination sphere exhibit the highest relaxivity because this places the protons closest to the gadolinium ion (typically 3.1 Å). This is important for the orientation of the water protons with respect to the Gd−O bond. Relaxivity also depends on the hydration number. The *in vitro* and *in vivo* chemical results reported by Tweedle *et al.*[373] support the usefulness of strongly chelated Gd^{3+} complexes as contrast agents. The choice of the proper compound is based on the evaluation of several parameters, such as solubility in water, high water proton relaxivity, better bodily distribution, and extremely inert to the loss of the metal ion, which is very poorly tolerated *in vivo* as the free ion.[374] They should also have an increased molecular reorientation time which results in increased solvent proton relaxation rates at the imaging magnetic fields and increased residence time in circulating blood and/or accumulation at the specific target tissue or organ.[375] Basically two properties are required for a Gd^{3+} complex to be considered a potential contrast agent in MRI: (i) high thermodynamic and possibly kinetic stability; and (ii) presence of at least one water molecule in the inner-coordination sphere. Paramagnetic compounds catalyze the proton relaxation of water in which they are dissolved.[376,377] The relaxation times of water protons are decreased typically by a factor of about 10^6 when the oxygen atom of water molecule becomes coordinated to a highly paramagnetic metal ion such as Gd^{3+}. As a result of decreasing both T_1 and T_2, the signal intensity is affected according to eq 7 where

$$SI = [H]H(v)\, e^{(-T_E/T_2)}(1 - e^{(-T_R/T_1)}) \qquad (7)$$

T_E and T_R are the echo delay time and pulse repetition time, respectively, $[H]$ is the concentration of water protons in the volume element, and $H(v)$ is a motion factor. When water-soluble paramagnetic compounds are involved the T_E and T_R are usually chosen to make the resulting signal intensity more sensitive to T_1 than to T_2 so as to increase the signal intensity. Relaxation catalysis by paramagnetic compounds is governed by a second-order rate constant called relaxivity, which describes the ability of a paramagnetic compound to catalyze relaxation of bulk water protons. The longitudinal or transverse relaxivity (R_1 or R_2) of a paramagnetic compound (p) is defined by eqs 8 and 9, where the term on the left

$$\Delta T_1^{-1} = R_1[p] \qquad (8)$$

$$\Delta T_2^{-1} = R_2[p] \qquad (9)$$

hand side is the difference in the reciprocal of the relaxation times measured in the presence and absence of p, and [p] is the concentration of p. Relaxation of paramagnetic metal complexes are highly dependent on the probe frequency at which the measurement is made, the temperature, and viscosity. Signal intensity is a complex function of the contrast enhancing agent, instrument, and tissue properties. The maximum signal intensity attained is determined by the R_2/R_1 ratio, with the highest signal intensity occurring when the ratio is unity.

The relaxivity of paramagnetic Gd^{3+} complexes depends on the magnitude of the dipole−dipole interaction between the electron spin on the metal and the proton spin on the water molecule(s) coordinated to the metal. The relaxivity is composed of inner- and outer-sphere contributions. Inner-sphere contributions arise when the water molecule is bound to gadolinium through its oxygen donor atom, whereas the outer-sphere contribution arises through hydrogen bonded water protons and translational diffusion. Correlation times characterize the time dependence of the motion which drive relaxation. When the gadolinium aqua ion is bound to proteins and macromolecules, its relaxivity is enhanced over that of the unbound ion due to increased correlation time, τ_c, which is dominated by the rotational correlation time, τ_r. Rotational correlation time increases as a function of molecular size and leads to increased relaxivity. This proton relaxation enhancement (PRE) effect increases with increasing molecular volume to the point where one or more of the other correlation times becomes dominant. NMRD (NMR dispersion) measurements are usually carried out to demonstrate PRE.

The theory of relaxation of solvent protons by small complexes of paramagnetic metal ions is well known[378] and has been reviewed in detail[20,379] and the essential equations pertinent to the Gd^{3+} case are summarized here as an essential basis to design suitable Gd^{3+} complexes which could serve as better contrast-enhancing agents. The observed water−proton longitudinal relaxation rate is given by the sum of three contributions:

$$R_1^{obs} = R_{1p}^{is} + R_{1p}^{os} + R_{1W} \quad (10)$$

where R_{1W} is the gadolinium-free water relaxation rate, R_{1p}^{is} represents the contribution due to the exchange of water molecules from the inner-coordination sphere of the metal ion to the bulk water, and R_{1p}^{os} is the contribution of the water molecules diffusing in the outer-coordination sphere of the paramagnetic center. The inner-sphere relaxation rate is described in terms of the following set of equations:

$$R_{1p}^{is} = \frac{Mq}{55.6}\frac{1}{T_{1M} + \tau_m} \quad (11)$$

$$\frac{1}{T_{1M}} = \frac{2}{15}\frac{\gamma_H^2 g^2 \beta^2 S(S+1)}{r^6} \times \left[\frac{7\tau_{c2}}{1 + (\omega_S\tau_{c2})^2} + \frac{3\tau_{c1}}{1 + (\omega_H\tau_{c1})^2}\right] \quad (12)$$

$$\frac{1}{\tau_{ci}} = \frac{1}{\tau_R} + \frac{1}{\tau_M} + \frac{1}{\tau_{Si}} \quad (13)$$

where $i = 1$ or 2 and

$$\frac{1}{\tau_{S1}} = \frac{1}{5\tau_{S0}}\left[\frac{1}{1 + (\omega_S\tau_V)^2} + \frac{4}{1 + (2\omega_S\tau_V)^2}\right] \quad (14)$$

$$\frac{1}{\tau_{S2}} = \frac{1}{10\tau_{S0}}\left[3 + \frac{5}{1 + (\omega_S\tau_V)^2} + \frac{2}{1 + (2\omega_S\tau_V)^2}\right] \quad (15)$$

In eqs 11−13, M is the molar concentration of the paramagnetic complex, q is the number of water molecules coordinated to the metal mon, τ_M is their mean residence lifetime, T_{1M} is their longitudinal relaxation time, S is the electron spin quantum number, γ_H is the proton nuclear magnetogyric ratio, g and β are the electronic g factor and Bohr magneton, respectively, r is the distance between the metal ion and protons of the coordinated water molecules, ω_H and ω_S are the proton and electron Larmor frequencies, respectively, τ_R is the rotational correlation time, and τ_{S1} and τ_{S2} are the longitudinal and transverse electron spin relaxation times. These last two are frequency dependent, according to eqs 14 and 15, and characterized by the correlation time of the modulation of the zero-field splitting (τ_V) and the electronic relaxation time at zero magnetic field (τ_{S0}).

The outer-sphere contribution may be calculated from Freed's equation:[380]

$$R_1^{os} = \frac{32\pi}{405}\gamma_H^2 g^2 \beta^2 S(S+1)\frac{N_A}{1000}\frac{M}{aD} \times [3j(\omega_H\tau) + 7j(\omega_S\tau)] \quad (16)$$

where N_A is Avagadro's number, a is the distance of closest approach between the paramagnetic center and the water molecules, and D is the relative diffusion coefficient for the water and paramagnetic complex. The spectral density function $j(\omega)$ is given by

$$j(\omega) = \mathrm{Re}\left[\frac{1 + {}^1/_4(i\omega\tau)^{1/2}}{1 + (i\omega\tau)^{1/2} + {}^4/_9(i\omega\tau) + {}^1/_9(i\omega\tau)^{3/2}}\right] \quad (17)$$

where $\tau = a^2/D$. In addition to the importance of the number of water molecules in the inner-coordination sphere (q) and the number of unpaired electron spins (s), the ligand environment plays an important role in determining the magnitude of the relaxivity of paramagnetic complexes.[381] Geraldes *et al.*[382] found that the relative relaxivities of polyamino carboxylate macrocyclic complexes of Gd^{3+} were reversed from that predicted based on the number of coordinated water molecules. The rational design of better MRI contrast agents thus requires a more detailed understanding of the influence of the structure and dynamics of the ligand on relaxivity and stability.

Analysis of $1/T_1$ NMRD profiles[372] of water protons in solutions of gadolinium(III) complexes may afford several important parameters such as the number of coordinated water molecules, their distance from the paramagnetic center, their mean residence lifetime, the reorientational correlation time of the complex, and the electronic relaxation time of the metal ion. Useful information may also be obtained from the armory of δ, j, T_1, and T_2 parameters of ^1H and ^{13}C NMR spectra.[383] The first example of a paramagnetic substance used for tissue discrimination in MRI was provided by Lauterbur *et al.*[377] Since then, a variety of paramagnetic contrast agents have been examined. Gadolinium(III) complexes derived from strongly binding anionic ligands, such as, DTPA,[20,384,385] **106**,[20,282,293,296,297,301] dacda,[20,386−388] and **131**[325,389] are among the most promising paramagnetic contrast agents currently being developed for use in MRI. Indeed two ionic complexes, $(NMG)_2$-[Gd(DTPA)][384] and (NMG)[Gd(**106**)],[374] and two neutral complexes, [Gd(**131**)][325,389] and [Gd(DTPA-BMA)][390] are at present used in humans. On the basis of its higher thermodynamic and kinetic stability, $[Gd(\mathbf{106})]^-$ [382] is currently preferred to $[Gd(DTPA)]^{2-}$, the first compound used as a contrast agent in MRI.[391] This unusual kinetic inertness probably stems from the tight packing and high rigidity of **106**.[297] The high stability constant of $[Gd(DTPA)]^{2-}$ reduces toxic effect of Gd^{3+} by lowering the concentration of free-metal ion. However, one factor limiting its effectiveness as a relaxation agent is the availability of only one water coordination site in the complex.[392] The relaxivity of $[Gd(DTPA)]^{2-}$ is a factor of 2−4 lower than that of the Gd^{3+} aqua ion. This can be attributed largely to the coordination of eight or nine water molecule in the aqua ion.[20] In comparison with the linear analogs EDTA and DTPA, the

macrocyclic ligands **106** and **107** have a great advantage in forming more stable complexes. However, their slow complexation rates pose a serious setback in their practical use as contrast agents. Therefore, there is significant room for the improvement in making contrast agents with higher relaxivities. The challenge is to design metal complexes that have multiple water coordination sites and yet remain intact under physiological conditions.

Although $[Gd(DTPA)]^{2-}$ and $[Gd(\mathbf{106})]^{-}$ are water soluble and stable both are charged complexes and the osmolarity of the solution injected intravenously is quite high. Consequently, neutral complexes of the 9-membered triaza tricarboxylate ligand **110** was studied by Sherry and his co-workers.[305,308,382] The complex [Gd(**110**)] has a higher water proton relaxivity, but both the thermodynamic and kinetic stabilities are lower than that of $[Gd(DTPA)]^{2-}$ and $[Gd(\mathbf{106})]^{-}$.[282,305] In an attempt to obtain stable, water-soluble, and neutral Gd^{3+} complexes Dischino *et al.*[325] synthesized the tetraaza triacetate macrocycle, 1,4,7-tris(carboxymethyl)-1,4,7,10-tetraazacyclododecane (**130**) which forms desirable Gd^{3+} complex, a chemically useful MRI contrast agent. This ligand can be easily derivatized to produce potentially octadentate ligands, such as, **131** and bifunctional chelating agents. Brucher *et al.*[309] have synthesized the triazatricarboxylate ligands **113**–**115** and studied the effect of the macrocyclic ring size and the rigidity on the complexation of these ligands. The Gd^{3+} complexes of these ligands exhibit increased thermodynamic and kinetic stability.

Kodama *et al.*[304] have designed the macrocyclic pentaamino pentacarboxylate ligand **108** and the hexaamino hexacarboxylate ligand **109**. The thermodynamic and kinetic properties of lanthanide complexes of these ligands show that the complexation is complete at pH 7 and the relative complexation rate of **109** with Gd^{3+} is 10 times slower than that of DTPA but 100 times faster than that of **106**. The stability constant of [Gd(**109**)] (log $K_{[Gd(\mathbf{109})]}$) is 22.95, compared to that of DTPA (log $K_{[Gd(DTPA)]}$ = 22.5)[393] and **106** (log $K_{[Gd(\mathbf{90})]}$ = 24.6).[282] The macrocycle **109** seems to be promising as another appropriate chelating agent to find use in MRI. In an attempt to obtain highly stable complexes of Gd^{3+}, which would also allow coordination of several water molecules for enhanced relaxivity Smith *et al.*[148] studied the Gd^{3+} complex of **27**. The longitudinal relaxivity of $[Gd(\mathbf{27})(CH_3COO)_2]Cl{\cdot}4H_2O$ is comparable to that of the Gd^{3+} ion, which suggests that the expectation of increased relaxivity in complexes with multiple open coordination sites is realized. However, it is apparent that the relaxivities observed are not solely a function of q. The longitudinal relaxivities of $[Gd(\mathbf{27})(CH_3COO)_2]Cl{\cdot}4H_2O$, $[Gd(H_2O)_9]^{3+}$, $[Gd(DTPA)]^{2-}$, and $[Gd(EDTA)]^{2-}$ are presented in Table 6. Chen *et al.*[323] have synthesized the 18-membered N_3O_3 triacetic acid **129** and its Gd^{3+} complex. It has been shown to exert moderate relaxivity of the NMR water signal in the *in vitro* tests.

Currently the search for new contrast agents for MRI is directed toward the synthesis of Gd^{3+} complexes of functionalized derivatives of macrocycles without altering their chelating abilities.[303] The water proton relaxation enhancement induced by these paramagnetic chelates can be increased by conjugating them to macromolecules such as albumin. This is achieved via the formation of an amide bond between an acetate group of the complex and an amino group of the macromolecule.[394,395] Aime *et al.*[311] reported the synthesis of Gd^{3+} complexes of macrocyclic polyamino polycarboxylic ligands **117**–**120** bearing β-(benzyloxy)-α-propionate residues. Substitution for acetate of β-(benzyloxy)-α-propionate groups in the framework of **106** results in a linear increase in the longitudinal and transverse relaxivities. The correlation between the relaxivity and molecular weight indicates that the chemical modification of the acetate groups of **106** did not result in an increase in the number of water molecules coordinated to the metal ion, as also suggested by the high values of the stability constants. The $1/T_1$ NMRD profiles of the Gd^{3+} complexes of **117**–**120** are consistent with the presence of one water molecule in the inner-coordination sphere. The results indicate that these complexes have significantly higher relaxivities than $[Gd(\mathbf{106})]^{-}$. The value of τ_{S0} reflects the changes in symmetry introduced in the coordination sphere of the Gd^{3+} ion by the insertion of one, two, or three β-(benzyloxy)-α-propionate residues. The value of τ_{S0} depends not only on the change introduced in the molecular geometry but also on the nature of the substituent group. In fact, as reported by Sherry *et al.*,[303] the amidation of the carboxyl group of **106** produces a dramatic decrease in τ_{SO}, which results in a lower water proton relaxivity at low fields. The NMRD studies indicate that the Gd^{3+} complexes of **117** and **120** are useful contrast agents at low magnetic field. Introduction of (benzyloxy)-methyl residues onto the macrocyclic framework of **106** does not alter its very favorable thermodynamic stability. Thus the type of substitution introduced in **117**–**120** reduces the *in vivo* toxicity associated with the release of Gd^{3+} ions.[311]

In another study Aime *et al.*[313] reported the synthesis of polyhydroxy (benzyloxy)propionamide substituted macrocycles **121** and **122** and the corresponding derivatives **123** and **124** with an −OH function by modifying **106**. Water proton relaxation rates of aqueous solutions of [Gd(**121**)], [Gd(**122**)], [Gd(**123**)], and [Gd(**124**)] suggest that these complexes contain only one molecule in their inner-coordination sphere

Table 6. Longitudinal Relaxivities of Selected Gadolinium Complexes

complex	R_1, $mM^{-1}\,s^{-1}$	frequency, MHz	T, °C	ref(s)
$[Gd(\mathbf{27})(CH_3COO)_2]Cl{\cdot}4H_2O$	9.7[a]	300	25	148
$[Gd(H_2O)_9]^{3+}$	9.0[a]	300	25	148
$[Gd(\mathbf{27})(CH_3COO)_2]Cl{\cdot}4H_2O$	9.7[a]	20	30	148
$[Gd(H_2O)_9]^{3+}$	9.1	20	35	*b*
$[Gd(DTPA)]^{2-}$	4.1	20	35	*c*
	3.7	20	37	20, 22
	4.5	20	37	20, 384
$[Gd(EDTA)]^{-}$	6.6	20	35	*c*
	5.4	20	37	20, 22
	6.9	20	37	384

[a] Correlation coefficients for the relaxivities measured were 0.98–0.99. [b] Koenig, S. H.; Brown, R. D., III. In *Magnetic resonance Annual 1987*; Kressel, H. Y., Ed.; Raven: New York, 1987. [c] Koenig, S. H.; Baglin, C. K.; Brown, R. D., III; Brewer, C. F. *Magn. Reson. Med.* **1984**, *1*, 496.

Table 7. Longitudinal and Transverse Relaxivities of Gd^{3+} Complexes at 20 MHz, 39 °C, pH 7.3

complex	R_1, $mM^{-1}\ s^{-1}$	R_2, $mM^{-1}\ s^{-1}$	ref
[Gd(**67**)]$^{2+}$	19.0 ± 1.5[a]		133
[Gd(**67**)]$^{2+}$	16.9 ± 1.5[b]		133
[Gd(**106**)][c]	3.56	4.70	311
	3.5 ± 0.1[d,e]		
[Gd(**117**)][c]	4.16	5.70	311
[Gd(**118**)][c]	5.10	6.95	311
[Gd(**119**)][c]	4.87	6.94	311
[Gd(**120**)][c]	5.66	8.00	311
[Gd(**121**)][f]	4.49	5.99	313
[Gd(**122**)][f]	5.19	7.29	313
[Gd(**123**)][f]	4.03	5.35	313
[Gd(**124**)][f]	4.33	6.36	313
[Gd(**129**)][g]	1.48		393
[Gd(**130**)][e]	4.8 ± 0.1		396
[Gd(**131**)][e]	3.7 ± 0.1		396
[Gd(**133**)]	4.4 ± 0.1		329

[a] At 25 °C. [b] At 50 MHz and 25 °C. [c] Measurements were carried out using Gd^{3+} complexes of concentration 1.5 mM. The accuracy of the measurements, repeated at least five times, is estimated as better than 2%. [d] Reference 396. [e] At 20 MHz and 40 °C. [d] Measurements were carried out using Gd^{3+} complexes prepared from a 0.01 M stock solution by diluting with 0.15 M NaCl. [g] The field strength is not indicated.

Table 8. NMRD Parameters Obtained From the Fitting of NMRD Profiles for the Gd^{3+} Complexes[a]

complex	τ_{S0}, ps	τ_V, ps	τ_R, ps	r, Å
Gd(**106**)[b]	460 ± 20	26 ± 8	72 ± 1	3.16 ± 0.01
Gd(**117**)[b]	417 ± 18	20 ± 6	86 ± 1	3.06 ± 0.01
Gd(**118**)[b]	275 ± 14	21 ± 6	115 ± 2	3.09 ± 0.01
Gd(**119**)[b]	443 ± 20	14 ± 4	115 ± 2	3.07 ± 0.01
Gd(**120**)[b]	300 ± 13	22 ± 6	133 ± 2	3.03 ± 0.01
Gd(**121**)[c]	137	16	92	3.02
Gd(**122**)[c]	140	25	123	3.00
Gd(**123**)[c]	142	21	81	3.08
Gd(**124**)[c]	122	25	96	3.00

[a] The experimental data were fitted by the Solomon–Bloembergen–Morgan equations (eqs 11–17) using r, τ_R, τ_{S0}, and τ_V as adjustable parameters (refs 311 and 313). [b] The parameters are obtained from the fitting of the NMRD profiles with the inner- and outer-sphere relaxation theory, the standard deviation for the calculated relaxivity is less than 0.01 (ref 311). [c] The parameters are obtained from the fitting of the NMRD profiles with the inner-sphere relaxation theory (ref 313).

as was found for the parent complex of **106**. The longitudinal and transverse relaxivities of Gd^{3+} complexes of **106**, **117**–**124**, and **129** are presented in Table 7. The $1/T_1$ NMRD profiles of aqueous solutions of the Gd^{3+} complexes of **121**–**124** reveal that at higher frequencies the solvent proton relaxation rates are dominated by the molecular reorientational time τ_R; i.e., the observed relaxivities are linearly related to the molecular size. However, the main effect associated with the transformation of carboxylate to carboxamide is the drastic reduction of the electronic relaxation time τ_{S0}, which is responsible for a decrease in relaxivity at low fields.[313] The NMRD parameters for the Gd^{3+} complexes of **106** and its derivatives **117**–**124** are presented in Table 8.

The complexes [Gd(**130**)] and [Gd(**106**)]$^-$ exhibit both inner- and outer-sphere relaxivities, whereas the relaxivities of [Fe(**106**)]$^-$ and [Fe(**130**)] are clearly outer-sphere. Therefore, [Gd(**106**)]$^-$ and [Gd(**130**)] are more effective water proton relaxation agents

Table 9. Stability Constants (log $K_{[GdL]}$) of Gadolinium(III) Complexes of Macrocyclic Polyamino Carboxylates

macrocycle	stability constant: log $K_{[GdL]}$
106	25.8,[a] 25.3,[b,c] 24.6,[d] 28.0,[e] 24.0 ± 0.1,[f] 24.9[g]
107	14.73,[h] 15.75[i]
108	15.88[h]
109	22.95[h]
110	13.7[j]
113	15.1 ± 0.3[k]
114	14.7 ± 0.3[k]
115	10.4 ± 0.2[k]
129	18.02[l]
130	21.1[a]
131	23.8[a]
133	25.3[a]

[a] At 25 °C, μ = 0.1 M Me_4NCl (ref 329). [b] Reference 327. [c] Reference 326. [d] Reference 282. [e] Desreux, J. F. *Bull. Cl. Sci. Acad. R. Belg.* **1978**, *64*, 814. [f] At 25 °C, μ = 0.1 M KCl (Clarke, E. T.; Martell, A. E. *Inorg. Chim. Acta* **1991**, *190*, 37). [g] At 25 °C, μ = 0.1 M Me_4NNO_3 (Broan, C. J.; Cox, J. P. L.; Craig, A. S.; Kataky, R.; Parker, D.; Harrison, A.; Randall, A. M.; Ferguson, G. J. *J. Chem. Soc., Perkin Trans. 2* **1991**, 87). [h] Reference 304. [i] At 80 °C, μ = 1 M NaCl (ref 296). [j] Reference 309. [k] At 25.0 ± 0.1 °C, μ = 1 M NaCl (ref 309). [l] Reference 324.

than the corresponding Fe^{3+} chelates.[360] The inner-sphere relaxivities for Gd(**130**)$(H_2O)_{1.8}$ and Gd(**106**)-$(H_2O)_{1.0}$, where the hydration numbers were determined for the Tb^{3+} complexes of the same ligands,[396] are found to be 2.9 and 1.5 $mM^{-1}\ s^{-1}$, respectively.[360] In general, the relaxivities of the Gd^{3+} complexes are much greater than that for most 3d-transition metal complexes, roughly in proportion to the ratio of their squared magnetic moments. The $4f^7$ Gd^{3+} complexes with relatively higher inner- and outer-sphere relaxivities are, in general, more effective T_1 relaxation agents in MRI than the structurally similar $3d^5$ Fe^{3+} transition metal complexes.[360] The longitudinal relaxivity of [Gd(**133**)][329] is found to be 4.4 ± 0.1 $mM^{-1}\ s^{-1}$ while that of [Gd(**130**)][396] is 4.8 ± 0.1 $mM^{-1}\ s^{-1}$. For small monomeric chelates with similar charge types, the primary determinant of relaxivity is the hydration number. The stability constants of gadolinium(III) complexes of the various macrocyclic polyamino carboxylates are presented in Table 9.

The ligands **99** and **100** containing three pendant acetate groups have been designed to synthesize neutral Gd^{3+} complexes. The ligand **99** forms the dinuclear Gd^{3+} complex $[Gd_2(\mathbf{99})_2(H_2O)_2]\cdot 14H_2O$ in which the two metal ions are located between two ligand molecules, whereas **100** forms the mononuclear complex $[Gd(\mathbf{100})(H_2O)]\cdot 3H_2O$. Both the complexes are water soluble, and the solubility of the latter is much higher than that of the former.[220] The trinuclear gadolinium(III) complex $[Gd_3(\mathbf{101})(OH)_2(NO_3)_4]\cdot 4H_2O$ is stable in water, suggesting its potential use as an *in vivo* MRI contrast enhancing agent.

The synthesis of Gd^{3+} complexes of other macrocycles remain of interest, since such systems might have greater kinetic stability, superior relaxivity, or better biodistribution properties than the existing carboxylate-based contrast agents. Gd^{3+} complexes of water-soluble porphyrin derivatives, such as, tetrakis(4-sulfonatophenyl)porphyrin and tetra-

kis(*N*-methyl-4-pyridiniumyl)porphyrin have been studied.[397-399] Unfortunately, the larger Gd^{3+} ion cannot be accommodated well within the relatively small porphyrin binding core, and as a consequence, gadolinium porphyrin complexes are invariably hydrolytically unstable.[397,398,400-402] In order to circumvent the problem associated with the cation–cavity mismatch Sessler *et al.*[187] have prepared water-soluble Gd^{3+} complexes of the texaphyrin **65**.[183] It is found that the strong hydrolytic stability of this complex is in marked contrast to that observed for simple water-soluble gadolinium porphyrins. The longitudinal relaxivity, R_1, of Gd(**67**) was found to be 19.0 ± 1.5 mM^{-1} s^{-1} at 20 MHz and 25 °C in aqueous solution. In another independent measurement the R_1 relaxivity was found to be 16.9 ± 1.5 mM^{-1} s^{-1} at 50 MHz in aqueous solution and found it to be invariant in magnitude over a period of 4 days. The solubility in water and the high R_1 relaxivity of Gd(**67**) promise its effective use as a potential contrast-enhancing agent in MRI.[133] The longitudinal relaxivities of Gd^{3+} complexes of **67**, **131**, and **133**, are presented in Table 7.

XV. Use of Macrocyclic Complexes of Lanthanides in Radioimmunotherapy

An important feature of modern medical technology has been the development of monoclonal antibodies which when injected bind firmly to tumor-associated compounds (antigens).[8,403] Such antibodies can function as specific carriers for the transport of imaging or cytotoxic agents to tumors for use in clinical diagnosis or therapy. A radionuclide–antibody conjugate can be used for both imaging and therapy but in both cases it is essential that the radionuclide does not dissociate from the antibody conjugate *in vivo*. The conjugation of metals, particularly radionuclides, to monoclonal antibodies results in agents for radioimmunotherapy and other medical applications.[9,404-407] Conventionally the metal radionuclide has been complexed to an acyclic chelate, such as EDTA and DTPA, which is covalently linked to the antibody. None of these chelates were adequate because the metal tends to dissociate *in vivo*. The pathway for the metal ion loss involves acid- (or metal-) catalyzed dissociation so that in liver and other tissues of locally low pH metal loss will occur readily. Chelators that can hold radiometals with high stability under physiological conditions are essential to avoid metal ion dissociation and excessive radiation damage to non target cells.[10,11] A prerequisite for the use of these isotopes *in vivo* is that their complexes should be kinetically inert, resisting acid or cation mediated decomplexation and subsequent exchange with serum proteins such as transferrin.[408] The released radioisotope may then be bound by serum proteins such as transferrin or may build up in radiosensitive organs such as the bone/bone marrow or in gastrointestinal mucosa. The build up of significant amount of the radioisotope in these organs may have lethal consequences. These problems may be obviated by using judiciously chosen macrocyclic ligands which form kinetically inert complexes with metals. Derivatives of polyazamacrocycles bearing a C-substituted functional group for antibody attachment can exhibit remarkable kinetic inertness. Thus the introduction of macrocycle conjugated monoclonal antibodies is a key feature to the successful application of radiolabeled tumor localizing antibodies for use in tumor imaging and therapy.[409-411] For radioimmunoscintigraphy (γ-scintigraphy)[13,14] the most promising radionuclides are the γ-emitting radioisotopes ^{99m}Tc ($t_{1/2}$ 6.02 h), ^{111}In ($t_{1/2}$ 2.83 d), and ^{67}Ga ($t_{1/2}$ 3.25 d), while the positron emitting radioisotopes ^{64}Cu ($t_{1/2}$ 12.8 h) and ^{68}Ga ($t_{1/2}$ 68 min) are used for positron emission tomography (PET).[15,16] Radionuclides, such as, ^{90}Y ($t_{1/2}$ 64 h) and ^{67}Cu, conjugated to monoclonal antibodies, are used in radioimmunotherapy.

The C-functionalized macrocyclic ligands **106**, **110**, and cyclam derivatives which are covalently attached[412-414] to the monoclonal antibody B-72.3 and radiolabeled with ^{64}Cu, ^{111}In, or ^{90}Y form kinetically stable complexes *in vivo*. The potential application of these macrocycle–antibody conjugate in tumor therapy is being actively pursued. The Ga^{3+} complex of **110** exhibits remarkable kinetic inertness as evidenced from ^{71}Ga NMR spectroscopy: the spectrum is unchanged after 60 days in HNO_3 (6 M) or in LiOH (0.01 M). The electrical neutrality of this complex together with its low molecular weight and stability in acidic medium augur well for its use as a radiopharmaceutical.[415] The tetraaza tetraacetate macrocycle **135** containing *p*-nitrobenzyl side chain,

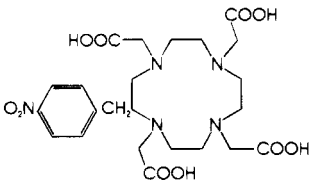

135

synthesized by Moi *et al.*[416] via peptide synthesis and intramolecular tosylamide ring closure, forms stable complex with $^{88}Y^{3+}$. The stability of the complex under physiological conditions was assessed by measuring the rate of transfer of the metal ion from the complex to serum proteins at high dilution in sterile human serum at 37 °C and pH 7.4. The remarkable kinetic stability of this complex promises its potential application in radioimmunotherapy. The introduction of bifunctional macrocyclic complexing agents has led to more promising results *in vivo* due to their slow rate of decomposition.[409,413,414,417] Synthesis of ^{111}In-, ^{67}Ga-, ^{68}Ga-, ^{64}Cu-, ^{67}Cu-, and ^{90}Y-labeled monoclonal antibodies bearing functionalized derivatives of **106** and **110** and their biodistribution studies have been reported.[412-416,418-420]

A. Synthesis of Macrocycle-Conjugated Antibodies

In order to synthesize the most suitable ligand to develop the radiolabeled monoclonal antibody two exacting criteria are defined: (i) the ligand, covalently bound to the protein, should bind the radioisotope rapidly and quantitatively under physiological conditions, (ii) the complex should be stable with respect to cation release over the pH range 2–8, and in the presence of the cations found in serum

(e.g., Ca^{2+}, Zn^{2+}, and Mg^{2+}). Macrocyclic ligands bearing carboxylate groups as pendant arms have been preferred to synthesize neutral and water-soluble complexes of the radionuclides. These ligands should bear a functionalized derivative to be attached to the monoclonal antibody. The synthesis of a C-functionalized macrocycle and the method of effecting the selective linkage of the macrocycle to the antibody is illustrated here.

The C-functionalized macrocycle **136** is prepared by the reaction of cyclam with diethyl *p*-cyanobenzylmalonate followed by reduction with BH_3·THF. The related macrocycle **137** bearing a phenolic sub-

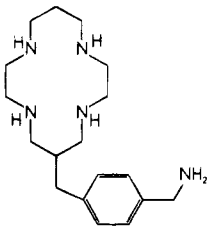

136

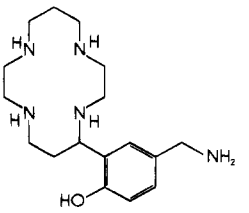

137

stituent which may act as a fifth axial donor is synthesized by the condensation of 6-cyanocumarin with cyclam followed by reduction with BH_3·THF.[409,412] The next problem is to effect a selective linkage of this macrocycle to the antibody. This is achieved by the use of a bifunctional linker molecule which could be selectively attached to the primary amine group and which bear a second functional group for reaction with a thiol residue on the antibody. The 2-vinylpyridine derivative **138**, synthesized for this purpose,[409] reacts selectively with thiol groups in the pH range 5–9 while primary and secondary amine groups are unaffected under these conditions. It is therefore possible to form an amide bond by the reaction of **136** and **137** with the active ester of **138**, generating the stable and isolable vinylpyridine intermediates **139** and **140**. The conjugates **139** and **140** react selectively with thiol residues on the antibody to yield stable macrocycle–antibody conjugate. Free thiol groups on the antibody may be generated either by recombinant antibody methods by the cleavage of the antibody disulfide links or by treatment with 2-iminothiolane. In the latter method reaction of the antibody B72.3 with 2-iminothiolane gives typically 3 to 5 thiols per antibody by titration with Ellman's reagent.[421] Incubation of the functionalized macrocycles **139** and **140** with the modified antibody (pH 6, 15 h, 4 °C) gives the desired macrocycle antibody conjugate **141** and **142**. Similar functionalized thiol-sensitive macrocycles **143** and **144**, synthesized by Parker and his co-workers,[413,414] on incubation with the modified antibody gives the corresponding macrocycle–antibody conjugate. The number of macrocycles linked to each antibody is measured spectrofluorimetrically after exhaustic hydrolysis of the antibody conjugate followed by a standard *o*-phthalaldehyde assay[422] of the resultant macrocyclic primary amine residues. Up to three macrocycles per antibody are attached in this manner and no diminution of immunoreactivity is observed at this level of derivatization.

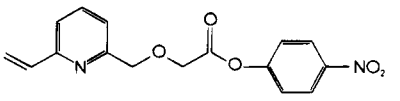

138

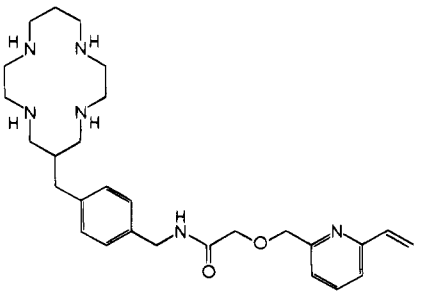

139

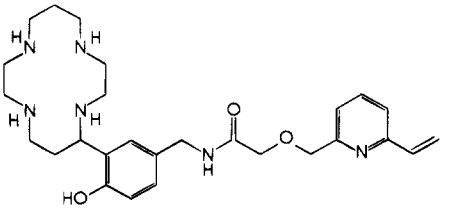

140

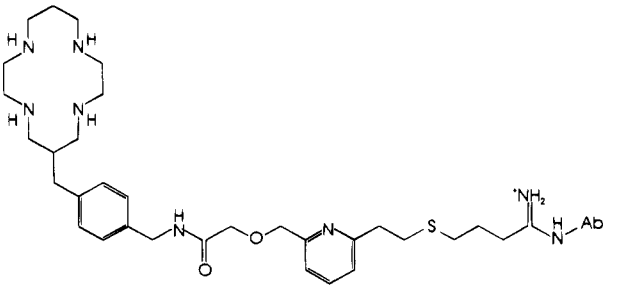

141

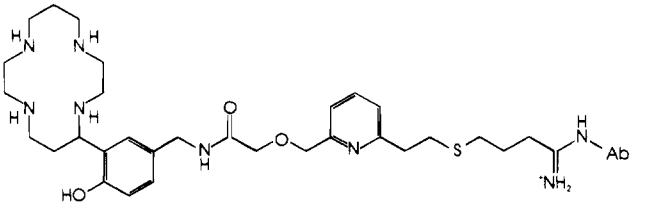

142

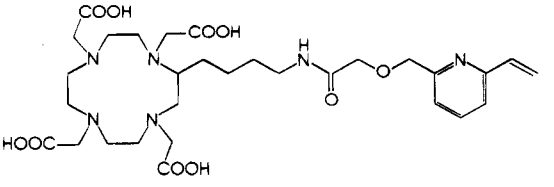

143

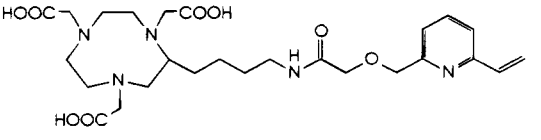

144

The yttrium(III) complex $[Y(\mathbf{127})]^-$ exhibits an invariant ^{31}P NMR shift in the pH range 2–12 and monoprotonation occurs only at pH 1.5. The formation and dissociation of $[Y(\mathbf{127})]^-$ has been studied using ^{90}Y radiolabeled complex: rapid complexation occurs above pH 6.5 and radiolabeling yields of ≥98% may be obtained at ligand concentrations of 5 μM (37 °C, 30 min). The complex $[^{90}Y(\mathbf{127})]^-$ clears rapidly from the body of injected mice and no measurable quantity of ^{90}Y was obtained in the femur (at 24 and 48 h post-injection period) consistent with the *in vivo* stability of the complex with respect to ^{90}Y loss.[319] The rate of dissociation of ^{90}Y from the complex, monitored in the pH range 1–2.7, is comparable with that obtained for $[^{90}Y(\mathbf{106})]^-$ under identical conditions.[420] In order to link **127** to a protein or oligonucleotide a C-functionalized variant bearing pendant functionality is required. Reaction of 2-(4-benzamidobutyl)-1,4,7,10-tetraazacyclododecane with $MeP(OC_2H_5)_2$ and $(CH_2O)_n$ in THF yielded **145** in 30% yield. Acid hydrolysis of **145** and reaction with the heterobifunctional coupling agent *N*-succinimido-3-maleimidopropionate [$(CH_3)_2SO$, *N*-methylmorpholine; 3 h; 20 °C] yielded the maleimide **146**. This has been coupled to the tumor-localizing antibody B72.3 and may be radiolabeled directly with ^{90}Y (pH 6.8, 15 min) to give labeling yields of 5 μCi per microgram of antibody.[319]

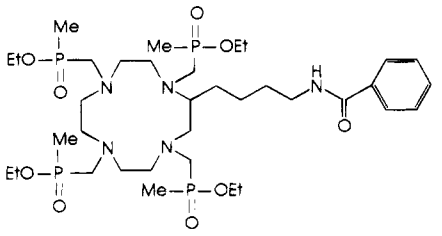

145

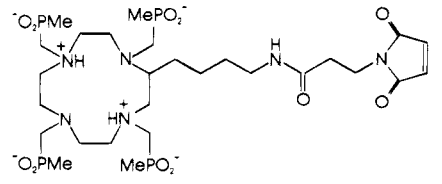

146

B. Labeling Methods

The introduction of the metal radioisotope into the macrocycle–antibody conjugate needs to be effected both rapidly and selectively in order to optimize the radiolabeling yield and obviate nonspecific metal binding to the protein. This is particularly difficult with ^{99m}Tc labeling ($t_{1/2}$ 6.02 h), as the reaction of "reduced technitium" with the macrocycle **136**, for example, is sluggish in the pH range 7–9. Binding of technitium by the phenolated macrocycles proceeds more rapidly. However, under these conditions, there is appreciable "nonspecific" binding of technitium by the protein. It is necessary therefore to form the technitium(V) dioxocomplexes of the vinylpyridine conjugates **139** and **140** prior to reaction with the antibody. This prelabeling strategy indeed results in a specifically labeled antibody. The limiting feature of this approach is that two separate steps are involved with a quickly decaying isotope, so that unless the linkage and purification steps are fast (<2 h) the overall radiolabeling yield is very low. The situation is more straightforward with copper. The macrocycle–antibody conjugates are radiolabeled with either carrier-free ^{64}Cu or ^{67}Cu in the presence of an anionic carboxylate buffer. Under these conditions nonspecific binding of Cu^{2+} to the protein is minimized. The radiolabeling yields are compared to the control antibody B72.3 which bears no macrocycles. After gel filtration the ratio of the activities associated with the conjugated and control antibodies is typically > 100. These labeled antibodies are then injected into the experimental animals and after a given period of time the biodistribution is studied. In order to selectively kill a tumor by radioimmunotherapy a β^-- (or α-) radiolabeled antibody conjugate is needed to selectively deliver a sterilizing dose of radiation without affecting healthy tissue. Possible therapeutic radioisotopes are listed in Table 10.

Table 10. Therapeutic Radioisotopes[a]

isotope	half-life, h	dose rate, (rad h^{-1} per μ lig^{-1})	mean range,[b] mm	total dose,[c] rad (τ_α)
^{67}Cu	62	0.58	0.2	52 (30)
^{90}Y	64	1.96	3.9	180 (180)
^{111}Ag	179	0.82	1.1	212 (198)
^{131}I	193	1.22	0.4	339 (115)
^{161}Tb	166	0.50	0.3	119 (101)
^{188}Re	17	1.91	3.3	47 (44)
^{199}Au	75	0.53	0.1	58 (47)

[a] Data from ref 12. [b] In healthy tissue. [c] Values in parentheses indicate electron dose.

XVI. Macrocycle–Cation Interaction and Separation of Metal Ions

Macrocyclic ligands are noted for their remarkable selectivity toward metal ions. The strong and selective interaction of macrocycles with specific metal ions make these ligands suitable candidates for use as reagents in separating metal ions which are otherwise difficult to separate.[58,59] The use of macrocycles to separate metal ions which are present in very low concentration from other more concentrated metal ions, and the separation of metal ions which do not differ in their ionic radii considerably are of particular interest. Macrocycles have been used to perform separation by the solvent extraction of the metal ion from aqueous solution into organic phases or by the membrane transport of metal ions from an aqueous source phase through an organic membrane phase containing the ligand with an aqueous receiving phase. Selective extraction of many cations using macrocyclic ligands have been achieved.[423–426] The crown ethers have proven to be excellent choices for the separation of metal ions because of their ability to complex a particular cation selectively.[427] The major problem encountered during the separation process using macrocyclic ligands by solvent extraction and liquid membrane transport are (i) maintaining the very expensive macrocycles in the organic phase, (ii) loss of extraction effectiveness when the concentration of the metal ions is very low, and (iii)

the relatively slow kinetics of extraction.[428] One way to overcome these problems is to attach covalently the macrocyclic ligands to a solid support. Early effort to accomplish the covalent attachment of macrocycles involved the use of benzocrown ethers to hydrophobic solid supports or to amide bonding groups of relatively low solubility.[429] Electron-withdrawing benzo groups on macrocycles reduce cation–macrocycle interaction,[58] and hydrophobic supports greatly reduce these interactions relative to those of the analogous unbound macrocycle due to the lack of wetting of the solid. Izatt and his coworkers[60,77,78,430–433] have described the use of ether and alkyl chains to connect the carbon framework of ether and diazamacrocycles to the siloxy component of silica gel. The macrocycle–silica gel bond is permanent and such systems have been used almost indefinitely to perform separation, recoveries, and determination without measurable loss of the crown. Separation is achieved by passing the aqueous metal ion solution through a column containing the macrocycle–silica gel material. 18-Crown-6 was the first macrocycle attached to silica gel through the very stable alkane–ether linkage.[434] The silica gel bound macrocycles have been found to have nearly the same affinity as the corresponding unbound macrocycles for metal ions.[60,77] Separation of metal ions has been effected through silica gel bound macrocycles, such as, 15-crown-5, 18-crown-6, 21-crown-7, pyridine-18-crown-6, 1,10-diaza-18-crown-6, 1,4,7,10-tetraaza-18-crown-6, triaza crowns, cyclam macrocycles with additional functionalities, pentaaza-15-crown-5 (cyclam-5), and hexaaza-18-crown-6 (cyclam-6) macrocycles.

The synthetic procedures used to covalently attach the macrocycle to the silica gel involves synthesizing the macrocycles in their pure form and reacting the silica gel with the appropriate silane followed by the macrocycle.[428] The detailed procedures are given elsewhere.[77,434,435] log K values for the interaction of the silica gel bound macrocycles with metal ions have been determined by equilibrating the silica gel material with known concentrations of the cations in well-defined matrices. After equilibrium is reached, the amount of bound cation is measured by stripping the gel with an acidic solution. The metal concentration in the eluate is then determined by atomic absorption spectrometry. Binding of the cations of interest to the silica gel sites is made negligible by including an excess of a cation, such as Mg^{2+}, which does not complex with the macrocycle but competes effectively with cations of interest for plain silica gel. Separations have been performed using alkali, alkaline earth, transition, and post transition metal ions.[436] The separation of trivalent lanthanide metal ions by these methods is expected to be difficult because these cations are similar to each other in size and in aqueous chemistry.[437] The large difference in the macrocycle **147** mediated flux of Eu^{3+} and Eu^{2+} in a $H_2O–CHCl_3–H_2O$ bulk liquid membrane system is exploited to separate Eu^{3+} selectively from other trivalent lanthanide ions.[61] The separation is effected using the crown ether mediated liquid membrane system by first reducing Eu^{3+} to Eu^{2+} in the source phase and then transporting the Eu^{2+} selectively using a crown ether type macrocycle as the carrier. In a study by Zhu and Izatt[62] the reduction of Eu^{3+} is accomplished electrically. The resulting Eu^{2+} has been separated from several lanthanides, and the fluxes of Eu^{2+} has been determined in competitive experiments using a modified thin sheet supported liquid membrane (TSSLM) system. However, the TSSLM system is not useful as a real separation process due to the small surface area of TSSLM and the decrease of transport for all cations when the electric field is applied. The TSSLM system can be modified to overcome these difficulties. The silica gel bound macrocycle **148** is used to separate quantitatively parts per billion (ppb) levels of toxic heavy metal ions, such as, Pb^{2+}, Hg^{2+}, Cd^{2+}, and Ag^{+} from potable water matrix.[435]

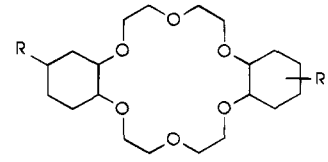

147

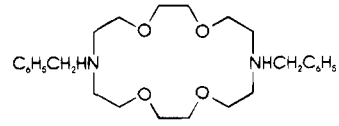

148

A. Extraction of Lanthanides and Actinides with Ionizable Macrocyclic Ligands

Actinide metal ions, such as Pu^{4+}, Am^{3+}, and Cm^{3+}, were studied for their extraction behavior using macrocyclic ligands as auxiliary ligands where they act as neutral oxo donors.[50–52] The complexation of tetravalent metal ions with neutral macrocycles is accompanied by large cation solvation energies with a concomitant decrease in the metal–ligand interaction energies. With the advent of ionizable macrocyclic ligands, the complexation of tri- and tetravalent cations has been studied. Chang and his coworkers[53–55] have studied the coordination behavior of ionizable macrocyclic ligands **111** and **149** with lanthanides and these ligands were found to exhibit selectivity effects. Ionizable macrocyclic ligands are

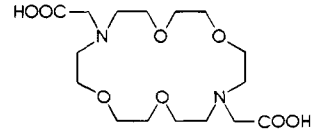

149

likely to have strong electrostatic interaction with actinide ions, along with guest–host interactions which are predominantly size selective in nature. These ligands are also important due to their ability to transfer metal ions toward nonaqueous media even in the absence of any other organophilic counteranion.[438] The complexation of trivalent europium and americium with **111** and **149** by Manchanda and Mohapatra,[56] studied by solvent extraction technique, reveals that both these metal ions form stronger complexes with **149** than with **111**. On the other

hand, **111** forms stronger complexes with plutonium(IV) than with **149**.[57] In view of the empirical guest–host size correlation arrived at by Christensen *et al.*[439] it is probable that Am^{3+} and Eu^{3+} are held in the cavity of **149**, whereas no such encapsulation is possible in **111**. The larger K values for Am^{3+} over Eu^{3+} may be explained on the basis of better availability of f-orbitals for participation in the bonding of the actinide ion.[56] The larger complex formation constant of Pu^{4+} with **111** ($\log K = 21.52$) compared to that with **149** ($\log K = 19.11$) is in sharp contrast to the observed behavior of Am^{3+} and Eu^{3+}, and is attributed to the encapsulation of Pu^{4+} into the cavity of **111** leading to a greater metal–ligand interaction. This is explained on the basis of better size compatibility of Pu^{4+} ion with **111**. The selective complexation of these metal ions with ionizable macrocycles is exploited for the extraction of metal ions.[56,57]

XVII. Lanthanide Complexes as NMR Shift Reagents

Paramagnetic lanthanide complexes have been used as NMR shift reagents for NMR-detectable alkali metal cations.[28,440–443] Water soluble anionic paramagnetic shift reagents have been used for distinguishing intra- and extracellular cations, particularly Li^+, Na^+, and K^+ by NMR spectroscopy in a variety of intact cells and tissues.[444–446] Aqueous shift reagents have been introduced in the past decade for the study of biologically important metal cations by NMR spectroscopy.[31] Because of their high negative charges, shift reagents are not soluble in the interior of the lipophilic membrane and are repelled by the negatively charged head groups of the phospholipids. Thus, shift reagents remain in the extracellular compartment during NMR experiments conducted on cell suspensions. With the use of shift reagents, the extracellular resonance is shifted away from the intracellular resonance, thus allowing the simultaneous observation of the two pools of metal ions. Information on metal cation transport and distribution in cell suspensions, and on enzymatic activity is then easily obtained by metal NMR spectroscopy in the presence of shift reagents. Several aqueous shift reagents for metal cation NMR spectroscopy have been reported.[28,444,445,447–449] They have been shown to be useful in membrane transport biochemistry, for example, in studies of alkali metal ion transport across vesicles[450,451] and red blood cell membranes.[441,444,452–454] Among the shift reagents reported thus far $[Ln(\mathbf{125})]^{5-}$ (Ln = Dy^{3+} or Tm^{3+}) are the only reagents derived from a macrocyclic ligand. $[Tm(\mathbf{125})]^{5-}$ has proven to be the most promising and found useful practical application for perfused heart studies[455,456] and *in vivo* rat brain ^{23}Na NMR spectroscopy.[457] The interaction of the shift reagents with metal ions depends on the counterions coordination in the second coordination sphere of the lanthanide ion. The lanthanide complexes of highly charged macrocycles bearing pendant arms are the likely candidates to effectively coordinate with countercations of large size and number. Thus the effectiveness of the shift reagents for the *in vivo* studies of the metal cation distribution and transport could be studied with such macrocyclic complexes.

One of the main problems with the acyclic shift reagents is their nonspecificity for particular biological cations, such as, Na^+. Competitive binding of other cations, especially Mg^{2+} and Ca^{2+}, present in physiological solution, decreases the $^{23}Na^+$-induced shift. Interaction of Ca^{2+} often results in the release of free lanthanide ions by competition or in the precipitation of binary calcium complex. The removal of free Ca^{2+} from bodily fluids by complexation or precipitation may often have a detrimental effect upon those tissues which depend upon low Ca^{2+} concentrations for survival. To explore the possibility of making shift reagents that are more specific for certain cations, Sink *et al.*[26] have synthesized the polyoxatetraazamacrocyclic tetraacetates **150–153**. The tetraaza tetraacetate portion of the macrocycle houses the lanthanide cation leaving the polyoxa cavity available for binding to alkali metal cations. It is found that Dy^{3+} complex of **151** produces the largest ^{23}Na paramagnetic shift.

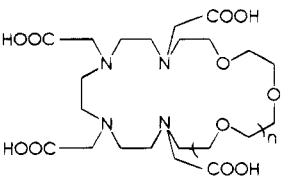

150, O_3N_4, n = 1

151, O_4N_4, n = 2

152, O_5N_4, n = 3

153, O_6N_6, n = 4

XVIII. Luminescence Quenching of Lanthanide Ions in Macrocyclic Complexes

Some lanthanide ions possess strongly emissive and long-lived excited states but do not exhibit intense absorption.[458] Therefore, considerable effort is devoted to the design of lanthanide complexes where light is absorbed by the ligands and the electronic energy is then transferred to the emitting metal ion (antenna effect).[37,75,459,460] The efficiency of conversion of absorbed light into emitted light can be increased by making use of energy transfer from excited photosensitive groups of organic ligands[461–463] bound to luminescent lanthanide ions. Europium cryptates, for example, exhibit notable emission in aqueous solution at room temperature, whereas simple aqua complexes do not luminesce under the same conditions.[464–467] This may be attributed to the protection of the cryptated europium ion from radiationless deactivation by solvent molecules.[73,464–470] Cryptate formation by inclusion of a metal ion into the intramolecular cavity of a macropolycyclic ligand provides efficient shielding of the bound species from interaction with solvent and solute molecules. Photoactive europium and terbium cryptates of macrobicyclic ligand **154** containing α,α′-bipyridine moiety as light absorber (photosensitizer) incorporate the three features, namely, inclusion, protection, and energy transfer from a ligand group required to achieve strong luminescence.[37] Strong red and green emissions, respectively, are readily observed for the Eu^{3+} and Tb^{3+} cryptates of **154** in aqueous solution

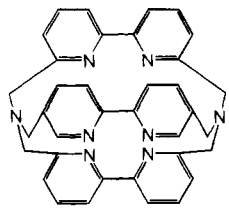

154

at room temperature. The UV light absorbed by the bipyridyl moiety is reemitted as visible light by the complexed lanthanide ions. These spectral properties may be ascribed to intramolecular energy transfer from the $\pi\pi^*$ excited states of the ligand groups to the excited levels of the Eu^{3+} and Tb^{3+} ions, which then emit from the $^5D_0$ and $^5D_4$ levels, respectively. The light conversion process, absorption–energy transfer–emission (A–ET–E), performed by these cryptates is represented in Figure 42.[37] The emission lifetime of this europium cryptate is longer than that of the aqua ion and even of the [Eu(2.2.2)] cryptate.[465] These photoactive Eu^{3+} and Tb^{3+} cryptates are efficient luminophores which function as A–ET–E light conversion molecular devices, transferring UV light absorbed by the ligand groups into visible lanthanide emission via intramolecular energy transfer.[37,38] Interesting photophysical and photochemical features of these and related complexes find potential applications, for instance, in the development of luminescent materials and of labels for biological applications, such as, time-resolved luminescence immunoassay[42] employing monoclonal antibodies. Because of their very intense absorption bands, which collect incident light, and their reasonably high ligand-to-metal energy transfer and luminescence efficiencies, the cryptates of **154** are excellent molecular devices to play the role of luminescence probes and luminescence concentrators (antenna effect). Even in very dilute aqueous solution the Eu^{3+} and Tb^{3+} cryptates of **154** are able to convert about 1% of the incident UV photons into emitted visible photons.[38] Higher conversion efficiency may be attained if structural modifications are found which increase both shielding of the enclosed ion and the yield of intramolecular energy transfer.

Bipyridine-type units are suitable building blocks to design macrocyclic,[39,471] macrobicyclic,[37,38,44,459,472] and podand-type ligands[473] capable of giving highly stable and strongly luminescent Eu^{3+} and Tb^{3+} complexes.[37,38,44,75,459,460,471,472–480] Absorption in the intense UV bands of the bipyridine type ligands can be followed by energy transfer to the strongly luminescent and long-lived excited state of the metal ion,[37,38] giving rise to molecular species that can be used as probes and labels for a variety of chemical and biological applications.[40,45,481–484] The Eu^{3+}, Tb^{3+}, and Gd^{3+} complexes of **155** show intense absorption. Excitation of the Tb^{3+} and Eu^{3+} complexes in the LC band causes the characteristics luminescence of the lanthanide ions.[476] The high luminescence quantum yield of $[Tb(\mathbf{155})]^{3+}$ could be exploited in its use as an excellent luminescence label. The ligand shields

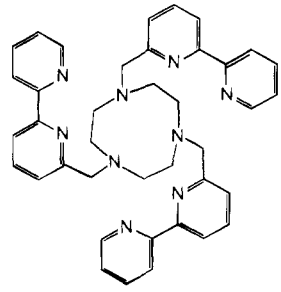

155

Tb^{3+} and Eu^{3+} metal ions from solvent interactions. Cerium(III) luminescence results from d → f transitions. Two emission bands are observed from the lowest excited state ^2D to the two spin–orbit components of the ground term, $^2F_{7/2}$ and $^2F_{5/2}$. The absorption spectrum for each distinct species may contain up to five bands resulting from the ground $^2F_{5/2}$ state to the components of the excited ^2D state, which may be split into as many as five levels under the influence of spin–orbit coupling and ligand field. The accessibility and environmental sensitivity of the

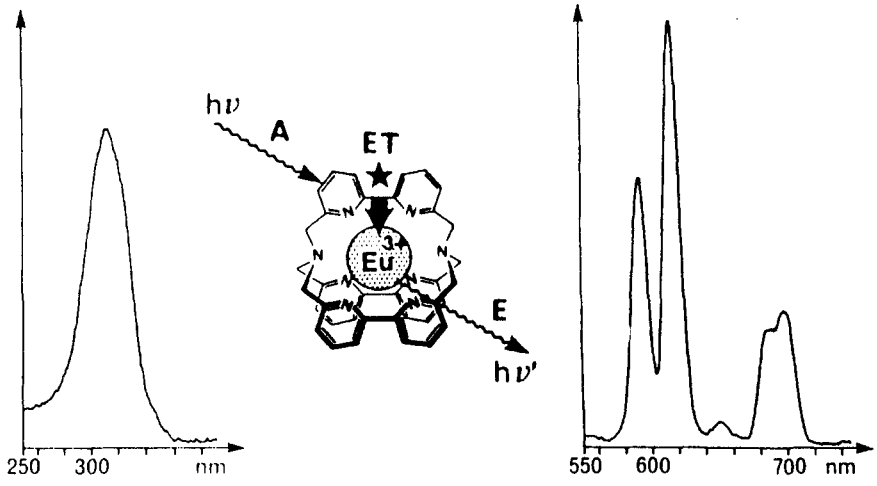

Figure 42. Illustration of the absorption-energy transfer emission A–ET–E light conversion process performed by the cryptate [Eu(**246**)] (center): left, excitation spectrum (emission at 700 nm); right, emission spectrum (excitation at 300 nm); 10^{-6} M aqueous solution of the nitrate at 20 °C. (Reprinted from ref 37. Copyright 1987 VCH Verlagsgesellschaft mbH.)

^2D state make the luminescence of Ce^{3+} useful in probing interaction of this metal ion with ligands. This property of Ce^{3+} could be exploited for its possible use as a probe of biomolecules.

Europium(III) is a valuable structural probe due to its ability to luminescence in solution at room temperature. It possesses the nondegenerate ground term $^7F_0$ and the first excited state $^5D_0$, neither of which can be split by the ligand field. The remaining energy levels of Eu^{3+} are degenerate in the free ion and will be split into the various Stark components depending on the symmetry of the ligand field. Eu^{3+} exhibits $^7F_0 \rightarrow {}^5D_0$ excitation and $^5D_0 \rightarrow {}^7F_2$ emission. The macrocyclic ligands **156**–**159** consisting of the

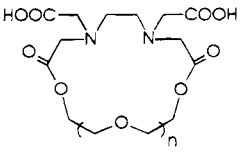

156, n = 0

157, n = 1

158, n = 2

159, n = 3

basic EDTA core in which two of the carboxylate arms are connected by varying lengths of polyether linkages, reported by Chang *et al.*,[485] form 1:1 complexes with Eu^{3+}. The $^7F_0 \rightarrow {}^5D_0$ excitation spectra indicate that for each of the complexes two isomers are present in fast exchange on the $^5D_0$ time scale. The coordination number for Eu^{3+} is found to be 8 or 9 for each of the macrocycles depending on whether or not both carboxylate moieties coordinate. The ether oxygen atoms of the macrocyclic ring do not coordinate. This indicates that macrocyclic cavity size might have been expected to be a minor factor in Eu^{3+} coordination. However, the formation constants of Eu^{3+} complexes of these ligands range over 4 orders of magnitude from 10.03–6.06 with **158** > **159** > **157** > **156**. This implies that macrocyclic cavity does play an important role even in the absence of the ether oxygen coordination. The importance of the macrocyclic cavity size of **156**–**159** is further reflected in the complex formation constants across the lanthanide series.[485] These values are at a maximum at Eu^{3+} for the ligands **157** and **158** and at Tb^{3+} for **159**. On the other hand, the complex formation constants for **156** increase steadily across the series from La^{3+} to Lu^{3+}, which suggests that the macrocyclic cavity of this ligand is too small to provide any selectivity among these ions.[486]

There has been great interest in the design, synthesis, and photophysics of luminescent lanthanide cryptates bearing heterocyclic units as potential probes in fluoroimmunoassay.[37,38,487,488] Aromatic *N*-oxides have been introduced into macrocyclic structure to achieve greater stability of the lanthanide complexes and good fluorescence properties in water. The Eu^{3+} complexes of **160**[39] shows very bright luminescence in aqueous solution when excited with UV radiation. Good luminescent characteristics and excellent stability of this complex in water seems to be very promising with respect to its potential ap-

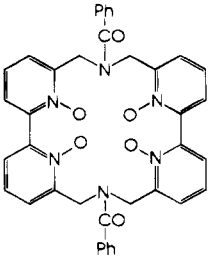

160

plications as fluorescent probe in fluoroimmunoassay. Strong circularly polarized luminescence was also detected for the Eu^{3+} and Tb^{3+} complexes of **40** due to its twisted chiral conformation.[158] A part of the excitation energy is transferred from the surrounding ligand to the Eu^{3+} or Tb^{3+} ion, and then the emission from the excited f–f states of these ions can be observed. The intramolecular energy-transfer process occurs between the π^* electronic states of the ligand and the 4f levels of the central metal ion. Modification of the ligand with extensive delocalization of electron density may have profound effect on the luminescence properties.

Excitation into the $^5D_6$ level of europium(III) in $[Eu(\mathbf{27})(CH_3COO)_2]Cl{\cdot}4H_2O$ at 394 nm resulted in the $^5D_0 \rightarrow {}^7F_2$ emission. The luminescence of the Eu(**27**) moiety is enhanced by axial coordination of organic ligands that are better chromophores than acetates which enhance energy transfer to Eu^{3+}. A variety of neutral and anionic oxygen-donor ligands were screened as potential enhancers and it is found that the heteroaromatic monocarboxylic acids enhance the luminescence of the Eu(**27**) moiety.[233,489–491] The emission intensity of $[Eu(\mathbf{27})(CH_3COO)_2]Cl{\cdot}4H_2O$ was increased to 7–12-fold in the presence of 2-thiophenecarboxylate, 2-pyridinecarboxylate, or 2-furancarboxylate.[29] However, no change in intensity of the typical europium(III) emission was observed in the presence of N-donor ligands.[151]

Molecular recognition events in which lanthanide(III) cation pairs are formed have been studied using the heterodinuclear lanthanide(III) complexes of **96** by luminescence decay dynamics. The luminescence spectra of $(Sm_{1-x}Eu_x)_2(\mathbf{96})(NO_3)_4{\cdot}H_2O$ are dominated by strong emission from the $^5D_0$ level of Eu^{3+} at 77 K. The emissions from the $^4G_{5/2}$ state of Sm^{3+} is apparently quenched by Eu^{3+}. The short-lived Eu^{3+} luminescence has a decay rate constant $k_1 \approx 8200$ s^{-1} while the cumulative average decay rate constant is $k_2 \approx 1400$ s^{-1}. The $(Tb_{1-x}Pr_x)_2(\mathbf{96})(NO_3)_4{\cdot}H_2O$ system emits when the $^5D_4$ state of Tb^{3+} is directly excited and is similar to the behavior of $(Sm_{1-x}Eu_x)_2(\mathbf{96})(NO_3)_4{\cdot}H_2O$ complexes. These results reveal that there are two microscopic environments for Eu^{3+} and Tb^{3+} which are attributed to the homodinuclear molecules, $Ln_2(\mathbf{96})(NO_3)_4{\cdot}H_2O$ (Ln = Eu or Tb) and the heterodinuclear molecules, $SmEu(\mathbf{96})(NO_3)_4{\cdot}H_2O$ and $PrTb(\mathbf{96})(NO_3)_4{\cdot}H_2O$. The luminescence decay rate constants for the intramolecularly coupled Eu–Sm and Pr–Tb pairs are 8200 and 12500 s^{-1}, which yield coupling constants of 2.9×10^{-53} and 4.7×10^{-53} m^6 s^{-1}, respectively, when dominant dipolar interactions are assumed. The ratio of the Eu–Eu to Eu–Sm cation pairing selectivity constants of 1:1.5 sup-

ports the intervention of molecular recognition processes favoring the homo to hetero paired species in the ion pairing events leading to the formation of $(Sm_{1-x}Eu_x)_2$(**96**)$(NO_3)_4 \cdot H_2O$ compounds. The study reveals that the formation of dinuclear lanthanide complexes of the macrocycle **96** is governed by molecular recognition processes in which the homo- and heterolanthanide cations are recognized and paired on the basis of their cooperative effects.[79]

The complexes Ln_2(**96**)$(NO_3)_4$] exhibit either ligand fluorescence for Ln = La, phosphorescence for Ln = Gd, and ligand sensitized Ln^{3+} luminescence for Ln = Eu and Tb.[217] Europium(III) luminescence originates from the $^5D_0$ state to the ^7F_J stark levels.[492,493] The short luminescence lifetime of the $^5D_0$ state indicates Eu–Eu interactions.[494] Terbium luminescence originates from the $^5D_4$ state to the ^7F_J Stark levels and is effectively sensitized by the blue shoulder of the ligand (**96**) triplet state. The laser-excited luminescent spectra of homo- and heterodinuclear complexes of the cyclic compartmental Schiff base macrocycle **97**, reported by Guerriero *et al.*,[218] have been used to assess the local site symmetry and chemical environment of coordinated metal ions, fluxionality of the ligand framework, metal–metal distances in dinuclear complexes, and metal–metal interactions. The luminescence study also indicates absorption of energy by the ligand followed by the energy transfer from the ligand to Eu^{3+}, and the $Tb^{3+} \rightarrow Eu^{3+}$ energy transfer within the macrocyclic framework. Absorption of light by the ligand and an efficient energy transfer from the ligand to Tb^{3+} and energy transfer from Tb^{3+} to Eu^{3+}, Nd^{3+}, and Ho^{3+} is also observed in the heterodinuclear lanthanide(III) complexes of *p-tert*-butylcalix[8]arene by Bunzli *et al.*[353] Thus, dinuclear lanthanide(III) complexes of ligands, such as, *p-tert*-butylcalix[8]arene which exhibit intense absorption due to the antenna effect of the ligand framework may yield highly luminescent labels by the excitation of the lanthanide(III) ion by an efficient intramolecular ligand-to-metal energy transfer.[459] The dinuclear Eu^{3+} and Tb^{3+} complexes of the branched hexaazacyclooctadecane ligand **98** containing six pendant 2,2′-bipyridine units exhibit metal-centered luminescence. Energy transfer from the coordinated bipyridine units to Eu^{3+} and Tb^{3+} is observed in acetonitrile.[219]

The luminescence quenching studies have also been exploited to demonstrate the existence of macrocyclic lanthanide(III) complexes as monomeric species in solution. The intermolecular energy-transfer luminescence quenching in fluid solution may take place by dynamic (collisional in nature) or static (formation of an associated species between donor and acceptor) processes.[495,496] The two quenching mechanisms can be differentiated by comparing the Stern–Volmer emission intensity quenching constant, k^{ϕ}_{SV} and the Stern–Volmer emission lifetime quenching constant, k^{τ}_{SV}. The k^{τ}_{SV} values, obtained from luminescence lifetime measurements, is a measure of dynamic quenching alone, as static quenching does not affect the observed emission lifetime.[495] It follows thus that for monomeric compounds with no tendency for association in solution, the Stern–Volmer quenching constants obtained from emission intensity and lifetime measurements should be equal, i.e., $k^{\phi}_{SV} = k^{\tau}_{SV}$. Since static quenching is normally much more effective in deexcitation of the emissive donor species than is dynamic quenching, the formation of associated species in solution to any significant extent is usually marked by a large inequality in the Stern–Volmer quenching constants obtained from luminescence intensity and lifetime measurements, i.e., $k^{\phi}_{SV} \gg k^{\tau}_{SV}$. The k^{ϕ}_{SV} values of the Tb^{3+} and Eu^{3+} complexes of the macrocyclic polyamino carboxylates **106**, **130**, and **131** are in the vicinity of the k^{τ}_{SV} values, indicating that these macrocyclic complexes show little self-association.[396]

XIX. Molecular Mechanics and Molecular Graphics Techniques in the Design of Macrocycles

The techniques of molecular mechanics and molecular graphics have been used to investigate different structural problems concerned with macrocycles. These include prediction of detailed molecular geometry, calculations of the "goodness of fit" of a metal ion inside a particular macrocycle in terms of defined geometric and energetic parameters, interactions between macrocyclic complexes and other molecules, and positioning of solvent guests within the macrocycle.[497] A promising approach to the design of macrocycles for selective complexation involves the use of molecular mechanics concept. The empirical force field (EFF),[498,499] also called molecular mechanics,[500] is a set of functions whose sum is expected to represent the energy of a molecule as a function of its conformation. Molecular mechanics is a modern tool in coordination chemistry used to design macrocycles which are sterically efficient.[306,501,502] The lower the steric strain generated in the complex on coordination of the ligand to the metal ion, the more sterically efficient is the ligand. Thus synthesis of suitable ligands with requisite ligand design features to achieve high complex stability and metal ion selectivity involves the use of molecular mechanics calculations to design more sterically efficient ligands. Molecular mechanics calculations could be used to study the relative stabilities of different conformers of macrocycles in producing metal ion selectivity.

There are two major problems in using molecular mechanics in the study of macrocyclic complexes: false minima and parametrization of the force field. No known method finds the optimal energy minima; what are found are local minima. Attempts have been made to overcome this problem through molecular dynamics, distance geometry, tree-searching,[503] artificial intelligence,[504] and a truth maintenance system,[505] but none of these methods are as yet foolproof. Molecular graphics is an invaluable technique in this process. Molecules can be built up from their substituent parts; atoms can be added or removed, or changed from one atom type to another; individual sections can be translated, rotated and fitted together. The complete molecule can then be viewed from any direction, rotated, magnified, and represented in different forms as required. This visualization of the molecule is of enormous importance in the understanding of molecular shape. Thus

molecular graphics is an invaluable tool for the finetuning of the ligand design features to tailor a required macrocycle.

Molecular mechanics calculations and molecular dynamics simulation were used to examine the molecular structure and the stabilities of ligands and their Gd^{3+} complexes. The magnitude of various factors determining the stability of multidentate Gd^{3+} complexes including the energy loss due to change of ligand conformation by complexation, the energy gain from cation−ligand attraction, and the effects of intramolecular hydrogen bonding were calculated by molecular mechanics. The cation−cavity "best fit" is examined by molecular graphics techniques. Intramolecular hydrogen bonds in the free ligands usually disfavor the complex formation due to disruption of hydrogen bond during complex formation. On the other hand, intramolecular hydrogen bond may contribute to complex stability if they make their desolvation energy of the free ligand smaller.[506]

XX. Glossary

DMSO	dimethyl sulfoxide
DMF	dimethylformamide
edta	ethylenediaminetetraacetic acid
DTPA	diethylenetriaminepentaacetic acid
MRI	magnetic resonance imaging
THF	tetrahydrofuran
cp	cyclopentadienyl radical
NMRD	nuclear magnetic resonance dispersion
T_1	longitudinal relaxation time
T_2	transverse relaxation time
T_E	echo delay time
T_R	pulse repetition time
R_1	longitudinal relaxivity
R_2	transverse relaxivity
τ_c	correlation time
τ_r	rotational correlation time
PRE	proton relaxation enhancement
PET	positron emission tomography
dacda	1,10-diaza-4,7,13,16-tetraoxacyclooctadecane-*N,N'*-diacetic acid
NMG	*N*-methylglucamine
DTPA-BMA	*N,N''*-bis[(methylcarbamoyl)methyl]-*N,N',N''*-tris(carboxymethyl)diethylenetriamine
cyclen	1,4,7,10-tetraazacyclododecane
en	1,2-diaminoethane
cyclam	1,4,8,11-tetraazacyclotetradecane
TSSLM	thin sheet supported liquid membrane system
EFF	empirical force field

XXI. Acknowledgments

With pleasure and gratitude I thank my enthusiastic research scholars V. Arul Joseph Aruna, A. N. Paul Angelo, D. Suresh Kumar, and Shaji James for all their committed and prompt service throughout the preparation of this review and for the neat and speedy typing of the manuscript. I thank the authors and the publishers for granting permission to reprint the published figures from literature: The Royal Society of Chemistry (Figures 1, 2, 20, 22, 23a, 23b, 24, 25, and 29), Elsevier Sequoia (Figures 9, 10, 11, 19, 21, 31a, 31b, 32, 36, and 41), Pergamon Press Ltd. (Figures 4, 5, 6a, 6b, 7, 27, and 28), and VCH Verlagsgesellschaft (Figure 42). I express my sincere thanks to John A. Joseph and Kottaiah Daniel of JOJO Graphics, Madras-600 094, for drawing the structures and schemes elegantly on the computer. This work is supported in part by the SERC grant from the Department of Science and Technology and the BRNS grant from the Department of Atomic Energy of the Government of India. Financial assistance from the International Affairs Committee of the Royal Society of Chemistry, London, is also gratefully acknowledged.

XXII. References

(1) Melson, G. A., Ed. *Coordination Chemistry of Macrocyclic Compounds*; Plenum: New York, 1979.
(2) Izatt, R. M., Christensen, J. J., Eds. *Synthesis of Macrocycles: The Design of Selective Complexing Agents, Progress in Macrocyclic Chemistry*; Wiley-Interscience: New York, 1987; Vol. 3.
(3) Lindoy, L. F. *The Chemistry of Macrocyclic Ligand Complexes*; Cambridge University Press: Cambridge, 1989.
(4) Dalley, N. K. In *Synthetic Multidentate Macrocyclic Compounds*; Izatt, R. M., Christensen, J. J., Eds.; Academic Press: New York, 1978.
(5) Fenton, D. E.; Vigato, P. A. *Chem. Soc. Rev.* **1988**, *17*, 69.
(6) Vallarino, L. M. *J. Less-Common Met.* **1989**, *149*, 121.
(7) Fritzberg, A. R., Ed. *Radiopharmaceuticals: Progress and Clinical Perspectives*; C. R. C. Press: Boca Raton, 1986; Vols. 1 and 2.
(8) Kohler, G.; Milstein, C. *Nature* **1975**, *256*, 495.
(9) Hnatowich, D. J.; Layne, R. L.; Lanteigne, D.; Davis, M. A.; Griffin, D. W.; Doherty, P. W. *Science* **1983**, *220*, 613.
(10) Klein, J. L.; Leichner, P. K.; Callahan, K. M.; Kopher, K. A.; Order, S. E. *Antibody, Immunoconjugates, Radiopharm.* **1988**, *1*, 55.
(11) Meares, C. F.; Wensel, T. G. *Acc. Chem. Res.* **1984**, *17*, 202.
(12) Parker, D.; Morphy, J. R.; Karl Jankowski; Jonathan Cox. *Pure Appl. Chem.* **1989**, *61*, 1637.
(13) Koizumi, M.; Endo, K.; Kunimatsu, M.; Sakahara, H.; Nakashima, T.; Kawamura, Y.; Watanabe, Y.; Ohmomo, Y.; Arano, Y.; Yokoyama, A.; Torizuka, K. *J. Immunol. Methods* **1987**, *104*, 93.
(14) Alvarez, V. L.; Wen, M. L.; Lee, C.; Lopes, A. D.; Rodwell, J. D.; McKearn, T. J. *Nucl. Med. Biol.* **1986**, *13*, 347.
(15) Raicle, M. E. *Adv. Chem. Ser.* **1981**, *197*, 419.
(16) Loc'h, C.; Maziere, B.; Comar, D. *J. Nucl. Med.* **1980**, *21*, 171.
(17) Partain, C. L.; James, A. E.; Rollo, F. D.; Price, R. R. *Nuclear Magnetic Resonance (NMR) Imaging*; W. B. Saunders: Philadelphia, 1983.
(18) Mansfield, P.; Morris, P. G. In *Advances in Magnetic Resonance*; Waugh, J. S., Ed.; Academic Press: New York, 1982; Supplement 2.
(19) Tweedle, M. F. In *Lanthanide Probes in Life, Chemical, and Earth Sciences*; Bunzli, J.-C. G., Choppin, G. R., Eds.; Elsevier: Amsterdam, 1989; Chapter 5.
(20) Lauffer, R. B. *Chem. Rev.* **1987**, *87*, 901.
(21) Kumar, K.; Tweedle, M. F. *Pure Appl. Chem.* **1993**, *65*, 515.
(22) Tweedle, M. F.; Brittain, H. G.; Eckelman, W. C.; Gaughan, G. T.; Hagan, J. J.; Wedeking, P. W.; Runge, V. M. In *Magnetic Resonance Imaging*, 2nd ed.; Partain, C. L., Ed.; W. B. Sanders: Philadelphia: 1988; Vol. 1, p 793.
(23) Moonen, C. T.; van-Zijil, P. C.; Frank, J. A.; Le-Bihan, D.; Becker, E. D. *Science* **1990**, *250*, 53.
(24) Morris, P. G. *Nuclear Magnetic Resonance Imaging in Medicine and Biology*; Clarendon Press: Oxford, England, 1986.
(25) Young, S. W. *Magnetic Resonance Imaging: Basic Principles*; Raven Press: New York, 1988; pp 1−282.
(26) Sink, R. M.; Buster, D. C.; Sherry, A. D. *Inorg. Chem.* **1990**, *29*, 3645.
(27) Ramasamy, R.; Mota de Freitas, D.; Jones, W.; Wezeman, F.; Labotka, R.; Geraldes, C. F. G. C. *Inorg. Chem.* **1990**, *29*, 3979.
(28) Sherry, A. D.; Malloy, C. R.; Jeffery, F. M. H.; Cacheris, W. P.; Geraldes, C. F. G. C. *J. Magn. Reson.* **1988**, *76*, 528.
(29) Fonda, K. K.; Smailes, D. L.; Vallarino, L. M.; Bombieri, G.; Benetollo, F.; Polo, A.; De Cola, L. *Polyhedron* **1993**, *12*, 549.
(30) Reuben, J.; Elgavish, G. A. In *Handbook on the Physics and Chemistry of Rare Earths*; Gschneider, K. A., Jr., Eyring, L., Eds.; North Holland: Amsterdam, 1979; Vol. 4, Chapter 38.
(31) Sherry, A. D.; Geraldes, C. F. G. C. In *Lanthanide Probes in Life, Chemical, and Earth Science*; Bunzli, J.-C. G., Choppin, G. R., Eds.; Elsevier: New York, 1989; Chapter 4.
(32) Balshi, J. A.; Kohler, S. J.; Bittl, J. A.; Springer, C. S.; Ingwall, J. S. *J. Magn. Reson.* **1989**, *83*, 138.
(33) Szklaruk, J.; Marecek, J. F.; Springer, A. L.; Springer, C. S., Jr. *Inorg. Chem.* **1990**, *29*, 660.
(34) Dick, L. R.; Geraldes, C. F. G. C.; Sherry, A. D.; Gray, C. W.; Gray, D. M. *Biochemistry* **1989**, *28*, 7896.

(35) Swinkels, D. W.; van Duynhoven, J. P. M.; Hilbers, C. W.; Tesser, G. I. *Recl. Trav. Chim. Pays-Bas.* **1991**, *110*, 124.
(36) Buster, D. C.; Castro, M. M. C. A.; Geraldes, C. F. G. C.; Malloy, C. R.; Sherry, A. D.; Siemers, T. C. *Magn. Reson. Med.* **1990**, *15*, 25.
(37) Alpha, B.; Lehn, J.-M.; Mathis, G. *Angew. Chem., Int. Ed. Engl.* **1987**, *26*, 266.
(38) Alpha, B.; Balzani, V.; Lehn, J.-M.; Perathoner, S.; Sabbatini, N. *Angew. Chem., Int. Ed. Engl.* **1987**, *26*, 1266.
(39) Pietraszkiewicz, M.; Pappalardo, S.; Finocchiaro, P.; Mamo, A.; Karpiuk, J. *J. Chem. Soc., Chem. Commun.* **1990**, 1907.
(40) Bunzli, J.-C. G. In *Lanthanide Probes in Life, Medical, and Environmental Sciences*; Choppin, G. R., Bunzli, J.-C. G., Eds.; Elsevier: Amsterdam, The Netherlands, 1989; Chapter 7.
(41) Evans, C. H. *Biochemistry of the Lanthanides*; Plenum Press: New York, 1990.
(42) Marshall, N. J.; Dakubu, S.; Jackson, T.; Ekins, R. P. In *Monoclonal Antibodies and Developments in Immunoassay*; Albertini, A., Ekins, R., Eds.; Elsevier/North-Holland Biomedical Press: Amsterdam, 1981; p 101.
(43) Leif, R. C.; Vallarino, L. M. In *Cell Separation Science and Technology*; Kompala, D. H., Todd, P., Eds.; ACS Symposium Series 464; American Chemical Society: Washington DC, 1991; p 41.
(44) Lehn, J.-M.; Pietraszkiewicz, M.; Karpiuk, J. *Helv. Chim. Acta* **1990**, *73*, 106.
(45) Richardson, F. S. *Chem. Rev.* **1982**, *82*, 541.
(46) Lehn, J.-M.; de Vains, J.-B. R. *Tetrahedron Lett.* **1989**, *30*, 2209.
(47) Lehn, J.-M.; Roth, C. O. *Helv. Chim. Acta* **1991**, *74*, 572.
(48) Horrocks, W. DeW., Jr.; Albin, M. *Prog. Inorg. Chem.* **1984**, *31*, 1.
(49) Moret, E.; Nicolo, F.; Plancherel, D.; Froidevaux, P.; Bunzli, J.-C. G. *Helv. Chim. Acta* **1991**, *74*, 65.
(50) Ensor, D. D.; Pruett, D. J. *Sep. Sci. Technol.* **1988**, *23*, 1345.
(51) Ally, H. F.; Khalifa, S. M.; Navratil, J. D.; Saba, M. T. *Solvent Extr. Ion Exch.* **1985**, *3*, 623.
(52) Mathur, J. L.; Khopkar, P. K. *Solvent Extr. Ion Exch.* **1988**, *6*, 111.
(53) Chang, C. A.; Rowland, M. E. *Inorg. Chem.* **1983**, *22*, 3866.
(54) Chang, C. A.; Ochaya, V. O. *Inorg. Chem.* **1986**, *25*, 355.
(55) Chang, C. A.; Chang, P. H.; Manchanda, V. K.; Kasprzyk, S. P. *Inorg. Chem.* **1988**, *27*, 3786.
(56) Manchanda, V. K.; Mohapatra, P. K. *Polyhedron* **1990**, *9*, 2455.
(57) Manchanda, V. K.; Mohapatra, P. K. *Radiochim. Acta* **1990**, *50*, 209.
(58) Izatt, R. M.; Bradshaw, J. S.; Neilsen, S. A.; Lamb, J. D.; Christensen, J. J.; Sen, D. *Chem. Rev.* **1985**, *85*, 271.
(59) Lehn, J.-M. *Science* **1985**, *227*, 849.
(60) Bradshaw, J. S.; Krakowiak, K. E.; Tarbet, B. J.; Bruening, R. L.; Biernat, J. F.; Bochenska, M.; Izatt, R. M.; Christensen, J. J. *Pure Appl. Chem.* **1989**, *61*, 1619.
(61) Brown, P. R.; Izatt, R. M.; Christensen, J. J.; Lamb, J. D. *J. Membr. Sci.* **1983**, *13*, 85.
(62) Zhu, C. Y.; Izatt, R. M. *J. Membr. Sci.* **1990**, *50*, 319.
(63) Morrow, J. R.; Buttrey, L. A.; Shelton, V. M.; Berback, K. A. *J. Am. Chem. Soc.* **1992**, *114*, 1903.
(64) Komryama, M.; Matsumura, K.; Matsumoto, Y. *J. Chem. Soc., Chem. Commun.* **1992**, 640.
(65) Breslow, R.; Hunang, D.-L. *Proc. Natl. Acad. Sci. U.S.A.* **1991**, *88*, 4080.
(66) Johnson, L. F.; Guggeinheim, H. J. *Appl. Phys. Lett.* **1971**, *19*, 44.
(67) Pollack, S. A.; Chang, D. B. *J. Appl. Phys.* **1988**, *64*, 2885.
(68) Killian, H. S.; Van Herwijnen, F. P.; Blasse, G. *J. Solid State Chem.* **1988**, *74*, 39.
(69) Blasse, G.; Bril, G. *Philips Tech. Rev.* **1970**, *31*, 303.
(70) Yeh, S. M.; Mears, C. F. *Biochemistry* **1980**, *19*, 5057.
(71) Mears, C. F.; Rice, L. S. *Biochemistry* **1981**, *20*, 610.
(72) Mears, C. F.; Yeh, M. S.; Stryer, L. *J. Am. Chem. Soc.* **1981**, *103*, 1607.
(73) Horrocks, W. DeW., Jr.; Sudnick, D. R. *Acc. Chem. Res.* **1981**, *14*, 384.
(74) Desvergne, J. P.; Fages, F.; Bouas-Laurent, H.; Marsau, P. *Pure Appl. Chem.* **1992**, *64*, 1231.
(75) Balzani, V.; Ballardini, R. *Photochem. Photobiol.* **1990**, *52*, 409.
(76) Davidson, R. S.; Hilchenbach, M. M. *Photochem. Photobiol.* **1990**, *52*, 431.
(77) Bradshaw, J. S.; Bruening, R. L.; Krakowiak, K. D.; Tarbet, B. J.; Bruening, M. L.; Izatt, R. M.; Christensen, J. J. *J. Chem. Soc., Chem. Commun.* **1988**, 812.
(78) Izatt, R. M.; Bruening, R. L.; Bruening, M. L.; Tarbet, B. J.; Krakowiak, K. E.; Bradshaw, J. S.; Christensen, J. J. *Anal. Chem.* **1988**, *60*, 1825.
(79) Matthews, K. D.; Fairman, R. A.; Johnson, A.; Spence, K. V. N.; Kahwa, I. A.; McPherson, G. L.; Robotham, H. *J. Chem. Soc., Dalton Trans.* **1993**, 1719.
(80) Guerriero, P.; Vigato, P. A.; Fenton, D. E.; Hellier, P. C. *Acta Chem. Scand.* **1992**, *46*, 1025.
(81) Vallarino, L. M. In *Handbook on the Physics and Chemistry of Rare Earths*; Gschneidner, K. A., Jr., Eyring, L., Eds.; Elsevier Science Publishers B. V.: Amsterdam, 1991; Vol. 15, Chapter 104.
(82) Bombieri, G. *Inorg. Chim. Acta* **1987**, *139*, 21.
(83) Ziegler, K.; Eberle, H.; Ohlinger, H. *Liebigs Ann.* **1933**, *504*, 94.
(84) Baker, W.; McOmie, J. W. F.; Ollis, W. D. *J. Chem. Soc.* **1951**, 200.
(85) Eliel, E. L. *Stereochemistry of Carbon Compounds*; McGraw Hill: New York, 1962.
(86) Shaw, B. L. *J. Am. Chem. Soc.* **1975**, *97*, 3856.
(87) Lindoy, L. F.; Busch, D. H. In *Preparative Inorganic Reactions*; Jolly, W. L., Ed.; Wiley-Interscience: New York, 1971; Vol. 6, p 1.
(88) House, D. A.; Curtis, N. F. *Chem. Ind.* **1961**, 1708.
(89) Thompson, M. C.; Busch, D. H. *J. Am. Chem. Soc.* **1964**, *86*, 3651.
(90) Nelson, S. M. *Pure Appl. Chem.* **1980**, *52*, 2461.
(91) Fenton, D. E. *Pure Appl. Chem.* **1986**, *58*, 1437.
(92) Nelson, S. M.; Knox, C. V.; McCann, M.; Drew, M. G. B. *J. Chem. Soc., Dalton Trans.* **1981**, 1669.
(93) Curtis, N. F. *J. Chem. Soc.* **1960**, 4409.
(94) Curtis, N. F. *Coord. Chem. Rev.* **1968**, *3*, 3.
(95) Comba, P. C.; Curtis, N. F.; Lawrence, G. A.; Sargenson, A. M.; Shelton, B. W.; White, A. H. *Inorg. Chem.* **1986**, *25*, 4260.
(96) Stelter, H.; Frank, W. *Angew. Chem.* **1976**, *88*, 760.
(97) Hafliger, H.; Kaden, Th. A. *Helv. Chim. Acta* **1976**, *88*, 760.
(98) Kaden, Th. A. *Top. Curr. Chem.* **1984**, *121*, 157.
(99) Xu Jide; Ni Shisheng; Lin Yujuan. *Inorg. Chim. Acta* **1986**, *111*, 61.
(100) Sellman, D.; Zapf, L. *Angew. Chem., Int. Ed. Engl.* **1984**, *23*, 807.
(101) Diel, B. N.; Haltiwanger, R. C.; Norman, A. D. *J. Am. Chem. Soc.* **1982**, *104*, 4700.
(102) Nelson, S. M.; McFall, S. G.; Drew, M. G. B.; Hamid bin Othmann, A. *Proc. R. Ir. Acad., Sect. B* **1977**, *77*, 523.
(103) Cook, D. H.; Fenton, D. E. *J. Chem. Soc., Dalton Trans.* **1979**, 266.
(104) Cook, D. H.; Fenton, D. E. *J. Chem. Soc., Dalton Trans.* **1979**, 810.
(105) Drew, M. G. B.; Hamid bin Othmann, A.; McFall, S. G.; Nelson, S. M. *J. Chem. Soc., Chem. Commun.* **1975**, 818.
(106) Fenton, D. E.; Cook, D. H.; Drew, M. G. B.; McFall, S. G.; Nelson, S. M. *J. Chem. Soc., Dalton Trans.* **1977**, 446.
(107) Fenton, D. E.; Cook, D. H.; Nowell, I. W.; Walker, P. E. *J. Chem. Soc., Chem. Commun.* **1978**, 279.
(108) Fenton, D. E.; Cook, D. H.; Nowell, I. W. *J. Chem. Soc., Chem. Commun.* **1977**, 274.
(109) Fenton, D. E.; Cook, D. H.; Nowell, I. W.; Walker, P. E. *J. Chem. Soc., Chem. Commun.* **1977**, 623.
(110) Drew, M. G. B.; Rodgers, A.; McCann, M.; Nelson, S. M. *J. Chem. Soc., Chem. Commun.* **1978**, 415.
(111) Cairns, C.; McFall, S. G.; Nelson, S. M.; Drew, M. G. B. *J. Chem. Soc., Dalton Trans.* **1979**, 446.
(112) Drew, M. G. B.; Hamid bin Othmann, A.; McFall, S. G.; McIlroy, P. D. A.; Nelson, S. M. *J. Chem. Soc., Dalton Trans.* **1977**, 1173.
(113) Drew, M. G. B.; Hamid bin Othmann, A.; McFall, S. G.; Nelson, S. M. *J. Chem. Soc., Dalton Trans.* **1977**, 438.
(114) Nelson, S. M.; Bryan, P.; Busch, D. H. *J. Chem. Soc., Chem. Commun.* **1966**, 641.
(115) Nelson, S. M.; Busch, D. H. *Inorg. Chem.* **1969**, *8*, 1859.
(116) Drew, M. G. B.; Hamid bin Othmann, A.; McIlroy, P. D. A.; Nelson, S. M. *J. Chem. Soc., Dalton Trans.* **1975**, 2507.
(117) Drew, M. G. B.; Hamid bin Othmann, A.; Nelson, S. M. *J. Chem. Soc., Dalton Trans.* **1976**, 1394.
(118) Drew, M. G. B.; Nelson, S. M. *Acta Crystallogr.* **1975**, *A31*, S140.
(119) Nelson, S. M.; McFall, S. G.; Drew, M. G. B.; Hamid bin Othmann, A.; Mason, N. B. *J. Chem. Soc., Chem. Commun.* **1977**, 167.
(120) Drew, M. G. B.; McFall, S. G.; Nelson, S. M. *J. Chem. Soc., Dalton Trans.* **1979**, 575.
(121) Fleischer, E.; Hawkinson, S. *J. Am. Chem. Soc.* **1967**, *89*, 720.
(122) Rest, A. J.; Smith, S. A.; Tyler, I. D. *Inorg. Chim. Acta* **1976**, *16*, L1.
(123) Cabral, J.; Cabral, M. F.; Drew, M. G. B.; Rodgers, A.; Nelson, S. M. *Inorg. Chim. Acta* **1978**, *30*, L313.
(124) Cook, D. H.; Fenton, D. E.; Drew, M. G. B.; Rodgers, A.; McCann, M.; Nelson, S. M. *J. Chem. Soc., Dalton Trans.* **1979**, 414.
(125) Drew, M. G. B.; Nelson, J.; Nelson, S. M. *J. Chem. Soc., Dalton Trans.* **1981**, 1678.
(126) Bailey, N. A.; Fenton, D. E.; Jackson, I. T.; Moody, R.; Rodriguez de Barbarin, C. O. *J. Chem. Soc., Chem. Commun.* **1983**, 1463.
(127) Adams, H.; Bailey, N. A.; Fenton, D. E.; Good, R. J.; Moody, R.; Rodriguez de Barbarin, C. O. *J. Chem. Soc., Dalton Trans.* **1987**, 207.
(128) Fenton, D. E. In *Comprehensive Coordination Chemistry*; Wilkinson, G., Gillard, R. D., McCleverty, J. A., Eds.; Pergamon Press: Oxford, 1987; Vol. 3, Chapter 23.
(129) Bailey, N. A.; Fenton, D. E.; Good, R. J.; Moody, R.; Rodriguez de Barbarin, C. O. *J. Chem. Soc., Dalton Trans.* **1987**, 207.

(130) Sessler, J. L.; Johnson, M. J.; Lynch, V. *J. Org. Chem.* **1987**, *52*, 4394.
(131) Sessler, J. L.; Mody, T. D.; Lynch, V. *Inorg. Chem.* **1992**, *31*, 529.
(132) Sessler, J. L.; Morishima, T.; Lynch, V. *Angew. Chem., Int. Ed. Engl.* **1991**, *30*, 977.
(133) Sessler, J. L.; Mody, T. D.; Hemmy, G. W.; Lynch, V. *Inorg. Chem.* **1993**, *32*, 3175.
(134) McMurry, T. J.; Raymond, K. N.; Smith, P. H. *Science* **1989**, *244*, 938.
(135) Backers-Dirks, J. D. J.; Gray, C. J.; Hart, F. A.; Hursthouse, M. B.; Schoop, B. C. *J. Chem. Soc., Chem. Commun.* **1979**, 774.
(136) De Cola, L.; Smailes, D. L.; Vallarino, L. M. *Inorg. Chem.* **1986**, *25*, 1729.
(137) Robinson, S. D.; Uttley, M. F. *J. Chem. Soc., Dalton Trans.* **1973**, 1912.
(138) Nakamoto, K. *Infrared and Raman Spectra of Inorganic and Coordination Compounds*, 3rd ed.; Wiley: New York, 1978; p 232.
(139) Radecka-Paryzek, W. *Inorg. Chim. Acta* **1981**, *52*, 261.
(140) Abid, K. K.; Fenton, D. E. *Inorg. Chim. Acta* **1984**, *95*, 119.
(141) Haque, Z. P.; McPartlin, M.; Tasker, P. A. *Inorg. Chem.* **1979**, *18*, 2920.
(142) Cairns, C.; McFall, S. G.; Nelson, S. M.; Drew, M. G. B. *J. Chem. Soc., Dalton Trans.* **1979**, 446.
(143) Abid, K. K.; Fenton, D. E.; Casellato, U.; Vigato, P. A.; Graziani, R. *J. Chem. Soc., Dalton Trans.* **1984**, 351.
(144) Abid, K. K. *Inorg. Chim. Acta* **1985**, *109*, L5.
(145) Radecka-Paryzek, W. *Inorg. Chim. Acta* **1980**, *45*, L147.
(146) Arif, A. M.; Backer-Dirks, J. D. J.; Gray, C. J.; Hart, F. A.; Hursthouse, M. B. *J. Chem. Soc., Dalton Trans.* **1987**, 1665.
(147) Bombieri, G.; Benetollo, F.; Polo, A.; De Cola, L.; Smailes, D. L.; Vallarino, L. M. *Inorg. Chem.* **1986**, *25*, 1127.
(148) Smith, P. H.; Brainard, J. R.; Morris, D. E.; Jarvinen, G. D.; Ryan, R. R. *J. Am. Chem. Soc.* **1989**, *111*, 7437.
(149) Bombieri, G.; Benetollo, F.; Hawkins, W. T.; Polo, A.; Vallarino, L. M. *Polyhedron* **1989**, *8*, 1923.
(150) Bombieri, G.; Benetollo, F.; Polo, A.; De Cola, L.; Hawkins, W. T.; Vallarino, L. M. *Polyhedron* **1989**, *8*, 2157.
(151) Fonda, K. K.; Vallarino, L. M.; Bombieri, G.; Benetollo, F.; Polo, A. *Polyhedron* **1991**, *10*, 1385.
(152) Stotz, R. W.; Stoufer, R. C. *J. Chem. Soc., Chem. Commun.* **1970**, 1682.
(153) Cabral, J. de O.; Cabral, M. F.; Drew, M. G. B.; Esho, F. S.; Haas, O.; Nelson, S. M. *J. Chem. Soc., Chem. Commun.* **1982**, 1066.
(154) Radecka-Paryzek, W. *Inorg. Chim. Acta* **1985**, *109*, L21.
(155) Benetollo, F.; Bombieri, G.; De Cola, L.; Polo, A.; Smailes, D. L.; Vallarino, L. M. *Inorg. Chem.* **1989**, *28*, 3447.
(156) Drew, M. G. B.; Cabral, J. de O.; Cabral, M. F.; Esho, F. S.; Nelson, S. M. *J. Chem. Soc., Chem. Commun.* **1979**, 1033.
(157) Benetollo, F.; Bombieri, G.; Fonda, K. K.; Polo, A.; Quagliano, J. R.; Vallarino, L. M. *Inorg. Chem.* **1991**, *30*, 1345.
(158) Tsubomura, T.; Yasaku, K.; Sato, T.; Morita, M. *Inorg. Chem.* **1992**, *31*, 447.
(159) Abid, K. K.; Fenton, D. E. *Inorg. Chim. Acta* **1984**, *82*, 223.
(160) Fenton, D. E.; Casellato, U.; Vigato, P. A.; Vidali, M. *Inorg. Chim. Acta* **1984**, *95*, 187.
(161) Pilkington, N. H.; Robson, R. *Aust. J. Chem.* **1970**, *23*, 2225.
(162) Lacroix, P.; Kahn, O.; Theobald, F.; Le Roy, J.; Wakselman, C. *Inorg. Chim. Acta* **1988**, *142*, 129.
(163) Bailey, N. A.; Fenton, D. E.; Roberts, P. B.; Walford, A. M. *J. Chem. Soc., Dalton Trans.* **1987**, 1865.
(164) Mandal, S. K.; Thompson, L. K.; Nag, K.; Charland, J. P.; Gabe, E. J. *Inorg. Chem.* **1987**, *26*, 1391.
(165) Lambert, S. L.; Spiro, C. L.; Gagne, R. R.; Hendrickson, D. N. *Inorg. Chem.* **1982**, *21*, 68.
(166) Luneau, D.; Savariault, J.-M.; Tuchageus, J.-P. *Inorg. Chem.* **1988**, *27*, 3912.
(167) Borovic, A. S.; Papaefthymiou, V.; Taylor, L. F.; Anderson, O. P.; Que, jun, L. *J. Am. Chem. Soc.* **1989**, *111*, 6183.
(168) Karlin, K. D.; Cruse, R. W.; Gultneh, Y.; Farook, A.; Hayes, R. M.; Zubieta, J. *J. Am. Chem. Soc.* **1987**, *109*, 2668.
(169) Buchanan, R. M.; Mashuta, M. S.; Oberhausen, K. J.; Richardson, J. F.; Qiaoying, I.; Hendrickson, D. N. *J. Am. Chem. Soc.* **1989**, *111*, 4497.
(170) Suzuki, M.; Oshio, H.; Ueharu, A.; Endo, K.; Yanaga, M.; Kida, S.; Saito, K. *Bull. Chem. Soc. Jpn.* **1988**, *61*, 3907.
(171) Bailey, N. A.; Fenton, D. E.; Moody, R.; Scrimshrie, P. J.; Beloritzky, E.; Fries, P. H.; Latour, J.-M. *J. Chem. Soc., Dalton Trans.* **1988**, 2817.
(172) Zanella, P.; Tamburini, S.; Vigato, P. A.; Mazzocchin, G. *Coord. Chem. Rev.* **1987**, *77*, 165.
(173) Guerriero, P.; Casellato, U.; Tamburini, S.; Vigato, P. A.; Graziani, R. *Inorg. Chim. Acta* **1987**, *129*, 127.
(174) Casellato, U.; Fregona, D.; Sitran, S.; Tamburini, S.; Vigato, P. A.; Fenton, D. E. *Inorg. Chim. Acta* **1985**, *110*, 181.
(175) Bunzli, J.-C. G.; Moret, E.; Casellato, U.; Guerriero, P.; Vigato, P. A. *Inorg. Chim. Acta* **1988**, *150*, 133.
(176) Tamburini, S.; Vigato, P. A.; Traldi, P. *Org. Mass Spectrom.* **1986**, *21*, 183.
(177) Bullita, E.; Guerriero, P.; Tamburini, S.; Vigato, P. A. *J. Less-Common Met.* **1989**, *153*, 211.
(178) Arif, A. M.; Gray, C. J.; Hart, F. A.; Hursthouse, M. B. *Inorg. Chim. Acta* **1985**, *109*, 179.
(179) Smith, P. H.; Raymond, K. N. *Inorg. Chem.* **1985**, *24*, 3469.
(180) Smith, P. H.; Reyes, Z. E.; Lee, C.-W.; Raymond, K. N. *Inorg. Chem.* **1988**, *27*, 4154.
(181) Creaser, I. I.; Geue, R. J.; Harrowfield, J. M.; Herlit, A. J.; Sargeson, A. M.; Snow, M. R.; Springborg, J. *J. Am. Chem. Soc.* **1982**, *104*, 6016.
(182) Raymond, K. N.; Smith, P. H. *Pure Appl. Chem.* **1988**, *60*, 1141.
(183) Sessler, J. L.; Murai, T.; Lynch, V.; Cyr, M. *J. Am. Chem. Soc.* **1988**, *110*, 5586.
(184) Maiya, B. G.; Mallouck, T. E.; Hemmi, G.; Sessler, J. L. *Inorg. Chem.* **1990**, *29*, 3738.
(185) Sessler, J. L.; Burrell, A. K. *Top. Curr. Chem.* **1991**, *161*, 177.
(186) Sessler, J. L.; Mody, T. D.; Ramasamy, R.; Sherry, A. D. *New J. Chem.* **1992**, *60*, 541.
(187) Sessler, J. L.; Murai, T.; Hemmi, G. *Inorg. Chem.* **1989**, *28*, 3390.
(188) Sessler, J. L.; Murai, T.; Lynch, V. *Inorg. Chem.* **1989**, *28*, 1333.
(189) Bauer, V. J.; Clive, D. L.; Dolphin, D.; Paine, J. B., III; Harris, F. L.; King, M. M.; Loder, H.; Wang, S.-W. C.; Woodward, R. B. *J. Am. Chem. Soc.* **1983**, *105*, 6429.
(190) Broadhurst, M. J.; Grigg, R.; Johnson, A. W. *J. Chem. Soc., Perkin Trans. 1* **1972**, 2111.
(191) Sessler, J. L.; Cyr, M. J.; Lynch, V.; McGhee, E.; Ibers, J. A. *J. Am. Chem. Soc.* **1990**, *112*, 2810.
(192) Sessler, J. L.; Cyr, M. J.; Burrell, A. K. *Syn. Lett.* **1991**, 127.
(193) Burrell, A. K.; Hemmi, G.; Lynch, V.; Sessler, J. L. *J. Am. Chem. Soc.* **1991**, *113*, 4690.
(194) Rexhausen, H.; Gossauer, A. *J. Chem. Soc., Chem. Commun.* **1983**, 275.
(195) Gossauer, A. *Bull. Soc. Chim. Belg.* **1983**, *92*, 793.
(196) Day, V. W.; Marks, T. J.; Wachter, W. A. *J. Am. Chem. Soc.* **1975**, *97*, 4519.
(197) Marks, T. J.; Stojakovic, D. R. *J. Am. Chem. Soc.* **1978**, *100*, 1695.
(198) Cuellar, E. A.; Stojakovic, D. R.; Marks, T. J. *Inorg. Syn.* **1980**, *20*, 97.
(199) Cuellar, E. A.; Marks, T. J. *Inorg. Chem.* **1981**, *20*, 3766.
(200) Marks, T. J.; Stojakovic, D. R. *J. Chem. Soc., Chem. Commun.* **1975**, 28.
(201) van Doorn, A. R.; Bos, M.; Harkema, S.; van Eerden, J.; Verboom, W.; Reinhoudt, D. N. *J. Org. Chem.* **1991**, *56*, 2371.
(202) Nijenhuis, W.; van Doorn, A. R.; Reichwain, A. M.; de Jong, F.; Reinhoudt, D. N. *J. Am. Chem. Soc.* **1991**, *113*, 3607.
(203) Chandra, R. *Synth. React. Inorg. Met.-Org. Chem.* **1990**, *20*, 645.
(204) Casellato, U.; Guerriero, P.; Tamburini, S.; Vigato, P. A.; Graziani, R. *J. Chem. Soc., Dalton Trans.* **1990**, 1533.
(205) El-Saied, F. A. *Inorg. Chim. Acta* **1989**, *165*, 147.
(206) van Staveren, C. J.; Fenton, D. E.; Reinhoudt, D. N.; van Eerden, J.; Harkema, S. *J. Am. Chem. Soc.* **1987**, *109*, 3456.
(207) De Cola, L.; Smailes, D. L.; Vallarino, L. M. *Inorg. Chim. Acta* **1985**, *110*, L1.
(208) Casellato, U.; Fregona, D.; Sitran, S.; Tamburini, S.; Vigato, P. A. *Inorg. Chim. Acta* **1985**, *110*, 161.
(209) Burrell, A. K.; Cyr, M. J.; Lynch, V.; Sessler, J. L. *J. Chem. Soc., Chem. Commun.* **1991**, 1710.
(210) Casellato, U.; Vidali, M.; Vigato, P. A. *Inorg. Nucl. Chem. Lett.* **1974**, *10*, 437.
(211) Vidali, M.; Vigato, P. A.; Casellato, U.; Tondello, E.; Traverso, O. *J. Inorg. Nucl. Chem.* **1975**, *37*, 1715.
(212) Casellato, U.; Sitran, S.; Tamburini, S.; Vigato, P. A.; Graziani, R. *Inorg. Chim. Acta* **1986**, *114*, 111.
(213) Casellato, U.; Guerriero, P.; Tamburini, S.; Vigato, P. A.; Graziani, R. *Inorg. Chim. Acta* **1986**, *119*, 215.
(214) Andrews, R. K.; Blakeley, R. L.; Zerner, B. *Adv. Inorg. Biochem.* **1984**, *6*, 245.
(215) van Staveren, C. J.; van Eerden, J.; van Veggel, F. C. J. M.; Harkema, S.; Reinhoudt, D. N. *J. Am. Chem. Soc.* **1988**, *110*, 4994.
(216) Kahwa, I. A.; Selbin, J.; Hsieh, T. C. Y.; Lane, R. A. *Inorg. Chim. Acta* **1986**, *118*, 179.
(217) Kahwa, I. A.; Folkes, S.; Williams, D. J.; Ley, S. V.; O'Mahoney, C. A.; McPherson, G. L. *J. Chem. Soc., Chem. Commun.* **1989**, 1531.
(218) Guerriero, P.; Vigato, P. A.; Bunzli, J.-C. G.; Moret, E. *J. Chem. Soc., Dalton Trans.* **1990**, 647.
(219) Ziessel, R.; Maestri, M.; Prodi, L.; Balzani, V.; Dorsselaer, A. V. *Inorg. Chem.* **1993**, *32*, 1237.
(220) Inoue, M. B.; Inoue, M.; Munoz, I. C.; Bruck, M. A.; Fernando, Q. *Inorg. Chim. Acta* **1993**, *209*, 29.
(221) Inoue, M. B.; Villegas, C. A.; Asano, K.; Nakamura, M.; Inoue, M.; Fernando, Q. *Inorg. Chem.* **1992**, *31*, 2480.
(222) McKee, V.; Shepard, W. B. *J. Chem. Soc., Chem. Commun.* **1985**, 158.
(223) Fenton, D. E.; Kitchen, S. J.; Spencer, C. M.; Tamburini, S.; Vigato, P. A. *J. Chem. Soc., Dalton Trans.* **1988**, 685.
(224) Aspinall, C. H.; Black, J.; Dodd, I.; Harding, M. M.; Winkley, S. J. *J. Chem. Soc., Dalton Trans.* **1993**, 709.

(225) Nelson, S. M.; McFall, S. G.; Drew, M. G. B.; Hamid bin Othmann, A. *Proc. R. Irish Acad.* **1977**, *77B*, 523.
(226) Day, V. W.; Marks, T. J.; Wachter, W. A. *J. Am. Chem. Soc.* **1975**, *97*, 4519.
(227) Marks, T. J.; Stojakovic, D. R. *J. Chem. Soc., Chem. Commun.* **1975**, 28.
(228) Nelson, S. M.; Esho, F. S.; Drew, M. G. B. *J. Chem. Soc., Chem. Commun.* **1981**, 388.
(229) Nelson, S. M.; Esho, F. S.; Drew, M. G. B. *J. Chem. Soc., Dalton Trans.* **1982**, 407.
(230) Nelson, S. M.; Esho, F. S. *J. Chem. Soc., Chem. Commun.* **1981**, 38.
(231) Drew, M. G. B.; Yates, P. C.; Grimshaw, J. T.; Lavery, A.; McKillop, K. P.; Nelson, S. M.; Nelson, J. *J. Chem. Soc., Dalton Trans.* **1988**, 347.
(232) Gray, C. J.; Hart, F. A. *J. Chem. Soc., Dalton Trans.* **1987**, 2289.
(233) Sabbatini, N.; De Cola, L.; Vallarino, L. M.; Blasse, G. *J. Phys. Chem.* **1987**, *91*, 4681.
(234) Izatt, R. M.; Bradshaw, J. S.; Neilson, S. A.; Lamb, J. D.; Christensen, J. J. *Chem. Rev.* **1985**, *85*, 271.
(235) Vögtle, F.; Weber, E. In *Crown Ethers and Analogs*; Patai, S., Rappoport, Z., Eds.; Wiley: New York, 1989; p 207.
(236) Cram, D. J. *J. Inclusion Phenom.* **1988**, *6*, 397.
(237) Lehn, J.-M. *J. Inclusion Phenom.* **1988**, *6*, 351.
(238) Pedersen, C. J. *J. Inclusion Phenom.* **1988**, *6*, 337.
(239) Raevskii, O. A. *Koord. Khim.* **1990**, *16*, 723.
(240) Fenton, D. E. *Pure Appl. Chem.* **1989**, *61*, 1563.
(241) Shinkai, S. *J. Inclusion Phenom. Mol. Recognit. Chem.* **1989**, *7*, 193.
(242) Chang, C. A.; Rowland, M. E. *Inorg. Chem.* **1983**, *22*, 3866.
(243) Adam, K. R.; Baldwin, D.; Duckworth, P. A.; Leong, A. J.; Lindoy, L. F.; McPartlin, M.; Tasker, P. A. *J. Chem. Soc., Chem. Commun.* **1987**, 1124.
(244) Fenton, D. E.; Murphy, B. P.; Price, R.; Tasker, P. A.; Winter, D. J. *J. Inclusion Phenom.* **1987**, *5*, 143.
(245) Fenton, D. E.; Murphy, B. P.; Leong, A. J.; Lindoy, L. F.; Bashall, A.; McPartlin, M. *J. Chem. Soc., Dalton Trans.* **1987**, 2543.
(246) Adam, K. R.; Dancey, K. P.; Harrison, B. A.; Leong, A. J.; Lindoy, L. F.; McPartlin, M.; Tasker, P. A. *J. Chem. Soc., Chem. Commun.* **1983**, 1351.
(247) Adam, K. R.; Leong, A. J.; Lindoy, L. F.; McCool, B. J.; Ekstrom, A.; Liepa, L.; Harding, P. A.; Henrick, K.; McPartlin, M.; Tasker, P. A. *J. Chem. Soc., Dalton Trans.* **1987**, 2537.
(248) Lindoy, L. F. In *Progress in Macrocyclic Chemistry*; Izatt, R. M., Christensen, J. J., Eds.; Wiley Interscience: New York, 1987; Vol. 3, p 53 and references therein.
(249) Adam, K. R.; Leong, A. J.; Lindoy, L. F.; Lip, H. C.; Skelton, B. W.; White, A. H. *J. Am. Chem. Soc.* **1983**, *105*, 4645.
(250) Adam, K. R.; Ansell, C. W. G.; Dancey, K. P.; Drummond, L. A.; Leong, A. J.; Lindoy, L. F.; Tasker, P. A. *J. Chem. Soc., Chem. Commun.* **1986**, 1011.
(251) Adam, K. R.; Dancey, K. P.; Leong, A. J.; Lindoy, L. F.; McCool, B. J.; McPartlin, M.; Tasker, P. A. *J. Am. Chem. Soc.* **1988**, *110*, 8471.
(252) Lindoy, L. F. *Pure Appl. Chem.* **1989**, *61*, 1575.
(253) Chen, C. S.; Wang, S. J.; Wu, S. C. *Inorg. Chem.* **1984**, *23*, 3901.
(254) Adam, K. R.; Leong, A. J.; Lindoy, L. F.; Anderegg, G. J. *J. Chem. Soc., Dalton Trans.* **1988**, 1733.
(255) Buschman, H. J. *J. Inclusion Phenom. Mol. Recognit. Chem.* **1989**, *7*, 581.
(256) Buschman, H.-J. *J. Solution Chem.* **1988**, *17*, 277.
(257) Soong, L. L.; Leroi, G. E.; Popov, A. I. *Inorg. Chem.* **1990**, *29*, 1366.
(258) Gholivand, M. B.; Shamsipur, M. *Inorg. Chim. Acta* **1986**, *121*, 53.
(259) Marolleau, E. V.; Gisselbrecht, J. P.; Gross, M.; Arnaud-Neu, F.; Schwing-Weill, M. J. *J. Chem. Soc., Dalton Trans.* **1990**, 1285.
(260) Schmidt, E.; Tremilon, J. M.; Kintzinger, J. P.; Popov, A. I. *J. Am. Chem. Soc.* **1983**, *105*, 7563.
(261) Bünzli, J.-C. G.; Giorgetti, A. *Inorg. Chim. Acta* **1985**, *110*, 225.
(262) Pett, V. B.; Leggett, G. H.; Cooper, T. H.; Reed, P. R.; Situm eang, D.; Ochrymowycz, L. A.; Rorabacher, D. B. *Inorg. Chem.* **1988**, *27*, 2164.
(263) Stöver, H. D.; Maurice, L. J.; Delville, A.; Detellier, C. *Polyhedron* **1985**, *4*, 1091.
(264) Motekaitis, R. J.; Martell, A. E.; Lehn, J.-M.; Watanabe, E. *Inorg. Chem.* **1982**, *21*, 4253.
(265) Van der Merwe, M. J.; Boeyens, J. C. A.; Hancock, R. D. *Inorg. Chem.* **1985**, *24*, 1208.
(266) Kulstad, S.; Malmsten, L. A. *J. Inorg. Chem.* **1980**, *42*, 573.
(267) Gokel, G. W.; Goli, D. M.; Minganta, C.; Echegoyen, L. *J. Am. Chem. Soc.* **1983**, *105*, 6786.
(268) Madeyski, C. M.; Michael, J. P.; Hancock, R. D. *Inorg. Chem.* **1984**, *23*, 1487.
(269) Hay, R. W.; Clark, D. M. S. *Inorg. Chim. Acta* **1984**, *83*, L23.
(270) Groth, P.; Crane, J. *J. Chem. Soc., Chem. Commun.* **1982**, 1172.
(271) Hancock, R. D.; Bhavan, R.; Wade, P. W.; Boeyens, J. C. A.; Dobson, S. M. *Inorg. Chem.* **1989**, *28*, 187.
(272) Hancock, R. D. *Pure Appl. Chem.* **1986**, *58*, 1445.
(273) Dermer, O. C.; Ham, G. E. *Ethyleneimine and Other Aziridines*; Academic Press: London, 1969.
(274) Deyrup, J. A. In *The Chemistry of Heterocycles*; Hassner, A., Ed.; Wiley: New York, 1983; Vol. 42, Part 1.
(275) Gauss, W.; Moser, P.; Schwartzenbach, G. *Helv. Chim. Acta* **1952**, *35*, 2359.
(276) Murase, I.; Mikuriya, M.; Sonoda, H.; Kida, S. *J. Chem. Soc., Chem. Commun.* **1984**, 692.
(277) Murase, I.; Mikuriya, M.; Sonoda, H.; Fukuda, Y.; Kida, S. *J. Chem. Soc., Dalton Trans.* **1986**, 953.
(278) Hediger, M.; Kaden, T. A. *J. Chem. Soc., Chem. Commun.* **1978**, 14.
(279) Pallavicini, P. S.; Perotti, A.; Poggi, A.; Seghi, B.; Fabrizzi, L. *J. Am. Chem. Soc.* **1987**, *109*, 5139.
(280) Hosseini, M. W.; Lehn, J.-M. *J. Am. Chem. Soc.* **1987**, *109*, 7047.
(281) Murase, I.; Ueda, I.; Marubayashi, N.; Kida, S.; Matsumoto, M.; Kudo, M.; Toyohara, M.; Hiute, K.; Mikuriya, M. *J. Chem. Soc., Dalton Trans.* **1990**, 2763.
(282) Cacheris, W. P.; Nickle, S. K.; Sherry, A. D. *Inorg. Chem.* **1987**, *26*, 958.
(283) Stetter, H.; Frank, W. *Angew. Chem., Int. Ed. Engl.* **1976**, *15*, 686.
(284) Delgado, R.; Frausto de Silva, J. R. *Talanta* **1982**, *29*, 815.
(285) Desreux, J. F.; Loncin, M. F. *Inorg. Chem.* **1986**, *25*, 69.
(286) Spirlet, M. R.; Rebizant, J.; Loncin, M. F.; Desreux, J. F. *Inorg. Chem.* **1984**, *23*, 4278.
(287) Wieghardt, K.; Bossek, U.; Chaudhuri, P.; Hermann, W.; Menke, B. C.; Weiss, J. *Inorg. Chem.* **1982**, *21*, 4308.
(288) Van der Merwe, M. J.; Boeyens, J. C. A.; Hancock, R. D. *Inorg. Chem.* **1983**, *22*, 3489.
(289) Bevilacqua, A.; Gelb, R. I.; Hebard, W. R.; Zompa, L. J. *Inorg. Chem.* **1987**, *26*, 2699.
(290) Chaudhuri, P.; Wieghardt, K. *Prog. Inorg. Chem.* **1986**, *35*, 329.
(291) Delgado, R.; Frausto de Silva, J. J. R. *Talanta* **1982**, *29*, 850.
(292) Stetter, H.; Frank, W.; Mertens, R. *Tetrahedron* **1981**, *37*, 767.
(293) Desreux, J. F. *Inorg. Chem.* **1980**, *19*, 1319.
(294) Desreux, J. F.; Merciny, E.; Loncin, M. F. *Inorg. Chem.* **1981**, *20*, 987.
(295) Graziani, R.; Vidali, M.; Casellato, U.; Vigato, P. A. *Acta Crystallogr., Sect. B* **1976**, *32*, 1681.
(296) Loncin, M. F.; Desreux, J. F.; Merciny, E. *Inorg. Chem.* **1986**, *25*, 2646.
(297) Wang, X.; Jin, T.; Comblin, V.; Lopez-Mut, A.; Merciny, E.; Desreux, J. F. *Inorg. Chem.* **1992**, *31*, 1095.
(298) Clark, E. T.; Martell, A. E. *Inorg. Chim. Acta* **1991**, *190*, 37.
(299) Chang, C. A. *Eur. J. Solid State Chem.* **1991**, *28*, 237.
(300) Aime, S.; Botta, M.; Ermondi, G. *Inorg. Chem.* **1992**, *31*, 4291.
(301) Spirlet, M.; Rebizant, J.; Desreux, J. F.; Loncin, M. F. *Inorg. Chem.* **1984**, *23*, 359.
(302) Brucher, E.; Laurenczy, G.; Makra, Z. *Inorg. Chim. Acta* **1987**, *139*, 141.
(303) Sherry, A. D.; Brown, R. D., III; Geraldes, C. F. G. C.; Koenig, S. H.; Kuan, K.; Spiller, M. *Inorg. Chem.* **1989**, *28*, 620.
(304) Kodama, M.; Koike, T.; Mahatma, A. B.; Kimura, E. *Inorg. Chem.* **1991**, *30*, 1270.
(305) Brucher, E.; Sherry, A. D. *Inorg. Chem.* **1990**, *29*, 1555.
(306) Hancock, R. D.; Martell, A. E. *Chem. Rev.* **1989**, *89*, 1875.
(307) Sekhar, V. C.; Chang, C. A. *Inorg. Chem.* **1986**, *25*, 2061.
(308) Cortes, S.; Brucher, E.; Geraldes, C. F. G. C.; Sherry, A. D. *Inorg. Chem.* **1990**, *29*, 5.
(309) Brucher, E.; Cortes, S.; Chavez, F.; Sherry, A. D. *Inorg. Chem.* **1991**, *30*, 2092.
(310) Carvalho, J. F.; Kim, S.-H.; Chang, C. A. *Inorg. Chem.* **1992**, *31*, 4065.
(311) Aime, S.; Botta, M.; Ermondi, G.; Fedeli, F.; Uggeri, F. *Inorg. Chem.* **1992**, *31*, 1100.
(312) Sherry, A. D.; Cacheris, W. P.; Kuan, K. T. *Magn. Reson. Med.* **1988**, *8*, 180.
(313) Aime, S.; Anelli, P. L.; Botta, M.; Fedeli, F.; Grandi, M.; Paoli, P.; Uggeri, F. *Inorg. Chem.* **1992**, *31*, 2422.
(314) Kabachnik, M. I.; Medved, T. Ya.; Polikarpov, Yu. M.; Pasechnik, M. P. *Izv. Akad. Nauk SSSR, Ser. Khim.* **1984**, 844.
(315) Delgado, R.; Siegfried, L. C.; Kaden, T. A. *Helv. Chim. Acta* **1990**, *73*, 140.
(316) Lazar, I.; Hrncir, D. C.; Kim, W.-D.; Kiefer, G. E.; Sherry, A. D. *Inorg. Chem.* **1992**, *31*, 4422.
(317) Geraldes, C. F. G. C.; Brown, R. D., III; Cacheris, W. P.; Koenig, S. H.; Sherry, A. D.; Spiller, M. *Magn. Reson. Med.* **1989**, *9*, 94.
(318) Dingwall, J. G.; Campbell, C. D.; Baylis, E. K. *J. Chem. Soc., Perkin Trans. 1* **1984**, 2845.
(319) Broan, C. J.; Jankowski, K. J.; Kataky, R.; Parker, D.; Randall, A. *J. Chem. Soc., Chem. Commun.* **1990**, 1739.
(320) Morrow, J. R.; Chin, K. O. A. *Inorg. Chem.* **1993**, *32*, 3357.
(321) Choppin, G. R. In *Lanthanide Probes in Life, Chemical, and Earth Sciences: Theory and Practice*; Bunzli, J.-C. G., Choppin, G. R., Eds.; Elsevier: New York, 1989; Chapter 1.
(322) Frechette, M.; Butler, I. R.; Hynes, R.; Detellier, C. *Inorg. Chem.* **1992**, *31*, 1650.
(323) Chen, D.; Squattrito, P. J.; Martell, A. E.; Clearfield, A. *Inorg. Chem.* **1990**, *29*, 4366.

(324) Delgado, R.; Sun, Y.; Motekaitis, R. J.; Martell, A. E. *Inorg. Chem.* **1993**, *32*, 3320.
(325) Dischino, D. D.; Delaney, E. J.; Emswiler, J. E.; Geughan, G. T.; Prasad, J. S.; Srivastava, S. K.; Tweedle, M. F. *Inorg. Chem.* **1991**, *30*, 1265.
(326) Kumar, K.; Chang, C. A.; Tweedle, M. F. *Inorg. Chem.* **1993**, *32*, 587.
(327) Kumar, K.; Tweedle, M. F. *Inorg. Chem.* **1993**, *32*, 4193.
(328) Brittain, H.; Desreux, J. F. *Inorg. Chem.* **1984**, *23*, 4459.
(329) Kang, S. I.; Ranganathan, R. S.; Emswiler, J. E.; Kumar, K.; Gougoutas, J. Z.; Malley, M. F.; Tweedle, M. F. *Inorg. Chem.* **1993**, *32*, 2912.
(330) Matthews, R. C.; Parker, D.; Ferguson, G.; Kaitner, B.; Harrison, A.; Royle, L. *Polyhedron* **1991**, *10*, 1951.
(331) Lyon, R. C.; Faustino, P. J.; Cohen, J. S.; Katz, A.; Mornex, F.; Colcher, D.; Baglin, C.; Koenig, S. H.; Hambright, P. *Magn. Reson. Med.* **1987**, *4*, 24.
(332) Hambright, P.; Adams, C.; Vernon, K. *Inorg. Chem.* **1988**, *27*, 1660.
(333) Haye, S.; Hambright, P. *J. Chem. Soc., Chem. Commun.* **1988**, 666.
(334) Streitwieser, A.; Muller-Westerhoff, U. *J. Am. Chem. Soc.* **1968**, *90*, 7364.
(335) Chang, A. H. H.; Pitzer, R. M. *J. Am. Chem. Soc.* **1989**, *111*, 2500.
(336) Streitwieser, A. In *Organometallics of the f-Elements*; Marks, T. J., Fisher, R. D., Eds.; Reidel: Holland, 1979; p 149.
(337) Brennan, J. G.; Green, J. C.; Redfern, C. M. *J. Am. Chem. Soc.* **1989**, *111*, 2374.
(338) Green, J. C.; Kelley, M. R.; Long, J. A.; Kanellakopulos, B.; Yarrow, P. I. W. *J. Organomet. Chem.* **1981**, *212*, 329.
(339) Bursten, B. E.; Casaril, M.; Ellis, D. E. A.; Fragala, I. L.; Marks, T. J. *Inorg. Chem.* **1986**, *25*, 1257.
(340) Streitwieser, A.; Linsley, S. A.; Rigsbee, J. A.; Fragala, I. L.; Ciliberto, E.; Rosch, N. *J. Am. Chem. Soc.* **1985**, *107*, 7786.
(341) Gulino, A.; Casirin, M.; Conticello, V. P.; Guadiello, J. G.; Mauermann, H.; Fragala, I. L.; Marks, T. J. *Organometallics* **1988**, *7*, 2360.
(342) Sockwell, S. C.; Hanusa, T. P. *Inorg. Chem.* **1990**, *29*, 76.
(343) Bursten, B. E.; Rhodes, L. F.; Strittmatter, R. J. *J. Am. Chem. Soc.* **1989**, *111*, 2758.
(344) Bursten, B. E.; Rhodes, L. F.; Strittmatter, R. J. *J. Am. Chem. Soc.* **1989**, *111*, 2756.
(345) Strittmatter, R. J.; Bursten, B. E. *J. Am. Chem. Soc.* **1991**, *113*, 552.
(346) Fagan, P. J.; Manriquez, J. M.; Jollmer, S. H.; Day, C. S.; Day, V. W.; Marks, T. J. *J. Am. Chem. Soc.* **1981**, *103*, 2206.
(347) Cramer, R. E.; Maynard, R. B.; Paw, J. C.; Gilje, J. W. *Organometallics* **1982**, *1*, 869.
(348) Fagan, P. J.; Manriquez, J. M.; Marks, T. J. *J. Am. Chem. Soc.* **1980**, *102*, 5393.
(349) Simpson, S. J.; Andersen, R. A. *J. Am. Chem. Soc.* **1981**, *103*, 4063.
(350) Marks, T. J.; Ernst, R. D. In *Comprehensive Organometallic Chemistry*; Wilkinson, G., Stone, F. G. A., Abel, E. W., Eds.; Pergamon Press: Oxford, 1982.
(351) Brennan, J. G.; Andersen, R. A.; Robbmns, J. L. *J. Am. Chem. Soc.* **1986**, *108*, 335.
(352) Bursten, B. E.; Strittmatter, R. J. *J. Am. Chem. Soc.* **1987**, *109*, 6606.
(353) Bunzli, J.-C. G.; Froidevaux, P.; Harrowfield, J. M. *Inorg. Chem.* **1993**, *32*, 3306.
(354) Blasse, G.; Dirksen, G. J.; Sabbatini, N.; Perathoner, S.; Lehn, J.-M.; Alpha, B. *J. Phys. Chem.* **1988**, *92*, 2419.
(355) Hart, F. A. In *Comprehensive Coordination Chemistry*; Wilkinson, G., Gillard, R. D., McCleverty, J. A., Eds.; Pergamon Press: Oxford, 1987.
(356) Backer-Dirks, J. D. J.; Cooke, J. E.; Galas, A. M. R.; Ghotra, J. S.; Gray, C. J.; Hart, F. A.; Hursthouse, M. B. *J. Chem. Soc., Dalton Trans.* **1980**, 2191.
(357) Bunzli, J.-C. G.; Klein, B.; Wessner, D.; Schenk, K. J.; Chapuis, G.; Bombieri, G.; De Paoli, G. *Inorg. Chim. Acta* **1981**, *54*, L43.
(358) Nicolo, F.; Plancherel, D.; Chapuis, G.; Bunzli, J.-C. G. *Inorg. Chem.* **1988**, *27*, 3518.
(359) Benetollo, F.; Polo, A.; Bombieri, G.; Fonda, K. K.; Vallarino, L. M. *Polyhedron* **1990**, *9*, 1411.
(360) Chang, C. A.; Francesconi, L. C.; Malley, M. F.; Kumar, K.; Gougoutas, J. Z.; Tweedle, M. F.; Lee, D. W.; Wilson, L. J. *Inorg. Chem.* **1993**, *32*, 3501.
(361) Dubost, J. P.; Legar, J. M.; Langlois, M. H.; Meyer, D.; Schaefer, M. *C.R. Acad. Sci. Paris Ser. 2* **1991**, *312*, 349.
(362) Forsellini, E.; Benetollo, F.; Bombieri, G.; Cassol, A.; DePaoli, G. *Inorg. Chim. Acta* **1985**, *109*, 167.
(363) Schaverien, C. J.; Orpen, A. G. *Inorg. Chem.* **1991**, *30*, 4968.
(364) Buchler, J. W.; De Cian, A.; Fischer, J.; Kihn-Botulinski, M.; Paulus, H.; Weiss, R. *J. Am. Chem. Soc.* **1986**, *108*, 3652.
(365) Buchler, J. W.; Scharbert, B. *J. Am. Chem. Soc.* **1988**, *110*, 4272.
(366) Buchler, J. W.; De Cian, A.; Fischer, J.; Kihn-Botulinski, M.; Paulus, H.; Weiss, R. *Inorg. Chem.* **1988**, *27*, 339.
(367) Buchler, J. W.; Kihn-Botulinski, M.; Loffler, J.; Wicholas, M. *Inorg. Chem.* **1989**, *28*, 3730.
(368) Buchler, J. W.; Loffler, J.; Wicholas, M. *Inorg. Chem.* **1992**, *31*, 524 and references cited therein.
(369) Buchler, J. W.; Scharbert, B. *J. Am. Chem. Soc.* **1988**, *110*, 4272.
(370) Potchen, J. E.; Koehler, P. R.; Davis, D. O. *Principles of Diagnostic Radiology*; McGraw-Hill: New York, 1971.
(371) Stark, D. D., Bradley, W. G., Jr., Eds. *Magnetic Resonance Imaging*; The C. V. Mosby Company: St. Louis, MO, 1988.
(372) Koenig, S. H. *Isr. J. Chem.* **1988**, *28*, 345.
(373) Tweedle, M. F.; Gaughan, G. T.; Hagan, J.; Wedeking, P. W.; Sibley, P.; Wilson, L. J.; Lee, D. W. *Nucl. Med. Biol.* **1988**, *15*, 31.
(374) Magerstadt, M.; Gansow, O. A.; Brechbiel, M. W.; Colcher, D.; Baltzer, L.; Knop, R. H.; Girton, M. E.; Naegele, M. *Magn. Reson. Med.* **1986**, *3*, 808.
(375) Lauffer, R. B.; Vincent, A. C.; Padmanabhan, J.; Meade, T. J. *J. Am. Chem. Soc.* **1987**, *109*, 2216.
(376) Bloch, F. *Phys. Rev.* **1946**, *70*, 460.
(377) Lauterbur, P. C.; Mendonca-Dias, M. H.; Rudin, A. M. In *Frontier of Biological Energetics*; Dutton, P. L., Leigh, L. S., Scarpa, A., Eds.; Academic: New York, 1978; p 752.
(378) Bertini, I.; Luchinat, C. *NMR of Paramagnetic Molecules in Biological Systems*; Benjamin/Cummins Publishing Co.: Menlo Park, 1986.
(379) Koenig, S. H.; Brown, R. D., III. *Magn. Reson. Med.* **1984**, *1*, 478.
(380) Aime, S.; Botta, M.; Ermondi, G. *J. Magn. Reson.* **1991**, *92*, 572.
(381) Tweedle, M. F.; Gaughan, G. T.; Hagan, J.; Wedeking, P. W.; Sibley, P.; Wilson, L. J.; Lee, D. W. *Nucl. Med. Biol.* **1988**, *15*, 31.
(382) Geraldes, C. F. G. C.; Sherry, A. D.; Brown, R. D., III; Koenig, S. H. *Magn. Reson. Med.* **1986**, *3*, 242.
(383) Choppin, G. R.; Baisden, P. A.; Khan, S. A. *Inorg. Chem.* **1980**, *18*, 1330.
(384) Weinmann, H. J.; Brasch, R. C.; Press, W. R.; Wesby, G. E. *AJR, Am. J. Roentgenol.* **1984**, *142*, 619.
(385) Koenig, S. H.; Spiller, M.; Brown, R. D.; Wolf, G. L. *Invest. Radiol.* **1986**, *21*, 697.
(386) Chang, C. A.; Sekhar, V. C. *Inorg. Chem.* **1987**, *26*, 1981.
(387) Chang, C. A.; Ochaya, V. O. *Inorg. Chem.* **1986**, *25*, 355.
(388) Chang, C. A.; Rowland, M. E. *Inorg. Chem.* **1983**, *22*, 3866.
(389) Tweedle, M. F.; Runge, V. M. *Drugs Future* **1992**, *17*, 187.
(390) Cacheris, W. P.; Quay, S. C.; Rocklage, S. M. *Magn. Reson. Imaging* **1990**, *8*, 467.
(391) Gries, H.; Miklautz, H. *Physiol. Chem. Phys. Med. NMR* **1984**, *16*, 105.
(392) Horrocks, W. DeW., Jr.; Sudnick, D. R. *J. Am. Chem. Soc.* **1979**, *101*, 334.
(393) Martell, A. E.; Smith, R. M. *Critical Stability Constants*; Plenum: New York, 1989; Vol. 6.
(394) Lauffer, R. B.; Brady, T. J. *Magn. Reson. Imaging* **1985**, *3*, 11.
(395) Ogan, M. D.; Schimiedl, U.; Mosely, M. E.; Grood, W.; Paajanen, H.; Brasch, R. C. *Invest. Radiol.* **1987**, *22*, 665.
(396) Zhang, X.; Chang, C. A.; Brittain, H. G.; Garrison, J. M.; Telser, J.; Tweedle, M. F. *Inorg. Chem.* **1992**, *31*, 5597.
(397) Horrocks, W. DeW., Jr.; Hove, E. G. *J. Am. Chem. Soc.* **1978**, *100*, 4386.
(398) Lyon, R. C.; Faustino, P. J.; Cohen, J. S.; Katz, A.; Mornex, F.; Colcher, D.; Baglin, C.; Koenig, S. H.; Hambright, P. *Magn. Reson. Med.* **1987**, *4*, 24.
(399) Radzki, S.; Krauz, P.; Gaspard, S.; Giannotti, C. *Inorg. Chim. Acta* **1987**, *138*, 139.
(400) Horrocks, W. DeW., Jr.; Wong, C. P. *J. Am. Chem. Soc.* **1976**, *98*, 7157.
(401) Wong, C. P.; Venteicher, R. F.; Horrocks, W. DeW., Jr. *J. Am. Chem. Soc.* **1974**, *96*, 7149.
(402) Srivastava, T. S. *Bioinorg. Chem.* **1978**, *8*, 61.
(403) DeNardo, S. J.; Peng, J. S.; DeNardo, G. L.; Mills, S. L.; Epstein, A. L. *Nucl. Med. Biol.* **1986**, *13*, 303.
(404) Order, S. E.; Klein, J. L.; Leichner, P. K.; Frinke, J.; Lollo, C.; Carlo, D. J. *Int. J. Radiat. Oncol. Biol. Phys.* **1986**, *12*, 277.
(405) Deshpande, S. V.; DeNardo, S. J.; Meares, C. F.; McCall, M. J.; Adams, G. P.; Moi, M. K.; DeNardo, G. L. *J. Nucl. Med.* **1988**, *29*, 217.
(406) Halpern, S. E.; Hagan, P. L.; Garver, P. R.; Kozol, J. A.; Chen, A. W. N.; Frincke, J. M.; Bartholomew, R. M.; David, G. S.; Adams, T. H. *Cancer Res.* **1983**, *43*, 5347.
(407) Pimm, M. V.; Perkins, A. C.; Baldwin, R. W. *Eur. J. Nucl. Med.* **1985**, *11*, 300.
(408) Harris, W. R.; Pecoraro, V. L. *Biochemistry* **1983**, *22*, 292.
(409) Morphy, J. R.; Parker, D.; Alexander, R.; Bains, A.; Carne, A. F.; Eaton, M. A. W.; Harrison, A.; Millican, A. T.; Phipps, A.; Rhind, S. K.; Titmas, R.; Weatherby, D. *J. Chem. Soc., Chem. Commun.* **1988**, 156.
(410) Moi, M. K.; Meares, C. F.; McCall, M. J.; Cole, W. C.; DeNardo, S. J. *Anal. Biochem.* **1985**, *148*, 249.
(411) Franz, J.; Freeman, G. M.; Barefield, E. K.; Volkert, W. A.; Ehrhardt, G. J.; Holmes, R. A. *Int. J. Appl. Radiat. Isot.* **1987**, *14*, 479.
(412) Morphy, J. R.; Parker, D.; Kataky, R.; Harrison, A.; Eaton, M. A. W.; Millican, A.; Phipps, A.; Walker, C. *J. Chem. Soc., Chem. Commun.* **1989**, 792.

(413) Craig, A. S.; Helps, I. M.; Jankowski, K. J.; Parker, D.; Beeley, N. R. A.; Boyce, B. A.; Eaton, M. A. W.; Millican, A. T.; Miller, K.; Phipps, A.; Rhind, S. K.; Harrison, A.; Walker, C. *J. Chem. Soc., Chem. Commun.* **1989**, 794.
(414) Cox, J. P. L.; Jankowski, K. J.; Kataky, R.; Parker, D.; Beeley, N. R. A.; Boyce, B. A.; Eaton, M. A. W.; Miller, K.; Millican, A. T.; Harrison, A.; Walker, C. *J. Chem. Soc., Chem. Commun.* **1989**, 797.
(415) Craig, A. S.; Parker, D.; Adams, H.; Bailey, N. A. *J. Chem. Soc., Chem. Commun.* **1989**, 1793.
(416) Moi, M. K.; Meares, C. F.; DeNardo, S. J. *J. Am. Chem. Soc.* **1988**, *110*, 6266.
(417) Morphy, J. R.; Kataky, R.; Parker, D.; Eaton, M. A. W.; Millican, A. T.; Phipps, A.; Harrison, A.; Walker, C. *J. Chem. Soc., Perkin Trans. 2* **1990**, 573.
(418) Cox, J. P. L.; Craig, A. S.; Helps, I. M.; Jankowski, K. J.; Parker, D.; Eaton, M. A. W.; Millican, A. T.; Miller, K.; Beeley, N. R. A.; Boyce, B. A. *J. Chem. Soc., Perkin Trans. 1* **1990**, 2567.
(419) Helps, I. M.; Jankowski, K. J.; Chapman, J.; Nicholson, P. E.; Parker, D. *J. Chem. Soc., Perkin Trans. 1* **1989**, 2079.
(420) Broan, C. J.; Cox, J. P. L.; Craig, A. S.; Kataky, R.; Parker, D.; Harrison, A.; Randall, A. M.; Ferguson, G. *J. Chem. Soc., Perkin Trans. 2* **1991**, 87.
(421) Ellman, G. L. *Arch. Biochem. Biophys.* **1959**, *82*, 70.
(422) Benson, J. R.; Hare, P. E. *Proc. Natl. Acad. Sci., U.S.A.* **1975**, *72*, 619.
(423) Dulyea, L. M.; Fyles, T. M.; Whitfield, D. M. *Can. J. Chem.* **1984**, *62*, 498.
(424) Bartsch, R. A.; Czech, B. F.; Kang, S. I.; Stewart, L. E.; Walkowiak, W.; Charewicz, W. A.; Heo, G. S.; Son, B. *J. Am. Chem. Soc.* **1985**, *107*, 4997.
(425) Gokel, G. W.; Goli, D. M.; Mingani, C.; Echegoyen, L. *J. Am. Chem. Soc.* **1983**, *105*, 6787.
(426) Izatt, R. M.; Bruening, R. L.; Bradshaw, J. S.; Lamb, J. D.; Christensen, J. J. *Pure Appl. Chem.* **1988**, *60*, 453.
(427) Lamb, J. D.; Izatt, R. M.; Christensen, J. J. In *Progress in Macrocyclic Chemistry*; Izatt, R. M., Christensen, J. J., Eds.; John Wiley & Sons: New York, 1981; Vol. 2, p 41.
(428) Izatt, R. M.; Bruening, R. L.; Tarbet, B. J.; Griffin, D.; Bruening, M. L.; Krakowiak, K. E.; Bradshaw, J. S. *Pure Appl. Chem.* **1990**, *62*, 1115.
(429) Takagi, M.; Nakamura, H. *J. Coord. Chem.* **1986**, *15*, 53.
(430) Bradshaw, J. S.; Izatt, R. M.; Christensen, J. J.; Krakowiak, K. E.; Tarbet, B. J.; Bruening, R. L. *J. Incl. Phenom.* **1989**, *7*, 127.
(431) Bradshaw, J. S.; Krakowiak, K. E.; Bruening, R. L.; Tarbet, B. J.; Savage, P. B.; Izatt, R. M. *J. Org. Chem.* **1988**, *53*, 3190.
(432) McDaniel, C. W.; Bradshaw, J. S.; Krakowiak, K. E.; Izatt, R. M.; Savage, P. B.; Tarbet, B. J.; Bruening, R. L. *J. Heterocycl. Chem.* **1989**, *26*, 413.
(433) Krakowiak, K. E.; Bradshaw, J. S.; Izatt, R. M. *Tetrahedron Lett.* **1988**, *29*, 3521.
(434) Izatt, R. M.; Lindh, G. C.; Bruening, R. L.; Huszthy, P.; Lamb, J. D.; Bradshaw, J. S.; Christensen, J. J. *J. Incl. Phenom.* **1987**, *5*, 739.
(435) Bradshaw, J. S.; Krakowiak, K. E.; Tarbet, B. J.; Bruening, R. L.; Griffin, L. D.; Cash, D. E.; Rasmussen, T. D.; Izatt, R. M. *Solvent Extr. Ion Exch.* **1989**, *7*, 855.
(436) Izatt, R. M.; Clark, G. A.; Bradshaw, J. S.; Lamb, J. D.; Christensen, J. J. *Sep. Purif. Methods* **1986**, *15*, 21.
(437) Cotton, F. A.; Wilkinson, G. *Advanced Inorganic Chemistry*, 5th ed.; John Wiley & Sons: New York, 1988; p 955.
(438) Kang, S. I.; Czech, A.; Czech, B. P.; Stewart, L. E.; Bartsch, R. A. *Anal. Chem.* **1985**, *57*, 1713.
(439) Christensen, J. J.; Hill, J. O.; Izatt, R. M. *Science* **1971**, *174*, 459.
(440) Chu, S. C.; Pike, M. M.; Fossel, E. T.; Smith, T. W.; Balschi, J. A.; Springer, C. S., Jr. *J. Magn. Reson.* **1984**, *56*, 33.
(441) Espanol, M. C.; Mota de Freitas, D. *Inorg. Chem.* **1987**, *26*, 4356.
(442) Ramasamy, R.; Espanol, M. T.; Long, K. M.; Mota de Freitas, D.; Geraldes, C. F. G. C. *Inorg. Chim. Acta* **1989**, *163*, 41.
(443) Kumar, A. M.; Gupta, R. K.; Spitzer, A. *Kidney Int.* **1988**, *33*, 792.
(444) Gupta, R. J.; Gupta, P. *J. Magn. Reson.* **1982**, *47*, 344.
(445) Pike, M. M.; Springer, C. S., Jr. *J. Magn. Reson.* **1982**, *46*, 348.
(446) Balschi, J. A.; Cirillo, V. P.; Springer, C. S., Jr. *Biophys. J.* **1982**, *38*, 323.
(447) Pike, M. M.; Yarmusch, D.; Balschi, J. A.; Lenkinski, R. E.; Springer, C. S., Jr. *Inorg. Chem.* **1983**, *22*, 2388.
(448) Buster, D. C.; Castro, M. M. C. A.; Geraldes, C. F. G. C.; Malloy, C. R.; Sherry, A. D.; Siemers, T. C. *Magn. Reson. Med.* **1990**, *13*, 239.
(449) Szklaruk, J.; Marecek, J. F.; Springer, A. L.; Springer, C. S., Jr. *Inorg. Chem.* **1990**, *29*, 660.
(450) Pike, M. M.; Simon, S. R.; Balschi, J. A.; Springer, C. S., Jr. *Proc. Natl. Acad. Sci. U.S.A.* **1982**, *79*, 810.
(451) Shinar, H.; Navon, G. *J. Am. Chem. Soc.* **1986**, *108*, 5005.
(452) Brophy, P. J.; Hayer, M. K.; Riddell, F. G. *Biochem. J.* **1983**, *210*, 961.
(453) Ogino, T.; Shulman, G. I.; Avison, M. G.; Gullans, S. R.; den Hollander, J. A.; Shulman, R. G. *Proc. Natl. Acad. Sci. U.S.A.* **1985**, *82*, 1099.
(454) Pettegrew, J. W.; Post, J. F. M.; Panchalingam, K.; Whiters, G.; Woessner, D. E. *J. Magn. Reson.* **1987**, *71*, 504.
(455) Pike, M. M.; Frazer, J. C.; Dedrick, D. F.; Ingwall, J. S.; Allen, P. D.; Springer, C. S., Jr.; Smith, T. W. *Biophys. J.* **1985**, *48*, 159.
(456) Malloy, C. R.; Buster, D. C.; Castro, M. M. C. A.; Geraldes, C. F. G. C.; Jeffrey, F. M. H.; Sherry, A. D. *Magn. Reson. Med.* **1990**, *15*, 33.
(457) Naritomi, H.; Kanashiro, M.; Sasaki, M.; Kuribauashi, Y.; Sawada, T. *Biophys. J.* **1987**, *52*, 611.
(458) Carnall, W. T. In *Handbook on the Physics and Chemistry of Rare Earths*; Gschmeidner, K. A., Jr., Eyring, L., Eds.; Elsevier: Amsterdam, 1987; Vol. 3, p 171.
(459) Alpha, B.; Ballardini, R.; Balzani, V.; Lehn, J.-M.; Perathoner, S.; Sabbatini, N. *Photochem. Photobiol.* **1990**, *52*, 299.
(460) Balzani, V.; Scandola, F. *Supramolecular Photochemistry*; Horwood: Chichester, England, 1991.
(461) Heller, A.; Wasserman, E. *J. Chem. Phys.* **1965**, *42*, 949.
(462) Charles, R. G.; Riedel, E. P.; Haverlack, P. G. *J. Chem. Phys.* **1966**, *44*, 1356.
(463) Abusaleh, A.; Meares, C. F. *Photochem. Photobiol.* **1984**, *39*, 763.
(464) Sabbatini, N.; Ciano, M.; Dellonte, S.; Bonazzi, A.; Balzani, V. *Chem. Phys. Lett.* **1982**, *90*, 265.
(465) Sabbatini, N.; Dellonte, S.; Ciano, M.; Bonazzi, A.; Balzani, V. *Chem. Phys. Lett.* **1984**, *107*, 212.
(466) Sabbatini, N.; Ciano, M.; Dellonte, S.; Bonazzi, A.; Bolletta, F.; Balzani, V. *J. Phys. Chem.* **1984**, *88*, 1534.
(467) Sabbatini, N.; Dellonte, S.; Blasse, G. *Chem. Phys. Lett.* **1986**, *129*, 541.
(468) Adachi, G.-Y.; Sorita, K.; Kawata, K.; Tomokiyo, K.; Shiokawa, *J. Less-Common Met.* **1983**, *93*, 81.
(469) Halverson, F.; Brinen, J. S.; Leto, J. R. *J. Chem. Phys.* **1964**, *41*, 157.
(470) Horrocks, W. DeW., Jr.; Sudnick, D. R. *J. Am. Chem. Soc.* **1979**, *101*, 334.
(471) Balzani, V.; Lehn, J.-M.; Van Loosdrecht, J.; Mecati, A.; Sabbatini, N.; Ziessel, R. *Angew. Chem., Int. Ed. Engl.* **1991**, *30*, 190.
(472) Sabbatini, N.; Perathoner, S.; Balzani, V.; Alpha, B.; Lehn, J.-M. In *Supramolecular Photochemistry*; Balzani, V., Ed.; Reidel: Dordrecht, The Netherlands, 1987; p 187.
(473) Balzani, V.; Berghmans, E.; Lehn, J.-M.; Sabbatini, N.; Therorde, R.; Ziessel, R. *Helv. Chim. Acta* **1990**, *73*, 2083.
(474) Buonocore, G. E.; Li, H. *Coord. Chem. Rev.* **1990**, *99*, 55.
(475) Bunzli, J.-C. G. In *Handbook on the Physics and Chemistry of Rare Earths*; Gschneidner, K. A., Jr.; Eyring, L., Eds.; Elsevier: Amsterdam, 1987; Vol. 9, Chapter 60.
(476) Prodi, L.; Maestri, M.; Ziessel, R.; Balzani, V. *Inorg. Chem.* **1991**, *30*, 3798.
(477) Pietraszkiewicz, M.; Pappalardo, S.; Finocchiaro, P.; Mamo, A.; Karpiuk, J. *J. Chem. Soc., Chem. Commun.* **1990**, 1907.
(478) Prodi, L.; Maestri, M.; Balzani, V.; Lehn, J.-M.; Roth, C. *Chem. Phys. Lett.* **1991**, *180*, 45.
(479) Buonocore, G. E.; Li, H. *Coord. Chem. Rev.* **1990**, *99*, 55.
(480) Sabbatini, N.; Guardigli, M.; Lehn, J.-M. *Coord. Chem. Rev.* **1993**, *123*, 201.
(481) Sabbatini, N.; Guardigli, N.; Mecata, A.; Balzani, V.; Engaro, R.; Ghidini, E.; Casnati, A.; Pochini, A. H. *Angew. Chem., Int. Ed. Engl.* **1991**, *30*, 854.
(482) Horrocks, W. DeW., Jr.; Albin, M. *Prog. Inorg. Chem.* **1984**, *31*, 1.
(483) Hemmila, I. A. *Application of Fluorescence in Immunoassay*; Winefordner, J. D., Ed.; Wiley: New York, 1991.
(484) Lehn, J.-M. In *Supramolecular Photochemistry*; Balzani, V., Ed.; Reidel: Dordrecht, The Netherlands, 1987; p 29.
(485) Chang, C. A.; Chang, P. H.-L.; Qin, S.-Y. *Inorg. Chem.* **1988**, *27*, 944.
(486) Holz, R. C.; Chang, C. A.; Horrocks, W. DeW., Jr. *Inorg. Chem.* **1991**, *30*, 3270.
(487) Rodriguez-Ubis, J. C.; Alpha, B.; Plancherel, D.; Lehn, J.-M. *Helv. Chim. Acta* **1984**, *67*, 2264.
(488) Reichstein, E.; Shami, Y.; Ramjeesing, M.; Diamandis, E. P. *Anal. Chem.* **1988**, *69*, 1069.
(489) Choppin, G. R.; Goedken, M. P.; Gritmon, T. F. *J. Inorg. Nucl. Chem.* **1977**, *39*, 2025.
(490) Gritmon, T. F.; Goedken, M. P.; Choppin, G. R. *J. Inorg. Nucl. Chem.* **1977**, *39*, 2021.
(491) Gharia, K. S.; Singh, M.; Mathur, S.; Sankhla, B. S. *J. Ind. Chem. Soc.* **1983**, *60*, 315.
(492) Forsberg, J. H. *Coord. Chem. Rev.* **1973**, *10*, 195.
(493) Sinha, S. P.; Butter, E. *Mol. Phys.* **1969**, *16*, 285.
(494) Kahwa, I. A.; Selbin, J.; O'Connor, C. J.; Foise, J. W.; McPherson, G. L. *Inorg. Chim. Acta* **1988**, *148*, 265.
(495) Brittain, H. G. In *Metal Containing Polymeric Systems*; Carraher, C. E., Sheats, J., Pittman, C., Eds.; Plenum Press: New York, 1985; p 451.
(496) Spauldine, L.; Brittain, H. G. *Inorg. Chem.* **1983**, *22*, 3486.
(497) Drew, M. G. B.; Yates, P. C. *Pure Appl. Chem.* **1989**, *61*, 835.
(498) Lifson, S. In *Structural Molecular Biology: Methods and Applications*; Davies, V. D., Saenger, U., Danyluck, S. S., Eds.; Plenum Press: New York, 1982; p 359.

(499) Pifat, G., Herak, J. N., Eds. *Supramolecular Structure and Function*; Plenum Press: New York, 1983.
(500) Burkert, V.; Allinger, N. L. *Molecular Mechanics*, ACS Monograph 177; American Chemical Society: Washington, DC, 1982.
(501) Brubaker, G. R.; Johnson, D. W. *Coord. Chem. Rev.* **1984**, *53*, 14.
(502) Hancock, R. D. *Prog. Inorg. Chem.* **1989**, *36*, 187.
(503) Lipton, M.; Still, W. C. *J. Comput. Chem.* **1988**, *9*, 343.
(504) Dolata, D.; Leach, A.; Prout, K. *J. Comput.-Aided Mol. Des.* **1987**, *1*, 73.
(505) Koschmann, T.; Snyder, J. P.; Johnson, P.; Grace, T.; Evens, M. W. *J. Mol. Graphics* **1988**, *6*, 74.
(506) Fossheim, R.; Dugstad, H.; Dahl, S. G. *J. Med. Chem.* **1991**, *34*, 819.